School of Doctoral Studies in Biological Sciences
University of South Bohemia in České Budějovice, Faculty of Science

Molecular Factors of Cell Antiviral Immunity

Ph.D. Thesis

Mgr. Martin Selinger

Supervisor: prof. RNDr. Libor Grubhoffer, CSc., Hon. D.Sc., dr. h. c.

University of South Bohemia in České Budějovice, Faculty of Science,
Czech Republic
&
Biology Centre of the Czech Academy of Sciences, Institute of Parasitology,
Czech Republic

České Budějovice 2019

This thesis should be cited as:

Selinger, M., 2019: Molecular Factors of Cell Antiviral Immunity. Ph. D. Thesis Series 20, University of South Bohemia, Faculty of Science, School of Doctoral Studies in Biological Sciences, České Budějovice, Czech Republic, 186 pp.

Annotation:

The proposed thesis focuses on the description of flavivirus-host interactions in case of tick-borne encephalitis virus (TBEV) and Zika virus (ZIKV). In more detail, the TBEV-induced host responses in human cells of neural origin and interferon-mediated protection were described together with the identification of a new phenomenon of TBEV-induced host transcriptional and translational shut-off. In addition, virus-derived molecules with hypothetical immunomodulatory characteristics, TuORF and ZIKV sfRNA, were analysed for their presence and possible function during the infection.

Declaration [in Czech]:

Prohlašuji, že v souladu s § 47b zákona č. 111/1998 Sb. v platném znění souhlasím se zveřejněním své disertační práce, a to v úpravě vzniklé vypuštěním vyznačených částí archivovaných Přírodovědeckou fakultou elektronickou cestou ve veřejně přístupné části databáze STAG provozované Jihočeskou univerzitou v Českých Budějovicích na jejích internetových stránkách, a to se zachováním mého autorského práva k odevzdanému textu této kvalifikační práce. Souhlasím dále s tím, aby toutéž elektronickou cestou byly v souladu s uvedeným ustanovením zákona č. 111/1998 Sb. zveřejněny posudky školitele a oponentů práce i záznam o průběhu a výsledku obhajoby kvalifikační práce. Rovněž souhlasím s porovnáním textu mé kvalifikační práce s databází kvalifikačních prací Theses.cz provozovanou Národním registrem vysokoškolských kvalifikačních prací a systémem na odhalování plagiátů.

České Budějovice, 29.11. 2019

…………….…………………
Mgr. Martin Selinger

This thesis originated from a partnership of Faculty of Science, University of South Bohemia, and Institute of Parasitology, Biology Centre CAS, supporting doctoral studies in the Molecular and Cell Biology and Genetics study programme.

best sister in the world. Most importantly, I would like to thank my beloved wife Pája, for her patience, love and care.

And the last "thank you", and also the dedication of this work, goes to my grandparents. All of them are not with us anymore, but I will remember their unconditional love and limitless support for the rest of my life.

List of papers and author's contribution

The thesis is based on the following papers (listed chronologically):

I.   Černý, J., **Selinger, M.**, Palus, M., Vavrušková, Z., Tykalová, H., Bell-Sakyi, L., Štěrba, J., Grubhoffer, L., Růžek, D., 2016: Expression of a second open reading frame present in the genome of tick-borne encephalitis virus strain Neudoerfl is not detectable in infected cells. Virus Genes 52(3): 309-316. DOI: 10.1007/s11262-015-1273-y (IF = 1.537)

Martin Selinger was responsible for the preparation and imaging of TBEV-infected cells and participated in the revision of the manuscript.

II.   Donald, C.L., Brennan, B., Cumberworth, S.L., Rezelj, V.V., Clark, J.J., Cordeiro, M.T., Franca, R.F.D., Pena, L.J., Wilkie, G.S., Filipe, A.D., Davis, C., Hughes, J., Varjak, M., **Selinger, M.**, Zuvanov, L., Owsianka, A.M., Patel, A.H., McLauchlan, J., Lindenbach, B.D., Fall, G., Sall, A.A., Biek, R., Rehwinkel, J., Schnettler, E., Kohl, A., 2016: Full Genome Sequence and sfRNA Interferon Antagonist Activity of Zika Virus from Recife, Brazil. PLoS Neglected Tropical Diseases 10(10): e0005048. DOI: 10.1371/journal.pntd.0005048 (IF = 4.72)

Martin Selinger was responsible for the cloning of ZIKV sfRNA and sfRNA/IFN assays, and participated in the revision of the manuscript.

III.   **Selinger, M.**, Wilkie, G.S., Tong, L., Gu, Q., Schnettler, E., Grubhoffer, L., Kohl, A., 2017: Analysis of tick-borne encephalitis virus-induced host responses in human cells of neuronal origin and interferon-mediated protection. Journal of General Virology 98(8): 2043-2060. DOI: 10.1099/jgv.0.000853 (IF = 2.693)

Corrigendum:

Selinger, M., Wilkie, G.S., Tong, L., Gu, Q., Schnettler, E., Grubhoffer, L., Kohl, A., 2018: Analysis of tick-borne encephalitis virus-induced host responses in human cells of neuronal origin and interferon-mediated protection. Journal of General Virology 99(8):1147-1149. DOI: 10.1099/jgv.0.001109

Martin Selinger was responsible for the design of the study and participated in experimental procedures, data processing and analysis, and writing the manuscript.

IV.   Věchtová, P., Štěrbová, J., Štěrba, J., Vancová, M., Rego, R.O.M., **Selinger, M.**, Strnad, M., Golovchenko, M., Rudenko, N., Grubhoffer, L., 2018: A bite so sweet – the glycobiology interface of tick-host-pathogen interactions. Parasites & Vectors 11(1): 594. DOI: 10.1186/s13071-018-3062-7. (IF = 3.408)

Martin Selinger was responsible for the writing of "N-linked glycans of flaviviruses" chapter and participated in the revision of the manuscript.

V.   **Selinger, M.**, Tykalová, H., Štěrba, J., Věchtová, P., Vavrušková, Z., Lieskovská, J., Kohl, A., Schnettler, E., Grubhoffer, L., 2019: Tick-borne encephalitis virus downregulates rRNA synthesis and host protein production in human cells of neuronal origin. PLoS Neglected Tropical Diseases 13(9): e0007745. DOI: 10.1371/journal.pntd.0007745. (IF = 4.487)

Martin Selinger was responsible for the design of the study and participated in experimental procedures, data processing and analysis, and writing the manuscript.

Contents:

1 Preface

Arthropod-borne viruses (arboviruses) represent a paraphyletic group of viruses with a world-wide impact on human and animal health, with millions of cases reported per year. According to their name, arboviruses are defined as viruses that are maintained in nature *via* biological transmission between susceptible vertebrate hosts and invertebrate vectors (haematophagous arthropods – ticks, mosquitoes, midges, sandflies, etc.). Arboviruses include species from various families, e.g., *Reoviridae*, *Flaviviridae*, *Togaviridae*, *Nairoviridae*, *Phenuiviridae*, *Peribunyaviridae*, and *Asfaviridae*.

Virus species, which were the object of this thesis' research, belong to the *Flaviviridae* family, genus *Flavivirus*. As stated above, flaviviruses being arboviruses are important human pathogens. Almost the whole human population lives in areas where at least one flavivirus species is endemic. Among the medically most important flavivirus species belong dengue virus (DENV), yellow fever virus (YFV), West Nile virus (WNV), Zika virus (ZIKV), Japanese encephalitis virus (JEV), tick-borne encephalitis virus (TBEV) and many others. As vaccination against most flaviviruses is missing or the population is not sufficiently vaccinated, a specific anti-flaviviral cure, which is also currently unavailable, is urgently needed.

Research interests of our laboratory include mainly the description of TBEV-host interactions and do not involve the direct characterization of an antiviral agent. However, we believe that by understanding the nature of TBEV pathogenesis in the central nervous system (CNS) we could help to find the way for identifying a suitable treatment against TBEV infection. Therefore, we are focused on the identification of viral factors responsible for the modulation of host immune response on one side and the description of host response to TBEV infection on the other side.

The proposed thesis tries to at least partially explore and describe the vast universe of virus-host interactions by studying TBEV infection in cells of neural origin. In more detail, the host response in terms of gene and protein expression was studied as well as the modulatory effects of particular viral components from TBEV and ZIKV.

2 Introduction

2.1 Flaviviruses

According to the phylogenetic relationships, family *Flaviviridae* shows clustering into four currently assigned genera – *Flavivirus*, *Hepacivirus*, *Pestivirus*, and *Pegivirus* (Fig. 1). However, only species belonging to the genus *Flavivirus* are characterized as arboviruses. Based on their vector, flaviviruses can be further divided into mosquito-borne flaviviruses (currently 34 species), tick-borne flaviviruses (currently 13 species), or flaviviruses with no known vector (currently 13 species) [1]. Disease severity of flaviviral infections ranges from asymptomatic or mild flu-like/febrile illness to severe encephalitis, haemorrhagic fever, jaundice or developmental disorders. Basic information about the most important flaviviruses is described in the following text.

2.1.1 Mosquito-borne flaviviruses

Dengue virus

DENV circulates in endemic areas of tropic and subtropic Asia, Africa, Australia, and both Americas (Fig. 2). Its vectors are mosquitoes from the *Aedes* genus, with *A. aegypti* being the principal one. DENV infection is very often asymptomatic (~75% of the cases), however, it can also develop into dengue fever (headache, severe muscle and joint pain, and rash) or into potentially lethal dengue haemorrhagic fever (increased vascular permeability and plasma leakage from blood vessels into tissues accompanied by significant thrombocytopenia). Four distinct serotypes (DENV1–4) have been classified. Recovery from the primary infection with one serotype provides life-long immunity. However, secondary infection with a different serotype may lead to an increased risk of sever dengue fever thanks to the antibody-dependent enhancement [2, 3].

Based on the report from WHO, the number of reported DENV cases increased dramatically in the last years from 2.2 million (2010) to 3.34 million (2016) in Americas, South-East Asia and Western Pacific [4]. The exact numbers of annual DENV cases worldwide are not available. However, the study of Bhatt *et al.* estimates 390 million cases per year,

of which 96 million manifested clinically [5]. Currently, 20 countries have approved the use of dengue tetravalent vaccine CYD-TDV (Dengvaxia®; Sanofi Pasteur), which was licensed in 2015. Based on several studies, the vaccine was proved to be efficient. However it is recommended that the vaccine should be given only to patients with confirmed prior dengue virus infection [4, 6, 7].

Yellow fever virus

YFV is the prototype virus of the *Flavivirus* genus (lat. *flavus* – yellow – one of the yellow fever symptoms is jaundice). Three different transmission cycles have been described for YFV (sylvatic/jungle, intermediate, and urban), with monkeys being the natural reservoir. The vectors are mosquitoes of the *Haemogogus*, *Aedes*, and *Sabethes* genera. The geographical distribution includes tropical and subtropical areas of Africa and South America (Fig. 2). The yellow fever disease follows a similar scheme as in the case of dengue – only low percentage of infected people manifest symptoms. These could be characterized as fever, muscle pain, headache, loss of appetite, and nausea or vomiting. The vast majority of patients recover after several days, however, circa 14 % of patients develop a severe haemorrhagic form of the disease, which is accompanied by high fever, epigastric pain, jaundice (liver failure), renal failure, and bleeding from the eyes, nose, bladder, and rectum. The mortality rate of severe form reaches 30–60 % [8, 9].

Based on the data from Africa during the year 2013, it was estimated that there were 84 000–170 000 severe form cases, out of which 29 000–60 000 were lethal [10]. Fortunately, there is a very effective vaccine against YFV in the form of live attenuated strain YFV-17D with life-long protection.

Japanese encephalitis virus

Geographical distribution of JEV spreads across the vast area of Southeast Asia including China, India and Indonesia (Fig. 2). Vectors of JEV are mosquitoes from the *Culex* species (particularly *Cx. tritaeniorhynchus*) and the natural reservoir are domestic animals (pigs) and water birds; humans are dead-end hosts. Only 1 % of infected people will develop symptoms (fever, headache, and vomiting), however, a
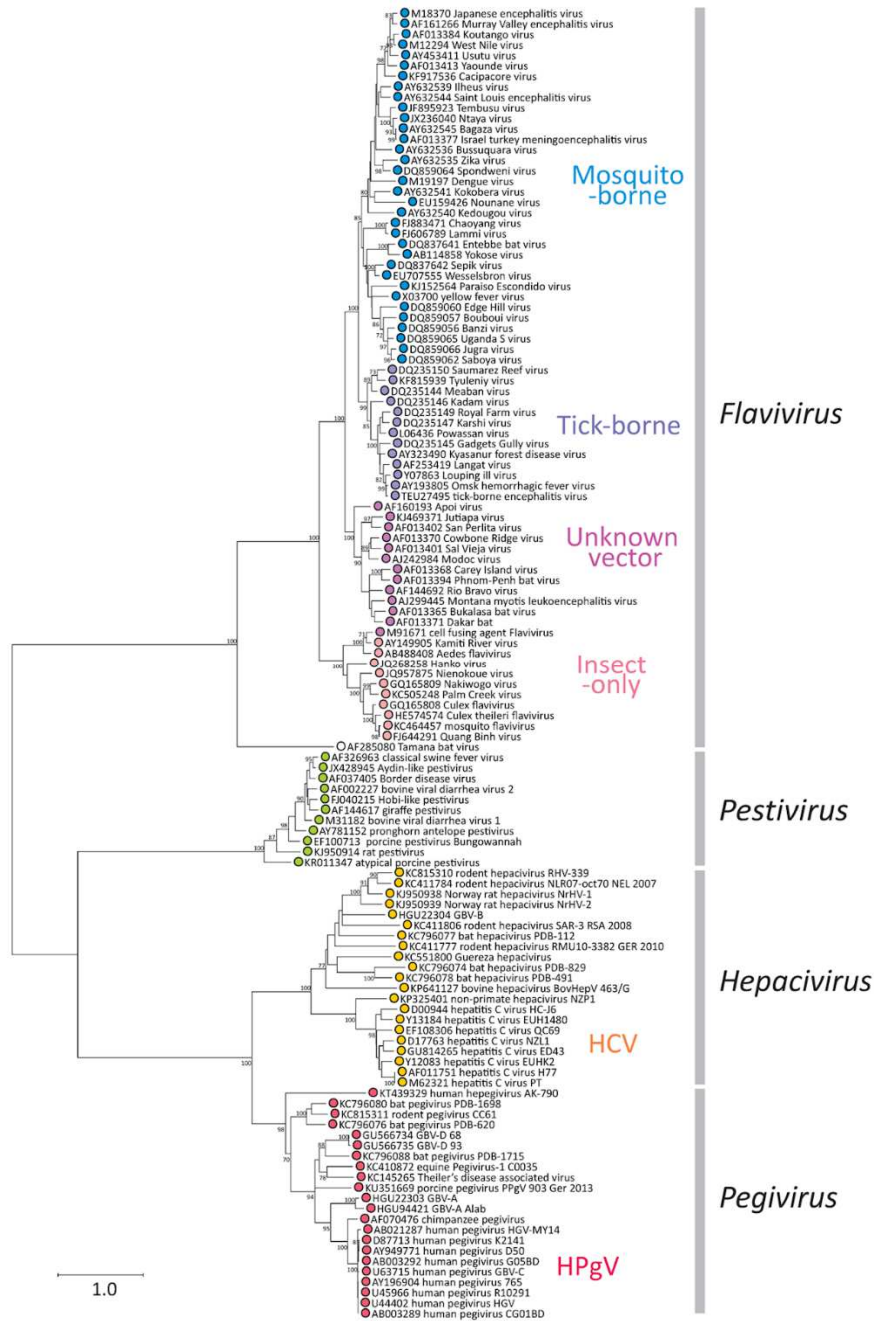
Figure 1: Maximum likelihood clustering model of phylogenetic relationships in *Flaviviridae* family based on the amino acid sequence from flaviviral RNA-dependent RNA polymerase conserved domain (adapted from ICTV; https://talk.ictvonline.org/ictv-reports/ictv_online_report/positive-sense-rna-viruses/w/flaviviridae).

4

relatively high portion of patients (up to 30 %) may develop severe encephalitis. The mortality rate for patients with severe encephalitis is 20–30 %. In addition, survivors often suffer with neurological sequelae (30–50 %) [11, 12].

Up to 68 000 clinical cases of Japanese encephalitis (JE) are estimated annually, with circa 13 600–20 400 deaths [13]. No specific treatment for JE exists, hence, vaccination is the main preventive measure. Currently, four different types of vaccines are at disposal in various countries around the world: (1) mouse brain-derived killed-inactivated, (2) cell culture-derived live-attenuated, (3) cell culture-derived killed-inactivated, and (4) genetically engineered live-attenuated chimeric [11].

West Nile virus

WNV circulates in bird-mosquito-bird cycle with humans as a dead-end host. It is believed that migratory birds and a considerably high number of sensitive mosquito species play a key role in the almost worldwide distribution of WNV (Fig. 2). Nevertheless, the main vectors of WNV are mosquitoes from the *Culex* genus (mainly *Cx. pipiens* and *Cx. quinquefasciatus*). Since WNV belongs to the JEV serocomplex, the disease characteristics are relatively similar to JEV. According to statistics, 20 % of infected people develop symptoms such as fever, headache, tiredness, body aches, nausea, and vomiting. Only a very low number of infected people (0.66 %) develop a severe form of the disease, West Nile encephalitis, which is characterised by high fever, headache, neck stiffness, stupor, disorientation, coma, tremors, convulsions, muscle weakness, vision loss, numbness, and paralysis. The severe form is fatal in 10 % of cases. No vaccine or specific antiviral treatment for WNV infection is available [14, 15].

Zika virus

ZIKV was firstly isolated in the Zika forest in Uganda in 1947 from a rhesus monkey (strain MR766) [16] and the first human infection was documented in 1954 in Nigeria [17]. For almost 50 years, ZIKV was considered a low-importance flavivirus with only 14 reported human cases in Africa and Asia [18]. However, starting in 2007, ZIKV caused large-scale outbreaks in Micronesia, French Polynesia (2013), New
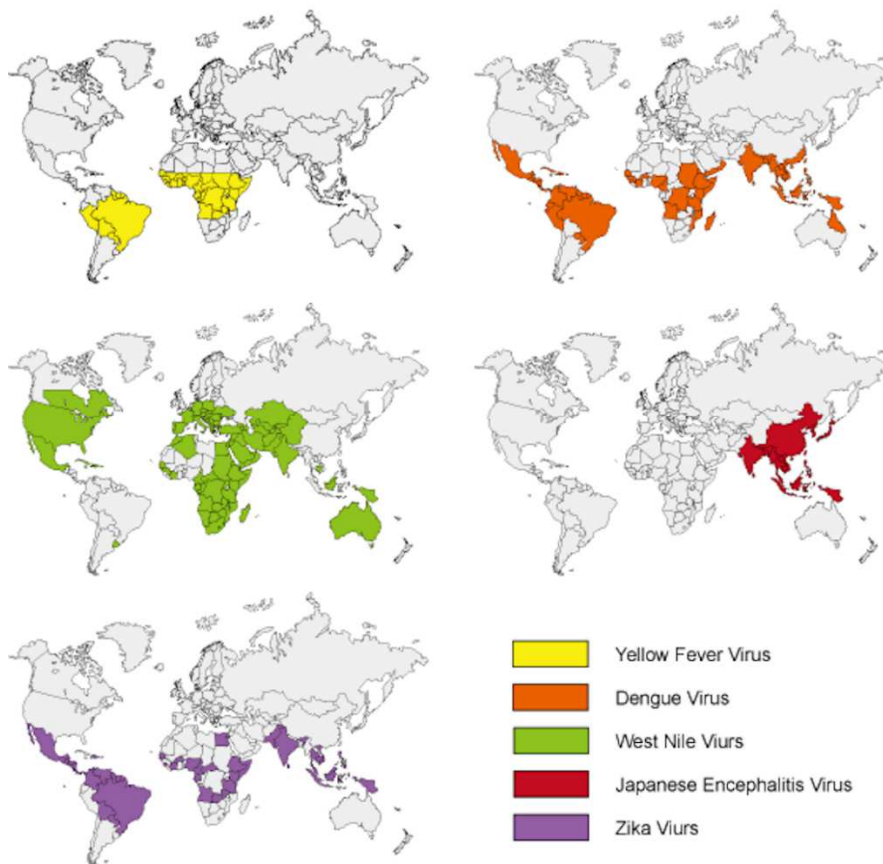
Figure 2: Geographic distribution of selected mosquito-borne flaviviruses (adapted from Creative Diagnostics®; https://www.creative-diagnostics.com/Flavivirus.htm).

Caledonia (2014), the Cook Islands (2014), Easter Island (2014), and in Americas (2015) (Fig. 2). These outbreaks have been associated with an increased frequency of neurological disorders, including Guillain-Barré syndrome, neuropathy, and myelitis in adults and microcephaly in newborns [19, 20]. Nevertheless, 80 % of the ZIKV infections are asymptomatic and most of the patients develop only mild symptoms such as fever, rash, conjunctivitis, muscle and joint pain, malaise, and headache [21].

ZIKV is transmitted by the bite of infected mosquitoes from the *Aedes* genus (*A. aegypti*, *A. albopictus*) [19], or, interestingly, by sexual contact and blood transfusions [22, 23]. In addition, ZIKV can be transmitted from

mother to foetus, resulting in the congenital Zika virus syndrome (microcephaly and developmental disorders) [24]. Currently, no vaccine or direct treatment exists.

2.1.2 Tick-borne flaviviruses

Group of tick-borne flaviviruses includes viruses such as TBEV, Louping ill virus (LIV), Powassan virus (POWV), Omsk haemorrhagic fever virus (OHFV), or Kyasanur forest disease virus (KFDV) [3, 25]. Geographic distribution encompasses North America and eastern Russia for POWV, India for KFDV, western Siberia for OHFV, and the majority of Eurasia for TBEV (Fig. 3).
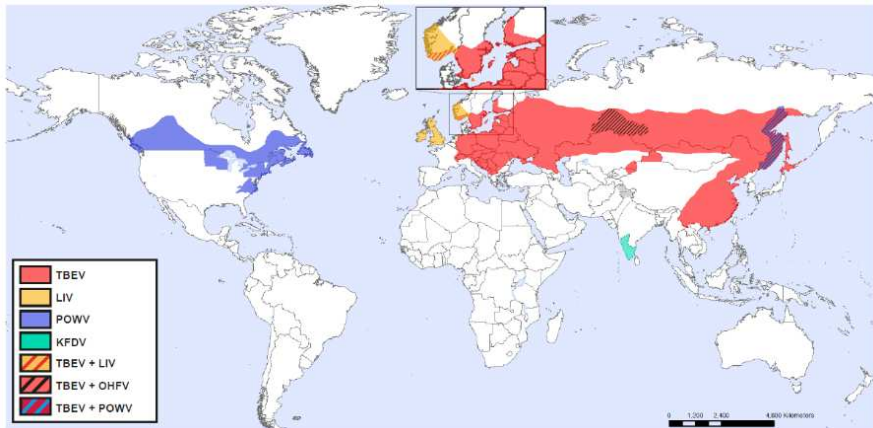
Figure 3: Geographic distribution of selected tick-borne flaviviruses (adapted from [25]).

Powassan virus

POWV was firstly identified in 1958 in the town of Powassan (Ontario, Canada) [26]. Until 1998, only 27 human cases of POWV infection were reported in North America. However, 152 cases of POWV infection were reported in USA since 1999. Main vectors of POWV are hard ticks, *I. scapularis* and *I. cookei*. The disease is mostly asymptomatic, however, severe encephalitis/meningitis cases with 10 % mortality rate were reported [27].

Kyasanur forest disease virus

KFDV was firstly described in 1957 in India (Kyasanur forest of Shimoga district, state of Karnataka) [28]. Annually, 400–500 cases of Kyasanur forest disease (KFD) are estimated with 3–5 % case fatality rate. Ticks from various genera were proved to be able to transmit the KFDV (*Haemaphysalis*, *Argas*, *Dermacentor*, *Hyalomma*, *Ixodes*, *Ornithodoros*, *and Rhipicephalus*). KFD is clinically characterized as a haemorrhagic disease with limited evidence of encephalitis [29].

Tick-borne encephalitis virus

The causative agent of viral encephalitis, TBEV, was firstly isolated in the eastern region of Russia in 1937 [30]. Endemic areas of TBEV are found in most European countries (except Great Britain, the Benelux countries, Portugal, and Spain) and in large parts of Asia, including Russia, northern and western China, and northern Japan (Fig. 3). As in the case of other flaviviruses, the geographic distribution of TBEV is expanding – in 2015, TBEV was confirmed in ticks and deer in the Netherlands [31]. Shortly after, in 2016, the first human case of tick-borne encephalitis (TBE) acquired in the Netherlands was reported as well [32].

TBEV is further subdivided into three subtypes based on the serological analyses: a European subtype (TBEV-EU), Siberian subtype (TBEV-Sib) and Far Eastern subtype (TBEV-FE) [33, 34]. These subtypes are varying in clinical outcome, the main natural vector and geographical distribution. The Far-Eastern subtype is seasonally epidemic in scattered foci in the far eastern part of the former USSR and extending across into China and Japan, while the Siberian subtype occurs in the Urals, Siberia and far-eastern Russia. The European subtype includes most virus isolates from Europe [35]. However, all three subtypes occur in Europe, because the TBEV-Sib and TBEV-FE subtypes were recently detected in the Baltic republics and Finland [36-38].

The principal vectors of TBEV are hard ticks from the *Ixodes* genus and the geographical distribution of particular TBEV subtypes strongly correlates with the geographical distribution of their main tick vector: TBEV-EU is transmitted mainly by *I. ricinus* in Europe and Scandinavia; *I. gibbosus* was shown to be a potent TBEV vector in the Mediterranean.

I. persulcatus is the principal vector of both TBEV-FE and TBEV-Sib subtypes, less often *I. ovatus* together with ticks belonging to the *Dermacentor* and *Haemaphysalis* genera. Competent vertebrate hosts and reservoirs of TBEV are small forest mammals, especially rodents and insectivores. Although other larger animals, including birds, deer and horses also serve as hosts for ticks, they are not considered to be important hosts for virus transmission between ticks [35, 39, 40].

TBEV transmission is realized in several ways; the virus can be transmitted tran-ovarially to the progeny of an infected female tick [41], or uninfected larvae and nymphs can get infected by feeding on a viremic animal or by co-feeding next to an infected tick. The co-feeding mechanism enables a transmission in the absence of significant viremia, even on immune hosts, and is probably the most relevant pathway for viral spread among ticks in nature [42, 43]. Once a tick gets infected, it carries the virus for the rest of its life – TBEV infection is then maintained throughout the developmental stages (trans-stadial transmission). Humans are dead-end hosts from the epidemiologic point of view, and they do not play any role in the maintenance of the virus in nature. There are two ways how people can get infected by TBEV: (1) by a bite of an infected tick, or (2) by consumption of unpasteurised milk and dairy products from infected goat, cow or sheep [44]. Despite the knowledge of TBEV transmission *via* raw milk, several outbreaks of TBEV coming from this source were recently reported [45, 46].

After the bite of an infected tick and the release of TBEV-containing saliva into the human body, various cell types in the skin are infected, namely epidermal Langerhans cells, which are among the first and most important host cells to be infected [47, 48]. These cells then transport the virus to the draining lymph nodes and initiate the spread of infection to lymphoid compartments. Virus replication in these and other tissues leads to viremia and systemic infection including the central nervous system (CNS), which can be invaded only under high-level viremia conditions. How the neurotropic TBEV gains access to the CNS remains incompletely understood, but interactions at the blood-brain barrier (BBB) are critical. Proposed mechanisms include active replication within the endothelial cells, passive transfer across the BBB or within leukocytes that migrate across the barrier [49, 50]. Recently, the transcellular pathway of crossing

BBB was suggested [51]. The primary human microvascular endothelial cells (HBMECs) were proved to be susceptible to TBEV infection and produced high titres of TBEV despite relatively low infection rate (> 5%). In addition, TBEV infection of HBMECs in an *in vitro* BBB model did not compromise its integrity and transcellular transport of TBEV was observed.

Once TBEV enters the CNS, neurons are the predominantly infected cell type. Immunocytochemistry analysis of brain autopsies from fatal TBE cases detected widespread localization of viral antigens in the spinal cord, brainstem, cerebellum, and basal ganglia. Prominent labelling was consistently found in perikarya and processes of Purkinje cells and large neurons of dentate nucleus, inferior olives, and anterior horns [52]. Astrocytes were recently also shown to be susceptible to TBEV infection, however, no cytopathic effect was observed [53]. The suggested mechanism of neural tissue damage during TBEV infection is virus-associated cell death combined with an immunopathogenic role of cellular and humoral responses of the host immune system, especially CD8^{+} granzyme B–releasing cytotoxic T cells and macrophages/microglia [54, 55].

According to WHO, 10 000–12 000 cases of TBE are reported annually worldwide [56]. Czech Republic reported 681 cases per year on the average from 2003 to 2009, which represents the second highest incidence of TBE in Europe after Russia [57]. The number also represents 25 % of all the TBE cases reported in the European Union between 2000–2010 [58]. The clinical outcome of TBEV infection in humans depends on the respective TBEV subtype. While the early stage of the disease is more or less similar during the infections caused by all three TBEV subtypes, the late neurological symptoms are varying in frequency and severity. Regardless of disease severity, the incubation period of TBE on average lasts between 7 and 14 days (4–28 days in extreme cases). The early stage is characteristic by unspecific influenza-like symptoms including fever (99 %), fatigue (63 %), general malaise (62 %), headache and body pain (54 %). Nevertheless, acute neuroinvasive disease is the most commonly recognized clinical manifestation of TBE with the following forms described: febrile, meningeal, meningoencephalitic, poliomyelitic, polyradiculoneuritic and chronic. A significant proportion of the patients

suffered with various long-term subjective and objective sequelae [59, 60].

The TBEV-EU strain is associated with high ratio of sub-clinical or asymptomatic cases (estimated 70–95 %). Typically, the disease is biphasic in 72–87 % of patients. The first stage is characterized by viremia and influenza-like symptoms. This is often followed by asymptomatic interval ranging from 1 to 33 days. 20–30 % of infected patients develop the symptoms typical for the second meningoencephalitic phase. In the second stage, the clinical spectrum ranges from mild meningitis to severe encephalitis with or without myelitis and spinal paralysis. Neurologic sequelae were reported up to 30 % of the patients and case fatality in adult patients is < 2 % [61]. Human infection with a TBEV-FE subtype viruses results in the most severe form of CNS disorder with a tendency for the patient to develop focal meningoencephalitis or polyencephalitis accompanied by loss of consciousness and prolonged feelings of fatigue during recovery. The course of the disease is mostly monophasic (85 % of patients) and the case fatality ranges between 20 and 40 %. TBEV-Sib subtype viruses induce a less severe acute period and a high prevalence of the non-paralytic febrile form of encephalitis. Case fatality rates rarely exceed 6–8 %. Instead, there is a tendency for patients to develop chronic TBE, when several cases were reported in Western and Eastern Siberia and of Central Russia [39, 60].

2.1.3 Structure of flaviviruses

All members of the genus *Flavivirus* share similar architecture of their virions, genomic organization and life cycle. Fig. 4 shows composition of the flaviviral particle – virions are about 50 nm in diameter and are composed of an electron dense core surrounded by a lipid bilayer containing two glycoproteins – E (envelope) and prM/M (membrane). The core includes single stranded RNA genome of positive polarity, which is approximately 11 kb long and a capsid composed of protein C (capsid) units. The TBEV E protein is responsible for yet unknown receptor binding and membrane fusion; it also acts as a main antigen inducing production of neutralizing antibodies and protective immune response. The prM protein in immature virus particles protects the E protein from premature

membrane fusion. The pr fragment of M is cleaved by the host protease furin in the trans-Golgi network enabling secretion of mature virions from the infected cells [62, 63].
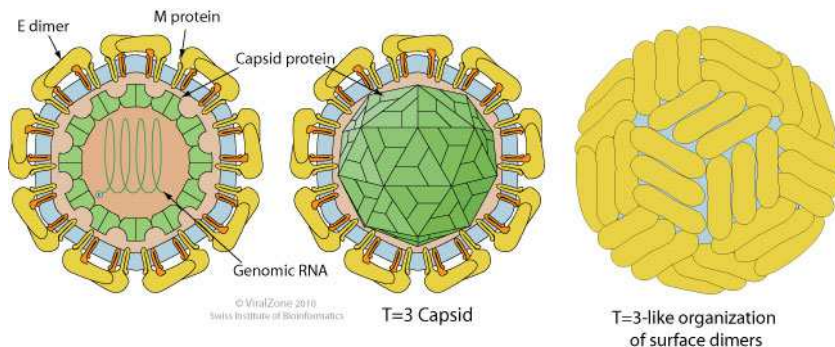
Figure 4: Schematic illustration of flaviviral virion (adapted from http://viralzone.expasy.org).

Because of its (+) orientation, the flaviviral genomic RNA acts directly as an mRNA and contains only one open reading frame flanked by 5' (ca. 130 nt) and 3' (400-700 nt) UTRs. The flaviviral genome further possesses a 5' type I cap structure (m7GpppAmpN1), but lacks a poly-(A) tail at the 3' end [64]. Interestingly, a poly-(A) sequence is found in the variable region of 3' UTR of some TBEV isolates, including Neudoerfl [65]. A single ORF encodes a polyprotein of 3 392–3 433 amino acids (depending on the species). This polyprotein is co-translationally and post-translationally cleaved by viral and cellular proteases to three structural (C, prM and E) and seven non-structural proteins (NS1, NS2A, NS2B, NS3, NS4A, NS4B, NS5) (see Fig. 5). As mentioned above, three structural proteins are responsible for virion composition, while non-structural proteins play a key role during TBEV life cycle in host cell – viral replication and virion assembly [62, 63]. Functional characteristics of all 10 proteins are depicted in detail in Fig. 5.

The various stages of the flavivirus life cycle seems to be coordinated and strictly regulated. Among others, cis-acting RNA structures within the viral genome play an important role in the regulation – specific RNA secondary structures located in both UTRs are involved in translation, cyclization and initiation of genomic RNA replication and probably determine the genome packaging [65-69]. Interestingly, 3' UTR of TBEV was shown to play a crucial role also in the virulence [70].
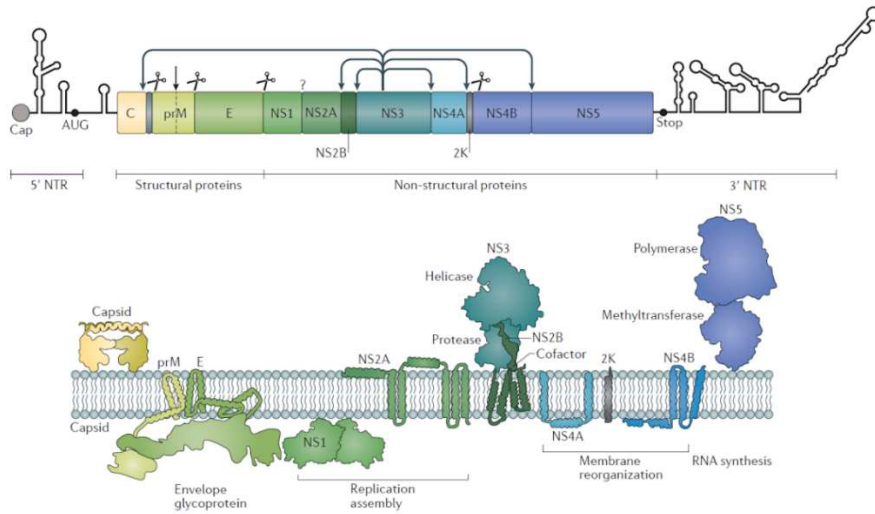
Figure 5: Flaviviral genome organization and viral protein functions. The single open reading frame encodes a polyprotein precursor that is co- and post-translationally cleaved into three structural proteins and seven non-structural proteins. Putative functions of these proteins during infection are described. Simplified RNA secondary and tertiary structures within the 5' and 3' non-translated regions (NTRs) are indicated. Adapted from [71].

More recently, several studies have described the presence of a 0.3–0.8 kb long non-coding RNA derived from the 3' UTR of flaviviral genomes. This so-called sfRNA (subgenomic flaviviral RNA) was detected in cells infected with WNV [72], JEV [73], DENV [74], TBEV and LGTV [75]. The origin of sfRNA was outlined in the case of WNV by Pijlman *et al.* – sfRNA molecules are produced by degradation of viral genome by the cellular 5'-3' exonuclease XRN1 [72]. The same study showed that sfRNA is also required for viral pathogenicity in a mouse model, which corresponds to the findings of Sakai *et al.* [70].

2.1.4 Replication cycle of flaviviruses

Replication and translation processes occur in special virus-induced membranous structures derived from endoplasmic reticulum of the host cells (Fig. 6). These large morphological changes are typical for flaviviruses in general. Using 3D tomography and electron microscopy, it was shown that replication of flaviviral RNA takes place in vesicle packets (VPs) and translation occurs in convoluted membranes [53, 76-79]. The VP membranes do not only promote viral replication, but also contribute

to the protection of viral factors from detection by the host immune system [80, 81]. The viral genomic RNA is translated into a transmembrane polyprotein that is processed by viral protease NS2B-3 and host signal peptidase at the luminal and cytoplasmic site of ER, respectively (Fig. 6). Interestingly, all virus-induced membrane compartments are interconnected and constitute a single endo-membrane system in which all the steps necessary for viral replication and virion assembly take place [77].
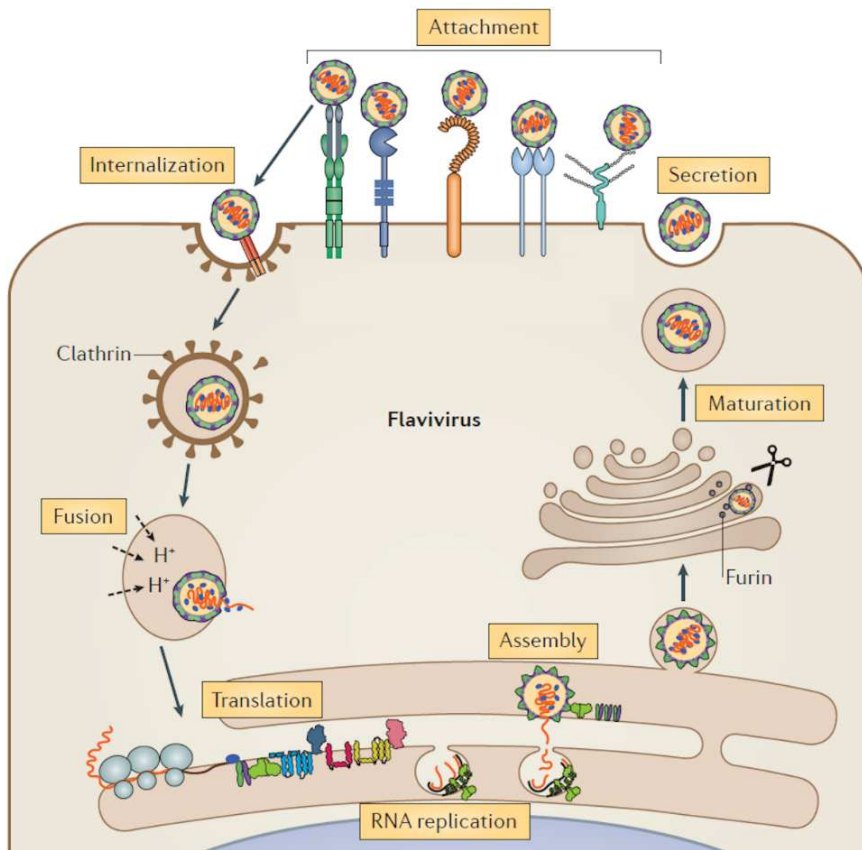
Figure 6: Flavivirus infectious life cycle. Flaviviruses are internalized by receptor-mediated endocytosis and transported to endosomes, where the acidic environment induces fusion between the virus and the host membrane resulting in the release of genomic (+) RNA (gRNA). Translation of viral gRNA is followed by processing of the resulting polyprotein by host and virus-proteases. Subsequently, a replication complex is assembled and associated to virus-induced vesicular packets where viral replication takes place. The replication complex produces (-) gRNA strands, which then serves as template for new (+) gRNA synthesis. Progeny (+) gRNA strands can either initiate a new translation cycle or be assembled into virions. Packaging takes place on the surface of the ER, followed by budding of the structural proteins and newly synthesized RNA into the lumen of the ER. The resultant immature virions are transported to the trans-Golgi where furin-mediated cleavage of prM to M generates mature infectious particles that are released by exocytosis. Adapted from [71].

Following the replication of flaviviral genomic RNA in VPs, progeny strands are incorporated into the nucleocapsid as they exit VP pores. Nucleocapsids are then transported through an adjacent ER membrane and acquire the lipid envelope containing the prM-E heterodimers. These immature virions accumulate in ER cisternae prior to transport to the Golgi apparatus. Immature individual virions are conveyed within individual ER-derived vesicles to the Golgi apparatus; here they are exposed to acidic pH allowing the host enzyme furin to proteolytically cleave prM resulting in the formation of a mature virion. Mature virion particles are then assumed to be secreted at the plasma membrane immediately [76, 82].

2.2 Immune system and its response to the viral infection

After a virus infects a human, antiviral responses are generated that attempt to prevent virus dissemination. The human immune response generally acts on two levels: (1) the innate immune system represents the early non-specific reaction; (2) the adaptive immune system is triggered when a virus evades the innate immune system and generates a threshold level of antigen. The effectors of the innate immune system can either eliminate the virus or interfere with the infection process providing sufficient time for slower antigen-specific adaptive immune response. Although these two arms of the immune system have distinct functions, there is an interplay between both systems, when components of the innate immune system influence the adaptive immune system and vice versa.

2.2.1 Adaptive immune response

The adaptive immune system consists of two arms: the humoral immune response (B lymphocytes) and the cellular immune response (CD4+ and CD8+ T lymphocytes). Studies have shown common and disparate features among the flaviviruses in the induction of both the humoral and the cellular arms of the adaptive immune responses which play a central

role in the disease pathogenesis and outcome of flavivirus infection (see below). Generally, to initiate an adaptive immune response, sensing by a subset of immune cells, the antigen-presenting cells (APCs), is required. The most potent antigen-presenting cells are dendritic cells (DCs) which can be described as sentinels of immunity [83]. However, Langerhans cells are susceptible to TBEV infection and may contribute to the spread of TBEV to uninfected cells at the same time [47].

The humoral immune response is crucial in controlling flaviviral infection and dissemination. The passive immunization by application of monoclonal and polyclonal antibodies protects mice against WNV [84], DENV [85], and JEV [86]. Moreover, mice lacking B lymphocytes are more vulnerable to lethal WNV infection [84]. Much of the humoral immune control is provided by neutralizing antibodies, which recognize epitopes located predominantly in the viral E glycoprotein. NS1-specific antibodies were also documented to prevent mice from flavivirus-induced disease in case of TBEV and DENV [87, 88]. On the other hand, the phenomenon of antibody-dependent enhancement (ADE) of infection was described for DENV [89, 90], thus the humoral immune response can also favour arboviral infection as a side effect.

In addition to host humoral immunity, the activation of cellular immunity is usually required for the clearance of established infection. Viral peptides, which are generated by either proteasome machinery (cytosolic antigens) or lysosomal pathway (internalized antigens), are translocated into the endoplasmic reticulum where they are loaded onto major histocompatibility complex class I or II (MHCI or II) molecules and transported to the cell surface to promote antigen-restricted recognition by CD8+ T lymphocytes (MHCI) or CD4+ T lymphocytes (MHCII) [91]. For example, mice that lacked CD8+ T cells were inflicted with more severe CNS damage and higher mortality rate, when infected by WNV [92]. Importance of CD8+ T cells was also demonstrated in case of DENV and JEV [93, 94]. CD4+ T cells were required for clearance of WNV from CNS in infected mice [95]. Surprisingly, differential targeting of viral components by CD4+ and CD8+ T cells was documented in case of DENV and TBEV. Whereas CD4+ are directed to recognize viral components that are also targeted by B cells (E, C and NS1) for both DENV and TBEV, CD8+ T cell epitopes preferentially target non-structural

proteins (NS3, NS5) in case of DENV [96, 97]. The complexity of flavivirus-adaptive immunity interactions is demonstrated by *in vivo* studies with TBEV, where activation of the cytotoxic T lymphocytes (CTLs) contributes to the disease pathogenesis [55, 98].

2.2.2 Innate immune response

Innate immune system acts as the first line of defence for sensing a viral infection. It includes the rapid recognition of pathogen-associated molecular patterns (PAMPs) in immune and non-immune cells by the pattern-recognition receptors (PRRs) and subsequent response including IFN signalling pathway, inflammatory cytokines, complement response, natural killer cells, apoptosis and autophagy. All these components play complementary roles limiting the viral replication and dissemination, as well as initiation of the adaptive immune response.

2.2.2.1 Natural killer cells

Natural killer (NK) cells are a class of lymphocytes that contain cytoplasmic granules filled with chemicals and enzymes that are toxic to the target cells. NK cells recognize and kill abnormal cells (e.g. cancer or virus-infected cells) *via* receptor-mediated granule exocytosis. Furthermore, a wide range of cytokines, including IFN-γ, is produced by NK cells [99]. Significant increase of NK cell number and their activation was detected in patients infected with DENV, TBEV, and YFV [100-102]. Transient activation of NK cells was observed even in WNV-infected mice [103], however, the depletion of murine NK cells did not alter morbidity or mortality in infected individuals [104].

2.2.2.2 Complement

The complement system includes more than 50 soluble and membrane-associated proteins that recognize exogenous, altered, or potentially harmful endogenous ligands. Activation of these proteins triggers several antiviral responses including opsonisation (marking of pathogen by specific molecules for phagocytosis), release of

anaphylotoxins (attracting leucocytes) or formation of the membrane attack complex, which lyses the infected cells. The complement cascade can be activated by one of the three distinct pathways – the alternative, the classical or the lectin pathway, depending on a specific recognition molecules [105]. In connection with flaviviral infections, complement system acts as one of the antiviral effector pathways, however, it can also contribute to the eliciting of the flaviviral pathogenic effect. The protective effect of the complement was described in the case of WNV and DENV [106, 107]. In addition, an interesting study of Mehlhop *et al.* demonstrated that complement protein C1q is a potent inhibitor of antibody-dependent enhancement in case of *in vitro* and *in vivo* DENV infection [108].

2.2.2.3 Interferons (IFNs)

Despite the innate response being enormously multifaceted, IFNs possess a central role and are responsible for inducing a cellular antiviral state, which plays a major role in limiting the early replication and spread of many viruses. Two key steps are required to trigger IFN-mediated antiviral state in infected cells: (1) PAMP recognition by PRRs, resulting in an activation of signalling cascade, which induces IFN expression, (2) expression of effector interferon-stimulated genes (ISGs) *via* the IFN-mediated pathway. Depending on the mechanism of action, cellular localization and type of the ligand, PRRs are divided into several groups: (1) Toll-like receptors (TLRs), (2) retinoic acid-inducible gene I (RIG-I)-like receptors (RLRs), (3) NOD-like receptors (NLRs), (4) C-type lectin receptors (CLRs), and AIM2-like receptors (ALRs). A particular virus may be sensed by several PRRs and, *vice versa*, particular PRR may sense several types of viruses [109, 110]. More details about selected PRRs are stated in Table 1.

Among other pathways being induced downstream after the activation of PRRs, expression of IFNs represents the crucial point of the innate immune response. An activated IFN signalling pathway eventually results in expression of hundreds of genes in order to elicit the antiviral state in infected (autocrine signalling) or neighbouring (paracrine signalling) cells. IFNs also possess potent immune-modulating activities, and thus serves

18

to regulate the responses of other parts of the innate immune system (CTLs and NK cells). The immune-modulating activities of IFNs were also described for adaptive immune system (dendritic cells, B cells and T cells). So far, three classes of IFNs have been described – type I, II, and III.

Table 1: List of PRRs known to play a role in virus detection in host cells (summarized from [109, 110]).

class	receptor	localization	ligand	downstream signalling pathway
TLRs	TLR2	cell surface	viral proteins	MyD88 --> MAPK/NF-κB
	TLR3	endosome	viral dsRNA	TRIF --> IRF3/IRF7/MAPK/NF-κB
	TLR4	cell surface	viral proteins	MyD88/TRIF --> IRF3/MAPK/NF-κB
	TLR7/8	endosome	viral ssRNA	MyD88 --> IRF7/MAPK/NF-κB
	TLR9	endosome	viral DNA	MyD88 --> IRF7/MAPK/NF-κB
RLRs	MDA5	cytosol	viral dsRNA	MAVS --> IRF3/IRF7
	RIG-I	cytosol	viral ssRNA/dsRNA	MAVS --> IRF3/IRF7
	LGP2	cytosol	viral RNA	enhances/inhibits other RLRs
NLRs	NLRP3	cytosol	viral proteins	forming inflammasome complex and maturation of IL-1β
	NOD2	cytosol	viral ssRNA	MAVS --> IRF3
ALRs	IFI16	cytosol/nucleus	viral DNA	STING --> NF-κB
	DAI	cytosol	viral DNA	STING --> NF-κB
	AIM12	cytosol	viral DNA	forming inflammasome complex and maturation of IL-1β
CLRs	DC-SIGN	cell surface	carbohydrates	phospholipase C --> Raf-1

Type I IFNs

The class of type I IFNs represents the largest group comprising of IFN-α, IFN-β, IFN-ε, IFN-κ, and IFN-ω. Out of these, IFN-α and IFN-β are considered to be the most important in the early response to viral infection, since they are almost ubiquitously expressed. Their importance in the case of flaviviral infections was well-documented by several studies. For instance, *in vitro* pre-treatment of cells by IFN-α/β substantially reduced viral replication in case of DENV and WNV [111, 112]. The role of IFN-β in preventing the viral infection of neuronal cells *in vitro* was shown for human granule cell neurons and cortical neurons, when IFN-β

19

pre-treatment resulted in inhibition of both, WNV and Saint Louis encephalitis virus (SLEV) [113]. More recently, IFN-α/β signalling was proved to be crucial in eliciting an antiviral state in murine astrocytes. Astrocytes derived from IFNAR$^{-/-}$ mice showed higher sensitivity to TBEV, JEV, WNV, and ZIKV in comparison to the wild-type [114]. *In vivo* experiments with knockout mice (IFNAR1$^{-/-}$ or IFN-β$^{-/-}$) supported the observations from *in vitro* experiments – defective type I IFN signalling resulted in rapid development of neurological symptoms and higher mortality upon LGTV and TBEV infections [115].

Receptor of type I IFNs is a heterodimer (IFNAR1 and IFNAR2 subunits) localized on the cell surface. Binding of IFN to the receptor activates receptor-associated tyrosine kinases JAK1-TYK2 resulting in the phosphorylation of STAT1 and STAT2. These proteins subsequently heterodimerize and bind to a third component, IRF9/p48, creating interferon-stimulated gene factor 3 complex (ISGF3), which is subsequently translocated into the nucleus and activates expression of various ISGs (Fig. 7) [116].

Type II IFNs

The class of type II IFNs includes IFN-γ, which was described to be produced in immune cells only. These include T lymphocytes, B lymphocytes, and various APCs including NK cells, dendritic cells, and macrophages [117]. IFN-γ was also shown to be an important player in the immune response against flaviviruses. The pre-treatment with IFN-γ resulted in reduced infection and replication rate of DENV *in vitro* [111]. In addition, lack of IFN-γ or impaired IFN-γ signalling lead to an increased vulnerability to lethal WNV infection in mice [118].

Receptor complex for IFN-γ is composed of two ligand-binding IFNGR1 subunits and two signal-transducing IFNGR2 subunits (Fig. 7). As in the case of type I IFNs, binding of IFN-γ to the receptor triggers the JAK-STAT signalling pathway. However, small differences in signal transduction were described – IFNGR utilizes JAK1-JAK2-TYK2 tyrosine kinases, which phosphorylates STAT1 to form a homodimer (GAF complex). GAF

is then translocated into the nucleus, where it activates expression of ISGs containing GAS sequence in their promoters [117].
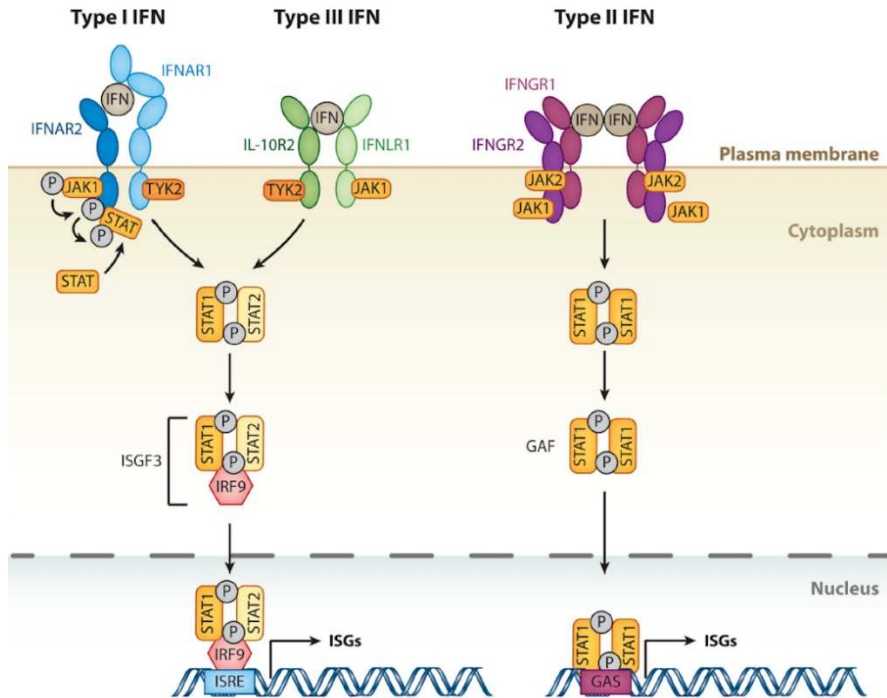
Figure 7: Signalling pathways for all types of IFNs (adapted from [119]).

Type III IFNs

Type III IFNs are the newest class of IFNs being identified in 2003 [120, 121]. Up to date, type III IFNs include IFN-λ, which is further divided into four subtypes (λ1-λ4). Type III IFN receptor is a heterodimer composed of IL10Rβ and IFNLR1/IL28Rα subunits. Although there are different receptors for type I and III IFNs, the downstream signalling utilizes the same pathway (Fig. 7). As a result of this shared downstream signalling cascade for both, type I and III IFNs, the spectrum of ISGs up-regulated upon IFN-λ stimulation overlaps strongly with that up-regulated upon IFN-α/β [122, 123]. However, a strong tissue specificity was described for IFN-λ/IFNLR expression in comparison to IFN-α/β/IFNAR in the study of Sommereyns *et al.*; in addition, cells of epithelial origin were

predominantly sensitive to IFN-λ stimulus in analysed tissues [124]. IFN-λ was also proven to control the infection of several flaviviruses. In more detail, IFN-λ restricted replication of DENV in epithelial cell line C-33A *via* up-regulation of OAS1 and Mx1 ISGs [125]. Furthermore, an interesting study of Lazear *et al.* documented that IFN-λ decreased the permeability of BBB *in vivo*, which resulted in a reduced WNV infection rate of brain tissue. Detailed *in vitro* experiments revealed the nature of this phenomenon: IFN-λ modulated the localization of tight junction proteins in microvascular endothelial cells [126]. IFN-λ was also shown to confer protection against ZIKV in the case of primary human trophoblasts (cells responsible for the formation of placenta) [127].

2.2.2.4 Interferon-stimulated genes

As already stated above, autocrine or paracrine IFN signalling results in an induction of expression of hundreds of genes (Fig. 8). The spectrum of ISGs being up-regulated strongly depends on the context, i.e. the type of IFN and the type of tissue. Depending on the function, several groups of ISGs could be distinguished: (1) ISGs with direct antiviral effect, (2) ISGs with positive regulatory effect, and (3) ISGs with negative regulatory effect. Among ISGs with positive regulatory effect belong many PRRs and IRFs, whose production leads to the sensitization of pathogen sensing in infected and also neighbouring cells thanks to the paracrine signalling effect of IFNs. The desensitization process is done *via* USP18 and SOCS proteins, which belong to the group of negative regulators of the IFN response [119].

ISGs with direct antiviral effect represent the most intriguing category with promising candidates for the treatment of flaviviral infections. An extensive number of studies describing the mechanisms and effects of particular ISGs has been published in the last decade. As type I IFN signalling represents the main effector pathway of the early innate immune response, the following text is focused on selected type I IFN-induced ISGs with direct antiviral effect.

PKR

One of the first ISGs to be linked with an antiviral response was the

22
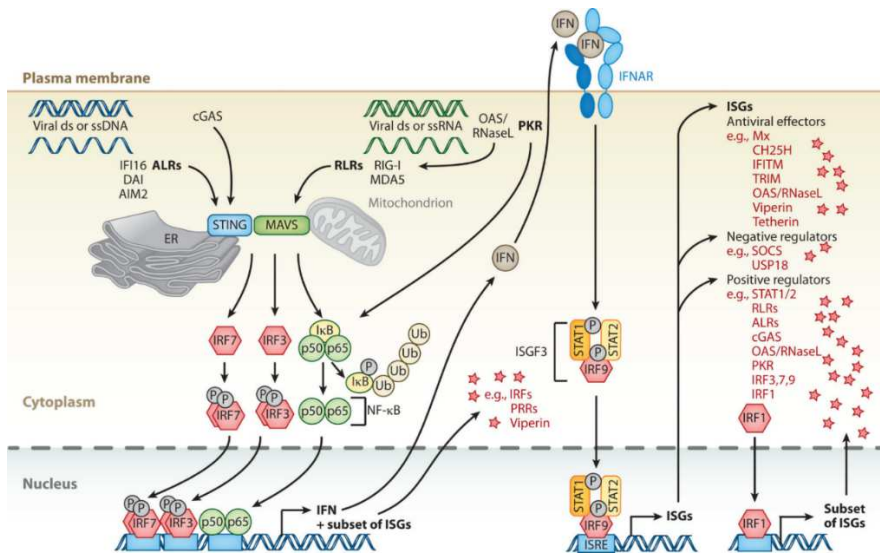
Figure 8: Signalling pathway of type I IFNs (adapted from [119]).

dsRNA-dependent Protein Kinase R (PKR). PKR is a serine/threonine kinase composed of an N-terminal regulatory domain that contains two dsRNA binding motifs and a C-terminal kinase domain [128, 129]. Under normal circumstances, PKR is maintained as an inactive monomer, and activation of PKR by dsRNA results in the formation of dimers that are stabilized by autophosphorylation at multiple residues [130]. PKR belongs to the family of stress-responsive kinases that regulate protein synthesis *via* phosphorylation of eIF2α translation initiation factor (PRK, PERK, GCN2, HRI) [131].

Basal levels of PKR are maintained in all tissues and type I and III IFN stimulation leads to PKR up-regulation [132]. Besides the translational arrest, PKR utilizes other mechanisms in order to antagonize viral replication including posttranscriptional regulation of IFN-β levels [133], activation of MDA5 signalling or induction of IFN production *via* MAVS [134].

Experiments with transgenic mice or mouse embryonic fibroblasts showed that PKR is crucial in protection against HCV [135], WNV [136], and vesicular stomatitis virus (VSV) [137]. Moreover, it was shown recently that DENV replication triggers autophosphorylation of PKR, however, no phosphorylation of eIF2α was observed. This striking

observation thus suggests a possible DENV-driven interference of PKR downstream signalling [138].

TRIM proteins

Tripartite motif (TRIM) proteins represent a large family of more than 80 genes with various functions including the regulation of innate immunity, transcription, apoptosis, autophagy, oncogenesis, etc. The "tripartite motif" name corresponds to the unique structure of TRIM proteins, which includes three conserved N-terminal domains: (1) a Really Interesting New Gene (RING) domain, (2) one or two zinc-finger domains called B-Boxes (B1/B2), and (3) a coiled-coil (CC) domain, all together referred as RBBC. The structural diversity of TRIM proteins is further enlarged by the occurrence of various C-terminal domains and their combinations. The identified C-terminal domains include COS domain, fibronectin type III repeat, PRY domain, SPRY domain, acid-rich region, filamin-type IG domain, NHL domain, PHD domain, bromodomain, Meprin and TRAF-homology domain, ADP-ribosylation factor family domain, and transmembrane region [139, 140].

From the functional point of view most of the TRIM proteins are considered to be E3 ubiquitin ligases thanks to the presence of the RING domain. Indeed, the majority of the described antiviral effects by TRIM proteins in the case of flaviviral infections is realized *via* the RING domain. In more detail, TRIM69 inhibits DENV replication by ubiquitination and subsequent degradation of viral NS3 protein [141]. A similar scenario was described in the case of TRIM79α and TBEV, when TRIM79α targets the viral NS5 polymerase for degradation [142]. Furthermore, TRIM56 inhibits ZIKV replication *via* combination of two mechanisms: RING-mediated E3 ubiquitin ligase activity is needed as well as RNA binding activity *via* the C-terminal NHL-like domain [143]. On the other hand, JEV-induced expression of TRIM21 resulted in decreased production of IFN-β in human microglial cells, thus suggesting a possible strategy of JEV how to suppress the type I interferon response during the early course of infection [144].

IFIT proteins

Interferon-induced proteins with tetratricopeptide repeats (IFITs) represent a small group of ISGs capable of binding to various cellular and viral RNAs and proteins. So far, four IFIT family members have been characterized in humans (*IFIT1*, *IFIT2*, *IFIT3*, *IFIT5*). The tetratricopeptide repeat (TPR) motif comprises 34 amino acids and forms the HTH (helix-turn-helix) structural motif, which in tandem repetitions forms the TPR domain super structure serving as a protein-protein interaction module. The number of TPRs differs among IFITs and ranges from 4 to 8 [145, 146]. Surprisingly, structural studies revealed that the TPR domain selectively binds also specific RNAs [147, 148]. Moreover, C-terminal part of IFIT1 was shown to be necessary for RNA binding as well [149].

Currently described antiviral effects of IFIT proteins include several mechanisms. The first mechanism is based on the protein-protein interactions, when IFIT1 and IFIT2 restrict host translation *via* binding to the eIF3 complex [150, 151]. Next mechanism involves direct binding of IFIT1 to viral proteins in order to inhibit their function. This phenomenon was observed only in the case of human papilloma virus [152]. The last mechanism exploits the RNA-binding capabilities of IFIT proteins. IFIT1 protein is able to recognize 5'-triphosphorylated RNA (feature of many viral RNAs) and in co-operation with IFIT2 and IFIT3 prevents its utilization as a template for translation [153, 154]. Furthermore, IFIT1 also recognizes N1 and N2 ribose 2'-O-methylations [155, 156]. The recognition of 2'-O-unmethylated viral genomic RNA is the mechanism behind the antiviral effect of IFIT1 protein against JEV [157] and WNV [158]. In the case of WNV, *in vivo* experiments documented an important role in restricting the infection also for IFIT2 [159].

IFITM proteins

The family of IFITM (<u>i</u>nter<u>f</u>eron-<u>i</u>nduced <u>t</u>rans<u>m</u>embrane) proteins includes five membrane-bound genes (*IFITM1*, *IFITM2*, *IFITM3*, *IFITM5*, *IFITM10*), however, only *IFITM1-3* are considered as ISGs. Interestingly, *IFITM5* was not shown to be IFN-inducible and is expressed only in osteoblasts. Based on their structure, IFITMs belong to the CD225 protein superfamily and comprise of 5 structural domains: (1) N-terminal domain,

(2) intramembrane/transmembrane domain 1, (3) conserved intracellular loop, (4) intramembrane/transmembrane domain 2, and (5) C-terminal domain. The canonical CD225 domain spans across intramembrane/transmembrane domain 1 and conserved intracellular loop domain. Various post-translational modifications were documented for IFITM proteins as well, including phosphorylation, ubiquitination, and S-palmitoylation. The suggested mechanism of IFITMs antiviral effect arises from their transmembrane localization – the proposed model includes the interference with viral fusion on the host cytoplasmic or endolysosomal membranes in the case of enveloped viruses [160, 161].

Since flaviviruses belong to the group of enveloped viruses, it is not surprising that IFITMs were proved to inhibit some of them. In the case of DENV and WNV, IFITM3 was described to decrease the infection rate [162]. The restricting role of IFITM3 in the case of DENV infection was further supported by the study of Jiang *et al.*; in addition to IFITM3, IFITM2 was also shown to be a potent inhibitor of DENV infection [163]. Recently, Savidis *et al.* documented that IFITM1 and IFITM3 interferes also with ZIKV infection. In more detail, IFITM3 was described to inhibit early stages of ZIKV replication process [164]. Moreover, an interesting localization of IFITM3 in exosomes was documented during DENV infection. The IFITM3-containing exosomes were shown to fuse with cell membranes of other cells, thus transmitting antiviral agent *via* extracellular pathway [165].

ISG15

ISG15 is a 15 kDa ubiquitin-like protein, which has been described as one of the most highly induced ISGs. The structure of ISG15 is characteristic by two ubiquitin-like domains with the C-terminal LRLRGG motif, which is necessary for the conjugation reaction termed ISGylation [166-168]. ISGylation utilizes a three-step enzymatic mechanism similar to ubiquitination: (1) the activating E1 enzyme UBE1L forms an ATP-dependent thioester bond with ISG15, (2) activated ISG15 is then transferred to the conjugating E2 enzyme UBCH8; (3) finally, E3 ligases (ARIH1/TRIM25/HERC5) transfer ISG15 to lysine residues on target proteins. As for ubiquitylation, ISGylation is reversible due to the specific removal of ISG15 from conjugated proteins by the deconjugating enzyme

USP18. Apart ISGylation, ISG15 was detected in an unconjugated form as an extra- and intracellular protein. ISG15 thus represents an ISG with a complex range of functions including modulation of immune response, regulation of protein stability and translation, or direct inhibition of viral replication [169].

According to mass spectrometry data, hundreds of proteins were identified to be possibly ISGylated [170, 171]. ISGylation was also documented in case of viral proteins [172]. Thanks to the wide variety of ISGylation targets the full image of ISGylation effects is still incomplete. However, plenty of interesting effects have been already described. For example, ISGylation of USP18 plays a crucial role in desensitizing the type I IFN pathway [173], whereas ISGylation of TSG101 restricts release of influenza A virus (IAV) [174]. Several studies have also provided evidence that ISG15 plays a key role in the host antiviral response to flaviviruses. ISG15 was shown to inhibit replication of JEV [175], DENV and WNV [176]. On the other hand, ISG15 functions also as a proviral factor, as it is necessary for HCV replication cycle [177].

OAS/RNase L system and OASL

Family of IFN-inducible oligoadenylate synthethases (OASs) is known to co-operate with the cellular RNase L, thus creating a unique system of antiviral defence. The human OAS family consists of three isoforms – OAS1, OAS2, and OAS3. All three isoforms are active enzymes synthesizing 2'-5'-linked oligoadenylates *via* the OAS domain, which activate the cellular RNase L resulting in general degradation of ssRNA. The produced short RNAs serve then for induction of IFN-β expression via RLRs [178]. Activation of RNase L also leads to the general inhibition of protein production *via* digestion of Y-RNAs and tRNAs [179], but also specific mRNAs [180]. OAS1 can occur in four isoforms (42, 44, 46, and 48 kDa), and OAS2 produces four alternatively spliced transcripts that encode two proteins (69 and 71 kDa). OAS3 encodes a single transcript that produces a 100 kDa protein. Tandem repeat of two and three OAS domains is present in OAS2 and OAS3, respectively. OAS1 contains only one OAS domain [181, 182].

The importance of OAS1 in antiviral immunity was highlighted on the example of WNV infection, when OAS1 was shown to be activated by WNV stem loops located in 5' UTR [183] and mutations in the OAS1 gene lead to increased susceptibility to WNV infection [184]. In addition, DENV replication was shown to be blocked by OAS1 p42, OAS1 p49, and OAS3 isoforms [185].

Another example of recently identified ISG is the OAS-like protein (OASL), which is a member of the OAS family. The *OASL* gene encodes a two-domain protein, where the N-terminal OAS-like domain is fused to a C-terminal part containing two tandem ubiquitin-like domains [186]. Unlike other members of the OAS family, OASL does not possess the 2-5A activity [187]. Nevertheless, OASL was proved to be a potent antiviral ISG in the case of HCV infection, when both structural domains were found to be necessary [188, 189]. Surprisingly, OASL did not restrict DENV replication in A549 and HEK293T cells [185]. So far, three spliced transcripts have been identified in humans – OASL a, OASL b, and OASL d [190].

Viperin

One of the most currently studied ISGs is viperin (<u>v</u>irus <u>i</u>nhibitory <u>p</u>rotein, <u>e</u>ndoplasmic <u>r</u>eticulum-associated, <u>in</u>terferon-inducible) coded by *RSAD2* gene. This antiviral protein was first identified as an ISG expressed in fibroblasts upon infection with human cytomegalovirus (HCMV) [191]. Viperin is a 42 kDa protein composed of three structural/functional domains: (1) N-terminal domain, which contains an amphipathic α-helix and a leucine zipper motif, responsible for anchoring viperin in the ER membrane e (2) a highly conserved radical SAM domain forming a [4Fe-4S] cluster, and (3) a C-terminal domain that also shows high similarity across different species [192, 193].

Various mechanisms of an antiviral effect have been described for viperin, suggesting a virus- and cell-specific mode of action. In the case of HCV, viperin C-terminus was shown to interact with the viral NS5A protein [194] and to deplete the pro-viral host cell factor hVAP-33 [195]. Helbig *et al.* and Wang *et al.* further showed that viperin inhibits virus release by budding *via* modification of the lipid environment within the cell or at the

cell surface [194, 196]. Multiple mechanisms of viperin antiviral effect in the case of TBEV were described. First, SAM domain was shown to be crucial in an antiviral response against TBEV in HEK293 cells, where viperin inhibited the production of viral genomic RNA [197]. In addition, viperin-induced secretion of uninfectious TBEV particles was suggested as another mechanism of antiviral action [198]. The most recent study by Panayiotou *et al.* documented viperin-mediated degradation of viral NS3 protein in the case of TBEV and ZIKV [199]. An interesting study by Lindqvist *et al.* described more about the specificity of viperin recruitment against TBEV. Viperin antiviral effect was restricted only to specific CNS regions and cell types [200]. Except TBEV and ZIKV, other flaviviruses were shown to be restricted by viperin as well, including WNV and DENV [163].

As was mentioned above, viperin expression is stimulated by IFN signalling, however, there are viruses, which can induce viperin expression by an IFN-independent way. These include JEV [201], HCMV [202], and Vesicular stomatitis virus (VSV) [203]. An interesting combination of IFN-dependent and independent expression of viperin was described in the study of Dixit *et al.* [204]: upon reovirus or IAV infection, rapid and transient IFN-independent expression of viperin resulted in a short-term protection against the invading virus, whereas delayed IFN-dependent viperin expression amplified and stabilized the antiviral response afterwards.

As in the case of ISG15, viperin can act as a proviral factor, for example it is translocated to mitochondria during HCMV infection where it disrupts host cellular metabolism via reduction of ATP production [205].

2.2.3 Unfolded protein response

Apart from the induction of host immune system, flaviviral infection also triggers other signalling pathways, which contribute to the complexity of host response network. Documented enormous rearrangements of host ER membrane system accompanied by high levels of viral proteins and RNA during flaviviral replication play a significant role in the induction of ER stress [76-79]. Upon sensing the ER stress, the unfolded protein response (UPR) pathway is activated, resulting either in the recovery of

ER function or apoptosis. The UPR pathway employs various mechanisms, which serve to restore the ER homeostasis, including enhancement of protein-folding capacity, attenuation of mRNA production, and stimulation of the ER-associated degradation (ERAD) of misfolded proteins. Additionally, UPR activation was also shown to increase the rate of autophagy, stress granule formation and potentiation of antiviral inflammatory responses [206, 207].

Depending on the sensors of ER stress, three distinct arms of UPR have been described – (a) inositol-requiring protein 1 (IRE1) pathway, (b) PKR-like endoplasmic reticulum kinase (PERK) pathway, and (c) activating transcription factor 6 (ATF6) pathway (Fig. 9). Each of the UPR arms responds to both, unique and common stimuli, by either up-regulation of specific UPR target genes or by induction/inhibition of particular processes such as translation, autophagy, protein folding, lipid synthesis, apoptosis, etc. [206, 207].

Up to date, activation of UPR pathway was observed for DENV [138, 208], JEV [209], TBEV [210, 211], WNV [211, 212], and ZIKV [213, 214] infections. However, some of these studies also showed that flaviviruses are able to interfere with UPR signalling or even that UPR can act in a proviral way. For instance, IRE1-mediated UPR activation was shown to be essential for TBEV replication [210]. Furthermore, DENV and ZIKV were shown to inhibit formation of stress granules and phosphorylation of eIF2α [138, 213].
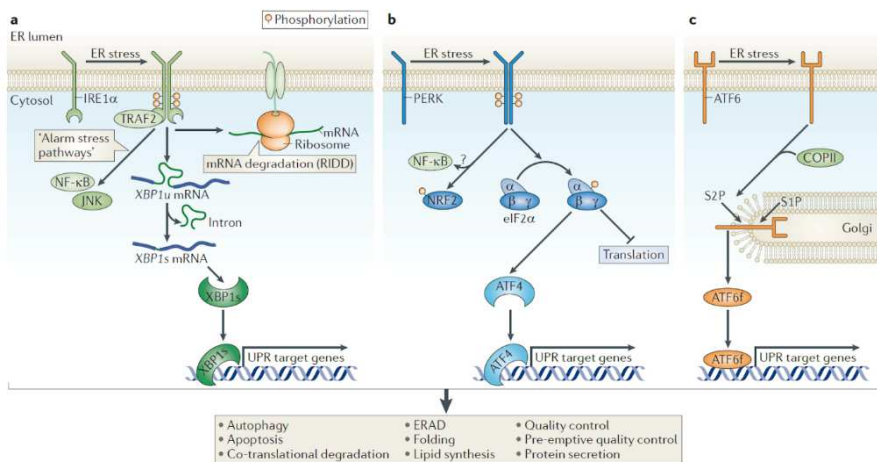

Figure 9: Schematic overview of UPR signalling pathway (adapted from [207]).

2.3 Viral evasion strategies of host immune system

The co-evolution of the host and pathogen led to creation of complex and sophisticated defence mechanisms, which should neutralize the invading pathogen in the host organism. As a countermeasure, pathogens, including viruses, employ a vast variety of mechanisms for evading such host defensive responses. Flaviviruses represent no exception to this phenomenon and multiple intriguing evasion strategies have been already described. Most commonly, the non-structural proteins are responsible for the interference with the host immune response. However, it has been reported that particular parts of the viral RNA and structural proteins can also act as important modulators of the host immune response. In order to get more insight into this complex interaction network, the following chapters will describe the present knowledge about the flaviviral evasion mechanisms including both types of effector molecules – viral RNA and viral proteins.

In addition, it is worth mentioning that many of the described evasion mechanisms are, in fact, part of the viral life cycle itself. The formation of VPs and replication factories in the host ER prevents the virus to be sensed by host PRRs in the early stages of infection [53, 76, 77, 79-81]. Moreover, the membrane-associated replication of flaviviruses also results in an altered lipid production and distribution. For instance, WNV-driven increase in cholesterol production and its redistribution in host membrane/protein system resulted in decreased responsiveness to IFN [215]. Another interesting observation documents that TBEV-induced autophagy in human neurons favours viral replication [79].

2.3.1 Viral RNA

Cellular mRNAs in eukaryotes have been described to be chemically tagged ("capped") at the initial stage of transcription by the addition of 7-methylguanosine to the 5' end. The cap plays an important role in the stability of mRNA and also in the self-discrimination from foreign RNAs. The capping process starts by the dissociation of γ-phosphate from the 5' nucleotide (RNA triphosphatase), then, 7-methylguanosine is added *via*

5'-5' triphosphate bond (guanylyltransferase). Eventually N7-guanine methyltransferase completes the process by addition of methyl to N^7 (cap0). Higher eukaryotes further employ 2'-O-methyltransferases for the generation of cap1 and cap2 types (Fig. 10) [216].

It was already mentioned that 2'-O-methylation of cellular mRNA plays an important role in IFIT-mediated antiviral response. Remarkably, flaviviruses are able to counteract this immune response by capping the viral genomic RNA on their own. Among other enzymatic functions, the viral NS3 protein acts as an RNA triphosphatase. In addition, the viral NS5 protein serves as a polymerase, methyltransferase, and guanylyltransferase. Therefore, the combination of NS3 and NS5 enzymatic activities results in the generation of capped transcripts. Truly, DENV and WNV mutants lacking the NS5 methyltransferase activity were strongly attenuated by IFITs [217, 218].
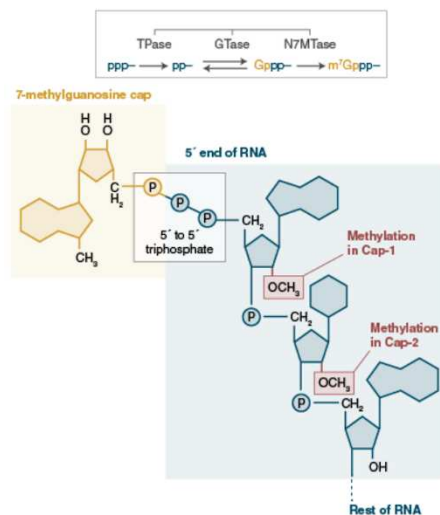
Figure 10: Schematic overview of the capping enzymatic reaction together with depicted cap types and their structures (adapted from NEB (https://international.neb.com/products/m0366-mrna-cap2-o-methyltransferase#Product%20Information).

A specific 0.3–0.8 kb long non-coding RNA, termed sfRNA, is generated during the flaviviral infection (see Chapter 2.1.3.). Surprisingly, sfRNA seems to play an important role in evading the host immune system. For instance, JEV sfRNA was suggested to inhibit IFN production by blocking the phosphorylation of IRF3 [73], whereas DENV and WNV sfRNA was

shown to interfere with RNAi machinery in the infected cells [74]. The broad variety of sfRNA functions is further supported by the study of Bidet *et al.* where DENV sfRNA, for a change, binds to three RNA-binding proteins involved in mRNA stability regulation, thus preventing the translation of selected ISGs with direct antiviral effect [219]. A similar finding was documented in the study of Manokaran *et al.*, where sfRNA was observed to bind TRIM25 and prevent its deubiquitination required for an activation of RIG-I signalling [220]. An incredible variety of sfRNA modulation functions was further enlarged by the study of Göertz *et al.* – WNV sfRNA was proved to modulate the virus transmissibility by *C. pipiens* mosquitoes [221].

2.3.2 Viral proteins

As stated in the beginning of this chapter, the non-structural proteins are considered to be mostly responsible for the interference with the host antiviral response. However, later findings point towards the key antagonistic properties of structural proteins as well. For instance, an elegant study of Arjona *et al.* described that WNV E protein blocks the production of TNF-α, IFN-β, and IL-6 cytokines *via* binding to RIPK1 (Receptor Interacting Serine/Threonine Kinase 1), which results in the inhibition of RIG-I signalling. However, a specific glycosylation pattern is required for this unique feature of WNV E [222]. In addition to E protein, an alternative role for C protein during the infection was demonstrated as well. Binding of DENV or WNV C protein to Sec3p protein was shown to trigger its proteasome-driven degradation [223]. The decrease of Sec3p levels resulted in higher rate of viral replication/translation since Sec3p was shown to sequester EF1α translation elongation factor as a host response to the infection [224]. Interestingly, YFV C protein was documented to suppress RNA silencing machinery in *A. aegypti* mosquitoes [225].

In the case of flaviviral non-structural proteins, almost all of them were described to possess a wide range of activities, which interfere with the host antiviral responses. It is not surprising that most of these target IFN and PRR signalling. For example, ZIKV NS1 protein was shown to interfere with RIG-I signalling *via* binding to its downstream signal kinase,

TBK1 (TANK Binding Kinase 1). NS1-induced decrease of TBK1 activity due to its impaired phosphorylation resulted in the inhibition of IFN-β expression [226]. The complexity of the NS1 interactions is further developed by an intriguing finding that the extracellularly secreted DENV NS1 negatively affects endothelial permeability, which results in a vascular leakage. This phenomenon was shown to strongly enhance the severity of DENV infection [227].

For NS2A protein, inhibition of IFN-β promoter activity was documented in case of WNV and ZIKV [226, 228]. Similar to ZIKV NS1, DENV NS2B/3 protease complex interferes with the RIG-I downstream signalling by binding to IκB kinase ε (IKKε) and preventing its functionality. Non-functional IKKε does not phosphorylate IRF3, thus preventing its nuclear translocation and activation of IFN expression [229]. Inhibition of IFN-β production and signalling was documented for DENV NS4A and NS4B proteins as well [230]. In this case, NS4A/B proteins were shown to inhibit RIG-I/TBK1 signalling as in the case of ZIKV NS1. Interestingly, NS2A protein was shown to contribute to the NS4B-induced inhibition of TBK1 and IRF3 phosphorylation [231].

So far, NS5 protein seems to be the most potent effector of viral fight against the host innate immune system. Its role in restricting the IFN signalling was described in case of many flaviviruses, including DENV, KFDV, TBEV, WNV, and ZIKV. The mechanism of inhibition includes binding to type I IFN receptors (TBEV) or NS5-directed degradation of STAT proteins (DENV) [226, 232-235].

3 Aims and objectives

The presented Ph.D. thesis focuses on the host-virus interactions during flaviviral infection in cells of neural origin. In particular, the innate immune response of TBEV-infected cells was studied together with the roles of specific IFNs and ISGs. Furthermore, an additional aim was the identification of possible viral inhibitors of the host innate immunity.

Specific aims:

1. To analyse the role of viperin and OASL ISGs during TBEV infection in human neural cells.
2. To describe the response of host innate immune system in reaction to TBEV infection.
3. To characterize possible viral counter measurements against the host innate immune system.

4 Research papers

Černý, J., **Selinger, M.**, Palus, M., Vavrušková, Z., Tykalová, H., Bell-Sakyi, L., Štěrba, J., Grubhoffer, L., Růžek, D., 2016: Expression of a second open reading frame present in the genome of tick-borne encephalitis virus strain Neudoerfl is not detectable in infected cells. Virus Genes 52(3): 309-316. DOI: 10.1007/s11262-015-1273-y (IF = 1.537)

CrossMark

Expression of a second open reading frame present in the genome of tick-borne encephalitis virus strain Neudoerfl is not detectable in infected cells

Jiří Černý[1,2,3] · Martin Selinger[1,2] · Martin Palus[1,2,3] · Zuzana Vavrušková[1] ·
Hana Tykalová[1,2] · Lesley Bell-Sakyi[4] · Ján Štěrba[1,2] · Libor Grubhoffer[1,2] ·
Daniel Růžek[1,3]

Abstract A short upstream open reading frame (uORF) was recently identified in the 5′ untranslated region of some tick-borne encephalitis virus (TBEV) strains. However, it is not known if the peptide encoded by TBEV uORF (TuORF) is expressed in infected cells. Here we show that TuORF forms three phylogenetically separated clades which are typical of European, Siberian, and Far-Eastern TBEV subtypes. Analysis of selection pressure acting on the TuORF area showed that it is under positive selection pressure. Theoretically, TuORF may code for a short hydrophobic peptide embedded in a biological membrane. However, expression of TuORF was detectable neither by immunoblotting in tick and mammalian cell lines infected with TBEV nor by immunofluorescence in TBEV-infected mammalian cell lines. These results support the idea that TuORF is not expressed in TBEV-infected cell or expressed in undetectably low concentrations. Therefore we can assume that TuORF has either minor or no biological role in the TBEV life cycle.

Keywords TBEV · uORF · TuORF · Immunoblotting · Immunofluorescence

Edited by Hartmut Hengel.

✉ Jiří Černý
cerny@paru.cas.cz

1   Institute of Parasitology, Biology Centre of the Czech Academy of Sciences, Branišovská 31, 370 05 České Budějovice, Czech Republic

2   Faculty of Science, University of South Bohemia in České Budějovice, Branišovská 31, 370 05 České Budějovice, Czech Republic

3   Veterinary Research Institute, Hudcova 296/70, 621 00 Brno, Czech Republic

4   The Pirbright Institute, Ash Road, Pirbright, Woking, Surrey GU24 0NF, UK

Introduction

Tick-borne encephalitis virus (TBEV), the causative agent of tick-borne encephalitis (TBE), is a typical representative of the genus *Flavivirus*, family *Flaviviridae* [1, 2]. It is endemic in most of Central and Eastern Europe and North Asia [3] where it is the most medically important flavivirus [4]. Despite the availability of effective vaccination in endemic regions, TBEV infects thousands of people annually. Many of them develop clinical manifestations of TBE, often followed by permanent decrease in their life quality. TBEV mortality varies according to the TBEV subtype [4].

The TBEV genomic RNA, which is approximately 11,000 nt long, serves also as viral mRNA. It contains a single open reading frame (ORF) encoding one polyprotein. Translation of this ORF is initiated by a classical cap-dependent scanning mechanism [5]. The polyprotein is co- and post-translationally cleaved into three structural (C, ,M and E) and seven nonstructural (NS1, NS2A, NS2B, NS3, NS4A, NS4B, and NS5) proteins [6]. Apart from the major proteins, some flaviviruses such as Japanese encephalitis virus (JEV) and West Nile virus (WNV) produce minor proteins and peptides. Each minor protein is usually specific only for a narrow group of closely related flaviviruses. NS1′ produced by JEV [7, 8] and WARF4 produced by WNV [9, 10] are typical examples of such flaviviral minor proteins. Both these minor proteins are

⊘ Springer

encoded by alternative open reading frames and produced via a ribosome frame-shifting process [11, 12]. While the role of WARF4 is unknown, JEV NS1′ plays an important role in virus–host interaction, especially in virus neuroinvasiveness [8, 13] and JEV genomic RNA replication [14].

The presence of a short upstream open reading frame (uORF) in the 5′ untranslated region (UTR) of some TBEV strains has been reported [15]. Expression and functional importance of this second ORF (here called TuORF) remain unknown. In the present study, we investigated the expression of the hypothetical TuORF-encoded peptide in mammalian and tick cells by Western blotting and indirect immunofluorescence.

Methods

TBEV strains, cell lines, synthetic TuORF peptide, and anti-TuORF antibodies

Low-passage TBEV strain Neudoerfl (4th passage) (kindly provided by F. X. Heinz) and the strain Hypr (unknown passage history) were used in this study. TuORF presence and absence in TBEV strains Neudoerfl and Hypr, respectively, were verified by sequencing. Human cell lines of neural origin comprising neuroblastoma (UKF-NB-4), medulloblastoma (DAOY), and glioblastoma cells [16] and the *Ixodes ricinus* tick cell line IRE/CTVM19 [17] were used. A synthetic version of the TuORF peptide (sequence MRLLRTALAAVGLKKKC) and anti-TuORF protein A-purified mouse and rabbit polyclonal antibodies were produced by GenScript (USA). Because of high hydrophobicity, the most hydrophilic part of the peptide was synthesized together with an additional hydrophilic tail (KKC) in order to obtain sufficient yields of the artificial peptide.

Bioinformatics characterization of TBEV 5′ UTR and TuORF peptide

One hundred closest homologs of the TBEV strain Neudoerfl 5′ UTR were identified in GenBank using the blastn algorithm [18]. TBEV strains containing uORF were manually selected and classified into appropriate TBEV subtypes. Alignment of selected 5′ UTRs was constructed using ClustalX [19]. Protein sequences of hypothetical TuORF peptides were deduced from nucleotide sequences using the ExPASy—Translate tool [20].

Distant homologs of the TBEV TuORF peptide were sought using HHPred [21], HHblits [22], and Psi-blast algorithms [23]. Basic biophysical characteristics of the TuORF peptide from TBEV strain Neudoerfl were predicted using ProtParam [24]. TuORF peptide secondary structure was predicted using Jpred [25]. TuORF peptide

position in the cell membrane was predicted by TMpred [26].

Phylogenetic analysis and selective constraint calculation

Phylogenetic analysis of TuORF evolution was carried out using MEGA6 [27]. Protein and nucleic acid sequence alignments were processed by the neighbor-joining method using 1000 bootstrap replicates.

To calculate selective constraint, codon-based sequence alignment of TuORF was constructed on the GUIDANCE server [28, 29], using the implemented ClustalW algorithm [19]. The dN and dS difference was calculated in MEGA6 [27]. Analyses were conducted using the Nei-Gojobori method [30]. The analysis involved 17 nucleotide sequences. The variance of the difference was computed using 1000 bootstrap replicates. All ambiguous positions were removed for each sequence pair. There were a total of 29 positions in the final dataset. Wilcoxon tests were used to assess the significance of linked and unlinked synonymous and nonsynonymous scores, respectively.

Western blot assay

Mammalian and tick cell lines were infected with TBEV strain Neudoerfl at a multiplicity of infection (MOI) of 10. Virus adsorption was carried out for 1 h. Cells were harvested and lysed at several time points post infection (3, 6, 12, 18, 24, and 48 h in the case of mammalian cell lines, and 24, 92, 168, and 336 h in case of the tick cell line). Equal amounts of whole cell proteins were separated by Tricine-SDS-PAGE [31] and transferred to nitrocellulose membranes (0.2 μm porosity, Bio-Rad). Transferred proteins were labeled with primary mouse or rabbit polyclonal anti-TuORF antibodies (GenScript, USA). Both primary antibodies were diluted 1:200 in a 5 % skimmed milk powder in PBS (5 % milk). Subsequently, primary antibodies were detected by goat anti-rabbit secondary antibody conjugated with alkaline phosphatase (Vector Laboratories, USA) diluted 1:1000 in 5 % milk and tertiary horse anti-goat antibody conjugated with alkaline phosphatase (Vector Laboratories). Labeled proteins were visualized by chemiluminescence assay using CDPP-Star Reagent (NewEngland Bioloabs, USA).

Immunofluorescence staining

Neuroblastoma cells were infected with TBEV strains Neudoerfl and Hypr at an MOI of either 1 or 10. Virus adsorption was carried out for 1 h. At several time points post infection (12, 24, 48, and 72 h), cells were fixed in 4 % paraformaldehyde in PBS for 15 min, rinsed in PBS and

permeabilized with 0.1 % Triton X-100 in PBS for 5 min. Fixed cells were treated with PBS containing 50 mM NH$_4$Cl and a 1 % solution of bovine serum albumin (BSA) to block the formaldehyde autofluorescence. Further, cells were blocked with 3 % BSA dissolved in PBS and labeled with either mouse or rabbit polyclonal anti-TuORF antibody (GenScript) and with chicken polyclonal anti-NS3 antibody (reactive with TBEV NS3 protein, kindly provided by M. Bloom) [32]. After washing in PBS, the cells were labeled with goat anti-rabbit and goat anti-chicken secondary antibodies conjugated with DyLight 594 and DyLight488, respectively (Vector Laboratories). Subsequently, the cells were mounted in Vectashield mounting medium (Vector Laboratories). Examination was done on an Olympus BX-51 fluorescence microscope equipped with an Olympus DP-70 CCD camera.

Results

An upstream ORF is present in the 5′ UTR of numerous (but not all) TBEV strains as well as in the 5′ UTR of some other flaviviruses

A TuORF was identified in 43 of 100 tested TBEV strains. TuORF was present in strains representative of all TBEV subtypes (European, Siberian, and Far Eastern—Supplementary Table 1). The length of the TuORF varied between 36 and 93 nt; correspondingly, the length of coded peptides varied between 13 and 31 amino acid residues (Fig. 1). The modal length of the hypothetical TuORF peptide in European subtype TBEV strains was 23 amino acid residues. The most frequently seen length of the TuORF peptide in Siberian subtype TBEV strains was 21 amino acid residues. The longest TuORF peptide was in Far-Eastern TBEV strains where it is up to 31 amino acid residues in length. The N-terminal part of the TuORF peptide is conserved while its C-terminal part accommodates many substitutions typical for either European or Asian TBEV subtypes (Fig. 1b).

Among other tick-borne flaviviruses, uORFs were found in all 5′ UTR sequences of Langat virus (LGTV) (AF2534 19.1, AF253420.1, EU790644.1), Kama virus (KAMV) (NC_023439.1, KF815940.1), and Karshi virus (KARV) (DQ462443.1) available in GenBank (Supplementary Fig. 1). LANV and KAMV uORFs were, respectively, 339 and 51 nt long and they exceeded the 5′ UTR continuing also into the main ORF. In KARV, the initiating AUG codon was immediately followed by a UAG amber stop codon. Among mosquito-borne flaviviruses, the uORF was detected only in St. Louis encephalitis virus (DQ525916.1) (Supplementary Fig. 1). Sequences of these uORFs as well as the sequences of the possibly encoded peptides are

unrelated to TuORF. Sequences of other screened tick- and mosquito-borne flaviviruses did not contain any uORF (a complete list of flaviviruses that do or do not contain a uORF in their 5′ UTR is shown in Supplementary Table 2).

Evolutionary history of TuORF

Reconstruction of its evolutionary history and determination of any selection pressure would indicate if the TuORF peptide has a molecular function or whether it is only a free rider in the TBEV genome.

First we reconstructed phylogenetic relationships among the TuORFs of the different TBEV strains. Nucleic acid- and protein-based analysis revealed existence of three TuORF groups corresponding to the European, Siberian, and Far-Eastern TBEV strains (Supplementary Fig. 2). Only the position of the European strain Ek-328 in the phylogenetic tree is uncertain, possibly due to its origin. It was created by multiple passaging of TBEV in mice, which may have led to the accumulation of multiple mutations [33].

To see if the uORF coding for the TuORF peptide is under selection pressure, we compared the proportion of nonsynonymous (dN) and synonymous (dS) substitutions appearing in the TuORF of different TBEV strains. A dN higher than dS 1 implies positive selection, while a dN lower than dS 1 indicates negative (purifying) selection. In the case of TuORF, the overall average of dN and dS shows that the number of nonsynonymous mutations is significantly higher than the number of synonymous mutations which shows that TuORF is under positive selection pressure (Table 1). Nevertheless, this trend is only poorly or not at all visible in pairwise analyses or in overall analyses done on data subsets containing only individual TBEV subtypes (Supplementary Table 3).

Bioinformatics characterization of the putative TuORF peptide

The putative TuORF peptide is a highly hydrophobic peptide. According to in silico prediction, TuORF should form a single helix embedded into a membrane with its N-terminus protruding outside (Supplementary Table 4) possibly into the lumen of the endoplasmic reticulum. No TuORF peptide homologs were found among any other protein sequences in GenBank.

The TuORF peptide was not detected in TBEV-infected cells by immunoblotting

To test TuORF peptide expression in TBEV-infected cells, we infected three human neural cell lines and one tick cell line with TBEV Neudoerfl strain as described in Methods. Neither human nor tick cells were positive for TuORF

(A)

TBEV 5´UTR, strain Neudoerfl

```
001   AGATTTTCTT GCACGTGCA TGCGTTTGCT TCGGACAGCA TTAGCAGCGG TTGGTTTGAA AGAGATATTC TTTTGTTTCT ACCAGTCGTG   090
091   AACGTGTTGA GAAAAAGAC AGCTTAGGAG AACAAGAGCT GGGGATG          137
```

(B)

European TBEV strains:

```
Neu       ATG CGT TTG CTT CGG ACA GCA TTA GCA GCG GTT GGT TTG AAA GAG ATA TTC TTT TGT TTC TAC CAG TCG --- --- --- --- --- --- --- --- ---
KrM 93    ATG CGT TTG CTT CGG ACA GCA TTA GCA GCG GTT GGT TTG AAA GAG ATA TTC TTT TGT TTT TGC CAG TCG --- --- --- --- --- --- --- --- ---
AS33      ATG CGT TTG CTT CGG ACA GCA TTA GCA GCG GTT GGT TTG AAA GAG ATA TTC TTT TGT TTC TGT CAG TCG --- --- --- --- --- --- --- --- ---
tr263     ATG CGT TTG CTT CGG ACA GCA TTA GCA GCG GTT GGT TTG AAA GAG ATA TTC TTT TGT TTC TAC CAG TCG --- --- --- --- --- --- --- --- ---
T-2003    ATG CGT TTG CTT CGG ATA GCA TTA GCA GCG GTT GGT TTG AAA GAG ATT TTC TTT TGT TTC TAC CAG TCG --- --- --- --- --- --- --- --- ---
EK-328    ATG CGT TTG CTT CGG ACA GCA TTC GCA GCG GCC GGT --- --- --- --- --- --- --- --- --- --- --- --- --- --- --- --- --- --- ---
```

Siberian TBEV strains:

```
L23-3     ATG CGT TTG CTT CAG ATA GCA TTA GCA GCG GCA GGT TTG GAG GAG ACA TTG TCT CGT TTC TAC --- --- --- --- --- --- --- --- --- --- ---
i36-6     ATG CGT TTG CTT CAG ATA GCA TTA GCA GCG GCA GGT TTG GAA GAG ACA TTG TCT CGT TTC TAC --- --- --- --- --- --- --- --- --- --- ---
c19-5     ATG CGT TTG CTT CAG ATA GCA TTA GCA GCG GCA GGT TTG GAA GAG ACA TTG TCT CGT TTC TTC --- --- --- --- --- --- --- --- --- --- ---
O-13      ATG CGT TTG CTT CGG ATA GCA TTA GCA GCG GCA GGT TTG GAA GAG ACA TTG TCT CGT TTC TAC --- --- --- --- --- --- --- --- --- --- ---
L22       ATG CGT TTG CTT CGG ATA GCA TTA GCA GCG GCA GGT TGG GAA GAG ACA TTG TGT CGT TTC TAC --- --- --- --- --- --- --- --- --- --- ---
L22-3     ATG CGT TTG CTT CGG ACA GCA TTA GCA GCG GCA GGT TCG GAA GAG ACA TTG TCT CGT TTC TAC --- --- --- --- --- --- --- --- --- --- ---
L-1-96    ATG CGT TTG CTT CGG ATA GCA TTG GCA GCG GCT TGT TCG TCT CGA TTC TGC --- --- --- --- --- --- --- --- --- --- --- --- --- --- ---
Yar 71    ATG CGT TTG CTT CGG ATA GCA TTA GCA GCG GCT GGT TTG GAA GAG ATA TTG TCT CGA TTC TAC --- --- --- --- --- --- --- --- --- --- ---
```

Far East TBEV strains:

```
Osh5-10   ATG CGT TTG CTT CGG ATA GCA ACA GCA GCG GCG ACA GGC TTG AGA GAG ACA ATC TTT TGT TTG ATC AGT CGT GAA CGT GTT GAG AAA AAG ACA GCT
MDJ01     ATG CGT TTG CTC CGG ATA GCA ACA GCA GCG AGG TTT GAG AGA GAT AAT --T TTT CGC TTG ACC AGT CG- --- --- --- --- --- --- --- --- ---
Prot1     ATG CGT TTG CTT CGG ATA GCA ACA GCA GCG ACA GGT TTG AGA GAG ACA ATC TTT CGC TTG ATC AGT CGT GAA CGT GTT GAG AAA AAG ACA GCT
TE05      ATG CGT TTG CTC CGG ATA GCA ACA GCA GCG ACA GGT TTG AGA GAG GTA ATC CTT CGC TTG ATC AGT CGT GAA CGT GTT GAG AAA AAG ACA GCT
```

(C)

European TBEV strains:

```
Neu       MRLLRTALAAVGLKEIFFCFYQS--------
KrM 93    MRLLRTALAAVGLKEIFFCFCQS--------
AS33      MRLLRTALAAFGLKEIFFCFYQS--------
tr263     MRLLRTALAAFGLKEIFFCFYQS--------
T-2003    MRLLRIALAAVGLKEIFFCFYQS--------
EK-328    MRLLRTAFAAAG------------------
```

Siberian TBEV strains:

```
L23-3     MRLLQIALAAAGLEETLSRFY----------
i36-6     MRLLQIALAAAGLEETLSRFY----------
c19-5     MRLLQIALAAAGLEETLSRFF----------
O-13      MRLLRIALAAAGLEETLSRLY----------
L22       MRLLRIALAAAGWEETLSRFY----------
L22-3     MRLLRIALAAAGSEETLSRFY----------
L-1-96    MRLLRIALAAAGLEETSSRFC----------
Yar 71    MRLLRIALAAAGLEEILSRFY----------
```

Far East TBEV strains:

```
Osh5-10   MRLLRIATAATGLRETIFRLISRERVEKKTA
MDJ01     MRLLRTATAAFRFRDN-FSLDQS--------
Prot1     MRLLRTATAATGLRETIFRLISRERVEKKTA
TE05      MRLLRIATAATGLREVILRLISRERVEKKTA
```

Fig. 1 Comparison of TuORF nucleotide and protein sequences: Full-length sequence of TBEV 5′UTR strain Neudoerfl (**a**). uORF sequence is marked in *color*, while remaining part of the 5′UTR is in *gray*. uORF start and stop codons as well as major ORF start codons are *underlined*. Alignment of uORF nucleotide sequences (**b**) and TuORF protein sequences (**c**) of various TBEV strains. GenBank accession numbers of all nucleotide sequences used in this study are listed in Supplementary Table 1. Protein sequences of hypothetical TuORF peptides were deduced from nucleotide sequences as described in Methods

Table 1 Determination of selection pressure on the TuORF peptide: Overall analysis revealed significant positive selection acting on the complete set of TuORF peptides

	Negative selection		Any selection pressure		Positive selection	
	dS–dN	P	dN–dS	P	dN–dS	P
all TuORFs	−2.4251	1	**2.2685**	**0.0251**	**2.3365**	**0.0106**
TuORFs of European TBEV strains	0.364	0.3583	−0.3907	0.6967	−0.3971	1
TuORFs of Siberian TBEV strains	−0.501	1	0.4858	0.628	0.4996	0.3091
TuORFs of Far-Eastern TBEV strains	0.3579	0.3605	−0.34	0.7392	−0.3348	1

This evolutionary trend was not confirmed at the level of TuORFs encoded by individual TBEV subtypes. The probability of rejecting the null hypothesis of strict neutrality (dN = dS) in favor of the alternative hypothesis (Negative selection: dN < dS, any selection pressure: dN ≠ dS, or positive selection: dN > dS) is shown. P values lower than 0.05 are considered significant at the 5 % level and are shown in bold type. The values were calculated as described in Methods

peptide expression at any time point tested while the positive control (synthetic peptide loaded onto the gel) returned a strong positive signal in all cases (Fig. 2). The results indicate that the TuORF peptide either was not expressed in the cell lines tested or its expression was extremely low, below the detection limit of the immunoblotting, which was 10 pg (Supplementary Fig. 3).

**TuORF peptide expression was not visible in TBEV-infected cells using indirect immunofluorescence**

To confirm the immunoblotting experiment results, we explored TuORF peptide expression in TBEV-infected neuroblastoma cells using indirect immunofluorescence. Both Neudoerfl (encodes for TuORF) and Hypr (does not encode for TuORF) strains of TBEV were used. Anti-TuORF staining with mouse (data not shown) or rabbit polyclonal antibodies (Fig. 3) did not produce any visible signal from either TBEV strain. Control anti-NS3 immunofluorescence staining showed a very bright signal increasing in intensity with the time post TBEV infection (Fig. 3). These results show that either TBEV Neudoerfl-infected cells do not express the TuORF peptide or that TuORF peptide expression was below the detection limit of the indirect immunofluorescence.

Discussion

Minor peptides occur in some flaviviruses; for example JEV NS1′ protein [7, 8] and WNV WARF4 protein [9]. Presence of a uORF in the TBEV 5′ UTR was described

Fig. 2 Detection of the TuORF peptide by immunoblotting: Immunoblotting analysis using rabbit anti-TuORF antibodies, followed by goat anti-rabbit-AP and horse anti-goat-AP antibodies was done on human neuroblastoma, glioblastoma, and medulloblastoma cell lines and on the tick cell line IRE/CTVM19 infected with TBEV strain Neudoerfl as described in Methods. No positive signal was detected for TuORF peptide in the cell lysates, while the positive control (artificial TuORF—marked by *asterisk*) always gave a very strong response
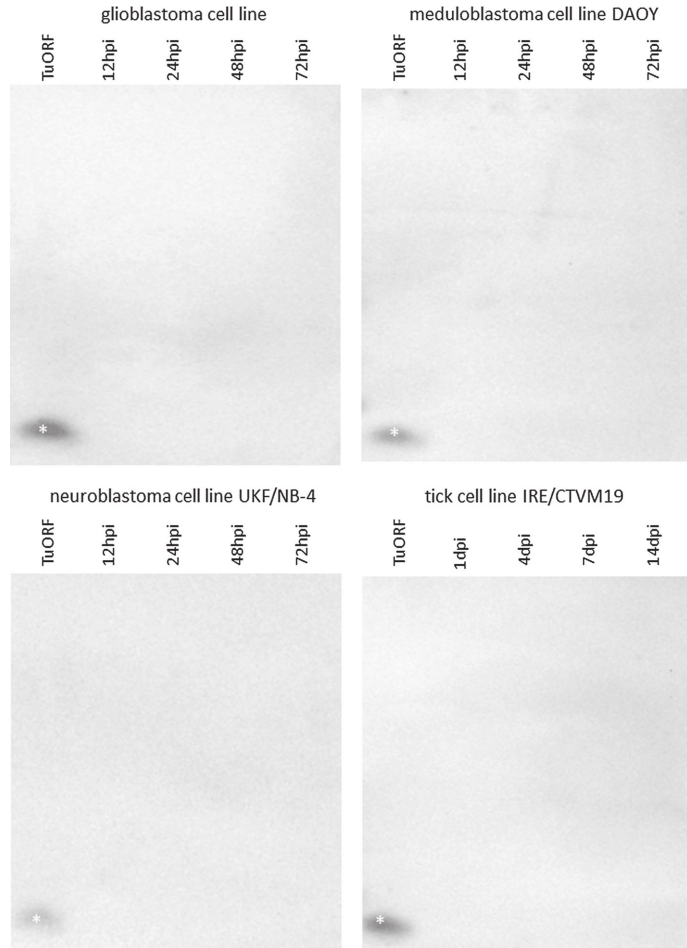
previously [15]. However, it has not been determined whether or not a peptide coded by TBEV uORF is expressed in TBEV-infected cells.

Here we showed that the putative peptide coded by the TBEV strain Neudoerfl uORF was not detectably expressed in the TBEV-infected human or tick cell lines tested. As two sets of polyclonal antibodies were used for TuORF peptide detection it is very unlikely that the negative results were caused by the inability of the antibodies to detect the natural TuORF peptide.

These results can be explained in at least three different ways. (i) The simplest explanation is that the TuORF peptide is not produced in TBEV-infected cells and TuORF

itself is just a product of random mutation. This explanation is also supported by evolutionary analyses. (ii) The TuORF peptide may be produced under different conditions from those tested in our experiments; TBEV infects various cell types during mammalian host infection and neural cells are only the final targets [34]. Other target cells such as dendritic cells, macrophages, and spleen cells are infected during primary viremia; in some of these cells the TuORF peptide may be produced. (iii) TuORF peptide is expressed in TBEV-infected cells but is rapidly degraded and therefore it is impossible to detect it.

The bioinformatics analyses showed that TuORF is present in some (but not all) TBEV strains belonging to all
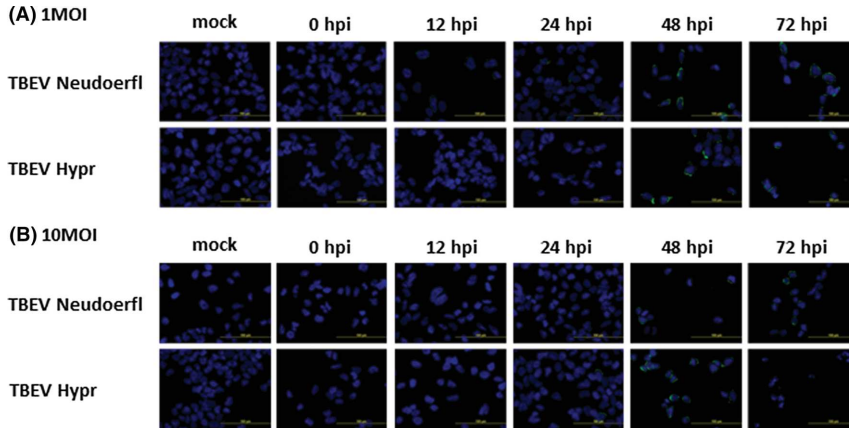
Fig. 3 Attempted detection of TuORF peptide expression by immunofluorescence: Human neuroblastoma cells were infected by TBEV strains Neudoerfl (sample, TuORF containing TBEV strain) and Hypr (negative control, TuORF lacking TBEV strain). Mock- and TBEV-infected (MOI of 1, *panel A*; MOI of 10, *panel B*) cells grown and fixed at various time points were stained with anti-NS3 antibody (*green*) and anti-TuORF antibody (*red*), and counterstained with DAPI (*blue*). No positive response for TuORF was detected at any time post infection while NS3 protein was already detectable 12 h post infection. The size of *yellow* measure line is 100 μm

three TBEV subtypes. Individual TuORFs specific for European, Siberian, and Far-Eastern subtypes differ in both nucleotide and amino acid sequence (Fig. 1) and they form three monophyletic clades which can be clearly distinguished in the phylogenetic tree (Supplementary Fig. 3). TBEV is not the only Flavivirus containing a uORF in its 5′ UTR. uORFs were also detected in other flaviviruses namely LGTV, KAMV, KARV, and SLEV (Supplementary Table 2). Nevertheless these uORFs do not share any sequence similarity with TuORF (Supplementary Fig. 1).

It is likely that TuORF evolved by mutation of the GUG codon, which is present in TBEV strains without TuORF, to an initiating AUG codon. The TBEV 5′ UTR is extremely structured [35]. All the structures are very conserved and they have crucial functions in TBEV genome replication [36] and polyprotein expression [37]. Therefore all mutations in the TuORF peptide have to be assessed in respect of preservation of the 5′ UTR structure. The GUG/AUG codon is positioned at the base of the stem loop 1 (SL1) structure [35]. As the first guanosine in GUG is not a part of SL1 but is located in the preceding internal loop, GUG can mutate to AUG without affecting the 5′ UTR secondary structure.

The TBEV 5′ UTR has numerous sequence variable but structurally extremely conserved regions, which affect TBEV replication and translation [38]. Mutational analyses of these regions showed that secondary structures, but not primary sequence, in these regions are responsible for their

function [39, 40]. TuORF is located in SL1, which is one of the most important structures in the TBEV 5′ UTR [38]. Therefore it is not surprising that the proportion of non-synonymous mutations (dN) exceeds the proportion of synonymous mutations (dS) in this region which would allow retention of the keep native SL1 structure in all tested TBEV strains (data not shown). This indicates that the putative TuORF peptide, if expressed, does not have an exact, precisely defined role in the TBEV life cycle.

It is possible that TuORF can regulate expression of the major TBEV ORF by itself. Translation regulation by uORFs is a well-known and intensively studied process. In most cases uORF down-regulates gene expression [41]. The rate of down-regulation depends on sequence context of the uORF initiation codon, uORF length, and the distance between uORF and major ORF [42]. In the case of TuORF, down-regulation of the major ORF would not be great. The AUG codon initiating TuORF is in a suboptimal sequence context (acgTgcAUGC) which is far from the optimal Kozak sequence (gccRccAUGG) [43, 44]. Also the length of TuORF is rather short and the distance between TuORF and the major TBEV ORF is sufficient for possible translation reinitiation. This allows us to speculate that a high proportion of ribosomes would pass the TuORF initiation codon by leaky scanning and initiate translation on the major TBEV ORF initiation codon. Nevertheless, the exact effect of TuORF presence on major TBEV polyprotein production remains unknown.

Summary

We showed that uORFs are present in some strains of TBEV, LGTV, KAMV, KARV, and SLEV. TuORF sequence conservation among different TBEV subtypes is low. The TuORF peptide was not detectably expressed in TBEV strain Neudoerfl-infected human neural or tick cells. Therefore, we can assume that the uORF plays either a minor or no role in TBEV infection of these cell types.

Authors contribution JC did all the bioinformatics predictions and phylogenetic calculations; he participated in the immunofluorescence and Western blot experiments and he drafted the manuscript. JC, MS, MP, HT, and ZV grew the cells and did TBEV infections. JS, MS, and ZV carried out the immunofluorescence and Western blot experiments, assisted by JC, HT, and MP. LBS provided the tick cell line and critically revised the manuscript. LG and DR supervised all work and participated in the manuscript revisions.

Compliance with ethical standards

Conflict of interest The authors have declared no competing interests.

References

1. T.S. Gritsun, P.A. Nuttall, E.A. Gould, Adv. Virus Res. **61**, 317–371 (2003)
2. A.M.Q. King, M.J. Adams, E.B. Carstens, E.J. Lefkowitz, *Virus Taxonomy: Classification and Nomenclature of Viruses: Ninth Report of the International Committee on Taxonomy of Viruses* (Elsevier Academic Press, San Diego, 2012)
3. M. Ecker, S.L. Allison, T. Meixner, F.X. Heinz, J. Gen. Virol. **80**(Pt 1), 179–185 (1999)
4. T.S. Gritsun, V.A. Lashkevich, E.A. Gould, Antiviral Res. **57**, 129–146 (2003)
5. V.M. Hoenninger, H. Rouha, K.K. Orlinger, L. Miorin, A. Marcello, R.M. Kofler, C.W. Mandl, Virology **377**, 419–430 (2008)
6. E. Harris, K.L. Holden, D. Edgil, C. Polacek, K. Clyde, Novartis Found Symp **277**, 23–39 (2006). **discussion 40, 71-23, 251-253**
7. B.J. Blitvich, D. Scanlon, B.J. Shiell, J.S. Mackenzie, R.A. Hall, Virus Res. **60**, 67–79 (1999)
8. E.B. Melian, E. Hinzman, T. Nagasaki, A.E. Firth, N.M. Wills, A.S. Nouwens, B.J. Blitvich, J. Leung, A. Funk, J.F. Atkins, R. Hall, A.A. Khromykh, J. Virol. **84**, 1641–1647 (2010)
9. G. Faggioni, A. Pomponi, R. De Santis, L. Masuelli, A. Ciammaruconi, F. Monaco, A. Di Gennaro, L. Marzocchella, V. Sambri, R. Lelli, G. Rezza, R. Bei, F. Lista, Virol J **9**, 283 (2012)
10. G. Faggioni, A. Ciammaruconi, R. De Santis, A. Pomponi, M.T. Scicluna, K. Barbaro, L. Masuelli, G. Autorino, R. Bei, F. Lista, Int. J. Mol. Med. **23**, 509–512 (2009)
11. A.E. Firth, J.F. Atkins, Virol J **6**, 14 (2009)
12. J. Sun, Y. Yu, V. Deubel, Microbes Infect. **14**, 930–940 (2012)
13. Q. Ye, X.F. Li, H. Zhao, S.H. Li, Y.Q. Deng, R.Y. Cao, K.Y. Song, H.J. Wang, R.H. Hua, Y.X. Yu, X. Zhou, E.D. Qin, C.F. Qin, J. Gen. Virol. **93**, 1959–1964 (2012)
14. V. Satchidanandam, P.D. Uchil, P. Kumar, Novartis Found Symp **277**, 136–145 (2006). **discussion 145-138, 251-133**
15. E.V. Chausov, V.A. Ternovoi, E.V. Protopopova, J.V. Kononova, S.N. Konovalova, N.L. Pershikova, V.N. Romanenko, N.V. Ivanova, N.P. Bolshakova, N.S. Moskvitina, V.B. Loktev, Vector Borne Zoonotic Dis. **10**, 365–375 (2010)
16. D. Ruzek, M. Vancova, M. Tesarova, A. Ahantarig, J. Kopecky, L. Grubhoffer, J. Gen. Virol. **90**, 1649–1658 (2009)
17. L. Bell-Sakyi, E. Zweygarth, E.F. Blouin, E.A. Gould, F. Jongejan, Trends Parasitol. **23**, 450–457 (2007)
18. S.F. Altschul, W. Gish, W. Miller, E.W. Myers, D.J. Lipman, J. Mol. Biol. **215**, 403–410 (1990)
19. M.A. Larkin, G. Blackshields, N.P. Brown, R. Chenna, P.A. McGettigan, H. McWilliam, F. Valentin, I.M. Wallace, A. Wilm, R. Lopez, J.D. Thompson, T.J. Gibson, D.G. Higgins, Bioinformatics **23**, 2947–2948 (2007)
20. P. Artimo, M. Jonnalagedda, K. Arnold, D. Baratin, G. Csardi, E. de Castro, S. Duvaud, V. Flegel, A. Fortier, E. Gasteiger, A. Grosdidier, C. Hernandez, V. Ioannidis, D. Kuznetsov, R. Liechti, S. Moretti, K. Mostaguir, N. Redaschi, G. Rossier, I. Xenarios, H. Stockinger, Nucleic Acids Res. **40**, W597–W603 (2012)
21. J. Söding, A. Biegert, A.N. Lupas, Nucleic Acids Res. **33**, W244–W248 (2005)
22. M. Remmert, A. Biegert, A. Hauser, J. Söding, Nat. Methods **9**, 173–175 (2012)
23. S.F. Altschul, T.L. Madden, A.A. Schäffer, J. Zhang, Z. Zhang, W. Miller, D.J. Lipman, Nucleic Acids Res. **25**, 3389–3402 (1997)
24. E.H.C. Gasteiger, A. Gattiker, S. Duvaud, M.R. Wilkins, R.D. Appel, A. Bairoch, in *Protein Identification and Analysis Tools on the ExPASy Server*, ed. by J.M. Walker (Humana Press, New York, 2005), pp. 571–607
25. J.A. Cuff, M.E. Clamp, A.S. Siddiqui, M. Finlay, G.J. Barton, Bioinformatics **14**, 892–893 (1998)
26. K. Hofmann, W. Stoffel, Biol Chem Hoppe-Seyler **374**, 166 (1993)
27. K. Tamura, G. Stecher, D. Peterson, A. Filipski, S. Kumar, Mol. Biol. Evol. **30**, 2725–2729 (2013)
28. O. Penn, E. Privman, H. Ashkenazy, G. Landan, D. Graur, T. Pupko, Nucleic Acids Res. **38**, W23–W28 (2010)
29. O. Penn, E. Privman, G. Landan, D. Graur, T. Pupko, Mol. Biol. Evol. **27**, 1759–1767 (2010)
30. M. Nei, T. Gojobori, Mol. Biol. Evol. **3**, 418–426 (1986)
31. H. Schägger, Nat. Protoc. **1**, 16–22 (2006)
32. D.N. Mitzel, S.M. Best, M.F. Masnick, S.F. Porcella, J.B. Wolfinbarger, M.E. Bloom, Virology **381**, 268–276 (2008)
33. L.I.U. Romanova, A.P. Gmyl, T.I. Dzhivanian, D.V. Bakhmutov, A.N. Lukashev, L.V. Gmyl, A.A. Rumyantsev, L.A. Burenkova, V.A. Lashkevich, G.G. Karganova, Virology **362**, 75–84 (2007)
34. D. Růžek, G. Dobler, O.D. Mantke, Travel Med Infect Dis **8**, 223–232 (2010)

35. A. Tuplin, D.J. Evans, A. Buckley, I.M. Jones, E.A. Gould, T.S. Gritsun, Nucleic Acids Res. **39**, 7034–7048 (2011)
36. X.F. Li, T. Jiang, X.D. Yu, Y.Q. Deng, H. Zhao, Q.Y. Zhu, E.D. Qin, C.F. Qin, J. Gen. Virol. **91**, 1218–1223 (2010)
37. S.M. Paranjape, E. Harris, Curr. Top. Microbiol. Immunol. **338**, 15–34 (2010)
38. T.S. Gritsun, E.A. Gould, Virology **366**, 8–15 (2007)
39. L.G. Gebhard, C.V. Filomatori, A.V. Gamarnik, Viruses **3**, 1739–1756 (2011)
40. M.F. Lodeiro, C.V. Filomatori, A.V. Gamarnik, J. Virol. **83**, 993–1008 (2009)
41. A.E. Firth, I. Brierley, J. Gen. Virol. **93**, 1385–1409 (2012)
42. L.A. Ryabova, M.M. Pooggin, T. Hohn, Virus Res. **119**, 52–62 (2006)
43. M. Kozak, Nature **308**, 241–246 (1984)
44. M. Kozak, Cell **44**, 283–292 (1986)

Donald, C.L., Brennan, B., Cumberworth, S.L., Rezelj, V.V., Clark, J.J., Cordeiro, M.T., Franca, R.F.D., Pena, L.J., Wilkie, G.S., Filipe, A.D., Davis, C., Hughes, J., Varjak, M., **Selinger, M.**, Zuvanov, L., Owsianka, A.M., Patel, A.H., McLauchlan, J., Lindenbach, B.D., Fall, G., Sall, A.A., Biek, R., Rehwinkel, J., Schnettler, E., Kohl, A., 2016: Full Genome Sequence and sfRNA Interferon Antagonist Activity of Zika Virus from Recife, Brazil. PLoS Neglected Tropical Diseases 10(10): e0005048. DOI: 10.1371/journal.pntd.0005048 (IF = 4.72)

Full Genome Sequence and sfRNA Interferon Antagonist Activity of Zika Virus from Recife, Brazil

Claire L. Donald[1]☯, Benjamin Brennan[1]☯, Stephanie L. Cumberworth[1]☯, Veronica V. Rezelj[1], Jordan J. Clark[1], Marli T. Cordeiro[2], Rafael Freitas de Oliveira França[2], Lindomar J. Pena[2], Gavin S. Wilkie[1], Ana Da Silva Filipe[1], Christopher Davis[1], Joseph Hughes[1], Margus Varjak[1], Martin Selinger[3,4], Luíza Zuvanov[1], Ania M. Owsianka[1], Arvind H. Patel[1], John McLauchlan[1], Brett D. Lindenbach[5], Gamou Fall[6], Amadou A. Sall[6], Roman Biek[7], Jan Rehwinkel[8], Esther Schnettler[1¤a], Alain Kohl[1]*

1 MRC-University of Glasgow Centre for Virus Research, Glasgow, Scotland, United Kingdom, **2** Fundação Oswaldo Cruz-PE/Centro de Pesquisas Aggeu Magalhães, Departamento de Virologia, Campus da UFPE-Cidade Universitária, Recife/PE, Brasil, **3** Faculty of Science, University of South Bohemia, České Budějovice, Czech Republic, **4** Institute of Parasitology, Biology Centre of the Academy of Sciences of the Czech Republic, České Budějovice, Czech Republic, **5** Department of Microbial Pathogenesis, Yale University, New Haven, Connecticut, United States of America, **6** Pole de Virologie, Unité des arbovirus et virus des fièvres hémorragiques, Institut Pasteur de Dakar, Dakar, Senegal, **7** Boyd Orr Centre for Population and Ecosystem Health, Institute of Biodiversity, Animal Health and Comparative Medicine, College of Medical Veterinary and Life Sciences, University of Glasgow, Glasgow, Scotland, United Kingdom, **8** Medical Research Council Human Immunology Unit, Weatherall Institute of Molecular Medicine and Radcliffe Department of Medicine, University of Oxford, Oxford, England, United Kingdom

☯ These authors contributed equally to this work.
¤a Current address: Bernhard Nocht Institute for Tropical Medicine, Hamburg, Germany
* alain.kohl@glasgow.ac.uk

OPEN ACCESS

Abstract

Background

The outbreak of Zika virus (ZIKV) in the Americas has transformed a previously obscure mosquito-transmitted arbovirus of the *Flaviviridae* family into a major public health concern. Little is currently known about the evolution and biology of ZIKV and the factors that contribute to the associated pathogenesis. Determining genomic sequences of clinical viral isolates and characterization of elements within these are an important prerequisite to advance our understanding of viral replicative processes and virus-host interactions.

Methodology/Principal findings

We obtained a ZIKV isolate from a patient who presented with classical ZIKV-associated symptoms, and used high throughput sequencing and other molecular biology approaches to determine its full genome sequence, including non-coding regions. Genome regions were characterized and compared to the sequences of other isolates where available. Furthermore, we identified a subgenomic flavivirus RNA (sfRNA) in ZIKV-infected cells that has antagonist activity against RIG-I induced type I interferon induction, with a lesser effect on MDA-5 mediated action.

46

Conclusions/Significance

The full-length genome sequence including non-coding regions of a South American ZIKV isolate from a patient with classical symptoms will support efforts to develop genetic tools for this virus. Detection of sfRNA that counteracts interferon responses is likely to be important for further understanding of pathogenesis and virus-host interactions.

Author Summary

The current ZIKV outbreak is a major public health concern in the Americas. To further understand the virus, and to develop tools and potentially vaccines, more information on the virus strains circulating in the Americas is required. Here we describe the full-length sequence of a ZIKV isolate from a patient with classical symptoms, including the complete non-coding regions which are missing from many currently available sequences, and put these in context. Moreover, we also demonstrate the production of an RNA molecule derived from the 3' untranslated region that counteracts interferon responses and may therefore be important for understanding the pathogenesis of ZIKV infection.

Introduction

Zika virus (ZIKV) is a mosquito-transmitted arbovirus in the *Flavivirus* genus, *Flaviviridae* family. This previously obscure virus has recently caused large scale outbreaks in French Polynesia in 2013 [1, 2], New Caledonia [3], the Cook Islands [4] and Easter Island [5] in 2014 and the Americas in May 2015, beginning in Brazil [6, 7]. These outbreaks have been characterized by an increased prevalence of neurological syndromes, such as Guillain-Barré syndrome and microcephaly [8–13], which has heightened public concern. As of April 2016 the World Health Organization (WHO) announced that 60 countries had reported autochthonous transmission in the escalating epidemic originating in Bahia, Brazil in 2015 that has so far resulted in over 1.5 million suspected cases [14]. This unprecedented spread combined with the associated neurological conditions resulted in WHO declaring a global public health emergency in February 2016.

Brazil has the greatest burden of dengue virus (DENV), a related flavivirus, in the world and the ongoing ZIKV epidemic is occurring in areas where such mosquito-borne arboviruses are a major public health problem. This is due to widespread arbovirus vectors such as *Aedes aegypti* and *Ae. albopictus* which are important vectors of DENV and chikungunya virus (CHIKV, *Togaviridae*), as well as ZIKV [15–19]. Clinical manifestations of ZIKV are similar to symptoms of DENV or CHIKV infections making misdiagnosis common [3, 20]. Only 20% of ZIKV infections are thought to progress to clinical symptoms, which present as an acute, self-limiting illness comprising fever, myalgia, headache, polyarthralgia, nonpurulent conjunctivitis and maculopapular rash. The largest public health risk from ZIKV is its association with neurological conditions such as Guillain-Barré syndrome and microcephaly which place substantial strains on local communities and healthcare providers.

As is characteristic of flaviviruses, ZIKV possesses a linear single-stranded, positive-sense RNA genome. The flavivirus genome has a single open reading frame that encodes all structural and non-structural proteins flanked by 5′ and 3′ untranslated regions (UTRs) [21]. Phylogenetic analysis of partial ZIKV sequence data revealed isolates may be categorised into

47

African and Asian lineages, of which the African lineage is further subdivided into Nigerian and MR766 prototype strain clades [22, 23]. Recently obtained sequences from the current epidemic are of Asian lineage and are most closely related to strains from the French Polynesian outbreak in 2013 [5, 6, 24]. However, there are currently few full-length complete sequences that include the genome termini. One of these is from the Americas and was derived from a microcephaly case [10]. Nonetheless, such information is important given the relevance of the genome termini and non-coding regions in virus translation, replication and pathogenesis. The 5' and 3' non-translated regions of flavivirus genomes have been shown to demonstrate conserved secondary structures, cyclization elements, and are important for binding to several host proteins in addition to proteins involved in viral replication complexes [25, 26]. Furthermore, the 3'UTR encodes subgenomic flavivirus RNA (sfRNA) which is produced by the incomplete degradation of viral RNA by a cellular 5'-3' exoribonuclease [27, 28]. These molecules have been shown to be more than a by-product and are involved in viral interference with innate immune responses in both vertebrates and invertebrates through antagonizing type I interferon and RNA interference responses respectively [29–36].

Herein we present the complete genome sequence of a ZIKV isolate derived from a patient in Brazil with classical disease symptoms. This will be important for future studies and the development of reagents, such as reverse genetics systems, for ZIKV. We also identified ZIKV-derived sfRNA in infected cells and show that it functions as an antagonist of RIG-I mediated induction of type I interferon, while a lesser effect on MDA-5 mediated induction was observed. The production of sfRNA in ZIKV infection may be an important contributor to associated pathogenesis.

Materials and Methods

Ethics statement

This study was approved by the Brazilian Ethics Committee, Process number: IMIP Human Ethics Research Committee Approval number 4232, PlatBr580.333 and 44462915.8.2004.5190. The virus reported here, *ZIKV/H. sapiens/Brazil/PE243/2015* (abbreviated to ZIKV PE243), was isolated in Recife (Brazil) in 2015 from a patient (rash on face and limbs; arthralgia hands, fist/wrist, ankle; edema on hands, fist/wrist; no neurological symptoms). All patients who agreed to participate in this study were asked to sign an informed consent form.

Virus isolation from cell culture

ZIKV from positive serum samples was isolated at Fundação Oswaldo Cruz (FIOCRUZ), Recife (Brazil) by amplification in C6/36 *Ae. albopictus* cells. then Vero cells, which are frequently used for virus isolation and were obtained from collections at FIOCRUZ. Briefly, 50 μl of positive serum was incubated for 1 h at room temperature on monolayers of C6/36 cells. The cells were then further incubated for 7 days. Following this, ZIKV infection was confirmed by RT-PCR as described below.

Viral RNA extraction and RT-PCR

Viral RNA was extracted from serum of suspected acute DENV/ZIKV cases using the QIAmp Viral RNA Mini kit (Qiagen) following the manufacturer's instructions. RNA was extracted from 140 μl of the sample and stored at -70°C prior to downstream applications. RT-PCR was carried out using the QIAGEN OneStep RT-PCR kit in a final volume of 25 μl following previously established protocols and primers [22].

Virus growth and titration by plaque assay

Vero E6 cells, a commonly used cell line for the growth of viruses [37] were infected with ZIKV PE243 for the preparation of virus stocks which were collected upon detection of cytopathic effect. ZIKV PE243 infected cells tested positive with mouse anti-ZIKV serum (provided by G. Fall and A. A. Sall, Institut Pasteur de Dakar, Senegal) as well as with commercially obtained ZIKV E protein-specific antibodies by western blotting and immunofluorescence (S1 File). For titration, Vero E6 cells were infected with serial dilutions of virus and incubated under an overlay consisting of DMEM supplemented with 2% FCS and 0.6% Avicel (FMC BioPolymer) at 37°C for 5–7 days. Cell monolayers were fixed with 4% formaldehyde. Following fixation, cell monolayers were stained with Giemsa to visualize plaques. Plaque assays for plaque size comparisons were also performed using A549 and A549/BVDV-Npro cell lines (provided by R. E. Randall, University of St Andrews, UK) [37–39].

Detection of ZIKV PE243 sfRNA by northern blot

Denatured total RNA (3.5 μg per sample; isolated from Vero E6 cells infected with ZIKV PE243 at an multiplicity of infection [MOI] of 1 by Trizol followed by Direct-zol RNA purification) was separated on a denaturing formaldehyde agarose gel (1.5% agarose, 1x MOPS buffer [Fisher Scientific], 12.3 M formaldehyde) in 1x MOPS running buffer. RNA was transferred onto a Hybond-N+ membrane (GE Healthcare Life Sciences) via capillary transfer action using 10x SSC (1.5 M NaCl, 150 mM trisodium citrate). RNA was crosslinked to the membrane by UV (120 mJ/cm^2). Following transfer, the membrane was prehybridized for 2 h in PerfectHyb Plus Hybridization buffer (Sigma-Aldrich) at 65°C. Specific oligonucleotides for the sfRNA region of the ZIKV PE243 3'UTR (forward: AGCTGGGAAACCAAGCCTAT, reverse: GTGGTGGAAAC TCATGGAGTCT) were used to amplify a fragment by PCR with KOD polymerase (Merck Millipore). Following this 250 ng of the PCR product was end-labelled with ^{32}P using T4 Polynucleotide Kinase (NEB) and [γ-^{32}P]Adenosine 5'-triphosphate (PerkinElmer) to produce a probe. The probe was denatured for 5 min at 95°C and added to prehybridization mixture which was incubated on the membrane overnight at 65°C. The membrane was then washed twice for 15 min at 65°C with each of the following three buffers: 2x SSC and 0.5% SDS, 2x SSC and 0.2% SDS, 0.2x SSC and 0.1% SDS. RNA species were detected by phosphorimaging.

Cloning of ZIKV 3'UTR

The Gateway cloning system was used for cloning the 3'UTR of ZIKV, potentially containing the sfRNA sequence, fused to hepatitis delta virus ribozyme (HDVr) into pDEST40 (mammalian expression vector [Invitrogen]). The 3'UTR of ZIKV PE243 was amplified by PCR using 1 μl of the 3' end RACE reaction as a template. Subsequently, fusion PCR was performed using the primers described in Table 1. The resulting fragment was inserted into the pDONR207 using BP Clonase II kit (Invitrogen) and sequenced using the pDONR201 forward primer. LR Clonase II kit (Invitrogen) was used for the recombination of pDONR207-ZIKV PE243-3'UTR (entry vector) and the empty pDEST40 resulting in pDEST40-ZIKV PE243-3'UTR. The sequence of pDEST40-ZIKV PE243-3'UTR was validated using the T7 promoter forward primer. Similar cloning strategies have been used for other flavivirus 3'UTRs containing sfRNA [29, 30].

Interferon assays

In vitro type I interferon assays were performed using the human A549 cell line [37] to analyze the activity of the IFN-β promoter in the presence of plasmids expressing flavivirus 3'UTRs containing the sfRNA sequence. A549 cells were grown in DMEM (supplemented with 10%

Table 1. Primers used for cloning of ZIKV 3'UTR containing sfRNA.

Primer	Use	Sequence (5'-3')
ZIKV-3'UTR-FW	ZIKV 3'UTR amplification	GCACCAATCTTAATGTTGTCAGG
ZIKV-3'UTR-RV		AGACCCATGGATTTCCCC
ZIKV-3'UTR-attB-FW	amplification of attB-ZIKV 3'UTR-HDVr fragment	GGGGACAAGTTTGTACAAAAAAGCAGGCTTCGCACCAATCTTAATGTTGTC
ZIKV-3'UTR-HDVR-RV		CATGCCGACCCAGACCCATGGATTTCCCCA
HDVR-ZIKV-3'UTR-FW	amplification of ZIKV 3'UTR-HDVr-attB fragment	GAAATCCATGGGTCTGGGTCGGCATGGCATCTC
HDVR-attB-RV (E10)		GGGGACCACTTTGTACAAGAAAGCTGGGTTTTCCGATAGAGAATCGAGAGAAAA
pDONR201 forward	sequencing (pDONR207)	TCGCGTTAACGCTAGCATGGATCTC
T7 promoter (F)	sequencing (pDEST40)	TAATACGACTCACTATAGGG

doi:10.1371/journal.pntd.0005048.t001

FBS, 1000 units/ml penicillin and 1 mg/ml streptomycin) at 37°C with 5% CO_2. Briefly, 24 h prior to transfection, A549 cells were seeded in 24 well plates at a density of $1.2x10^5$ cells/well to reach 70% confluency the following day. Cells were first co-transfected with 400 ng p125Luc IFN-β promoter reporter vector expressing Firefly luciferase [40], 2 ng pRL-CMV (internal control, expressing *Renilla* luciferase), and 500 ng of either pDEST40 expressing DENV [29] or ZIKV 3'UTRs (constructs described in this study) or a MBP-HDVr (maltose-binding protein-HDVr) control using Opti-MEM and Lipofectamine2000 (Invitrogen) according to the manufacturer's protocol. Following a further 24 h incubation, type I interferon induction was stimulated by transfecting the cells a second time with either 10 μg/well poly I:C, 50 ng Vero cell produced EMCV RNA or 50 ng Neo[1-99] IVT-RNA (universal, MDA-5 specific and RIG-I specific type I interferon agonists respectively) [41, 42]. Cells were lysed in 1x passive lysis buffer (Promega) 24 h after the second transfection and Firefly and *Renilla* luciferase activities determined using a Dual-Luciferase reporter assay kit (Promega) in a GloMax luminometer.

Virus infection for RNA sequencing

Vero E6 cells were infected with ZIKV at an MOI of 0.001 in triplicate. At 48 h post infection (p.i.), cell culture supernatant was harvested and clarified by low speed centrifugation. Following clarification, 6 ml of infected cell supernatant was concentrated to 250 μl using an Ultra-15 Centrifugal Filter Units with 100 kDa molecular weight cut-off (Amicon). Concentrated supernatant was then added to Direct-zol solution and RNA extracted using a Direct-zol RNA mini kit (Zymogen) according to the manufacturer's instructions. Purified RNA was then stored at -80°C for further downstream processing.

RACE analysis of viral genome termini

Sequencing of the 5' and 3' termini of the viral genome was performed using a 5'/3' RACE kit (Roche) following the manufacturer's protocol. All primers used are described in Table 2. To

Table 2. Primers sequences used for 5'/3' RACE of ZIKV viral termini.

Primer	Use	Sequence (5'-3')
SP1	cDNA synthesis	CTCATGGTGGCATCACACATGTGTCCAAGATCC
5' PCR	PCR amplificiation	TGCACTCCCACGTCTAG
3' PCR	PCR amplification	TGGCCAATGCCATTTGTTCATCTGTGC
5' SEQ	Sequencing	CATCTATTGATGAGACCCAGTGATGGC
3' SEQ	Sequencing	GAAGACTTGTGGTGTGGATCTCTCATAGGGCACAG
3' SEQ2	Sequencing	GCCTGAACTGGAGATCAGCTGTGGATC

doi:10.1371/journal.pntd.0005048.t002

50

obtain the 5' end sequence of the ZIKV genome 5' RACE was performed. Briefly, 1 μg total RNA was extracted from ZIKV-infected Vero E6 cells using a Direct-zol RNA mini kit and reverse transcribed using the ZIKV specific primer, SP1. The synthesized cDNA was purified using the illustra GFX PCR DNA and Gel Band Purification kit (GE Healthcare) according to the manufacturer's instructions. This was prior to polyadenylation at the 3' end and amplification using the PCR anchor primer and a ZIKV specific primer (5' PCR). 3' RACE was carried out to obtain the 3' end sequence using 1 μg total RNA extracted from ZIKV infected Vero cells which was polyadenylated at the 3' end using Poly(A) polymerase (New England Biolabs) following the manufacturer's guidelines. cDNA synthesis was performed by reverse transcribing the RNA using the oligo (dT) anchor primer. Amplification of the cDNA was achieved by using the PCR anchor primer and a ZIKV specific primer (3' PCR). The PCR cycling conditions were 95°C for 2 min then 35 cycles of 95°C 20 sec, 56°C (5' RACE) or 68°C (3' RACE) for 10 sec, 70°C for 15 sec and 70°C for 7 min.

cDNA synthesis and NGS library preparation

A volume of 25 μl of cell culture supernatant was treated with RNase-free DNase I (Ambion), purified with RNAClean XP magnetic beads (Beckman Coulter) and eluted in 11 μl of water. In parallel, an equivalent sample was concentrated from 25 to 11 μl using magnetic beads as indicated above, in the absence of DNase I treatment. In addition, 45 μl of extracted total cellular nucleic acid was treated with RNase-free DNase I and purified as above. Half of the volume was further depleted of ribosomal RNA (RiboZero Gold) according to the manufacturer's protocol.

All samples were reverse-transcribed using Superscript III (Invitrogen) followed by dsDNA synthesis with NEB Next(r) mRNA Second Strand Synthesis Module (New England Biolabs). Libraries were prepared using a KAPA DNA Library Preparation Kit (KAPA Biosystems), utilizing a modified protocol that includes ligation of the NEBnext adapter for Illumina (New England Biolabs), followed by indexing with TruGrade oligonucleotides (Integrated DNA Technologies) to eliminate tag crossover. Resulting libraries were quantified using a Qubit 3.0 fluorometer (Invitrogen) and their size determined using a 2200 TapeStation (Agilent). Libraries were pooled in equimolar concentrations.

Sequencing analysis

Samples from different passages were sequenced on a NextSeq500 platform (Ilumina). This obtained 24,275,098 read pairs (2x150bp) and 88.8% of reads had a quality score of >Q30.

Bioinformatic analysis

Reads were first checked for quality using FASTQC (http://www.bioinformatics.babraham.ac.uk/projects/fastqc/) and trimmed for adapter sequences and quality filtered using trim_galore (http://www.bioinformatics.babraham.ac.uk/projects/trim_galore/). These were subsequently mapped to the ZIKV complete genome KU321639 using two different aligners: Tanoti (http://www.bioinformatics.cvr.ac.uk/tanoti.php) and Bowtie2 [43]. The assembly was parsed using customized scripts to determine the frequency of nucleotides at each site and reconstruct a consensus with nucleotides above 50%. The complete genome was extended at the 5' and 3'UTRs by extracting additional reads that overlapped with the terminal ends of the consensus sequence. The sequence of the ZIKV PE243 genome has been deposited in GenBank with the accession number KX197192.

51

Phylogenetic and sequence analysis

Phylogenetic and comparison analyses were carried out using full coding sequence alignments that were generated using MUSCLE [44] within the program suite Geneious (version 7.1.8: http://www.geneious.com) [45]. These alignments were created using our ZIKV PE243 sequence in addition to publicly available coding sequences on GenBank. All Asian and African lineage ZIKV sequences used for the analysis are described in S1 Table. A single African sequence (MR-766, accession NC_012532) was used as an outgroup. Before generating phylogenies, the data set was analyzed for the presence of recombination. The Recombination Detection Program version 4 (RDP4) [46] software was utilized, specifically the programs RDP, Chimaera, BootScan, 3Seq, GENECONV, MacChi & SiScan. Phylogenies were generated with both maximum likelihood and Bayesian inference methods using the software packages PhyML [47] and MrBayes (version 3.2.6) [48] respectively. Support for the maximum likelihood tree topology was generated by 1,000 non-parametric bootstrap replicates. For the Bayesian analysis one MCMC run of four heated chains of length 1,000,000 was utilized to ensure an effective sample size of at least 200. The run was sampled every 200th generation and the first 10% of samples were discarded as burn-in. The generalized time reversible (GTR) substitution model with gamma distribution (+G) was found to suit the data set best, as selected by both jModel Test [49] and HyPhy [50] software packages. The topologies of both the Bayesian and maximum likelihood trees were identical; here we present only the Bayesian tree.

Statistical analysis

All data were analysed using Prism 5 software (GraphPad) and presented as mean ± standard error. Statistical significance for the comparison of means between groups was determined by a two-way ANOVA; p values ≤ 0.05 were considered significant.

Results and Discussion

Characterization of *ZIKV/H. sapiens/Brazil/PE243/2015*

At the time of writing, 62 ZIKV genomes are available on GenBank, of which 37 are published. Of these only 11 showed both 5' and 3' complete UTRs (accessed 16th April 2016). A summary of currently available strain information and accession numbers is presented in S1 Table. ZIKV PE243 was isolated from a patient presenting with classical symptoms associated with ZIKV infection and the complete viral genome sequence including the non-coding regions was determined. The UTRs are largely missing in many sequences from the Americas, with some exceptions including the Natal isolate derived from a case presenting with microcephaly [10]. Only recently have more full-length ZIKV sequences been described [51, 52].

Our phylogenetic analysis uses the entire protein-coding region and the position of our isolate was supported by a posterior probability node support of 1. Recombination screening prior to analysis also produced no signals. The sequence of ZIKV PE243 used for further analysis (as deposited in GenBank) derives from virus that had been passaged five times in Vero E6 cells upon receipt by the Centre for Virus Research (Glasgow, UK) on a NextSeq500 (average depth of coverage of 5637, range 52–13691). Three nucleotide substitutions were observed following the sequencing of this virus compared to a previous passage of the isolate (passage two) that had been sequenced on a MiSeq platform (these earlier data did not generate complete coverage; average depth of coverage of 1158, range 2–2944). The mutations observed are as follows: site 2784, 1149 out of 1159 reads had A in the MiSeq run (after two passages) and 3508 out of 3910 reads had G in the NextSeq run after a further three passages. The mutation A2784G corresponds to the amino acid substitution R893G in NS1. The mutations observed in

52

NS3 (U5231C: 1727/1730 Ts in passage two versus 7031/7623 Cs in passage five) and NS4B (A7637G: 1835/1846 As in passage two versus 9578/10587 Gs in passage five) were synonymous. These three substitutions represent mutations obtained during adaptation in cell culture between passage two and passage five. The mutations A2784G and U5231C are unique to ZIKV PE243 and are not found in any other strains published to date. Phylogenetic analysis based on the entire protein coding region grouped the ZIKV PE243 isolate with another 2015 Brazilian isolate (KU321639, 'ZikaSPH2015') with 100% posterior support (Fig 1). As expected, our isolate clusters with other strains from the Americas which belong to the Asian lineage that is attributed to the epidemic in French Polynesia in 2013 (Fig 1). Previous findings have shown that American isolates are genetically very comparable, with approximately 99% homology at the nucleotide level, and there is less than 12% diversity between strains from both African and Asian lineages [24, 53]. Our data are in agreement with this as ZIKV PE243 demonstrates a strong degree of conservation at amino acid level (98.3% pairwise identity) with sequences from 62 isolates (Fig 2). ZIKV PE243 shares the greatest level of similarity with the Brazilian isolate ZikaSPH2015 (99.9% at the nucleotide level and 99.97% at amino acid level) [54] and the passage two isolate matched the coding region precisely. There is no obvious virological explanation, based upon our sequence analysis, for the increased occurrence of neurological disease cases associated with the outbreak in Brazil. This is in accordance with other findings which have similarly suggested that there are no specific mutations in the viral genome associated with severe cases [54]. However, the role of mutations in ZIKV isolates needs to be assessed by reverse genetics approaches to provide conclusive evidence.

We also successfully sequenced both the 5' and 3' non-coding regions (Figs 3 and 4). Of the 62 sequences publicly available (as of 16th April 2016), 48 sequences with 5'UTR information are shown in the consensus alignment (Fig 3). ZIKV strains ZIKV/*Homo sapiens*/NGA/ibH-30656_SM21V1-V3/1968 and ZIKV/*Macaca mulatta*/UGA/MR-766_SM150-V8/1947 contain large insertions and were subsequently excluded from 5'UTR analysis. The 5'UTR of ZIKV PE243 shares 100% sequence identity with the consensus sequence (the most common bases between all sequences analyzed) and overall very few mismatches are detected across all 48 sequences studied. The 5'UTR is largely conserved between isolates of the same lineage and is approximately 107 nucleotides long in isolates from the Asian lineage, similar to the length shown for MR766 strain and other African lineage viruses. There was strong similarity between ZIKV PE243 and Natal RGN, a Brazilian isolate associated with microcephaly [10], while ZIKV PE243 was associated with classical symptoms. Similarly, there are few mismatches between known 3'UTRs (Fig 4). These non-coding regions are expected to be approximately 428 nucleotides in length as seen for many Asian and African isolates.

ZIKV PE243 produces interferon antagonist sfRNA

The host interferon response is known to be essential for fighting viral infections and preventing virus replication, including mosquito-borne flaviviruses [55–58]. This has been specifically illustrated for ZIKV as *in vivo* pathogenesis studies require murine models lacking type I interferon [59], while type III interferon has been shown to have a protective role against ZIKV infection in human placental cells [60]. Furthermore, ZIKV NS5 has recently been described as a type I IFN signaling antagonist that targets STAT2 [61]. Indeed, ZIKV PE243 was also susceptible to type I interferon responses and produced much larger plaque sizes in the type I interferon incompetent A549/BVDV-Npro cell line than in A549 cells (S1 Fig).

However, viruses also employ mechanisms that allow them to counteract the host's interferon responses in order to replicate efficiently. Mosquito- and tick-borne flaviviruses express sfRNA derived from the 3' terminus, which is resistant to RNase (XRN1)-mediated virus
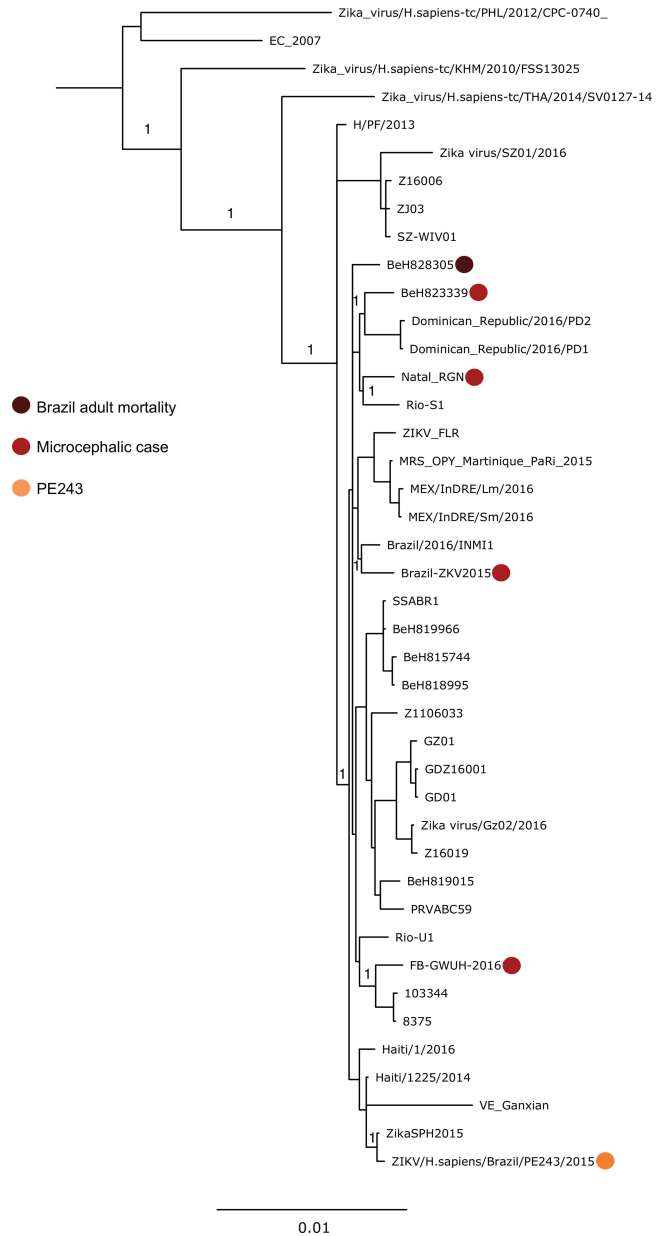
53

54

Fig 1. Bayesian maximum clade credibility tree generated from coding sequence data. Bayesian posterior probabilities are given at nodes of importance. Isolates which have been implicated in particular diseases are highlighted, as is the ZIKV PE243 isolate we have sequenced. GenBank accession numbers of all sequences used are given in S1 Table. EC_2007 refers to the epidemic consensus sequence generated from the Yap Island outbreak in 2007 (EU545988).

doi:10.1371/journal.pntd.0005048.g001

genome degradation due to RNA stem loop structures and pseudoknots in this region [27, 28]. Interestingly, sfRNA has been implicated in pathogenesis, immune evasion and inhibition of small RNA-based responses [29–34]. Thus, a similar subgenomic RNA produced during ZIKV infection could be important in the development of disease and virus-host interactions. Based on our sequence data and comparisons to other mosquito-borne flavivirus 3'UTRs, we predicted the structure of ZIKV PE243 sfRNA (Fig 5). Secondary structures, specific for flavivirus 3'UTRs, were detected in the 3'UTR of ZIKV PE243 by Clustal alignments of the 3'UTR of ZIKV PE243, yellow fever virus (X03700, K02749), DENV2 (M19197), Kunjin virus (AY274504), Japanese encephalitis virus (AF014161) and Murray Valley encephalitis virus
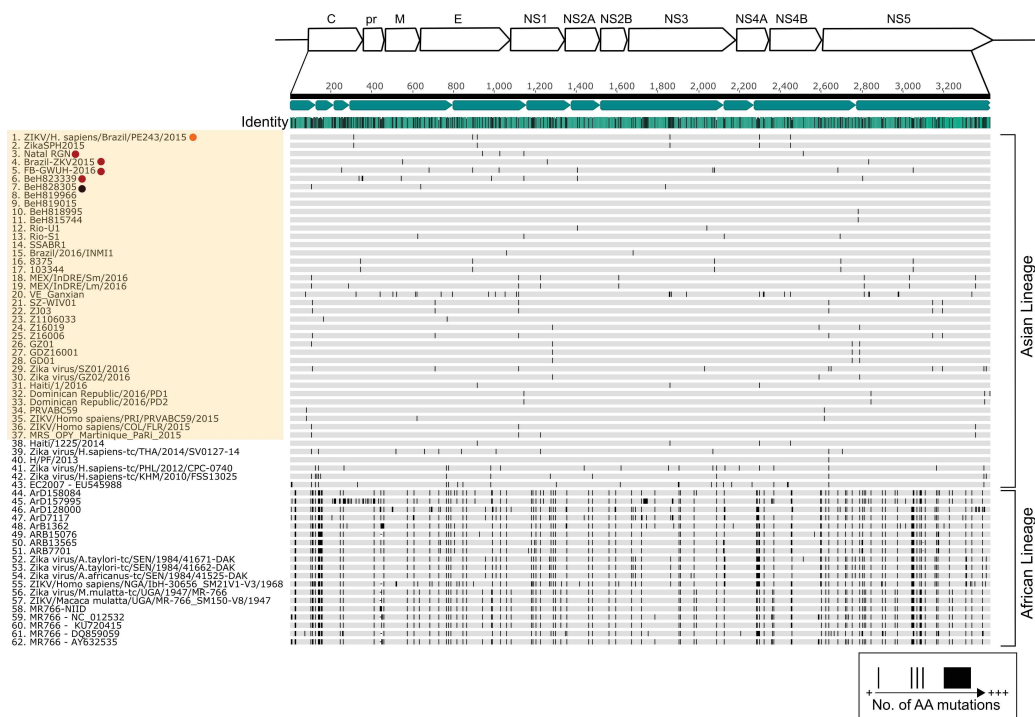
Fig 2. Comparison of African and Asian lineage ZIKV protein coding regions. The mean pairwise identity of all pairs at a given position is indicated by the identity bar; light blue denotes 100% pairwise identity, dark blue highlights positions possessing less than 100% pairwise identity. Positions and quantity of amino acid substitutions are indicated by black bands within grey sequence bars. Sequences 1–37, highlighted yellow, correspond to the outbreak originating in 2015 in South America. Microcephaly, adult mortality and ZIKV PE243 associated sequences are highlighted as previously described in Fig 1.

doi:10.1371/journal.pntd.0005048.g002

55

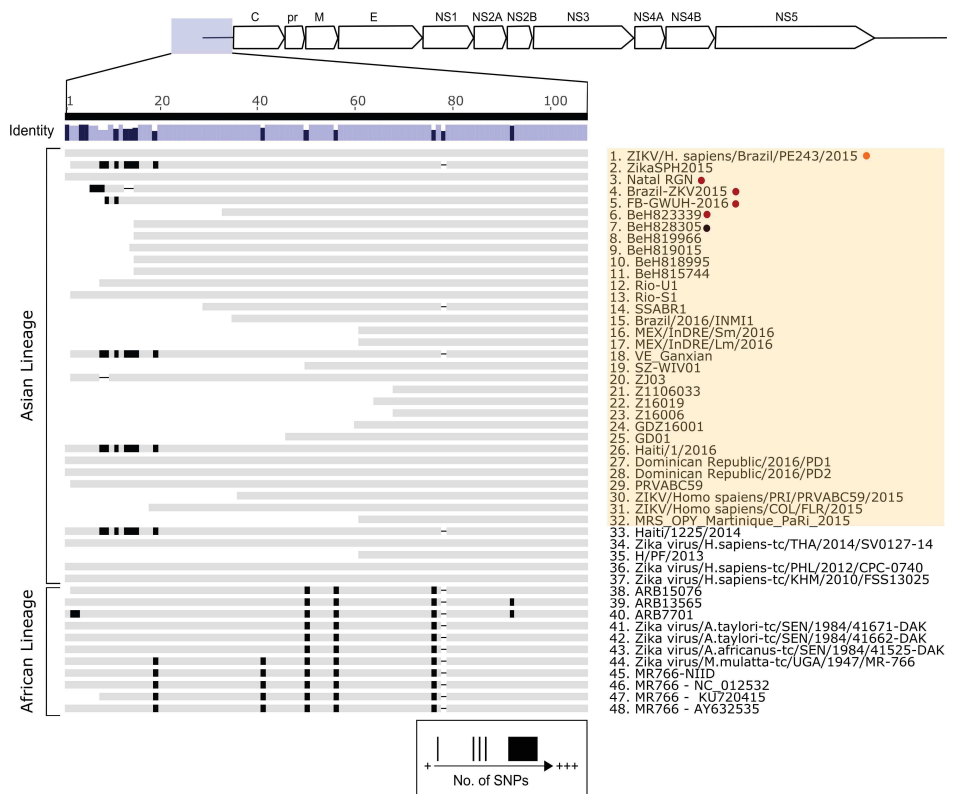**Fig 3. Comparison of the 5'UTR nucleotide sequences of Asian and African ZIKV isolates.** The mean pairwise identity of all pairs at a given position is indicated by the identity bar; lilac is indicative of 100% pairwise identity, dark purple highlights positions possessing <100% pairwise identity. Positions and quantity of single nucleotide polymorphisms (SNPs) are represented as black bands within grey sequence bars. Sequences 1–32, highlighted orange, correspond to the outbreak originating in 2015 in Brazil. Microcephaly, adult mortality and ZIKV PE243 associated sequences are highlighted as previously described in Fig 1.

(AF161266) in combination with Mfold. Putative pseudoknot interactions were determined by hand. Further analysis was also carried out to compare the 3'UTR sequences between ZIKV PE243 and 3 African strain isolates (two MR766 isolates [AY632535, KX377335] and another African isolate [KU955592]). Our comparisons suggest that the sequence differences between these Asian and African isolates do not, or are unlikely to, affect the predicted sfRNA structure (S2 Fig, S3 Fig and S2 Table).

Our sequence data for ZIKV PE243 and predictive analysis suggested that the ZIKV sfRNA molecule begins 15 nt after the stop codon of the open reading frame and is 413 nt in length. This was further confirmed by northern blot analysis, which indicates a band at the anticipated size present only in ZIKV PE243 infected cell lysate (Fig 6). It is important to determine whether this molecule is involved in inhibition of type I IFN production as previously described for other flavivirus sfRNAs [27]. To test this hypothesis, cells were co-transfected
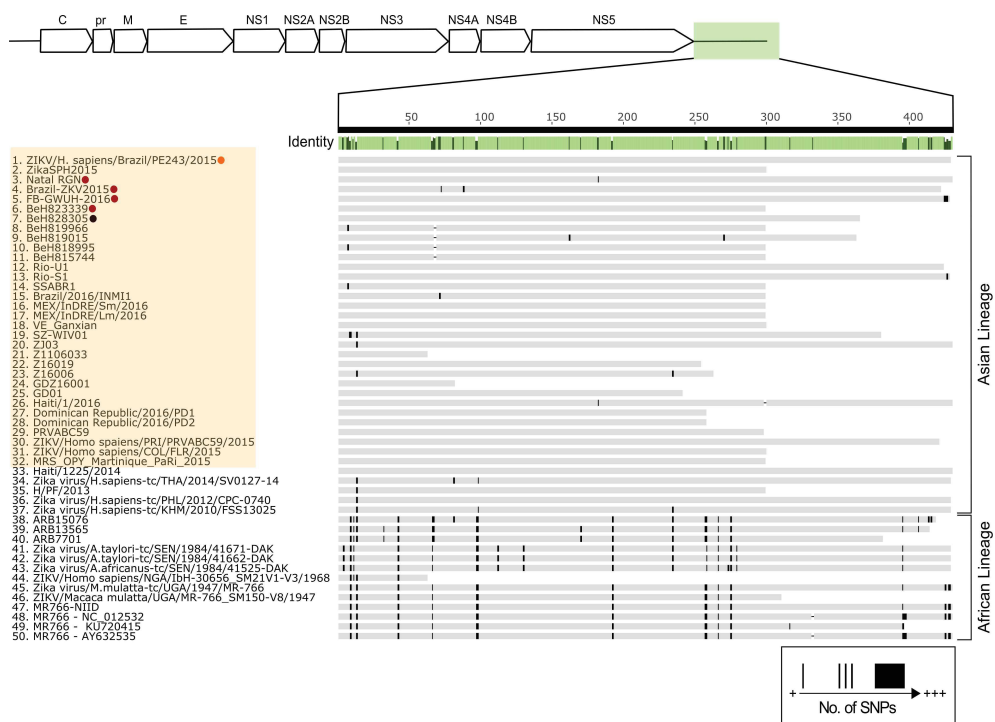
56

Fig 4. Comparison of the 3'UTR nucleotide sequences of Asian and African ZIKV isolates. The mean pairwise identity of all pairs at a given position is indicated by the identity bar; light green is indicative of 100% pairwise identity, dark green highlights positions possessing less than 100% pairwise identity. Sequences 1–32, highlighted orange, correspond to the outbreak originating in 2015 in Brazil. Microcephaly, adult mortality and ZIKV PE243 associated sequences are highlighted as previously described in Fig 1.

doi:10.1371/journal.pntd.0005048.g004

with a reporter plasmid (p125Luc) expressing Firefly luciferase under the control of the IFN-β promoter as well as plasmids expressing either ZIKV or DENV 3'UTRs which contain the sfRNA sequences. The IFN-β promoter was stimulated by treating with poly I:C (Fig 7).

As demonstrated in Fig 7, ZIKV PE243 sfRNA reduced activation of the IFN-β promoter to the same level as DENV sfRNA compared to MBP-HDVr control. This shows that ZIKV sfRNA functions in a similar manner to other flavivirus sfRNA molecules and interacts with important innate immune responses that may impact on virus replication and thus the severity of the clinical outcome.

To further understand the mechanism of action ZIKV sfRNA molecules use to antagonize the interferon response, the above assay was repeated this time using specific inducers of type I interferon induction components, RIG-I and MDA-5 [41, 42]. Receptors such as RIG-I and MDA-5 signal for the induction of IFN-α/β production through the detection of viral nucleic acid [62, 63]. As shown in Fig 8, stimulation of RIG-I (Fig 8A) results in a significant decrease in IFN-β promoter activity in the presence of both DENV and ZIKV sfRNAs compared to the control. In contrast MDA-5 (Fig 8B) stimulation did not alter the activity of the IFN-β promoter in the presence of DENV sfRNA, although a weak but significant decrease was observed
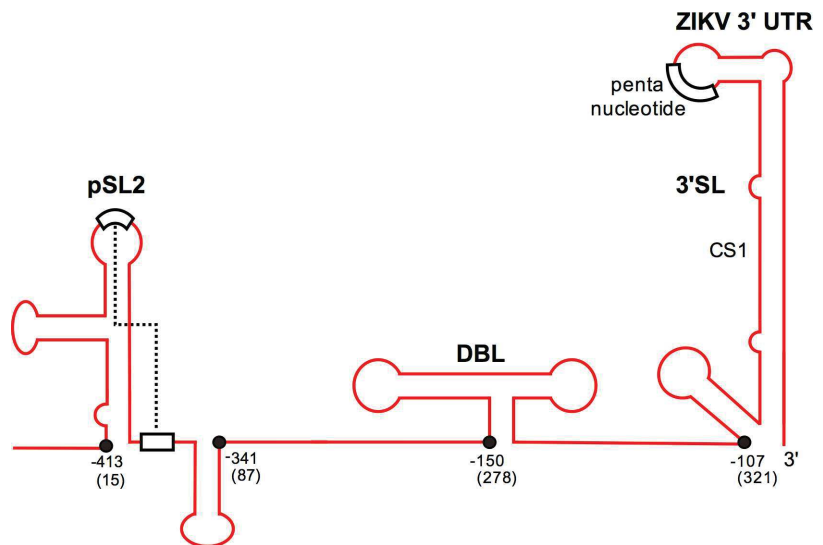
57

Fig 5. The predicted structure of ZIKV PE243 3'UTR. 5'-3' of the ZIKV PE243 3'UTR sequence, left to right. The arrow indicates the predicted start of sfRNA. Nucleotides are indicated either counted from the 3' (indicated as negative numbers) or from the start of the 3'UTR (positive number in brackets). SL, stem loop structure; DBL, dumbbell structure; 3'SL; 3' end stem loop structure. The dotted line represents the predicted pseudoknot.

in ZIKV sfRNA expressing cells. These data suggest that both ZIKV and DENV antagonize RIG-I mediated type I interferon induction. Our data is consistent with previous findings for DENV sfRNA which found that DENV sfRNA binds TRIM25 interfering with its deubiquitylation, consequently hindering RIG-I mediated interferon induction [34]. Only ZIKV sfRNA antagonized MDA-5 activity in this assay, although the biological significance of this is yet to be clarified.

Over the past 40 years there has be an upsurge in the number of cases of important arbovirus infections such as DENV, CHIKV and West Nile virus (WNV), and ZIKV is now another emerging arbovirus of significant clinical importance. The factors involved in the emergence of ZIKV from a rarely detected pathogen to a major epidemic are yet to be determined and could include genetic adaptation, environmental influences, interactions with other pathogens within infected individuals and changes in population dynamics of the virus. To date, the northeast region of Brazil has reported a significant increase in cases of microcephaly and it is important to understand the determinants that lead to this clinical outcome. It has been suggested that alterations in codon usage in the NS1 gene may have facilitated an adaptation towards improved fitness for human infections in the Asian lineage over the African [64]. These changes, combined with the geographical ranges throughout the Americas of its vector population, may have contributed to its accelerated spread. More work is required to analyze these possibilities, and reverse genetics systems in particular will be key to studying mutations and genetic diversity within viral populations. The 5' and 3'UTRs are important for virus replication and are therefore required for the development of such reverse genetic systems [65] that may be used in vaccine development or to advance knowledge of virus-host interactions. In
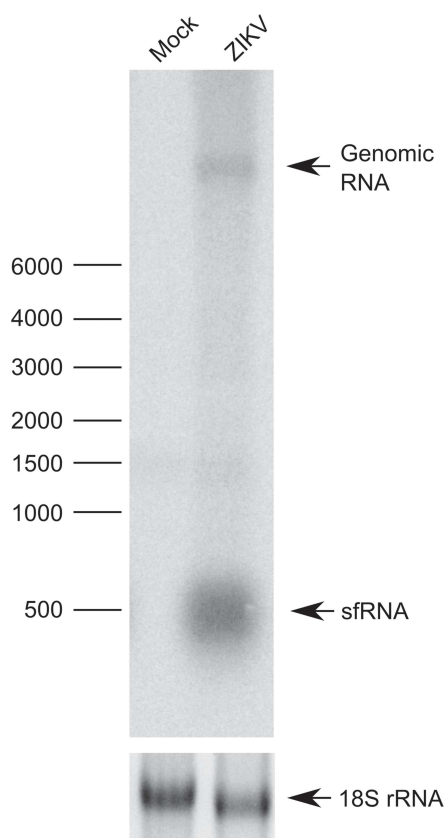
Fig 6. sfRNA production in ZIKV PE243 infection. Top panel: Vero E6 cells were infected with ZIKV isolate PE243 and sfRNA detected by northern blot. Total RNA isolated from Vero E6 cells infected with ZIKV PE243 was separated on a denaturing agarose gel and transferred to a nylon membrane as described in Materials and methods. Radiolabeled DNA probe complementary to 3'UTR was used to detect genomic RNA and sfRNA. Bottom panel: assessed amounts of 18S ribosomal RNAs (fluorescently labelled with ethidium bromide) prior to transfer.

doi:10.1371/journal.pntd.0005048.g006

order to understand not only ZIKV evolution and pathogenesis but also to support the development of virus-based tools, it is imperative to generate full virus genome sequences from ZIKV isolates in the Americas and elsewhere associated with classical and non-classical symptoms. Although new scientific information about ZIKV is published on a near daily basis, many avenues of research are yet to be fully explored in order to understand the clinical manifestations surrounding this outbreak. Characterization of the full sequence of ZIKV PE243 from a patient with symptoms classically associated with infection adds to our understanding of the virus genetics. We have also shown that ZIKV, like other pathogenic flaviviruses infecting humans, encodes sfRNA which inhibits type I interferon induction and thus is likely to
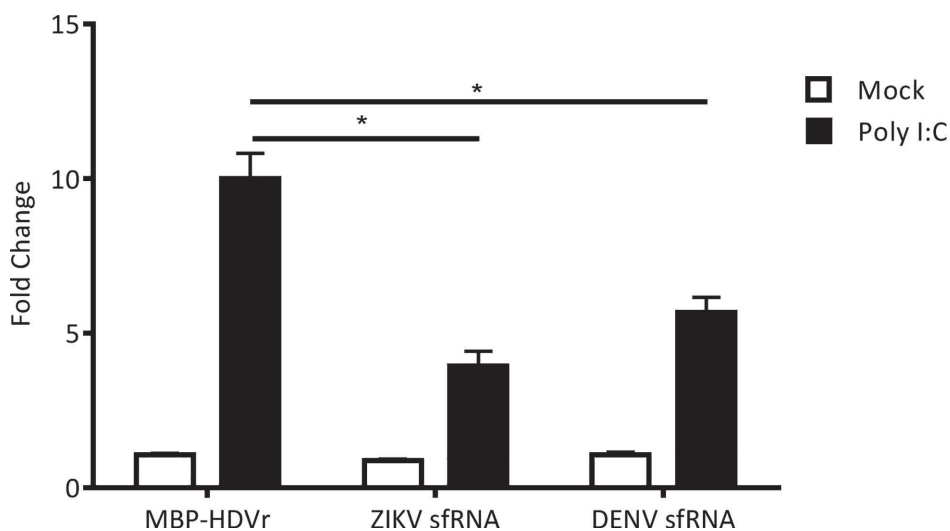
Fig 7. Activation of the IFN-β promoter by poly I:C in cells over expressing ZIKV sfRNA. A549 cells were co-transfected with either pDEST-DENV-3'UTR, pDEST-ZIKV PE243-3'UTR or pDEST40-MBP (sfRNA over-expression plasmids and MBP-HDVr control, respectively) and p125Luc IFN-β promoter reporter (expressing Firefly luciferase) along with pRL-CMV (internal control, expressing *Renilla* luciferase). The IFN-β promoter was stimulated by transfecting poly I:C 24 h after the primary transfection. The relative luciferase activity (Firefly/*Renilla*) was analyzed at 24 h following the second transfection. The mean with standard error is shown for three independent experiments performed in triplicate; values of independent experiments were used for analysis. The data were normalized to cells transfected with pDEST40-MBP without any poly I:C treatment. Asterisk (*) indicates significance (2-way ANOVA, $p < 0.05$).

doi:10.1371/journal.pntd.0005048.g007
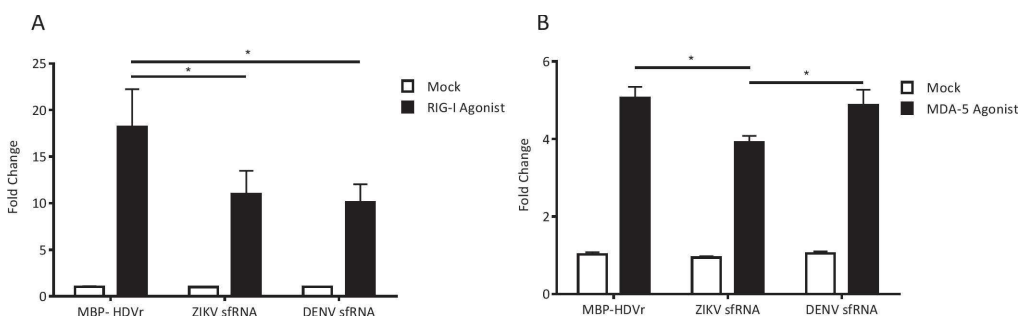
Fig 8. Activation of the IFN-β promoter by RIG-I or MDA-5 agonists in cells over-expressing ZIKV sfRNA. A549 cells were co-transfected as described with either pDEST-DENV-3'UTR, pDEST-ZIKV PE243-3'UTR or pDEST40-MBP and p125Luc IFN-β promoter reporter along with pRL-CMV. The IFN-β promoter was stimulated by transfecting either RIG-I agonist (Neo[1-99] IVT-RNA) (A) or MDA-5 agonist (Vero cell produced EMCV RNA) (B) 24 h after the primary transfection. The relative luciferase activity (Firefly/*Renilla*) was analyzed at 24 h following the second transfection. The mean with standard error is shown for three independent experiments performed in duplicate; values of independent experiments were used for analysis. The data were normalized to cells transfected with pDEST40-MBP without any agonist treatment. Asterisk (*) indicates significance (2-way ANOVA, $p < 0.05$).

doi:10.1371/journal.pntd.0005048.g008

60

contribute to viral pathogenesis. Our interferon induction assays suggest that ZIKV sfRNA may have broader antagonist activity compared to DENV sfRNA, which could contribute to disease outcome and requires further investigation. The data shown here give important insights into virus-host interactions that will help guide future research efforts in this field.

Supporting Information

S1 Table. ZIKV isolate information and data.
(DOCX)

S2 Table. Summary of 3'UTR mutations and associated secondary structures. Positions of single nucleotide mutations within the predicted sfRNA sequences of three African lineage isolates compared to ZIKV PE243 sfRNA. Mutations are described as Asian lineage: African lineage. * indicates MR766 conserved mutations.
(DOCX)

S1 Fig. Type I interferon inhibits ZIKV PE243. Virus growth was analyzed by plaque size comparisons in human A549 (interferon competent) and A549/BVDV-Npro (type I interferon incompetent) cell lines.
(TIF)

S2 Fig. Alignment and comparison between the 3'UTRs of ZIKV PE243 and 3 African lineage viruses. Accession numbers African ZIKV: MR766 isolates AY632535 and KX377335; further strain KU955592. Predicted sequence elements and structures are indicated.
(DOCX)

S3 Fig. Location of African ZIKV 3'UTR mutations relative to ZIKV PE243. Shown is 5'-3' of the ZIKV PE243 3'UTR sequence, left to right (as also shown in Fig 5). Asterisks indicate conserved mutations between all compared African lineage sequences (isolates AY632535, KX377335 and KU955592) and location in the predicted ZIKV PE243 sfRNA.
(TIF)

S1 File. Data and methods for use of mouse anti-ZIKV serum as well as antibodies against ZIKV E protein.
(DOCX)

Acknowledgments

We acknowledge colleagues worldwide for sharing sequence data on public databases to support ongoing research efforts. We also thank Professor Richard E Randall (University of St Andrews) for cell lines.

Author Contributions

Conceptualization: CLD BB SLC GSW JH RFdOF LJP JR AMO AHP JM BDL RB ES AK.

Data curation: JH AK.

Formal analysis: CLD BB SLC VVR JJC MS MV JH GSW ADSF CD RB ES AK.

Investigation: CLD BB SLC VVR JJC MTC RFdOF LJP GSW ADSF CD JH MV MS LZ.

Methodology: CLD BB SLC VVR GSW ADSF JH RFdOF LJP JR RB ES AK.

Project administration: AK ES.

61

Resources: JR MTC RFdOF LJP GF AAS.

Software: JH.

Supervision: AK ES RB.

Validation: CLD BB SLC VVR JJC MS GSW ADSF CD JH MV.

Visualization: CLD SLC BB VVR JJC MS MV ES AK.

Writing – original draft: AK CLD BB SLC RFdOF LJP GSW JH AHP JM RB ES.

Writing – review & editing: CLD BB SLC VVR JJC RFdOF LJP GSW ADSF CD JH MV MS AMO AHP JM JR BDL RB ES AK.

References

1. Hancock WT, Marfel M, Bel M. Zika virus, French Polynesia, South Pacific, 2013. Emerg Infect Dis. 2014; 20(11):1960. doi: 10.3201/eid2011.141380 PMID: 25341051; PubMed Central PMCID: PMCPMC4214323.

2. Cao-Lormeau VM, Musso D. Emerging arboviruses in the Pacific. Lancet. 2014; 384(9954):1571–2. doi: 10.1016/S0140-6736(14)61977-2 PMID: 25443481.

3. Dupont-Rouzeyrol M, O'Connor O, Calvez E, Daures M, John M, Grangeon JP, et al. Co-infection with Zika and dengue viruses in 2 patients, New Caledonia, 2014. Emerg Infect Dis. 2015; 21(2):381–2. doi: 10.3201/eid2102.141553 PMID: 25625687; PubMed Central PMCID: PMCPMC4313662.

4. Musso D, Nilles EJ, Cao-Lormeau VM. Rapid spread of emerging Zika virus in the Pacific area. Clin Microbiol Infect. 2014; 20(10):O595–6. doi: 10.1111/1469-0691.12707 PMID: 24909208.

5. Tognarelli J, Ulloa S, Villagra E, Lagos J, Aguayo C, Fasce R, et al. A report on the outbreak of Zika virus on Easter Island, South Pacific, 2014. Arch Virol. 2015. doi: 10.1007/s00705-015-2695-5 PMID: 26611910.

6. Campos GS, Bandeira AC, Sardi SI. Zika Virus Outbreak, Bahia, Brazil. Emerg Infect Dis. 2015; 21 (10):1885–6. doi: 10.3201/eid2110.150847 PMID: 26401719; PubMed Central PMCID: PMCPMC4593454.

7. Zanluca C, Melo VC, Mosimann AL, Santos GI, Santos CN, Luz K. First report of autochthonous transmission of Zika virus in Brazil. Mem Inst Oswaldo Cruz. 2015; 110(4):569–72. doi: 10.1590/0074-02760150192 PMID: 26061233; PubMed Central PMCID: PMCPMC4501423.

8. de Oliveira CS, da Costa Vasconcelos PF. Microcephaly and Zika virus. J Pediatr (Rio J). 2016; 92 (2):103–5. doi: 10.1016/j.jped.2016.02.003 PMID: 27036749.

9. Oehler E, Watrin L, Larre P, Leparc-Goffart I, Lastere S, Valour F, et al. Zika virus infection complicated by Guillain-Barre syndrome—case report, French Polynesia, December 2013. Euro Surveill. 2014; 19 (9). PMID: 24626205.

10. Mlakar J, Korva M, Tul N, Popovic M, Poljsak-Prijatelj M, Mraz J, et al. Zika Virus Associated with Microcephaly. N Engl J Med. 2016; 374(10):951–8. doi: 10.1056/NEJMoa1600651 PMID: 26862926.

11. Cao-Lormeau VM, Blake A, Mons S, Lastere S, Roche C, Vanhomwegen J, et al. Guillain-Barre Syndrome outbreak associated with Zika virus infection in French Polynesia: a case-control study. Lancet. 2016. doi: 10.1016/S0140-6736(16)00562-6 PMID: 26948433.

12. Schuler-Faccini L, Ribeiro EM, Feitosa IM, Horovitz DD, Cavalcanti DP, Pessoa A, et al. Possible Association Between Zika Virus Infection and Microcephaly—Brazil, 2015. MMWR Morb Mortal Wkly Rep. 2016; 65(3):59–62. doi: 10.15585/mmwr.mm6503e2 PMID: 26820244.

13. Rasmussen SA, Jamieson DJ, Honein MA, Petersen LR. Zika Virus and Birth Defects—Reviewing the Evidence for Causality. N Engl J Med. 2016:In press. doi: 10.1056/NEJMsr1604338 PMID: 27074377.

14. WHO. Situation Report: Zika virus, Microcephaly and Guillain-Barre syndrome. The World Health Organisation 2016.

15. Weaver SC, Costa F, Garcia-Blanco MA, Ko AI, Ribeiro GS, Saade G, et al. Zika virus: History, emergence, biology, and prospects for control. Antiviral Res. 2016; 130:69–80. doi: 10.1016/j.antiviral.2016.03.010 PMID: 26996139.

16. Weaver SC, Reisen WK. Present and future arboviral threats. Antiviral Res. 2010; 85(2):328–45. doi: 10.1016/j.antiviral.2009.10.008 PMID: 19857523; PubMed Central PMCID: PMCPMC2815176.

17. Chouin-Carneiro T, Vega-Rua A, Vazeille M, Yebakima A, Girod R, Goindin D, et al. Differential Susceptibilities of Aedes aegypti and Aedes albopictus from the Americas to Zika Virus. PLoS Negl Trop Dis. 2016; 10(3):e0004543. doi: 10.1371/journal.pntd.0004543 PMID: 26938868; PubMed Central PMCID: PMCPMC4777396.

18. Wong PS, Li MZ, Chong CS, Ng LC, Tan CH. Aedes (Stegomyia) albopictus (Skuse): a potential vector of Zika virus in Singapore. PLoS Negl Trop Dis. 2013; 7(8):e2348. doi: 10.1371/journal.pntd.0002348 PMID: 23936579; PubMed Central PMCID: PMCPMC3731215.

19. Grard G, Caron M, Mombo IM, Nkoghe D, Mboui Ondo S, Jiolle D, et al. Zika virus in Gabon (Central Africa)—2007: a new threat from Aedes albopictus? PLoS Negl Trop Dis. 2014; 8(2):e2681. doi: 10.1371/journal.pntd.0002681 PMID: 24516683; PubMed Central PMCID: PMCPMC3916288.

20. Villamil-Gomez WE, Gonzalez-Camargo O, Rodriguez-Ayubi J, Zapata-Serpa D, Rodriguez-Morales AJ. Dengue, chikungunya and Zika co-infection in a patient from Colombia. J Infect Public Health. 2016. doi: 10.1016/j.jiph.2015.12.002 PMID: 26754201.

21. Lindenbach BD, Murray CL, Thiel HJ, Rice CM. Flaviviridae. In: Knipe DM, Howley PM, editors. Fields Virology. 1. 6th ed. Philadelphia Lippincott Williams and W; 2013. p. 712–46.

22. Lanciotti RS, Kosoy OL, Laven JJ, Velez JO, Lambert AJ, Johnson AJ, et al. Genetic and serologic properties of Zika virus associated with an epidemic, Yap State, Micronesia, 2007. Emerg Infect Dis. 2008; 14(8):1232–9. doi: 10.3201/eid1408.080287 PMID: 18680646; PubMed Central PMCID: PMCPMC2600394.

23. Faye O, Freire CC, Iamarino A, Faye O, de Oliveira JV, Diallo M, et al. Molecular evolution of Zika virus during its emergence in the 20(th) century. PLoS Negl Trop Dis. 2014; 8(1):e2636. doi: 10.1371/journal.pntd.0002636 PMID: 24421913; PubMed Central PMCID: PMCPMC3888466.

24. Haddow AD, Schuh AJ, Yasuda CY, Kasper MR, Heang V, Huy R, et al. Genetic characterization of Zika virus strains: geographic expansion of the Asian lineage. PLoS Negl Trop Dis. 2012; 6(2):e1477. doi: 10.1371/journal.pntd.0001477 PMID: 22389730; PubMed Central PMCID: PMCPMC3289602.

25. Brinton MA, Basu M. Functions of the 3' and 5' genome RNA regions of members of the genus Flavivirus. Virus Res. 2015; 206:108–19. doi: 10.1016/j.virusres.2015.02.006 PMID: 25683510; PubMed Central PMCID: PMCPMC4540327.

26. Villordo SM, Carballeda JM, Filomatori CV, Gamarnik AV. RNA Structure Duplications and Flavivirus Host Adaptation. Trends Microbiol. 2016; 24(4):270–83. doi: 10.1016/j.tim.2016.01.002 PMID: 26850219; PubMed Central PMCID: PMCPMC4808370.

27. Roby JA, Pijlman GP, Wilusz J, Khromykh AA. Noncoding subgenomic flavivirus RNA: multiple functions in West Nile virus pathogenesis and modulation of host responses. Viruses. 2014; 6(2):404–27. doi: 10.3390/v6020404 PMID: 24473339; PubMed Central PMCID: PMCPMC3939463.

28. Clarke BD, Roby JA, Slonchak A, Khromykh AA. Functional non-coding RNAs derived from the flavivirus 3' untranslated region. Virus Res. 2015; 206:53–61. doi: 10.1016/j.virusres.2015.01.026 PMID: 25660582.

29. Schnettler E, Sterken MG, Leung JY, Metz SW, Geertsema C, Goldbach RW, et al. Noncoding flavivirus RNA displays RNA interference suppressor activity in insect and Mammalian cells. J Virol. 2012; 86(24):13486–500. doi: 10.1128/JVI.01104-12 PMID: 23035235; PubMed Central PMCID: PMCPMC3503047.

30. Schnettler E, Tykalova H, Watson M, Sharma M, Sterken MG, Obbard DJ, et al. Induction and suppression of tick cell antiviral RNAi responses by tick-borne flaviviruses. Nucleic Acids Res. 2014; 42 (14):9436–46. doi: 10.1093/nar/gku657 PMID: 25053841; PubMed Central PMCID: PMCPMC4132761.

31. Chang RY, Hsu TW, Chen YL, Liu SF, Tsai YJ, Lin YT, et al. Japanese encephalitis virus non-coding RNA inhibits activation of interferon by blocking nuclear translocation of interferon regulatory factor 3. Vet Microbiol. 2013; 166(1–2):11–21. doi: 10.1016/j.vetmic.2013.04.026 PMID: 23755934.

32. Moon SL, Dodd BJ, Brackney DE, Wilusz CJ, Ebel GD, Wilusz J. Flavivirus sfRNA suppresses antiviral RNA interference in cultured cells and mosquitoes and directly interacts with the RNAi machinery. Virology. 2015; 485:322–9. doi: 10.1016/j.virol.2015.08.009 PMID: 26331679; PubMed Central PMCID: PMCPMC4619171.

33. Pijlman GP, Funk A, Kondratieva N, Leung J, Torres S, van der Aa L, et al. A highly structured, nuclease-resistant, noncoding RNA produced by flaviviruses is required for pathogenicity. Cell Host Microbe. 2008; 4(6):579–91. doi: 10.1016/j.chom.2008.10.007 PMID: 19064258.

34. Manokaran G, Finol E, Wang C, Gunaratne J, Bahl J, Ong EZ, et al. Dengue subgenomic RNA binds TRIM25 to inhibit interferon expression for epidemiological fitness. Science. 2015; 350(6257):217–21. doi: 10.1126/science.aab3369 PMID: 26138103; PubMed Central PMCID: PMCPMC4824004.

35. Schuessler A, Funk A, Lazear HM, Cooper DA, Torres S, Daffis S, et al. West Nile virus noncoding subgenomic RNA contributes to viral evasion of the type I interferon-mediated antiviral response. J

63

Virol. 2012; 86(10):5708–18. doi: 10.1128/JVI.00207-12 PMID: 22379089; PubMed Central PMCID: PMCPMC3347305.

36. Bidet K, Dadlani D, Garcia-Blanco MA. G3BP1, G3BP2 and CAPRIN1 are required for translation of interferon stimulated mRNAs and are targeted by a dengue virus non-coding RNA. PLoS Pathog. 2014; 10(7):e1004242. doi: 10.1371/journal.ppat.1004242 PMID: 24992036; PubMed Central PMCID: PMCPMC4081823.

37. Brennan B, Welch SR, Elliott RM. The consequences of reconfiguring the ambisense S genome seg-ment of Rift Valley fever virus on viral replication in mammalian and mosquito cells and for genome packaging. PLoS Pathog. 2014; 10(2):e1003922. doi: 10.1371/journal.ppat.1003922 PMID: 24550727; PubMed Central PMCID: PMCPMC3923772.

38. Carlos TS, Young DF, Schneider M, Simas JP, Randall RE. Parainfluenza virus 5 genomes are located in viral cytoplasmic bodies whilst the virus dismantles the interferon-induced antiviral state of cells. J Gen Virol. 2009; 90(Pt 9):2147–56. doi: 10.1099/vir.0.012047–0 PMID: 19458173; PubMed Central PMCID: PMCPMC2885057.

39. Hilton L, Moganeradj K, Zhang G, Chen YH, Randall RE, McCauley JW, et al. The NPro product of bovine viral diarrhea virus inhibits DNA binding by interferon regulatory factor 3 and targets it for pro-teasomal degradation. J Virol. 2006; 80(23):11723–32. doi: 10.1128/JVI.01145-06 PMID: 16971436; PubMed Central PMCID: PMCPMC1642611.

40. Yoneyama M, Suhara W, Fukuhara Y, Fukuda M, Nishida E, Fujita T. Direct triggering of the type I interferon system by virus infection: activation of a transcription factor complex containing IRF-3 and CBP/p300. Embo J. 1998; 17(4):1087–95. doi: 10.1093/emboj/17.4.1087 PMID: 9463386.

41. Pichlmair A, Schulz O, Tan CP, Rehwinkel J, Kato H, Takeuchi O, et al. Activation of MDA5 requires higher-order RNA structures generated during virus infection. J Virol. 2009; 83(20):10761–9. doi: 10.1128/JVI.00770-09 PMID: 19656871; PubMed Central PMCID: PMCPMC2753146.

42. Rehwinkel J, Tan CP, Goubau D, Schulz O, Pichlmair A, Bier K, et al. RIG-I detects viral genomic RNA during negative-strand RNA virus infection. Cell. 2010; 140(3):397–408. doi: 10.1016/j.cell.2010.01.020 PMID: 20144762.

43. Langmead B, Salzberg SL. Fast gapped-read alignment with Bowtie 2. Nat Methods. 2012; 9(4):357–9. doi: 10.1038/nmeth.1923 PMID: 22388286; PubMed Central PMCID: PMCPMC3322381.

44. Edgar RC. MUSCLE: multiple sequence alignment with high accuracy and high throughput. Nucleic Acids Res. 2004; 32(5):1792–7. doi: 10.1093/nar/gkh340 PMID: 15034147; PubMed Central PMCID: PMCPMC390337.

45. Kearse M, Moir R, Wilson A, Stones-Havas S, Cheung M, Sturrock S, et al. Geneious Basic: an inte-grated and extendable desktop software platform for the organization and analysis of sequence data. Bioinformatics. 2012; 28(12):1647–9. doi: 10.1093/bioinformatics/bts199 PMID: 22543367; PubMed Central PMCID: PMCPMC3371832.

46. Martin DP, Murrell B, Golden M, Khoosal A, Muhire B. RDP4: Detection and analysis of recombination patterns in virus genomes. Virus Evolution. 2015; 1(1). doi: 10.1093/ve/vev003

47. Guindon S, Gascuel O. A simple, fast, and accurate algorithm to estimate large phylogenies by maxi-mum likelihood. Syst Biol. 2003; 52(5):696–704. PMID: 14530136.

48. Huelsenbeck JP, Ronquist F. MRBAYES: Bayesian inference of phylogenetic trees. Bioinformatics. 2001; 17(8):754–5. PMID: 11524383.

49. Darriba D, Taboada GL, Doallo R, Posada D. jModelTest 2: more models, new heuristics and parallel computing. Nat Methods. 2012; 9(8):772. doi: 10.1038/nmeth.2109 PMID: 22847109; PubMed Central PMCID: PMCPMC4594756.

50. Pond SL, Frost SD, Muse SV. HyPhy: hypothesis testing using phylogenies. Bioinformatics. 2005; 21 (5):676–9. doi: 10.1093/bioinformatics/bti079 PMID: 15509596.

51. Ladner JT, Wiley MR, Prieto K, Yasuda CY, Nagle E, Kasper MR, et al. Complete Genome Sequences of Five Zika Virus Isolates. Genome Announc. 2016; 4(3). doi: 10.1128/genomeA.00377-16 PMID: 27174284.

52. Giovanetti M, Faria NR, Nunes MR, de Vasconcelos JM, Lourenco J, Rodrigues SG, et al. Zika virus complete genome from Salvador, Bahia, Brazil. Infect Genet Evol. 2016. doi: 10.1016/j.meegid.2016.03.030 PMID: 27071531.

53. Lanciotti RS, Lambert AJ, Holodniy M, Saavedra S, Signor Ldel C. Phylogeny of Zika Virus in Western Hemisphere, 2015. Emerg Infect Dis. 2016; 22(5):933–5. doi: 10.3201/eid2205.160065 PMID: 27088323; PubMed Central PMCID: PMCPMC4861537.

54. Faria NR, Azevedo Rdo S, Kraemer MU, Souza R, Cunha MS, Hill SC, et al. Zika virus in the Americas: Early epidemiological and genetic findings. Science. 2016; 352(6283):345–9. doi: 10.1126/science.aaf5036 PMID: 27013429.

64

55. Diamond MS, Gale M Jr. Cell-intrinsic innate immune control of West Nile virus infection. Trends Immunol. 2012; 33(10):522–30. doi: 10.1016/j.it.2012.05.008 PMID: 22726607; PubMed Central PMCID: PMCPMC3461102.

56. Lazear HM, Diamond MS. New insights into innate immune restriction of West Nile virus infection. Curr Opin Virol. 2015; 11:1–6. doi: 10.1016/j.coviro.2014.12.001 PMID: 25554924; PubMed Central PMCID: PMCPMC4456296.

57. Green AM, Beatty PR, Hadjilaou A, Harris E. Innate immunity to dengue virus infection and subversion of antiviral responses. J Mol Biol. 2014; 426(6):1148–60. doi: 10.1016/j.jmb.2013.11.023 PMID: 24316047; PubMed Central PMCID: PMCPMC4174300.

58. Castillo Ramirez JA, Urcuqui-Inchima S. Dengue Virus Control of Type I IFN Responses: A History of Manipulation and Control. J Interferon Cytokine Res. 2015; 35(6):421–30. doi: 10.1089/jir.2014.0129 PMID: 25629430; PubMed Central PMCID: PMCPMC4490770.

59. Lazear HM, Govero J, Smith AM, Platt DJ, Fernandez E, Miner JJ, et al. A Mouse Model of Zika Virus Pathogenesis. Cell Host Microbe. 2016; 19(5):720–30. doi: 10.1016/j.chom.2016.03.010 PMID: 27066744; PubMed Central PMCID: PMCPMC4866885.

60. Bayer A, Lennemann NJ, Ouyang Y, Bramley JC, Morosky S, Marques ET Jr., et al. Type III Interferons Produced by Human Placental Trophoblasts Confer Protection against Zika Virus Infection. Cell Host Microbe. 2016; 19(5):705–12. doi: 10.1016/j.chom.2016.03.008 PMID: 27066743; PubMed Central PMCID: PMCPMC4866896.

61. Grant A, Ponia SS, Tripathi S, Balasubramaniam V, Miorin L, Sourisseau M, et al. Zika Virus Targets Human STAT2 to Inhibit Type I Interferon Signaling. Cell Host Microbe.In press.

62. Oshiumi H, Kouwaki T, Seya T. Accessory Factors of Cytoplasmic Viral RNA Sensors Required for Antiviral Innate Immune Response. Front Immunol. 2016; 7:200. doi: 10.3389/fimmu.2016.00200 PMID: 27252702; PubMed Central PMCID: PMCPMC4879126.

63. Yoneyama M, Onomoto K, Jogi M, Akaboshi T, Fujita T. Viral RNA detection by RIG-I-like receptors. Curr Opin Immunol. 2015; 32:48–53. doi: 10.1016/j.coi.2014.12.012 PMID: 25594890.

64. Freire CCdM, Iamarino A, Neto DFdL, Sall AA, Zanotto PMdA. Spread of the pandemic Zika virus lineage is associated with NS1 codon usage adaptation in humans. bioRxiv. 2015. doi: 10.1101/032839

65. Shan C, Xie X, Muruato AE, Rossi SL, Roundy CM, Azar SR, et al. An Infectious cDNA Clone of Zika Virus to Study Viral Virulence, Mosquito Transmission, and Antiviral Inhibitors. Cell Host Microbe. 2016:In press. doi: 10.1016/j.chom.2016.05.004 PMID: 27198478.

65

Selinger, M., Wilkie, G.S., Tong, L., Gu, Q., Schnettler, E., Grubhoffer, L., Kohl, A., 2017: Analysis of tick-borne encephalitis virus-induced host responses in human cells of neuronal origin and interferon-mediated protection. Journal of General Virology 98(8): 2043-2060. DOI: 10.1099/jgv.0.000853 (IF = 2.693)

Corrigendum:
Selinger, M., Wilkie, G.S., Tong, L., Gu, Q., Schnettler, E., Grubhoffer, L., Kohl, A., 2018: Analysis of tick-borne encephalitis virus-induced host responses in human cells of neuronal origin and interferon-mediated protection. Journal of General Virology 99(8):1147-1149. DOI: 10.1099/jgv.0.001109

Analysis of tick-borne encephalitis virus-induced host responses in human cells of neuronal origin and interferon-mediated protection

Martin Selinger,[1,2] Gavin S. Wilkie,[3] Lily Tong,[3] Quan Gu,[3] Esther Schnettler,[3]† Libor Grubhoffer[1,2] and Alain Kohl[3,*]

Abstract

Tick-borne encephalitis virus (TBEV) is a member of the genus *Flavivirus*. It can cause serious infections in humans that may result in encephalitis/meningoencephalitis. Although several studies have described the involvement of specific genes in the host response to TBEV infection in the central nervous system (CNS), the overall network remains poorly characterized. Therefore, we investigated the response of DAOY cells (human medulloblastoma cells derived from cerebellar neurons) to TBEV (Neudoerfl strain, Western subtype) infection to characterize differentially expressed genes by transcriptome analysis. Our results revealed a wide panel of interferon-stimulated genes (ISGs) and pro-inflammatory cytokines, including type III but not type I (or II) interferons (IFNs), which are activated upon TBEV infection, as well as a number of non-coding RNAs, including long non-coding RNAs. To obtain a broader view of the pathways responsible for eliciting an antiviral state in DAOY cells we examined the effect of type I and III IFNs and found that only type I IFN pre-treatment inhibited TBEV production. The cellular response to TBEV showed only partial overlap with gene expression changes induced by IFN-β treatment – suggesting a virus-specific signature – and we identified a group of ISGs that were highly up-regulated following IFN-β treatment. Moreover, a high rate of down-regulation was observed for a wide panel of pro-inflammatory cytokines upon IFN-β treatment. These data can serve as the basis for further studies of host–TBEV interactions and the identification of ISGs and/or lncRNAs with potent antiviral effects in cases of TBEV infection in human neuronal cells.

INTRODUCTION

Tick-borne encephalitis virus (TBEV) is a medically important tick-borne flavivirus and is the causative agent of tick-borne encephalitis (TBE). TBE is widespread in Europe and North Asia, and more than 10 000 cases per year are reported [1]. The Czech Republic has the second highest incidence of TBE in Europe after Russia [2]. The clinical outcome of TBE can vary from sub-clinical cases to severe encephalitis/meningoencephalitis. The European subtype of TBEV is associated with a high ratio of sub-clinical or asymptomatic cases (estimated 70–95 %). Neurologic sequelae were reported in up to 30 % of the patients and the case fatality in adult patients is <2 % [3].

The mechanism(s) by which TBEV crosses the blood–brain barrier (BBB) and enters the CNS are still not clear. Several

routes have been suggested: (i) direct infection of epithelial cells and transport of viruses across basolateral membranes, (ii) cytokine-mediated breakdown of BBB, or (iii) a 'Trojan horse' pathway in which TBEV-infected leukocytes can migrate across the BBB [4, 5]. Once TBEV enters the CNS, neurons are the predominantly infected cell type [6]. Astrocytes were recently also shown to be susceptible to TBEV infection [7]. Immunocytochemistry analysis of brain autopsies from fatal TBE cases detected localization of viral antigens in the spinal cord, brainstem, cerebellum and basal ganglia. Labelling was consistently found in the perikarya and processes of Purkinje cells, large neurons of the dentate nucleus, inferior olives and anterior horns [6]. The suggested mechanism of neural tissue damage during TBEV infection is virus-associated cell death combined with an immunopathogenic role of the cellular/humoral responses of the host

1

immune system, especially CD8+ granzyme B–releasing cytotoxic T cells and macrophages/microglia [8, 9].

The interferon (IFN) response is part of the innate immune system. IFNs activate the expression of hundreds of genes, known as IFN-stimulated genes (ISGs), which elicite the antiviral state [10–12]. In most cell types, type I IFNs (IFN-α and IFN-β), which signal through the IFNAR1/IFNAR2 receptors, are the primary IFNs produced. With regard to the production of type I IFNs in CNS, murine astrocytes and microglia were observed to be the main IFN producers following La Crosse virus (LACV) infection [13]. However, a study by Delhaye *et al.* showed that 16 % of IFN-producing cells in the CNS of mice infected with either Theiler's encephalomyelitis virus (TMEV) or LACV corresponded to neurons [14]. The importance of the type I IFN system in preventing CNS infection in mice was also characterized for West Nile virus (WNV) [15]. Furthermore, the role of IFN-β in preventing viral infection in neuronal cells was shown for human granule cell neurons and cortical neurons when IFN-β pre-treatment resulted in the inhibition of WNV and Saint Louis encephalitis (SLEV) flaviviruses [16]. Recently, type III IFNs were found to play an important role in the immune response to neurotropic viruses. IFN-λ1/2 pre-treatment of human neurons and astrocytes resulted in inhibition of herpes simplex virus 1 (HSV1) [17] and IFN-λ2 pre-treatment reduced WNV infection in murine CNS by decreasing BBB permeability [18]. Type III IFNs bind to IFNLR1/IL10β, which signals through a similar pathway to the type I IFN receptor complex and induces many of the same ISGs [19, 20].

To date, only the type I IFN system has been shown to be essential for control of TBEV and related Langat virus (LGTV) systemic infection of the murine CNS [21, 22]. Moreover, type I IFN responses have been shown to protect murine astrocytes – a CNS cell type – from tick-borne flavivirus infection [23]. IFN-α pre-treatment of murine neuroblastoma cells resulted in a decrease in the production of LGTV [24]. However, to date no study has described the host response of human neuronal cells upon TBEV infection. Here we investigated the responses to TBEV infection and type I IFNs in DAOY cells (human medulloblastoma cells derived from cerebellar neurons) by transcriptome analysis. We previously used this cell line to investigate morphological changes post-TBEV infection [25], and here expanded our study of virus–cell interactions. Our results show that in response to TBEV infection DAOY cells modulate the expression of ISGs, type III IFNs and pro-inflammatory cytokines. We found that the virus-induced responses differed from those induced by IFN-ß, with partial overlap. We examined the protective effect of type I and III IFNs on TBEV infection to assess pathways capable of eliciting an antiviral state in DAOY cells. Host responses mediated by type I but not type III IFNs mediated antiviral protection. Virus-specific host response signatures may be relevant for understanding TBEV pathogenesis.

RESULTS

Human DAOY medulloblastoma cell line expresses markers typical for neural precursor cells

As TBEV infection can result in CNS damage, we studied the antiviral host response against TBEV strain Neudoerfl (Western subtype) *in vitro* in the human medulloblastoma-derived neuronal cell line, DAOY HTB-186. These cells are derived from the cerebellum [26], one of the brain areas affected most during TBE infection [6], and were shown to be susceptible to TBEV strain Hypr [25]. In order to determine the infection rate of TBEV Neudoerfl, DAOY cells were infected at a multiplicity of infection (m.o.i.) of 0.1, 1, and 5, respectively, and levels of viral NS3 protein were analysed at 24 h post infection (h p.i.) using an immunofluorescence assay. The infection rates for an m.o.i. 0.1, 1 or 5 at 24 h p.i. were 1.5 % (SD ±0.44), 5.0 % (SD ±0.93) and 19.6 % (SD ±2.25), respectively (Fig. 1a). The m.o.i. refers to the TBEV titre in PS cells (see below); infection rates may therefore vary in other cell lines.

In order to verify the neuronal origin of DAOY cells, we analysed them for the presence of CNS biomarkers – tubulin beta 3 class III (TUBB3), vimentin (VIM) and myelin oligodendrocyte glycoprotein (MOG) [27]. These three CNS biomarkers were found to be among the genes with the highest expression according to transcriptomic analysis [see Tables S1 and S2 (available with the online Supplementary Material) for lists of glial and neuronal markers identified in DAOY cells]. In addition, we characterized the presence of glial fibrillary acidic protein (GFAP) in DAOY cells, which is a commonly used marker for glial cells [28]. The human glioblastoma cell line U-373 MG (Uppsala) was used as a control for glial origin [29]. The expression of GFAP was only detected in U373 cells (14.6 %, SD ±2.5), whereas MOG was detected in both DAOY (18.9 %, SD ±11.0) and U373 (23.4 %, SD ±10.4). Both cell lines were also positive for TUBB3 (45.4 %, SD ±13.1, and 81.7 %, SD ±12.2 for DAOY and U373, respectively) as well as VIM (100 %, SD ±0, and 100 %, SD ±0 for DAOY and U373, respectively), as shown in Fig. 1(b, c) (see also Fig. S1 for separate TUBB3/MOG staining).

Furthermore we analysed the expression of selected glial/neuronal markers in DAOY cells upon TBEV infection, and whether TBEV preferentially targets certain cells (m.o.i. 5; analysis at 24 h p.i.). As shown in Fig. S2(a), the expression rates of TUBB3, MOG and VIM were not significantly changed upon TBEV infection in comparison to control cells (Student's *t*-test; *P*=0.9679, *P*=0.9249 and *P*=0.2244, respectively). No signal was detected for GFAP, which correlates with the data described in Fig. 1. In order to determine whether the presence of a particular marker affects the ability of DAOY cells to be infected with TBEV, we also quantified infected cells positive for TUBB3, MOG or VIM (30.4 %, SD ±5.1; 7.9 %, SD ±2.5; 100.0 %, SD ±0, respectively) (Fig. S2b). These numbers largely correlated with CNS marker expression levels in infected and uninfected cells, as
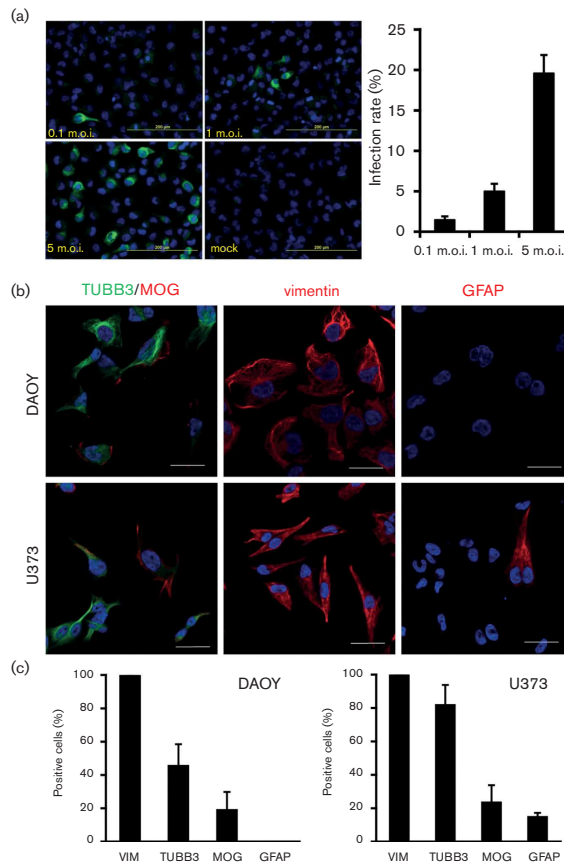
Fig. 1. DAOY cells were susceptible to TBEV infection and expressed both neuronal and glial markers. (a) DAOY cells were seeded on a chamber slide and infected at an m.o.i. of 0.1, 1 and 5 with TBEV Neudoerfl strain. Detection of viral NS3 protein via immunofluorescence was carried out at 24 h p.i. using anti-NS3 antibodies. Representative pictures from two independent experiments (in triplicate per experiment) are shown. The infection rate was calculated as a ratio of the total number of infected cells (positive signal for NS3) to the total number of cells. The average with standard deviation is shown. (b) DAOY and U373 cells were seeded on a chamber slide and incubated 24 h. Cells were stained with antibodies for TUBB3, MOG, VIM and GFAP. Representative pictures from two independent experiments (in triplicate per experiment) are shown. Scale bar represents 20 µm. (c) Cell counts for each of the markers are presented. The average with standard deviation from two independent experiments (in triplicate per experiment) is shown.

shown in Fig. S2(a), suggesting that TBEV did not preferentially infect cells expressing a specific marker.

IFN-β pre-treatment of DAOY cells resulted in reduced production of TBEV

It was previously shown that *in vitro* type I IFN pre-treatment of neuronal cells resulted in decreased production of several neurotropic RNA viruses, including LGTV, WNV and SLEV [16, 30]. To analyse whether IFN-β pre-

treatment can impair TBEV infection, DAOY and A549 cells were pre-treated with human recombinant IFN-β (10, 100, and 1000 ng ml^{-1}) and infected with TBEV 12 h later at an m.o.i. of 5. A549 cells were used as controls, given their wide use in type I IFN studies (for example [31–34]). Cells were incubated for 5 days until a virus-induced cytopathic effect (CPE) was observed in the control wells. Viability assays using MTT were subsequently performed (see the Methods section). We analysed the rescue of cell viability in

69

the presence of recombinant IFN-β compared to uninfected samples. In both cases, rescue effects were observed at IFN concentrations of 10 ng ml^{-1}, culminating at 100 ng ml^{-1} in DAOY cells (Fig. 2a). To further verify the antiviral effect of IFN-β and determine the kinetics of virus production, DAOY cells were treated with recombinant IFN-β (10 ng ml^{-1}) and subsequently infected with TBEV at an m.o.i. of 5 at 12 h post-IFN-β treatment. Samples were harvested at 12, 24, 48 and 72 h p.i. An over 10000-fold decrease in viral titres was observed starting at 24 h p.i. in IFN-β-pre-treated cells (Fig. 2b). Moreover, a decrease of viral NS3 protein levels in IFN-β-pre-treated cells was also observed, as shown in Fig. 2(c).

In order to analyse the activity of viral pattern-recognition/ signalling pathways leading to IFN-β expression, DAOY cells were co-transfected with the p125Luc plasmid encoding the Firefly luciferase reporter gene under the control of IFN-β promoter [35] and the pRL-CMV plasmid encoding *Renilla* luciferase as internal control. Cells were stimulated with poly I:C (1 or 10 µg ml^{-1}) at 24 h post-first transfection and luciferase actvity was determined 24 h post-second transfection. Again, A549 was used for positive controls [36]. No activation of IFN-β promoter was observed in DAOY cells upon poly I:C treatment (Fig. 2d).

IFN-β treatment and TBEV infection induce characteristic transcriptome changes in DAOY cells

To characterize the cellular response to TBEV infection and identify the differentially expressed genes responsible for the inhibition of TBEV replication after IFN-β treatment, an unbiased transcriptome analysis was performed. Infected (m.o.i. 5) and mock-infected DAOY cells at 24 h p.i. in the presence or absence of IFN-β pre-treatment (carried out 12 h prior to infection) were utilized for this analysis. Three biological replicates for each of the four combinations were prepared and successful infection was confirmed by plaque titration assays; again, a decrease in viral titre was observed in IFN-β-pre-treated cells (Fig. 3a). On average, ~48 million reads/sample were generated (Phred quality >30), and these were assembled against the *Homo sapiens* genome using TopHat2 [37]. In total, 94.3 % of the sequence reads were assembled to the reference genome. Differentially expressed genes (Benjamini Hochberg P-value$\leq$0.05 and fold change >1.5 or <−1.5) in comparison to mock-treated cells were identified using Cuffdiff2 [38]. The analysis showed that TBEV infection resulted in the differential expression of 498 genes (Fig. 3b; see Table S3 for a comprehensive list of differentially expressed genes). Moreover, either 155 or 778 genes were found to be differentially expressed in mock- or TBEV-infected cells pre-treated with IFN-β, respectively, thus confirming the high sensitivity of DAOY cells to IFN-β treatment (Fig. 3 and Table S3). Interestingly, IFN-β pre-treatment resulted in the altered expression of a rather unique set of genes: only 12.3 and 29.2 % of the differentially expressed genes identified in mock- and TBEV-infected cells that had been pre-treated with IFN-β were also identified in TBEV-infected cells. The differential expression

analysis was further validated by the relative quantification of eight selected genes using qRT-PCR (Fig. 3c). Significantly decreased numbers of reads mapped to the TBEV genome in IFN-β-pre-treated cells infected with TBEV (613 reads; SD ±61) compared to TBEV-infected cells without IFN-β pre-treatment (176 000 reads; SD ±15733) were observed (Student's t-test; P<0.0001). In addition, the Kraken tool was used to verify any contamination present in the samples. As shown in Table S4, the DAOY cells were free of bacterial or viral contamination, including *Mycoplasma* spp. or human cytomegalovirus, which might have interfered with host responses.

Host response-associated genes, including type III IFNs, are activated upon TBEV infection of DAOY cells

It was recently shown that TBEV infection of mouse brain and human astrocytes resulted in inflammatory responses, which included elevated production of cytokines (IL-1α, IL-1β, IL-6, IL-8, IFN-α and IFN-γ) and chemokines (CCL2/ MCP1, CCL3/MIP12α, CCL4/MIP1β, CCL5/RANTES and CXCL10/IP-10) [7, 39]. As shown in Fig. 4(a), DAOY cells activated a similar panel of cytokine-coding genes upon TBEV infection (CCL3/MIP1α, CCL4/MIP1β, CCL5/ RANTES, CXCL10/IP-10, IL-6 and TNF-α). In addition, five new cytokine-coding genes were identified as being significantly up-regulated, (CXCL2/MIP2α, CXCL11/IP-9, IL-12α, IL-15 and IL-23α), together with the IL-18 receptor accessory protein (IL18RAP). Hundreds of ISGs have been identified as being induced following viral infection (reviewed in [10–12]). Transcriptome analysis of TBEV-infected DAOY cells revealed significant induction of a number of ISGs (Table S3), including IFIT1, IFIT2, RSAD2, OASL, IFIT3, OAS2, ISG15 and ISG20 amongst the most up-regulated (fold-change >2.5; Fig. 4a and Table S5). RIG-I/DDX58 and MDA5/IFIH1 of the retinoic acid-inducible gene I-like receptor family, which are responsible for sensing viral RNA [40], were also significantly up-regulated. A TBEV-directed decrease in IL-2 and IL-4 mRNA levels was documented in the murine spleen [41]. A panel of 277 significantly down-regulated genes in TBEV-infected DAOY cells (fold-change >1.5; Fig. 3b and Table S3) was also observed. RNA28S5, RN7SL2, NOTCH3, COL1A1, BCL9L, BCORL1, POLR2A, FAM71D, IGF2, RN7SL3 and HSPG2 were found to be the most strongly down-regulated genes (fold-change >2.5; Fig. 4 and Table S5). Other than protein-coding genes, a number of non-coding RNAs were also identified as being differentially expressed upon TBEV infection, as shown in Fig. 4(b). However, of these, RN7SL2, RN7SL3 and RNA28S5 are the only RNA genes with known functions. The remaining differentially expressed RNAs were long non-coding RNAs (lncRNAs) with unknown functions. The observed pattern of general activation of host responses upon TBEV infection was also confirmed by Ingenuity Pathway Analysis (IPA) software. Table 1 shows the 10 most significantly affected canonical pathways that include IFN signalling. Furthermore, the unfolded protein response and endoplasmic reticulum stress pathways were
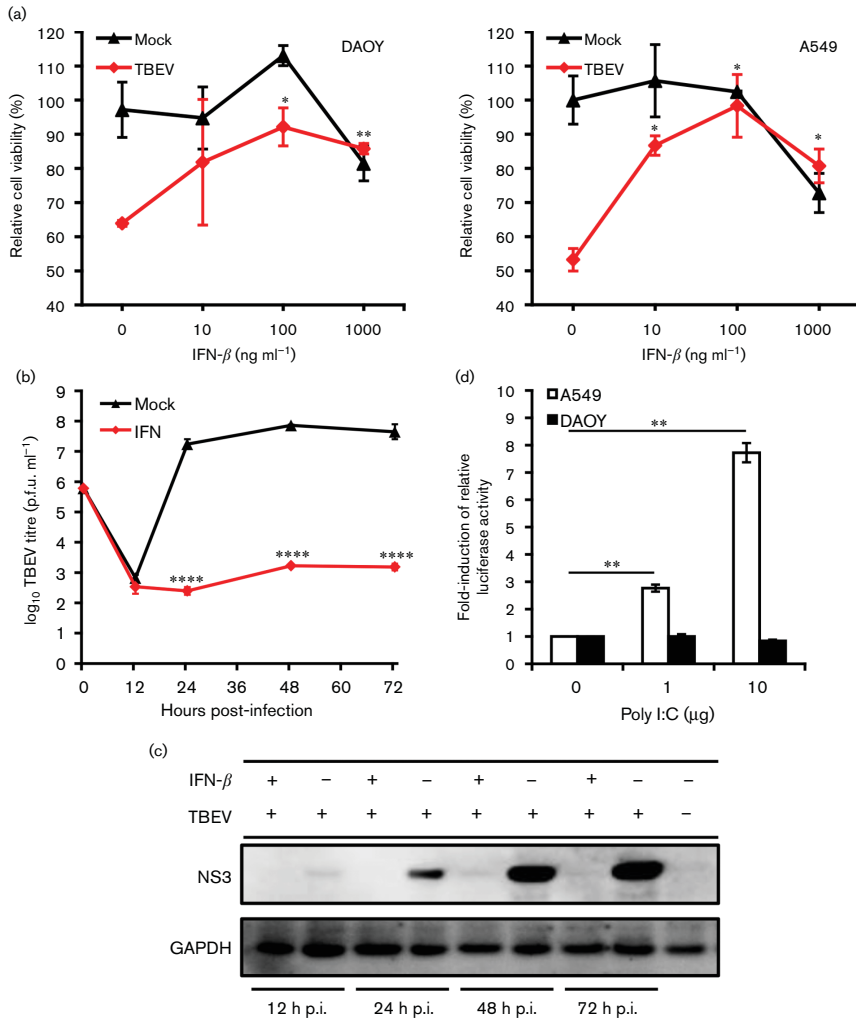
Fig. 2. IFN-β pre-treatment resulted in decreased virus production. (a) DAOY and A549 cells were treated with human recombinant IFN-β at concentrations of 10, 100 and 1000 ng ml^{-1}, and after 12 h infected with TBEV (m.o.i. 5). MTT viability assays were performed at 5 d p.i., when CPE was observed in infected cells without IFN pre-treatment. The numbers represents the percentage of living cells normalized to the untreated control. The average with standard deviation from three independent experiments (in triplicate per experiment) is shown. *Represent a significant difference from the TBEV-infected control as calculated by Student's *t*-test (*$P<0.05$; **$P<0.01$). (b) IFN-β- (10 ng ml^{-1}) or mock (no IFN-β)-treated DAOY cells were infected (m.o.i. 5) at 12 h post-treatment and viral titres (at 12, 24, 48 and 72 h p.i.) were determined by plaque assay. Time 0 stands for the initial infection input (6×10^5 p.f.u.). The average with standard deviation from three independent experiments is shown. Significant difference from the control was calculated by Student's *t*-test (****$P<0.0001$). (c) Cell lysates from (b) were used for the detection of viral NS3 levels by Western blot. GAPDH was used as a loading control. (d) DAOY and A549 cells were first co-transfected with p125Luc IFN-β promoter reporter expressing Firefly luciferase (500 ng well^{-1}) and pRL-CMV internal control expressing *Renilla* luciferase (2 ng well^{-1}). IFN-β promoter was stimulated following a secondary transfection of poly I:C (either 0, 1 or 10 µg well^{-1}) at 24 h post-first transfection. Relative luciferase activity was analysed at 24 h post-second transfection. The mean with standard error is shown for three independent experiments performed in

71

triplicate. Data were normalized to cells co-transfected with p125Luc and pRL-CMV without poly I:C treatment. Significant differences from the control were calculated by Student's *t*-test (**P<0.01).

also identified as being significantly affected. The TBEV-induced expression changes for genes that are functionally involved in these two pathways correlates with recent findings of TBEV-driven reorganization of the ER structure in infected cells [25, 42].

Basal expression of IFN-λ1 and its receptor, IFNLR1/IL10Rβ, was documented in human brain tissue and a set of human neuronal cells including primary human neurons, NT2-N neurons and neuroblastoma cell lines [43]. Our transcriptome data, together with qRT-PCR analysis, demonstrated that IFN-λ1 was expressed in non-infected

DAOY cells and highly up-regulated upon TBEV infection. Surprisingly, type I IFNs (IFN-α and IFN-β) as well as type II IFNs (IFN-γ) were not found to be up-regulated in response to TBEV infection in DAOY cells (Fig. 5a, b). In addition, the basal levels of IFN-α and IFN-β, but not INF-γ, were found to be significantly lower than the basal levels of IFN-λ1. IPA software analysis confirmed that a wide spectrum of genes involved in the IFN-λ signalling pathway were differentially expressed upon TBEV infection, as shown in Fig. 5(c). In order to assess the potential antiviral effect of IFN-λ1 on TBEV infection, we performed CPE
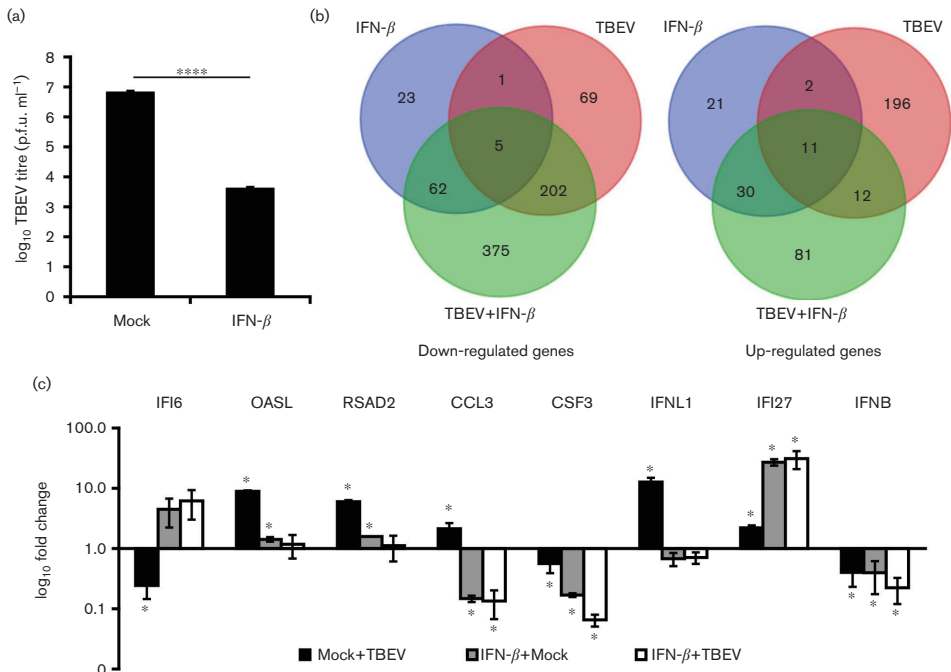
Fig. 3. Analysis of differentially expressed genes in DAOY cells upon TBEV infection and/or IFN-β treatment. (a) IFN-β- or mock-treated DAOY cells were infected (at 12 h post-treatment) with TBEV (m.o.i. 5) and viral titres were determined by plaque assay at 24 h p.i.; the mean of three biological replicates with standard deviation is shown. Significant difference from the control as calculated by Student's *t*-test (****P<0.0001). (b) Venn diagrams of either down-regulated (left) or up-regulated (right) transcripts in comparison to untreated mock-infected cells. In both diagrams, differentially expressed genes with a greater than 1.5-fold change as a cut-off condition are shown. (c) qRT-PCR validation of transcript level changes detected in transcriptome analysis for selected genes; the $\Delta\Delta$-ct method using HPRT as housekeeping gene was employed for relative fold-change calculation (control: mock-infected cells). The mean of three biological replicates with standard deviation is shown. Significant difference from control, as calculated by Student's *t*-test (*P<0.05).

72

Fig. 4. Overview of selected differentially expressed genes. DAOY cells were pre-treated with IFN-β (10 ng ml^{-1}) and/or infected with TBEV (m.o.i. 5) after 12 h. Three independent biological replicates were included for each of the combinations [untreated mock cells (control); IFN-β-treated mock cells; untreated cells infected with TBEV; IFN-β-pre-treated cells infected with TBEV]. Total cellular RNA was isolated at 24 h p.i. and used for transcriptome analysis. (a) List of selected protein-coding genes identified to be differentially

73

inhibition in pre-treated DAOY and A549 cells. The cells were pre-treated with human recombinant IFN-λ1 (10, 100 and 1000 ng ml^{-1}) and then the analysis was carried out 12 h p.i. with TBEV at m.o.i. 5. Cells were incubated for 5 days until a virus-induced CPE was observed in non-treated control cells and then viability assays using MTT were performed. A significant rescue effect by type III IFNs in A549 cells was only seen when 100 ng IFN-λ1/ml was applied. No significant rescue of cell viability was observed in the case of DAOY cells, as shown in Fig. 6(a). The potential antiviral effects of IFN-λ1 pre-treatment were further validated via plaque assays and the detection of TBEV NS3 protein by Western blot. Again, no significant changes were observed in the viral titres and protein levels of NS3 in DAOY cells pre-treated with either 10 or 100 ng ml^{-1} of IFN-λ1, as shown in Fig. 6(b, c). In order to verify whether these concentrations of IFN-λ1 are sufficient to trigger the expression of ISGs, we analysed the mRNA expression of six genes that were found to be up-regulated most after TBEV infection. This suggested that the activation of their expression could be influenced by elevated levels of endogenous IFN-λ. No ISG expression was observed in DAOY cells treated with 10 ng ml^{-1} of IFN-λ1, but in cells treated with 100 ng ml^{-1} of IFN-λ a strong induction of RSAD2 (viperin) gene expression was detected (Fig. 6d). Moreover, high basal mRNA expression of receptor subunits for both type I and type III IFNs was documented in DAOY cells (Fig. 6e).

IFN-β pre-treatment results in up-regulation of ISGs and down-regulation of pro-inflammatory cytokines

Transcriptome analysis showed that IFN-β treatment of DAOY resulted in the altered expression of 155 genes, as shown in Fig. 3(b), thus confirming the high sensitivity of human neuronal cells to type I IFNs. Based on the inhibitory effects observed following IFN-β pre-treatment in TBEV infected-DAOY cells, we speculated that IFN-β activates the expression of the genes responsible for this antiviral effect. We searched for genes that were highly up-regulated upon IFN-β pre-treatment in both mock- and TBEV-infected DAOY cells; 41 genes were found to be up-regulated in both data sets (Fig. 3b). Analysis of the literature showed that five genes (encoding BST2, IFI27, IFITM3, ISG15 and RSAD2) were also expressed in IFN-β-treated human granule and cortical neurons [16]. Out of the 41 identified genes, IFI27, IFI6, RMRP, RN7SK, IFITM1, BST2, EPSTI1, IFITM3 and CRABP2 were up-regulated most (fold-change >2.5; Fig. 4a Tables S6 and S7). IFI6 and IFI27 were both characterized as being most highly expressed

upon IFN-β treatment in mock- and TBEV-infected cells (Fig. 4a, Tables S6 and S7). Interestingly, a panel of genes down-regulated following IFN-β treatment consisted mainly of cytokine coding genes (Fig. 4a and Table S3). The same rate of down-regulation for CCL3/MIP1α, CSF3, CCL20/MIP3α, IL36RN, CXCL1/KC, CXCL2/MIP2α, CXCL3/MIP2β, CXCL5/ENA78, IL1α, IL1β, IL6, IL8 and IL11 was observed in both mock- and TBEV-infected DAOY cells pre-treated with IFN-β, but not in TBEV-infected cells (Fig. 4a). These data suggest a unique response of DAOY cells to type I IFN treatment in terms of the decreased mRNA levels of pro-inflammatory cytokines. The down-regulation of cytokine expression was by far the most significant expression pattern observed after IFN-β treatment. These findings were also supported by IPA analysis, which identified that for the most part cytokine-related canonical pathways were most significantly affected (Table 1). Our transcriptome analysis also revealed altered IFN-β-driven expression of a wide panel of non-coding RNAs (Fig. 3b). RNA5-8SP6, RMRP and RN7SK were the most up-regulated non-coding RNAs in this condition. Their expression may, however, be negatively influenced by TBEV, since a lower rate of up-regulation was seen for all three genes in IFN-β-treated cells subsequently infected with TBEV (Fig. 4b; Tables S6 and S7).

DISCUSSION

Here we established a model for studying the interactions between TBEV and cells of neural origin. Human DAOY medulloblastoma cells are derived from cerebellum and their neuronal origin was analysed using TUBB3, MOG, VIM and GFAP biomarkers. TUBB3 and VIM expression is typical for neural precursor cells; TUBB3 expression was documented in neuronal precursor cells [44], whereas vimentin is typical for radial glia, a primary progenitor cells capable of both neuro- and gliogenesis [27]. Therefore, our findings support the neuronal origin of DAOY cells, as well as their dedifferentiated state, which is typical for cancer cells. In the case of U373 cells, TUBB3 and VIM expression also points to a dedifferentiated state (especially TUBB3 for an ascending histological grade of malignancy). However, the presence of GFAP supports their glial origin. Despite its expression in radial glia, the presence of VIM in both cell lines may also serve as a cancer marker, since the high expression of VIM and CD44 results in an epithelial–mesenchymal transition that is typical for metastasis [45]. Relatively low expression of MOG, a minor component of myelin (0.05 %) in both cell lines, could point to an ascending histological grade of malignancy, since this protein is located in oligodendrocytes (a fully differentiated type of

Table 1. List of top 10 predicted canonical pathways affected by TBEV infection or IFN-β pre-treatment according to IPA software analysis

Untreated mock cells versus TBEV-infected cells

Canonical pathway	P-value	Pathway-associated genes found to be differentially expressed
Unfolded protein response	1,10E-13	DDIT3, DNAJB9, DNAJC3, EIF2AK3, ERO1LB, HSP90B1, HSPA1A, PPP1R15A, SEL1L, XBP1
Role of hypercytokinemia/hyperchemokinemia in the pathogenesis of influenza	5,09E-12	CCL3, CCL4, CCL5, CXCL10, IFNL1, IL6, IL15, IL12A, TNF
Pathogenesis of multiple sclerosis	5,93E-10	CCL3, CCL4, CCL5, CXCL10, CXCL11
Activation of IRF by cytosolic pattern recognition receptors	8,51E-10	CREBBP, DDX58, DHX58, IFIH1, IFIT2, IL6, ISG15, LTA, PPIB, TNF
VDR/RXR activation	2,39E-09	CCL5, CXCL10, EP300, IGFBP5, IGFBP6, IL12A, KLF4, LRP5, MXD1, NCOR2, RXRG
Differential regulation of cytokine production in macrophages and T helper cells by IL-17A and IL-17F	3,15E-09	CCL3, CCL4, CCL5, IL6, IL12A, TNF
Endoplasmic reticulum stress pathway	5,06E-09	DDIT3, DNAJC3, EIF2AK3, HSP90B1, HSPA5, XPB1
Role of macrophages, fibroblasts and endothelial cells in rheumatoid arthritis	5,98E-09	CCL5, CREBBP, EP300, FGF2, IL6, IL15, IL18RAP, JAK2, LRP5, LTA, MMP13, NFATC1, PLCD4, PLCG2, SFRP2, TCF7L2, TNF, TRAF1, WNT7B, WNT9A
Interferon signalling	7,53E-09	IFI6, IFIT1, IFIT3, IRF1, ISG15, JAK2, MX1
Granulocyte adhesion and diapedesis	9,68E-09	CCL3, CCL4, CCL5, CCL3L1, CCL4L2, CLDN1, CXCL2, CXCL10, CXCL11, IL18RAP, MMP13, MMP15, SDC4, TNF

Untreated mock cells vs IFN-β-treated cells

Canonical pathway	P-value	Pathway-associated genes found to be differentially expressed
Granulocyte adhesion and diapedesis	1,43E-07	CCL3, CCL4, CCL5, CCL3L1, CCL4L2, CLDN1, CXCL2, CXCL10, CXCL11, IL18RAP, MMP13, MMP15, SDC4, TNF
Agranulocyte Adhesion and Diapedesis	2,00E-07	CCL3, CCL20, CLDN1, CLDN14, CXCL1, CXCL2, CXCL3, CXCL5, CXCL8, IL1A, IL1B, IL1RN, IL36RN, MMP1
Differential regulation of cytokine production in macrophages and T helper cells by IL-17A and IL-17F	4,45E-07	CCL3, CCL4, CCL5, IL6, IL12A, TNF
Role of cytokines in mediating communication between immune cells	5,53E-07	CSF2, CSF3, CXCL8, IL6, IL1A, IL1B, IL1RN, IL36RN
Communication between innate and adaptive immune cells	6,11E-07	CCL3, CSF2, CXCL8, HLA-B, IL6, IL1A, IL1B, IL1RN, IL36RN
Differential regulation of cytokine production in intestinal epithelial cells by IL-17A and IL-17F	1,17E-06	CCL3, CSF2, CSF3, CXCL1, IL1A, IL1B
Role of hypercytokinemia/hyperchemokinemia in the pathogenesis of influenza	3,24E-06	CCL3, IL8, IL6, IL1A, IL1B, IL1RN, IL36RN
Role of IL-17F in allergic inflammatory airway diseases	4,30E-06	CSF2, CXCL1, CXCL5, CXCL8, IL6, IL11, IL1B
Role of IL-17A in psoriasis	7,89E-06	CCL20, CXCL1, CXCL3, CXCL5, CXCL8
Hematopoesis from pluripotent stem cells	2,10E-05	CSF2, CSF3, CXCL8, IL6, IL11, IL1A, LIF

Untreated mock cells versus IFN-β-treated cells infected with TBEV

Canonical pathway	P-value	Pathway-associated genes found to be differentially expressed
Hepatic fibrosis/hepatic stellate cell activation	6,85E-11	BCL2, COL13A1, COL1A1, COL1A2, COL3A1, COL4A2, COL5A1, COL5A3, COL6A1, CXCL3, CXCL8, ECE1, EGFR, IGF2, IGFBP3, IL6, IL1A, IL1B, MMP1, MMP9, MYH9, MYH14, PDGFA, PDGFRB, SERPINE1, TIMP2
Role of osteoblasts, osteoclasts and chondrocytes in rheumatoid arthritis	6,79E-08	BCL2, BMP5, CBL, COL1A1, FZD7, IL6, IL11, IL1A, IL1B, IL1RN, IL36RN, ITGA5, ITGB3, LRP1, MAP2K3, MMP1, MMP14, NFATC1, PIK3CD, SFRP2, SPP1, TCF7L1, WNT7B, WNT9A
Agranulocyte adhesion and diapedesis	8,17E-08	CCL3, CCL20, CLDN1, CLDN14, CXCL1, CXCL2, CXCL3, CXCL5, CXCL8, IL1A, IL1B, IL1RN, IL36RN, MMP1
Granulocyte adhesion and diapedesis	1,16E-07	CCL3, CCL4, CCL5, CCL3L1, CCL4L2, CLDN1, CXCL2, CXCL10, CXCL11, IL18RAP, MMP13, MMP15, SDC4, TNF
Atherosclerosis signalling	2,32E-07	APOC1, COL1A1, COL1A2, COL3A1, COL5A3, CXCL8, IL6, IL1A, IL1B, IL1RN, IL36RN, MMP1, MMP9, PDGFA, RARRES3, SELPLG, TNFSF14
Communication between innate and adaptive immune cells	2,95E-06	CCL3, CSF2, CXCL8, HLA-B, IL6, IL1A, IL1B, IL1RN, IL36RN
Role of IL-17F in allergic inflammatory airway diseases	5,92E-06	CSF2, CXCL1, CXCL5, CXCL8, IL6, IL11, IL1B
Graft versus host disease signalling	1,26E-05	HLA-B, HLA-C, HLA-DRA, HLA-F, IL6, IL1A, IL1B, IL1RN, IL36RN
Inhibition of matrix metalloproteases	1,92E-05	HSPG2, LRP1, MMP1, MMP9, MMP14, MMP15, THBS2, TIMP2
Role of IL-17A in psoriasis	2,74E-05	CCL20, CXCL1, CXCL3, CXCL5, CXCL8

glia) [46, 47]. Importantly, to the best of our knowledge, our data, as described below, also describe the innate immune properties of this cell line for the first time in the context of virus infection, and provide extensive transcriptome information. This is important information for others in the field who wish to make use of this particular cell line. It is often desirable in virology to use such cell lines before primary lines, which can be difficult to obtain, grow and infect. The data supplied here provide information on the nature of these cells, for example on how they compare to healthy neurons for experiments in virus–host interaction studies, drug screens, virus entry studies, etc.

Based on our transcriptome analysis, up-regulation of cytokines/chemokines as described here would mostly result in the activation/stimulation and chemotaxis of effector immune cells. This correlates with TBEV-associated immunopathogenesis in the brain [8, 9]. Transcriptome analysis of LGTV-infected HEK 293 T cells revealed enhanced expression of CCL5/RANTES, CXCL10/IP-10 and TNF-α cytokines [48]. CCR5 (specifically the CCR5Delta32 allele) has been associated with the severity of TBEV-induced disease, suggesting that differential regulation of CCL5/RANTES, etc. may be clinically relevant [49]. We did not observe up-regulation of IFN-α, which is intriguing and may point to a defect in its regulation. In addition, we identified that RIG-I/DDX58 and MDA5/IFIH1 (RIG-I like receptors, RLRs) are up-regulated upon TBEV infection. The involvement of RLRs in sensing TBEV RNA was documented previously [50]. Viral dsRNA 'hides' in endoplasmic reticulum-derived vesicle packets and thus prevents the activation of host receptors and subsequent IFN-mediated antiviral response [51]. Moreover, a recent study showed enhanced mortality rates of IPS-1/MAVS (a downstream factor involved in RIG-I and MDA5 signalling cascade) knockout mice infected with TBEV or LGTV [22]. In addition, RLR signalling can induce type III IFN expression [52]. Therefore, up-regulation of RIG-I and MDA5 in the case of TBEV-infected DAOY cells may also contribute to the observed induction of IFN-λ1.

Our study identified a wide panel of ISGs that were up-regulated in response to TBEV infection. These ISGs were found to inhibit a broad spectra of viruses [11, 53–57]. Viperin, encoded by the RSAD2 gene, was shown to inhibit TBEV replication in infected HEK293T cells [58]. Although various ISGs were up-regulated, high TBEV titres were observed in DAOY cells. This suggests the presence of counteracting measures by TBEV against host immune responses, at least in the infected cells. TBEV antagonizes type I IFN signalling in infected cells and NS5 protein inhibits JAK-STAT signalling [24, 59]. Although type I and type III IFNs signal through different receptors, downstream signalling pathways converge and lead to the formation of the ISGF3 transcription complex and subsequent expression of ISGs [60]. Whether IFN-λ1 signalling is antagonized via TBEV protein(s) is not known. Strong up-regulation of IFIT1, IFIT2 and RSAD2 transcripts in comparison to other

ISGs was detected. This could be a result of IFN-independent transcriptional induction of either IRF1 or IRF3, as IFN-independent ISG induction pathways were characterized for all three genes [61, 62].

We also identified a panel of genes that were down-regulated upon TBEV infection in DAOY cells. These genes are mostly involved in transcription and translation processes, as well as the regulation of cell proliferation. Down-regulation of effectors involved in either transcription (POLR2A) or translation (RNA28S5, RN7SL2, RN7SL3) suggests a possible TBEV-driven transcriptional or translational shut off in host cells. Both transcriptional and translational shut off are well-documented phenomena [63, 64]. Similar rates of RNA28S5, NOTCH3, COL1A1, BCL9L, BCOR1, POLR2A, FAM71D, IGF2 and HSPG2 down-regulation were also evident in IFN-β-pre-treated cells infected with TBEV, where significantly lower viral titres were determined. Intriguingly, down-regulation of these genes was not documented in only IFN-β-pre-treated cells. Therefore, the down-regulation observed for these genes could be considered to be a hallmark of TBEV infection in DAOY cells.

Altered expression of host lncRNAs was described in the case of influenza A virus and severe acute respiratory syndrome coronavirus (SARS-CoV) infection [65]. Furthermore, a wide panel of lncRNAs was found to be regulated by type I IFNs [66]. Therefore it may be that lncRNAs play an important role in IFN-stimulated host immune responses to viral infection. This hypothesis was recently supported by the identification of an IFN-λ3 up-regulated lncBST2/BISPR that positively regulates expression of BST2/tetherin [67], an ISG with antiviral effect in murine neurons against measles virus [68]. Further studies are required to elucidate the possible involvement of host lncRNAs in response to TBEV infection. The possible function of RNA5-8SP6 remains unclear, since it is classified as a 5.8S ribosomal RNA 6 pseudogene. RN7SK is involved in the regulation of transcription by RNA polymerase II. Its enhanced expression upon IFN-β treatment may increase the expression of other ISGs. RMRP was shown to interact with TERT, forming a complex with RNA-dependent RNA polymerase activity. This complex produces dsRNA that is processed into siRNAs in a Dicer-dependent manner [69], suggesting a possible role for RMRP in the decrease of TBEV levels by recruiting the RNA interference pathway. The phenomenon of type I IFN-dependent expression regulation of lncRNAs was recently described [66, 70]. We also report that TBEV infection results in the differential expression of genes coding for lncRNAs (Fig. 3b). No change in RN7SL3 expression was observed in IFN-β-pre-treated cells infected with TBEV, although down-regulation of RN7SL3 took place in TBEV-infected cells. This observation indicates a negative effect of TBEV on RN7SL3 expression, however this effect seems to be dose-dependent, since lowered titres of virus (as IFN pre-treatment resulted in lower TBEV production) did not affect the RN7SL3 expression at all. The biological relevance of these data, however, needs to be investigated.
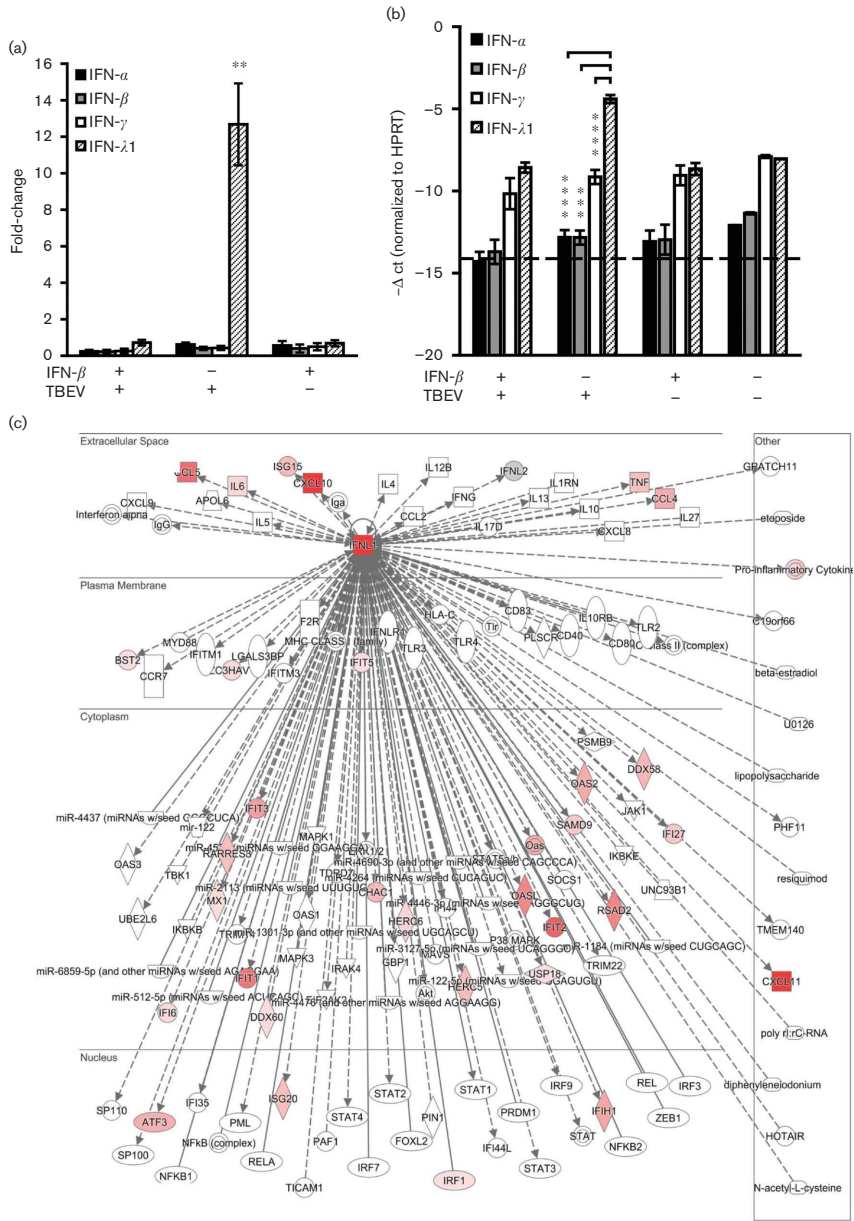
Fig. 5. Expression of type III IFN (IFN-λ1) is induced in DAOY cells following TBEV infection. DAOY cells were treated with IFN-β (10 ng ml⁻¹) and, where indicated, infected with TBEV after 12 h (m.o.i. 5), or only infected with TBEV, or mock-treated. Three independent bio-logical replicates were included for each of the combinations (untreated mock cells; IFN-β-treated mock cells; untreated cells infected

with TBEV; IFN-β-pre-treated cells infected with TBEV). Total cellular RNA was isolated at 24 h p.i. and further processed for transcriptome analysis. (a) Relative quantification of type I, II and III IFN mRNA levels in DAOY cells. The $\Delta\Delta$-ct method, using HPRT as a housekeeping gene, was employed for relative fold-change calculation; the mean of three biological replicates with standard deviation is shown. Significant differences to the control (mock-infected cells) were calculated by Student's *t*-test (**$P<0.01$). (b) -Δ ct values of type I, II and III IFNs normalized to the HPRT gene; the mean of three biological replicates with standard deviation is shown. The dotted line represents the sensitivity of the qPCR. Significant differences were calculated by Student's *t*-test (***$P<0.001$, ****$P<0.0001$). (**c**) Schematic overview of the IFN-λ (IFNL1) signalling network (as identified by IPA software). Identified up-regulated (red) transcripts in TBEV-infected DAOY cells are displayed.

With regard to IFNs, based on our data, DAOY cells seem to exclusively activate the IFN-λ1 (type III IFN) pathway in response to TBEV infection; our data suggest a defect in the recognition of viral RNA, given the inability the of the RIG-I/MDA-5 ligand poly I:C to induce a type I IFN reporter gene while type I IFN signalling itself is functional. This is likely to account at least in part for these observations. The unique pattern of IFN signalling in DAOY cells might be virus- and cell-type-specific, since previous work characterized IFN-λ as an inducer of IFN-α expression in HSV1-infected human neurons [17]. Furthermore, high up-regulation of IFN-β in LGTV-infected HEK 293T cells was also described [48]. However, DAOY cells express the type I IFN receptor and are responsive to IFN-β treatment. Furthermore, only IFN-β treatment resulted in significant inhibition of TBEV production. These results suggest that DAOY cells express IFN-λ1 in response to TBEV infection, however this endogenous response does not restrict TBEV production. However, it may be that TBEV does not inhibit the type III IFN pathway, because it does not affect virus replication, despite sharing elements of the signalling cascade [19, 20]. A comparable phenomenon was indeed observed for epithelial cell infection with human rotavirus [71].

We identified two genes that were highly up-regulated in IFN-β-treated DAOY cells, in the absence or presence of TBEV, IFI6 and IFI27. They belong to the FAM14 family of ISGs [72] and were documented as mitochondrial proteins involved in apoptosis regulation [73–75]. Over-expression of IFI6 inhibited DENV-induced apoptosis of endothelial cells [74, 75] and restricted HCV replication in hepatocarcinoma cells [76]. In addition, IFI6 was shown to block HCV entry into hepatocarcinoma cells [77]. IFI27 overexpression in human neurons resulted in decreased production of WNV, SLEV and MHV [16], while over-expression of murine IFI27 delayed Sindbis virus-induced encephalitis and death in neonatal mice [78]. This suggests that IFI6 and IFI27 are promising candidate proteinsthat may be responsible for the inhibition of TBEV infection in DAOY cells. Both IFITM1 and IFITM3 were documented to inhibit HCV entry into hepatocarcinoma cells [79, 80]. However, the antiviral effects of IFITMs seem to be RNA virus-specific [81]. An antiviral role in the case of HCV infection was also reported for EPSTI1, whose expression was induced upon IFN-λ2 treatment and resulted in a decreased rate of viral replication, assembly and release [82]. Moreover, BST2/tetherin inhibits HCV and DENV in

hepatocarcinoma cells [83, 84], as well as measles virus in murine neurons [68].

In summary, our results provide novel insights into the response of neuronal cells to TBEV infection and the antiviral effects of type I and III IFN. Importantly, we found a partial overlap of host-induced genes for TBEV and type I IFN. Whether genes induced by both pathways are particularly important in restricting infection, or whether virus-specific responses may have unique roles in pathogenesis, remains to be investigated. Our findings should influence and encourage further studies into the pathogenic effects of infection, as well as inhibitors of TBEV that can be further investigated and targeted.

METHODS

Cells, viruses and IFN pre-treatment

Human medulloblastoma (ATCC; DAOY HTB-186) and human lung adenocarcinoma (A549; available at the Institute of Parasitology, Biology Centre of the Academy of Sciences of the Czech Republic, Branišovská) lines were grown in low-glucose DMEM medium supplemented with 10 % foetal bovine serum (FBS), 1 % antibiotic/antimycotic (amphotericin B 0.25 µg ml^{-1}, penicillin G 100 units/ml and streptomycin 100 µg ml^{-1}) and 1 % L-glutamine. The human glioblastoma line (U373 MG Uppsala; kindly provided by T. Eckschlager, Charles University in Prague) was grown in IMDM medium supplemented with 10 % FBS, 1 % antibiotic/-antimycotic (amphotericin B 0.25 µg ml^{-1}, penicillin G 100 units/ml, and streptomycin 100 µg ml^{-1}) and 1 % L-glutamine. The DAOY medulloblastoma cell line was derived from desmoplastic cerebellar medulloblastoma [26], and the U373 MG Uppsala glioblastoma cell line was derived from malignant glioma/astrocytoma [29]. Porcine kidney stable (PS; cell line as in [85]; available at the Institute of Parasitology, Biology Centre of the Academy of Sciences of the Czech Republic, Branišovská) cells were grown in L15 medium with 3 % newborn calf serum (NCS), 1 % antibiotic/antimycotic and 1 % L-glutamine. All cell lines were grown at 37 °C and 5 % CO$_2$ (PS cells at 37 °C without additional CO$_2$).

The low-passage TBEV strain Neudoerfl (fourth passage in suckling mice brains; GenBank accession no. U27495) was provided by Professor F. X. Heinz (Medical University of Vienna, Austria) [86]. TBEV in growth medium was added to the cells 1 day post-seeding. Cells were incubated with the virus for 2 h, washed with PBS and then fresh pre-
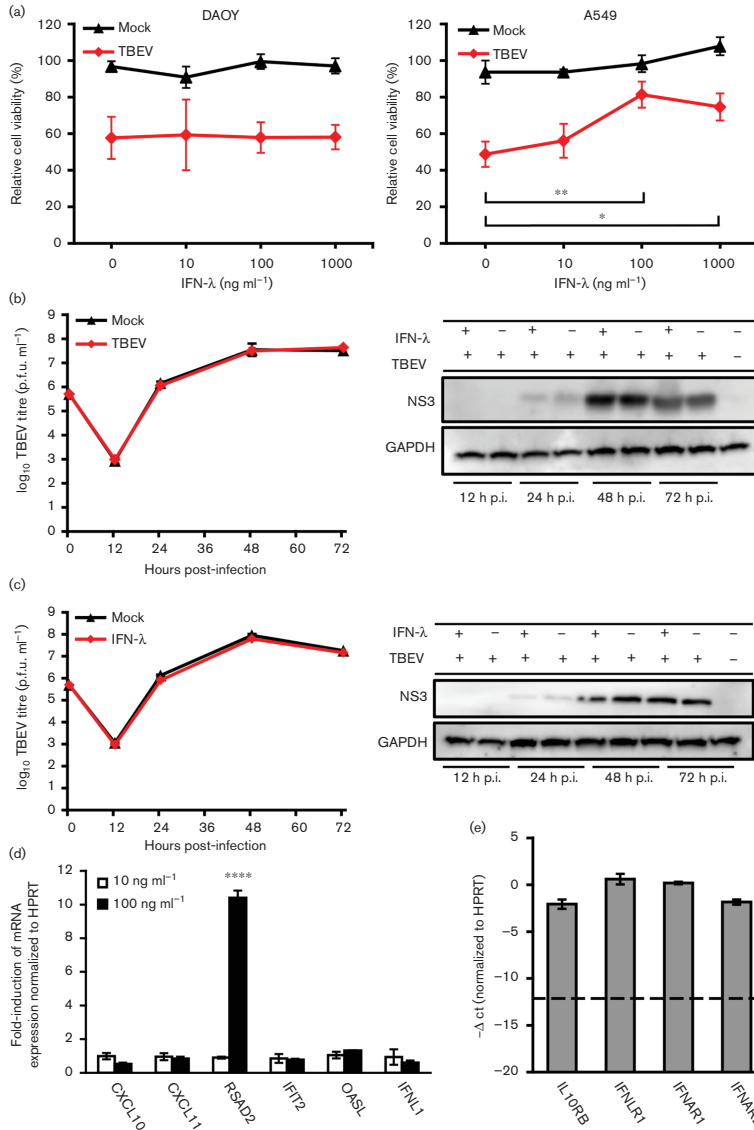
Fig. 6. IFN-λ1 pre-treatment results in non-altered virus production. (a) DAOY and A549 cells were first treated with human recombinant IFN-λ1 at concentrations of 10, 100 and 1000 ng ml^{-1}, and then after 12 h infected with TBEV (m.o.i. 5). MTT viability assays were performed at 5 d p.i. when the CPE was observed in infected cells in the absence of IFN pre-treatment. Numbers represents the percentage of living cells normalized to the untreated control. Averages with standard deviation from three independent experiments performed in triplicates are shown. Significant differences to control were calculated by Student's *t*-test (*$P<0.05$). (b, c) IFN-λ1 (10 and 100 ng ml^{-1}, respectively) or mock-treated DAOY cells were infected (m.o.i. 5) at 12 h post-treatment and viral titres (at 12, 24, 48 and 72 h p.i.) were determined by plaque assay. The time 0 value stands for the initial infection input (6×10^5 p.f.u.). Averages with standard

79

deviation from three independent experiments are shown. Cell lysates were further used for detection of the TBEV protein NS3 levels by Western blot. GAPDH was used as a loading control. A representative blot of three independent experiments is shown. (d) Total RNA isolated from DAOY cells 12 h post-IFN-λ1 treatment (10 ng ml^{-1}; 100 ng ml^{-1}) was used for relative quantification of the indicated ISG mRNAs. The $\Delta\Delta$-ct method, using HPRT as a housekeeping gene, was used for relative fold-change calculation; the mean of three independent experiments with standard deviation is shown. Significant difference from control was calculated by Student's *t*-test (****$P<0.0001$). (e) -Δ ct values of type I and III IFN receptor subunits normalized to the HPRT gene; the mean of three biological replicates with standard deviation is shown. The dotted line indicates the sensitivity of the assay.

warmed medium was added. Human INF-β 1a (RayBiotech) or IFN-λ1 (Sigma Aldrich) were added to the A549 or DAOY cells 12 h prior to infection.

Virus titration

Viral titres were determined by plaque assay [87], with minor modifications. Briefly, PS cell monolayers (9×10^4 cells per well) were grown in 24-well plates and incubated with $10\times$ serial dilutions of viral samples for 4 h at 37 $^{\circ}$C. The samples were then covered by a 1 : 1 (v/v) overlay mixture of carboxy-methyl cellulose and $2\times$ L15 medium including 6 % PTS, 2 % antibiotics and 2 % glutamine. After 5 days, the medium with overlay was removed, and the cells washed and subsequently fixed and stained with 0.1 % naphthalene black in 6 % acetic acid solution for 45 min. Virus-induced plaques were counted and the titres are stated as p.f.u./ml; it should be noted that infection rates can be different for other cell types.

IFN and antiviral activity assays

DAOY and A549 cells (1×10^4 cells well^{-1} and 2×10^4 cells well^{-1}, respectively) were seeded in 96-well plates 12 h prior pre-treatment with recombinant IFN-β and IFN-λ using concentrations of 10, 100 and 1000 ng ml^{-1}. Cells were infected at 12 h post-treatment with TBEV strain Neudoerfl at an m.o.i. of 5 and incubated at 37 $^{\circ}$C and 5 % CO$_2$ for 5 days until virus-induced the CPE was observed in control wells. Subsequently, an MTT assay with minor modifications was performed for the determination of cell viability [88]. Briefly, after removal of the medium, the cells were washed with PBS and 100 µl of fresh medium containing MTT (3-[4.5-dimethylthiazol-2-yl]−2,5-diphenyl tetrazolium bromide; Sigma Aldrich; 0,5 mg ml^{-1}) was added to each well. After incubation at 37 $^{\circ}$C for 2 h, the medium with MTT was removed and 100 µl of DMSO was added to each well. After shaking for 15 min at room temperature, the absorbance at 570 nm was determined using the microplate reader Synergy H1 (BioTek).

IFN-β promoter activity assay

The *in vitro* activity of the IFN-β promoter was analysed in DAOY and A549 cells using p125Luc reporter vector expressing Firefly luciferase under the control of IFN-β promoter [35] and pRL-CMV vector expressing *Renilla* luciferase as an internal control. Transfections were carried out using the PolyJet transfection reagent (SignaGen) according to the manufacturer's protocol. Briefly, cells (1.2×10^5 well^{-1} and 1.6×10^5 well^{-1} for DAOY and A549 cells, respectively) were seeded in 24-well plates 1 day prior to transfection.

The first co-transfection of p125Luc (500 ng) and pRL-CMV (2 ng) was followed by a second transfection of poly I: C (1 or 10 µg well^{-1}) after 24 h. Cells were lysed after a further 24 h in passive lysis buffer (Promega). The Firefly and *Renilla* luciferase activities were determined using a Dual Luciferase assay kit (Promega) in an H1 Synergy luminometer (BioTek).

RNA isolation

For transcriptome analysis, RNA from DAOY cells was extracted by using Trizol (Life Technologies). Briefly, cells were washed with phosphate buffer saline (PBS) and lysed in 1 ml Trizol. Chloroform (0.2 ml) was added, and the samples were mixed intensively and incubated for 5 min at room temperature. The upper aqueous phase was transferred to a new tube after centrifugation (12 000 *g*, 15 min, 4 $^{\circ}$C) and mixed with 0.5 ml of isopropanol. After incubation at 4 $^{\circ}$C for 10 min, the precipitated RNA was pelleted by centrifugation (12 000 *g*/15 min/4 $^{\circ}$C) and washed with 75 % ethanol. The RNA pellet was dissolved in 20 µl of RNase-free water. The RNA was stored at −80 $^{\circ}$C until further use.

For qRT-PCR analysis, total cellular RNA was isolated using the NucleoSpin RNA Plus kit (Macherey-Nagel).

Transcriptome analysis

RNA integrity was checked before sequencing using a 2200 TapeStation (Agilent). Five-hundred ng of total RNA from each sample was enriched for poly(A) RNA, and then fragmented and prepared for sequencing using a TruSeq stranded mRNA preparation kit (Illumina). Index-tagged libraries were pooled and single-end datasets with a read length of 76 nucleotides were generated on a NextSeq500 sequencer (Illumina). On average, 48 million reads were acquired for each sample.

FastQC software (http://www.bioinformatics.babraham.ac.uk/projects/fastqc) was used to check the RNA-Seq read quality. In order to check for possible contamination in the analysed samples we employed Kraken [89]. It is a system for assigning taxonomic labels to short DNA sequences, usually obtained through metagenomic studies. We mapped k-mers to a pre-built 4 GB database constructed from complete bacterial, archaeal and viral genomes in RefSeq. On average, only ~0.5 % reads aligned to the MiniKraken database constructed from bacterial, archaeal and viral genomes in RefSeq. TopHat2 [37], a fast splice junction mapper for RNA-Seq reads, aligns RNA-Seq reads to mammalian-sized genomes using the ultra high-throughput short-read aligner

Bowtie2, and then analyses the alignment results to identify splice junctions between exons. In the present research, we aligned the short reads to the *Homo sapiens* genome (GRCh37) downloaded via the Ensembl genome browser.

Cuffdiff was used to identify differentially expressed genes [38]. Cuffdiff is a program in the Cufflinks package (version 2.2.1). It adopts an algorithm that controls cross-replicate variability and read-alignment ambiguity by using a model for fragment counts based on a beta negative binomial distribution. It can identify differentially expressed (DE) transcripts and genes, differential splicing and promoter preference changes, and returns far more statistically significant differentially expressed genes than microarray analysis.

After identifying the DE genes, the software IPA was applied for the function annotation and pathway analysis. Sequencing data were deposited in EBI (study accession number: PRJEB14767).

Real-time qPCR

For qPCR validation of gene expression from samples used for transcriptome analysis, 1 µg of total RNA was first treated with DNase using the TURBO DNA-free kit (Life Technologies) and then reverse-transcribed by SuperScript III reverse transcriptase (Life Technologies) with 500 ng of oligo d(T)$_{15}$ primer according to the manufacturer's protocol. For qPCR reactions, 2 µl of 5× diluted cDNA reaction was used for the detection and amplification of selected genes; Fast SYBR Green Master Mix (Life Technologies) was used according to manufacturer's protocol.

For qPCR analysis of the IFN-λ1 treatment effect on DAOY cells, total RNA was first treated with dsDNase (Life Technologies) and 80 ng per reaction was used for RT-qPCR using the FAST Universal One-Step qRT-PCR kit (Kapa Biosystems) according to the manufacturer's protocol.

All data were analysed using the relative quantification $\Delta\Delta$ Ct method and HPRT as the reference gene. A full list of primers is outlined in Table S8.

Western blotting

Cells were washed with PBS and subsequently lysed on ice for 15 min in 1× cell lysis buffer (Cell Signalling Technology) including protease and phosphatase inhibitors (Life Technologies). Lysate was sonicated and centrifuged at 4 °C for 15 min at 14 000 g to eliminate cellular debris, and then analysed by BCA assay for protein concentration quantification. Using SDS-PAGE, 8–12 µg of protein extract per well was separated. The proteins were then subsequently transferred to a PVDF membrane (GE Healthcare). For TBEV NS3 detection, chicken polyclonal primary antibodies in 1 : 5000 dilution ratio were used (kindly provided by Dr M. Bloom, National Institute of Allergy and Infectious Diseases, USA). Goat polyclonal antibodies (Abcam) for the detection of GAPDH were used at 1 : 500 dilution. For NS3/ GAPDH detection, anti-goat and anti-chicken alkaline phosphatase-conjugated secondary antibodies (both 1 : 1000 dilution ratio; Vector Laboratories) were used and immuno-labelled proteins were visualized by chemiluminescence assay using Novex AP chemiluminescent substrate (CDP-Star) reagent (Life Technologies).

Immunofluorescence analysis

DAOY and U373 cells were seeded on a chamber slide (0.3 cm^2 well^{-1}; 1×10^4 cells well^{-1}). For the detection of CNS markers, cells were fixed after 24 h post-seeding, and in the case of TBEV NS3 detection, cells were infected with TBEV at an m.o.i. of 0.1, 1 or 5, and fixed at 24 h p.i. Fixation was carried out by using 4 % paraformaldehyde for 15 min; cells were subsequently rinsed in PBS and permeabilized with 0.1 % Triton X-100 for 15 min. Cells were also treated with 50 mM NH$_4$Cl in 1 % BSA in PBS to block formaldehyde auto-fluorescence. Following this, cells were blocked in 3 % BSA in PBS and incubated with chicken polyclonal anti-NS3, goat polyclonal anti-MOG (Abcam), rabbit polyclonal anti-TUBB3 (Abcam), rabbit polyclonal anti-VIM (Abcam), or rabbit polyclonal anti-GFAP (Dako) antibodies at 1 : 5000, 1 : 200, 1 : 200, 1 : 1000 and 1 : 500 dilutions, respectively. After washing with PBS, primary antibodies were labelled using DyLight488/594-conjugated secondary antibodies (Vector Laboratories) at a 1 : 1000 dilution. For MOG immunodetection, the Tyramide amplification signal kit (Life Technologies) was used according to the manufacturer's instructions. Subsequently, the cells were mounted in Vectashield (Vector Laboratories). Analysis of NS3-labelling was carried out on an Olympus BX-51 fluorescence microscope equipped with an Olympus DP-70 CCD camera. For CNS marker expression imaging, an Olympus Fluoview FV10i confocal microscope was used. In order to analyse the numbers of cells expressing NS3 or one of the CNS markers, four–nine images (100× magnification) were taken for NS3 or markers in two independent experiments. Subsequently, the total number of NS3 or CNS marker expressing cells (as indicated in figures) were counted and transformed to percentages relating to the total number of cells. Average values and standard deviations were calculated from two independent experiments.

References
1. **Kunz C, Heinz FX.** Tick-borne encephalitis. *Vaccine* 2003;21:S1–S2.
2. **Süss J.** Tick-borne encephalitis 2010: epidemiology, risk areas, and virus strains in Europe and Asia-an overview. *Ticks Tick Borne Dis* 2011;2:2–15.

81

3. **Kaiser R.** The clinical and epidemiological profile of tick-borne encephalitis in southern Germany 1994–98: a prospective study of 656 patients. *Brain* 1999;122:2067–2078.

4. **Dörrbecker B, Dobler G, Spiegel M, Hufert FT.** Tick-borne encephalitis virus and the immune response of the mammalian host. *Travel Med Infect Dis* 2010;8:213–222.

5. **Miner JJ, Diamond MS.** Mechanisms of restriction of viral neuroinvasion at the blood-brain barrier. *Curr Opin Immunol* 2016;38: 18–23.

6. **Gelpi E, Preusser M, Garzuly F, Holzmann H, Heinz FX et al.** Visualization of Central European tick-borne encephalitis infection in fatal human cases. *J Neuropathol Exp Neurol* 2005;64:506–512.

7. **Palus M, Bílý T, Elsterová J, Langhansová H, Salát J et al.** Infection and injury of human astrocytes by tick-borne encephalitis virus. *J Gen Virol* 2014;95:2411–2426.

8. **Gelpi E, Preusser M, Laggner U, Garzuly F, Holzmann H et al.** Inflammatory response in human tick-borne encephalitis: analysis of postmortem brain tissue. *J Neurovirol* 2006;12:322–327.

9. **Růžek D, Salát J, Palus M, Gritsun TS, Gould EA et al.** CD8+ T-cells mediate immunopathology in tick-borne encephalitis. *Virology* 2009;384:1–6.

10. **Melchjorsen J.** Learning from the messengers: innate sensing of viruses and cytokine regulation of immunity – clues for treatments and vaccines. *Viruses* 2013;5:470–527.

11. **Ivashkiv LB, Donlin LT.** Regulation of type I interferon responses. *Nat Rev Immunol* 2014;14:36–49.

12. **Schneider WM, Chevillotte MD, Rice CM.** Interferon-stimulated genes: a complex web of host defenses. *Annu Rev Immunol* 2014; 32:513–545.

13. **Kallfass C, Ackerman A, Lienenklaus S, Weiss S, Heimrich B et al.** Visualizing production of beta interferon by astrocytes and microglia in brain of La Crosse virus-infected mice. *J Virol* 2012; 86:11223–11230.

14. **Delhaye S, Paul S, Blakqori G, Minet M, Weber F et al.** Neurons produce type I interferon during viral encephalitis. *Proc Natl Acad Sci USA* 2006;103:7835–7840.

15. **Samuel MA, Diamond MS.** Alpha/beta interferon protects against lethal West Nile virus infection by restricting cellular tropism and enhancing neuronal survival. *J Virol* 2005;79:13350–13361.

16. **Cho H, Proll SC, Szretter KJ, Katze MG, Gale M et al.** Differential innate immune response programs in neuronal subtypes determine susceptibility to infection in the brain by positive-stranded RNA viruses. *Nat Med* 2013;19:458–464.

17. **Li J, Hu S, Zhou L, Ye L, Wang X et al.** Interferon lambda inhibits herpes simplex virus type I infection of human astrocytes and neurons. *Glia* 2011;59:58–67.

18. **Lazear HM, Daniels BP, Pinto AK, Huang AC, Vick SC et al.** Interferon-λ restricts West Nile virus neuroinvasion by tightening the blood-brain barrier. *Sci Transl Med* 2015;7:284ra59.

19. **Marcello T, Grakoui A, Barba-Spaeth G, Machlin ES, Kotenko SV et al.** Interferons α and λ inhibit hepatitis C virus replication with distinct signal transduction and gene regulation kinetics. *Gastroenterology* 2006;131:1887–1898.

20. **Bolen CR, Ding S, Robek MD, Kleinstein SH.** Dynamic expression profiling of type I and type III interferon-stimulated hepatocytes reveals a stable hierarchy of gene expression. *Hepatology* 2014; 59:1262–1272.

21. **Weber E, Finsterbusch K, Lindquist R, Nair S, Lienenklaus S et al.** Type I interferon protects mice from fatal neurotropic infection with Langat virus by systemic and local antiviral responses. *J Virol* 2014;88:12202–12212.

22. **Kurhade C, Zegenhagen L, Weber E, Nair S, Michaelsen-Preusse K et al.** Type I interferon response in olfactory bulb, the site of tick-borne flavivirus accumulation, is primarily regulated by IPS-1. *J Neuroinflammation* 2016;13:22.

23. **Lindqvist R, Mundt F, Gilthorpe JD, Wölfel S, Gekara NO et al.** Fast type I interferon response protects astrocytes from flavivirus infection and virus-induced cytopathic effects. *J Neuroinflammation* 2016;13:277.

24. **Best SM, Morris KL, Shannon JG, Robertson SJ, Mitzel DN et al.** Inhibition of interferon-stimulated JAK-STAT signaling by a tick-borne flavivirus and identification of NS5 as an interferon antagonist. *J Virol* 2005;79:12828–12839.

25. **Růžek D, Vancová M, Tesarová M, Ahantarig A, Kopecký J et al.** Morphological changes in human neural cells following tick-borne encephalitis virus infection. *J Gen Virol* 2009;90:1649–1658.

26. **Jacobsen PF, Jenkyn DJ, Papadimitriou JM.** Establishment of a human medulloblastoma cell line and its heterotransplantation into nude mice. *J Neuropathol Exp Neurol* 1985;44:472–485.

27. **Howard BM, Zhicheng Mo Z, Filipovic R, Moore AR, Antic SD et al.** Radial glia cells in the developing human brain. *Neuroscientist* 2008;14:459–473.

28. **Eng LF, Ghirnikar RS, Lee YL.** Glial fibrillary acidic protein: GFAP-thirty-one years (1969–2000). *Neurochem Res* 2000;25:1439–1451.

29. **Pontén J, Macintyre EH.** Long term culture of normal and neoplastic human glia. *Acta Pathol Microbiol Scand* 1968;74:465–486.

30. **Best SM, Morris KL, Shannon JG, Robertson SJ, Mitzel DN et al.** Inhibition of interferon-stimulated JAK-STAT signaling by a tick-borne flavivirus and identification of NS5 as an interferon antagonist. *J Virol* 2005;79:12828–12839.

31. **Bosworth A, Dowall SD, Garcia-Dorival I, Rickett NY, Bruce CB et al.** A comparison of host gene expression signatures associated with infection *in vitro* by the Makona and Ecran (Mayinga) variants of Ebola virus. *Sci Rep* 2017;7:43144.

32. **Voigt EA, Swick A, Yin J.** Rapid induction and persistence of paracrine-induced cellular antiviral states arrest viral infection spread in A549 cells. *Virology* 2016;496:59–66.

33. **Wang W, Wang WH, Azadzoi KM, Su N, Dai P et al.** Activation of innate antiviral immune response via double-stranded RNA-dependent RLR receptor-mediated necroptosis. *Sci Rep* 2016;6: 22550.

34. **Chiang C, Beljanski V, Yin K, Olagnier D, Ben Yebdri F et al.** Sequence-specific modifications enhance the broad-spectrum antiviral response activated by RIG-I agonists. *J Virol* 2015;89: 8011–8025.

35. **Yoneyama M, Suhara W, Fukuhara Y, Sato M, Ozato K et al.** Autocrine amplification of type I interferon gene expression mediated by interferon stimulated gene factor 3 (ISGF3). *J Biochem* 1996; 120:160–169.

36. **Donald CL, Brennan B, Cumberworth SL, Rezelj VV, Clark JJ et al.** Full Genome sequence and sfRNA interferon antagonist activity of Zika virus from Recife, Brazil. *PLoS Negl Trop Dis* 2016;10: e0005048.

37. **Kim D, Pertea G, Trapnell C, Pimentel H, Kelley R et al.** TopHat2: accurate alignment of transcriptomes in the presence of insertions, deletions and gene fusions. *Genome Biol* 2013;14:R36.

38. **Trapnell C, Hendrickson DG, Sauvageau M, Goff L, Rinn JL et al.** Differential analysis of gene regulation at transcript resolution with RNA-seq. *Nat Biotechnol* 2013;31:46–53.

39. **Palus M, Vojtíšková J, Salát J, Kopecký J, Grubhoffer L et al.** Mice with different susceptibility to tick-borne encephalitis virus infection show selective neutralizing antibody response and inflammatory reaction in the central nervous system. *J Neuroinflammation* 2013;10:77.

40. **Yoneyama M, Onomoto K, Jogi M, Akaboshi T, Fujita T et al.** Viral RNA detection by RIG-I-like receptors. *Curr Opin Immunol* 2015;32: 48–53.

41. **Tun MM, Aoki K, Senba M, Buerano CC, Shirai K et al.** Protective role of TNF-α, IL-10 and IL-2 in mice infected with the Oshima strain of Tick-borne encephalitis virus. *Sci Rep* 2014;4:5344.

42. **Miorin L, Romero-Brey I, Maiuri P, Hoppe S, Krijnse-Locker J et al.** Three-dimensional architecture of tick-borne encephalitis

virus replication sites and trafficking of the replicated RNA. *J Virol* 2013;87:6469–6481.

43. Zhou L, Wang X, Wang YJ, Zhou Y, Hu S *et al.* Activation of toll-like receptor-3 induces interferon-λ expression in human neuronal cells. *Neuroscience* 2009;159:629–637.

44. Katsetos CD, Herman MM, Mörk SJ. Class III β-tubulin in human development and cancer. *Cell Motil Cytoskeleton* 2003;55:77–96.

45. Päll T, Pink A, Kasak L, Turkina M, Anderson W *et al.* Soluble CD44 interacts with intermediate filament protein vimentin on endothelial cell surface. *PLoS One* 2011;6:e29305.

46. Johns TG, Bernard CC. The structure and function of myelin oligodendrocyte glycoprotein. *J Neurochem* 1999;72:1–9.

47. Solly SK, Thomas JL, Monge M, Demerens C, Lubetzki C *et al.* Myelin/oligodendrocyte glycoprotein (MOG) expression is associated with myelin deposition. *Glia* 1996;18:39–48.

48. Mlera L, Lam J, Offerdahl DK, Martens C, Sturdevant D *et al.* Transcriptome analysis reveals a signature profile for tick-borne flavivirus persistence in HEK 293T cells. *MBio* 2016;7:e00314-16.

49. Kindberg E, Mickiene A, Ax C, Akerlind B, Vene S *et al.* A deletion in the chemokine receptor 5 (*CCR5*) gene is associated with tick-borne encephalitis. *J Infect Dis* 2008;197:266–269.

50. Overby AK, Popov VL, Niedrig M, Weber F. Tick-borne encephalitis virus delays interferon induction and hides its double-stranded RNA in intracellular membrane vesicles. *J Virol* 2010;84:8470–8483.

51. Overby AK, Weber F. Hiding from intracellular pattern recognition receptors, a passive strategy of flavivirus immune evasion. *Virulence* 2011;2:238–240.

52. Odendall C, Dixit E, Stavru F, Bierne H, Franz KM *et al.* Diverse intracellular pathogens activate type III interferon expression from peroxisomes. *Nat Immunol* 2014;15:717–726.

53. Hornung V, Hartmann R, Ablasser A, Hopfner KP. OAS proteins and cGAS: unifying concepts in sensing and responding to cytosolic nucleic acids. *Nat Rev Immunol* 2014;14:521–528.

54. Lenschow DJ. Antiviral properties of ISG15. *Viruses* 2010;2:2154–2168.

55. Wang W, Xu L, Su J, Peppelenbosch MP, Pan Q *et al.* Transcriptional regulation of antiviral interferon-stimulated genes. *Trends Microbiol* 2017 [Epub ahead of print].

56. Fitzgerald KA. The interferon inducible gene: viperin. *J Interferon Cytokine Res* 2011;31:131–135.

57. Liu SY, Sanchez DJ, Cheng G. New developments in the induction and antiviral effectors of type I interferon. *Curr Opin Immunol* 2011; 23:57–64.

58. Upadhyay AS, Vonderstein K, Pichlmair A, Stehling O, Bennett KL *et al.* Viperin is an iron-sulfur protein that inhibits genome synthesis of tick-borne encephalitis virus via radical SAM domain activity. *Cell Microbiol* 2014;16:834–848.

59. Werme K, Wigerius M, Johansson M. Tick-borne encephalitis virus NS5 associates with membrane protein scribble and impairs interferon-stimulated JAK-STAT signalling. *Cell Microbiol* 2008;10:696–712.

60. Kotenko SV, Gallagher G, Baurin VV, Lewis-Antes A, Shen M *et al.* IFN-λ s mediate antiviral protection through a distinct class II cytokine receptor complex. *Nat Immunol* 2003;4:69–77.

61. Defilippis VR, Robinson B, Keck TM, Hansen SG, Nelson JA *et al.* Interferon regulatory factor 3 is necessary for induction of antiviral genes during human cytomegalovirus infection. *J Virol* 2006; 80:1032–1037.

62. Dixit E, Boulant S, Zhang Y, Lee AS, Odendall C *et al.* Peroxisomes are signaling platforms for antiviral innate immunity. *Cell* 2010; 141:668–681.

63. Rivas HG, Schmaling SK, Gaglia MM. Shutoff of host gene expression in influenza A virus and herpesviruses: similar mechanisms and common themes. *Viruses* 2016;8:102.

64. Walsh D, Mohr I. Viral subversion of the host protein synthesis machinery. *Nat Rev Microbiol* 2011;9:860–875.

65. Josset L, Tchitchek N, Gralinski LE, Ferris MT, Eisfeld AJ *et al.* Annotation of long non-coding RNAs expressed in collaborative cross founder mice in response to respiratory virus infection reveals a new class of interferon-stimulated transcripts. *RNA Biol* 2014;11:875–890.

66. Kambara H, Niazi F, Kostadinova L, Moonka DK, Siegel CT *et al.* Negative regulation of the interferon response by an interferon-induced long non-coding RNA. *Nucleic Acids Res* 2014;42:10668–10680.

67. Barriocanal M, Carnero E, Segura V, Fortes P. Long non-coding RNA BST2/BISPR is induced by IFN and regulates the expression of the antiviral factor tetherin. *Front Immunol* 2014;5:655.

68. Holmgren AM, Miller KD, Cavanaugh SE, Rall GF. Bst2/Tetherin is induced in neurons by type I interferon and viral infection but is dispensable for protection against neurotropic viral challenge. *J Virol* 2015;89:11011–11018.

69. Maida Y, Yasukawa M, Furuuchi M, Lassmann T, Possemato R *et al.* An RNA-dependent RNA polymerase formed by TERT and the RMRP RNA. *Nature* 2009;461:230–235.

70. Carnero E, Barriocanal M, Segura V, Guruceaga E, Prior C *et al.* Type I interferon regulates the expression of long non-coding RNAs. *Front Immunol* 2014;5:548.

71. Saxena K, Simon LM, Zeng XL, Blutt SE, Crawford SE *et al.* A paradox of transcriptional and functional innate interferon responses of human intestinal enteroids to enteric virus infection. *Proc Natl Acad Sci USA* 2017;114:E570–E579.

72. Parker N, Porter AC. Identification of a novel gene family that includes the interferon-inducible human genes 6-16 and ISG12. *BMC Genomics* 2004;5:8.

73. Rosebeck S, Leaman DW. Mitochondrial localization and pro-apoptotic effects of the interferon-inducible protein ISG12a. *Apoptosis* 2008;13:562–572.

74. Qi Y, Li Y, Zhang Y, Zhang L, Wang Z *et al.* IFI6 inhibits apoptosis via mitochondrial-dependent pathway in Dengue virus 2 infected vascular endothelial cells. *PLoS One* 2015;10:e0132743.

75. Huang J, Li Y, Qi Y, Zhang Y, Zhang L *et al.* Coordinated regulation of autophagy and apoptosis determines endothelial cell fate during Dengue virus type 2 infection. *Mol Cell Biochem* 2014;397:157–165.

76. Itsui Y, Sakamoto N, Kurosaki M, Kanazawa N, Tanabe Y *et al.* Expressional screening of interferon-stimulated genes for antiviral activity against hepatitis C virus replication. *J Viral Hepat* 2006; 13:690–700.

77. Meyer K, Kwon YC, Liu S, Hagedorn CH, Ray RB *et al.* Interferon-α inducible protein 6 impairs EGFR activation by CD81 and inhibits hepatitis C virus infection. *Sci Rep* 2015;5:9012.

78. Labrada L, Liang XH, Zheng W, Johnston C, Levine B *et al.* Age-dependent resistance to lethal alphavirus encephalitis in mice: analysis of gene expression in the central nervous system and identification of a novel interferon-inducible protective gene, mouse ISG12. *J Virol* 2002;76:11688–11703.

79. Wilkins C, Woodward J, Lau DT, Barnes A, Joyce M *et al.* IFITM1 is a tight junction protein that inhibits hepatitis C virus entry. *Hepatology* 2013;57:461–469.

80. Narayana SK, Helbig KJ, Mccartney EM, Eyre NS, Bull RA *et al.* The interferon-induced transmembrane proteins, IFITM1, IFITM2, and IFITM3 Inhibit hepatitis C virus entry. *J Biol Chem* 2015;290: 25946–25959.

81. Warren CJ, Griffin LM, Little AS, Huang IC, Farzan M *et al.* The antiviral restriction factors IFITM1, 2 and 3 do not inhibit infection of human papillomavirus, cytomegalovirus and adenovirus. *PLoS One* 2014;9:e96579.

82. Meng X, Yang D, Yu R, Zhu H. EPSTI1 is involved in IL-28A-mediated inhibition of HCV infection. *Mediators Inflamm* 2015; 2015:1–13.

83. Pan XB, Qu XW, Jiang D, Zhao XL, Han JC *et al.* BST2/Tetherin inhibits hepatitis C virus production in human hepatoma cells. *Antiviral Res* 2013;98:54–60.

84. **Pan XB, Han JC, Cong X, Wei L.** BST2/Tetherin inhibits dengue virus release from human hepatoma cells. *PLoS One* 2012;7: e51033.

85. **Kozuch O, Mayer V.** Pig kidney epithelial (PS) cells: a perfect tool for the study of flaviviruses and some other arboviruses. *Acta Virol* 1975;19:498.

86. **Heinz FX, Kunz C.** Homogeneity of the structural glycoprotein from European isolates of tick-borne encephalitis virus: comparison with other flaviviruses. *J Gen Virol* 1981;57:263–274.

87. **de Madrid AT, Porterfield JS.** A simple micro-culture method for the study of group B arboviruses. *Bull World Health Organ* 1969; 40:113–121.

88. **Zhang L, Li Y, Gu Z, Wang Y, Shi M *et al.*** Resveratrol inhibits enterovirus 71 replication and pro-inflammatory cytokine secretion in rhabdosarcoma cells through blocking IKKs/NF-κB signaling pathway. *PLoS One* 2015;10:e0116879.

89. **Wood DE, Salzberg SL.** Kraken: ultrafast metagenomic sequence classification using exact alignments. *Genome Biol* 2014;15:R46.

Five reasons to publish your next article with a Microbiology Society journal

1. The Microbiology Society is a not-for-profit organization.
2. We offer fast and rigorous peer review – average time to first decision is 4–6 weeks.
3. Our journals have a global readership with subscriptions held in research institutions around the world.
4. 80% of our authors rate our submission process as 'excellent' or 'very good'.
5. Your article will be published on an interactive journal platform with advanced metrics.

Find out more and submit your article at microbiologyresearch.org.

Corrigendum: Analysis of tick–borne encephalitis virus–induced host responses in human cells of neuronal origin and interferon–mediated protection

Martin Selinger,[1,2] Gavin S. Wilkie,[3] Lily Tong,[3] Quan Gu,[3] Esther Schnettler,[3]† Libor Grubhoffer[1,2] and Alain Kohl[3,*]

Due to a mistake in data set export, an error was introduced by which CTD-2328D6.1 was mistakenly switched to RNA28S5 in Table S5, leading to this gene wrongly being mentioned in the text on several occasions, and errors in Fig. 4.

The corrected Table S5 is shown in the supplementary material.

On page 2046, section, 'Host response-associated genes, including type III IFNs, are activated upon TBEV infection of DAOY cells', the first appearance of 'RNA28S5' should be changed to 'CTD-2328D6.1' and the final appearance of 'RNA28S5' should be removed from the following section of text.

'RNA28S5, RN7SL2, NOTCH3, COL1A1, BCL9L, BCORL1, POLR2A, FAM71D, IGF2, RN7SL3 and HSPG2 were found to be the most strongly down-regulated genes (fold-change >2.5; Fig. 4 and Table S5). Other than protein-coding genes, a number of non-coding RNAs were also identified as being differentially expressed upon TBEV infection, as shown in Fig. 4(b). However, of these, RN7SL2, RN7SL3 and RNA28S5 are the only RNA genes with known functions.'

This section should read as follows:

'CTD-2328D6.1, RN7SL2, NOTCH3, COL1A1, BCL9L, BCORL1, POLR2A, FAM71D, IGF2, RN7SL3 and HSPG2 were found to be the most strongly down-regulated genes (fold-change >2.5; Fig. 4 and Table S5). Other than protein-coding genes, a number of non-coding RNAs were also identified as being differentially expressed upon TBEV infection, as shown in Fig. 4(b). However, of these, RN7SL2 and RN7SL3 are the only RNA genes with known functions.'

On page 2052, right-hand column, paragraph 2, the first occurrence of 'RNA28S5' should be removed and the final appearance of 'RNA28S5' should be changed to 'CTD-2328D6.1' in the following section of text.

'Downregulation of effectors involved in either transcription (POLR2A) or translation (RNA28S5, RN7SL2, RN7SL3) suggests a possible TBEV-driven transcriptional or translational shut off in host cells. Both transcriptional and translational shut off are well-documented phenomena [63, 64]. Similar rates of RNA28S5, NOTCH3, COL1A1, BCL9L, BCOR1, POLR2A, FAM71D, IGF2 and HSPG2 down-regulation were also evident in IFN-β-pre-treated cells infected with TBEV, where significantly lower viral titres were determined.'

This section should read as follows:

'Downregulation of effectors involved in either transcription (POLR2A) or translation (RN7SL2, RN7SL3) suggests a possible TBEV-driven transcriptional or translational shut off in host cells. Both transcriptional and translational shut off are well-documented phenomena [63, 64]. Similar rates of CTD-2328D6.1, NOTCH3, COL1A1, BCL9L, BCOR1, POLR2A, FAM71D, IGF2 and HSPG2 down-regulation were also evident in IFN-β-pre-treated cells infected with TBEV, where significantly lower viral titres were determined.'

An error also occured in Table S3 due to a formatting mistake. The following changes are shown in the updated supplementary material:

'3.01' on page 1 in column 'IFN-β' was corrected to 'MARC1'.

'9.09' on page 10 in column 'TBEV' was corrected to 'SEPT9'.

'3.04' on page 12 in column 'TBEV' was corrected to 'MARCH4'.

'9.09' on page 14 in column 'IFN-β + TBEV' was corrected to 'SEPT9'.

'3.03' on page 20 in column 'IFN-β + TBEV' was corrected to 'MARCH3'.

Fig. 4. Overview of selected differentially expressed genes. DAOY cells were pre-treated with IFN-β (10 ng ml^{-1}) and/or infected with TBEV (m.o.i. 5) after 12 h. Three independent biological replicates were included for each of the combinations [untreated mock cells (control); IFN-β-treated mock cells; untreated cells infected with TBEV; IFN-β-pre-treated cells infected with TBEV]. Total cellular RNA was isolated at 24 h p.i. and used for transcriptome analysis. (a) List of selected protein-coding genes identified to be differentially expressed in at least one of the combinations over control (Benjamini Hochberg *P*-value $\leq$0.05 and fold change >1.5 or <$-$1.5; down-regulated in red and up-regulated in green). To emphasize the up-regulation of IFN-λ1, information for transcripts of IFN-α, IFN-β and IFN-γ was also included. (b) List of selected non-coding genes identified to be differentially expressed in at least one of the combinations over control (Benjamini Hochberg *P*-value $\leq$0.05 and fold change >1.5 or <$-$1.5; down-regulated in red and up-regulated in green).

Fig. 4 also required a correction in the heatmap and four genes that were in panel (a) should only be present in panel (b), with RNA28S5 deleted from the figure. The corrected Fig. 4 is shown above.

The authors apologise for any inconvenience caused.

Věchtová, P., Štěrbová, J., Štěrba, J., Vancová, M., Rego, R.O.M., **Selinger, M.**, Strnad, M., Golovchenko, M., Rudenko, N., Grubhoffer, L., 2018: A bite so sweet – the glycobiology interface of tick-host-pathogen interactions. Parasites & Vectors 11(1): 594. DOI: 10.1186/s13071-018-3062-7. (IF = 3.408)

REVIEW   **Open Access**

A bite so sweet: the glycobiology interface of tick-host-pathogen interactions

Pavlina Vechtova[1,2*†], Jarmila Sterbova[1,2†], Jan Sterba[1,2], Marie Vancova[1,2], Ryan O. M. Rego[1,2], Martin Selinger[1,2], Martin Strnad[1,2], Maryna Golovchenko[1], Nataliia Rudenko[1] and Libor Grubhoffer[1,2]

Abstract

Vector-borne diseases constitute 17% of all infectious diseases in the world; among the blood-feeding arthropods, ticks transmit the highest number of pathogens. Understanding the interactions between the tick vector, the mammalian host and the pathogens circulating between them is the basis for the successful development of vaccines against ticks or the tick-transmitted pathogens as well as for the development of specific treatments against tick-borne infections. A lot of effort has been put into transcriptomic and proteomic analyses; however, the protein-carbohydrate interactions and the overall glycobiology of ticks and tick-borne pathogens has not been given the importance or priority deserved. Novel (bio)analytical techniques and their availability have immensely increased the possibilities in glycobiology research and thus novel information in the glycobiology of ticks and tick-borne pathogens is being generated at a faster pace each year. This review brings a comprehensive summary of the knowledge on both the glycosylated proteins and the glycan-binding proteins of the ticks as well as the tick-transmitted pathogens, with emphasis on the interactions allowing the infection of both the ticks and the hosts by various bacteria and tick-borne encephalitis virus.

Keywords: Tick, Pathogen, Host, Glycan, Lectin, Glycobiology, *Borrelia*, *Anaplasma*, TBEV, Carbohydrate-binding

Background

Vector-borne diseases constitute 17% of all infectious diseases in the world [1]. Pathogenic viruses, bacteria, and protozoa are carried by blood-feeding arthropods on just about all the continents and both livestock and people tend to be affected by these. This becomes a large economic burden on the animal health sector and on the public health system of various countries. Ticks are the first among blood-feeding vectors in terms of the number of pathogens that they can transmit. Unfortunately, there are next to no vaccines against the tick-transmitted bacterial and protozoan diseases and very few against tick-borne viruses [2]. The only successful anti-tick vaccine, based on the glycoprotein Bm86 from the cattle tick *Rhiphicephalus microplus*, has been shown to be efficient against ticks of the genus *Rhiphicephalus* and Bm86 homologue vaccines have had some efficiency against at

least two species of the genus *Hyalomma*, but this is not the case for other ticks and the pathogens they transmit [3]. The European Centre for Disease Prevention and Control suggests that there will be a rise in tick-borne diseases based on changes in various factors including the environment and socio-economics [4]. Research efforts to combat tick-borne diseases have usually centred, as with most other infectious diseases, on determining the Achilles' heel of the pathogen. Most endeavours have focussed on understanding host-pathogen interactions, primarily at the vertebrate level. Protein-carbohydrate interactions between the pathogen and the host cell are of primary importance, in terms of attachment and/or invasion of the cell, whether in an invertebrate or vertebrate host. The observation that there is conservation in the protein-carbohydrate recognition strategies can be used as part of novel approaches for intervention [5]. It has been shown that many regulatory mechanisms are mediated by post-translational modifications (PTM). One example of a PTM that regulates protein degradation and signaling in eukaryotes is ubiquitination. Pathogens are known to exploit ubiquitination to infect mammalian cells and it

* Correspondence: vechtp00@jcu.cz
†Pavlina Vechtova and Jarmila Sterbova contributed equally to this work.
[1]Institute of Parasitology, Biology Centre, Czech Academy of Sciences, Branišovská 31, CZ-37005 České Budějovice, Czech Republic
[2]Faculty of Science, University of South Bohemia, Branišovská 1760, CZ-37005 České Budějovice, Czech Republic

has been shown that the ubiquitination machinery is present in the tick *Ixodes scapularis*. It was identified that the E3 ubiquitin ligase XIAP restricted bacterial colonization of the vector and *xiap* silencing significantly increased tick colonization by the bacterium *Anaplasma phagocytophilum*, the causative agent of human granulocytic anaplasmosis [6].

Over the last decade, there has been a slow increase in the knowledge of vector-host-pathogen interactions which start from the time a pathogen invades the vector within a blood meal and attaches to the tick midgut lumen. Later it traverses to the tick salivary glands and completes its life-cycle by transmission to a new mammalian host during the subsequent tick feeding [2].

Four possible routes that may facilitate pathogen survival and transmission by most arthropod vectors including ticks have been pointed out. These include: (i) pathogen carbohydrate-binding adhesins that attach to receptors in the tick midgut; (ii) the attachment of carbohydrate-binding proteins of the arthropod to the pathogen as part of its innate immunity; (iii) carbohydrate-binding proteins that are soluble and form a link between the pathogen and midgut surfaces; and (iv) the use of co-receptors to enhance the interactions within the vector [5].

In this review, we would like to highlight the glycobiological aspects of all four of these specific mechanisms that come into play when looking at the vector-pathogen interactions as well as glycobiology-associated processes between the mammalian host and the pathogen (see Fig. 1). Glycobiology of ticks and tick-borne pathogens is developing together with the increased availability and sensitivity of analytical methods; a short overview is listed below, together with some relevant references for readers seeking deeper knowledge.

Importance of glycosylation for protein functions

Post-translational modifications can be found in both prokaryotic and eukaryotic organisms; among them, glycosylation is one of the most abundant and most important. Protein glycosylation affects all the functions of proteins - their structure, activity, interactions with other molecules, half-life in the cell or organism; immune recognition is also dependent on the interaction of immune cells and receptors with glycosylated molecules. A wide variety of possible glycan structures and linkages increases the functionality of proteins [7].

The importance of carbohydrates for the function of proteins can be simply shown on complement proteins. The complement system comprises of more than 30 plasma- or membrane-bound components. Most of them are glycosylated to the various extent and the type of glycosylation generates tissue- or cell-specific population of glycoforms of each complement molecule. The specific
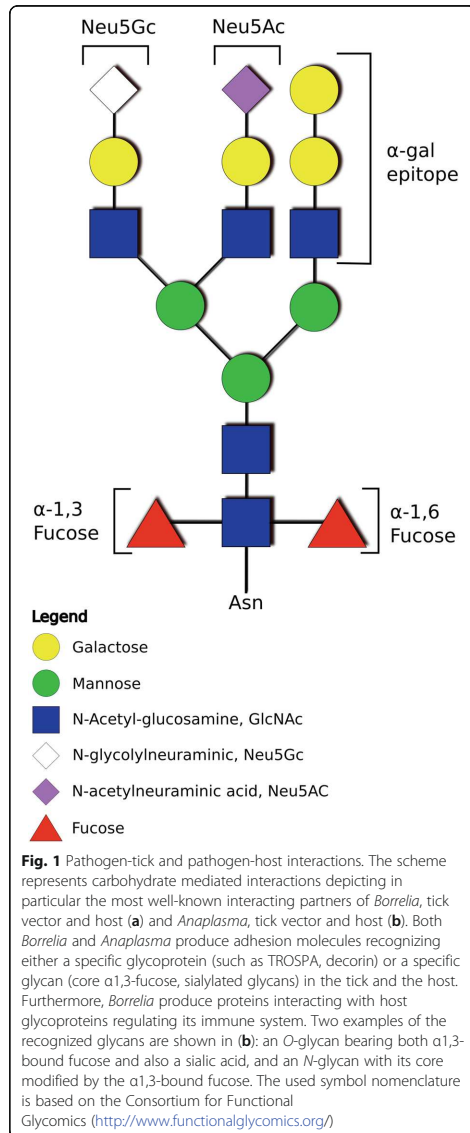
Fig. 1 Pathogen-tick and pathogen-host interactions. The scheme represents carbohydrate mediated interactions depicting in particular the most well-known interacting partners of *Borrelia*, tick vector and host (**a**) and *Anaplasma*, tick vector and host (**b**). Both *Borrelia* and *Anaplasma* produce adhesion molecules recognizing either a specific glycoprotein (such as TROSPA, decorin) or a specific glycan (core α1,3-fucose, sialylated glycans) in the tick and the host. Furthermore, *Borrelia* produce proteins interacting with host glycoproteins regulating its immune system. Two examples of the recognized glycans are shown in (**b**): an *O*-glycan bearing both α1,3-bound fucose and also a sialic acid, and an *N*-glycan with its core modified by the α1,3-bound fucose. The used symbol nomenclature is based on the Consortium for Functional Glycomics (http://www.functionalglycomics.org/)

glycoform population then secures functions that are required for a particular cell type or tissue. The repertoire of functions secured by glycans ranges from the control of protein folding, proper assembly within the endoplasmic reticulum, mechanistic shielding of the protein backbone

against protease degradation, preventing inappropriate protein-protein interactions or formation of proper spatial protein conformation or participation in recognition epitope formation [8]. Specific examples show interesting ways in which glycans influence or modulate the complement cascade.

C1q is a recognition molecule of classical complement pathway and mediates initiation of the pathway by binding to the antibody-antigen complexes. The proper function of the C1q is conditioned by the appropriate triple helix formation within C1q monomer and the formation of C1q hexamer whose spatial conformation may be secured by the presence of N-linked glycan of each monomer [9].

Glycosylation was also proven important in complement regulatory factors where factor H (fH) glycosylation mediates its proper folding within the endoplasmic reticulum (ER). The absence of glycosylation or its malfunctioning leads to in fH misfolding and retention in ER causing clinical symptoms in children in form of hypocomplementemic renal disease [10].

C1-inhibitor is a plasma glycoprotein and, along with other members of the serpin proteases, its inhibitory activities are enhanced by binding of negatively charged polysaccharides. Most of the polysaccharides binding to the C1-inhibitor induce allosteric changes of the inhibitor molecule causing potentiation of the attachment to the C1 proteases or, as in case of dermatan sulphate, the potentiation is caused by the formation of a negatively charged polysaccharide-mediated linkage between positively charged portions of the C1-inhibitor and C1 protease molecules [11]. Structural characterization of the C1-inhibitor reveals extensive O-glycosylation with a high number of sialylated glycans. The trials for functional characterization of C1-inhibitor glycosylation showed an increased resistance of highly O-glycosylated region against proteolytic degradation [12] and highlighted the importance of sialylation for prolonged serum half-life [13].

Advances in bioanalytical methods for glycobiology

The most frequently used methods in glycobiology are mass spectrometry in combination with chromatography or capillary electrophoresis, glycan/lectin microarrays, or lectin staining. All of these developed greatly recently; for example, the increasing number of mass spectrometers available throughout the world and the development of more sensitive instruments and specifically the introduction of the Orbitrap mass spectrometers, greatly advanced the possibilities for glycan and glycoprotein analysis [14, 15]. The number of commercially available microarrays is also increasing and nowadays allows more or less specific detection of almost any kind of glycan. The availability of lectins together with the possibility to synthesize specific glycan molecules allows also the preparation of in-house glycan-

or lectin-arrays; another possibility is the service provided by the Consortium for Functional Glycomics (http://www.functionalglycomics.org/).

Here, we review the current knowledge on how pathogens have evolved "sweet" strategies to overcome the immune responses within the vector and the mammalian host and the use of carbohydrate-binding properties to perpetuate their transmission and dissemination into a vertebrate host (Tables 1 and 2). We also provide a near comprehensive catalogue of all carbohydrate molecules that play a part in the disease cycle that have been characterized to date, be it within the tick or the mammalian host. We would like this to be the start of a renewed interest in the glycobiology of ticks and tick-borne diseases.

Glycosylation in the *Borrelia* infection cycle

Compared to eukaryotes, glycosylation in bacteria produces a much more diverse repertoire of glycoconjugate structures which are often species- or strain-specific. Most of the bacterial glycoconjugates are an integral part of the bacterial cell wall and provide the bacterial cell structural integrity. Additionally, the bacterial glycosylated cell surface structures mediate adhesion and interaction with its environment or host. Although the structural features of bacterial surface glycans have been well described, the function of many of them, including those in pathogenic bacteria, remain unexplored. In principle, pathogenic bacteria use glycosylation for two reasons; they synthesize host-like glycan structures to hide from the host immune system and, conversely, they produce glycosylated proteins that are able to bind more effectively the host immune molecules and thus influence their activity [16].

Since all *Borrelia* species are host-propagated bacteria that shuttle between a vertebrate host and an arthropod vector, these spirochetes have developed strategies to adjust to these diverse environments [17]. This is achieved by regulating the level of gene expression in response to changes in temperature, pH, salts, nutrient content, and other host- and vector-dependent factors. A significant number of *Borrelia* proteins mediate the interactions with host/vector molecules and thus enable *Borrelia* to complete its infectious cycle. Recent findings highlight the importance of carbohydrate moieties in these interactions and in the overall pathogenesis of this infectious spirochete.

Borrelia/tick glycosylated interactions

When entering the vertebrate host during tick-feeding, *Borrelia* must overcome several barriers to successfully invade and disseminate in the host body. The invasion of the host is difficult as it requires the interaction of the existing *Borrelia* surface structures with host tissues without being noticed by the host immune system. *Borrelia* have developed many elaborate strategies to recognize diverse host molecules and cell types to promote

Table 1 Summary of carbohydrate-binding proteins of *Borrelia* spp. recognizing tick or host receptors. The carbohydrate-binding proteins from *Borrelia* spp. are listed together with the recognized molecule from the vector or the host. Glycoproteins or glycans are listed as the recognized molecules depending on the available information. Majority of proteins from Lyme borreliosis spirochetes are listed; in the case of relapsing fever *Borrelia*, the bacterial species is defined

Borrelia spp. protein	Tick binding partner	Reference
Borrelia vs tick		
OspA	TROSPA	[236]
OspC	SALP15	[27]
TSLPI/P8	Mannose binding lectin (MBL)	[42]
Vsp33 (*B. hermsii*)	Unknown receptor in tick SG	[62]
Borrelia vs host		
Bgp (p26)	GAG	[294]
DbpA (p20)	Decorin/dermatansulfate	[48, 295]
DbpB (p19)	Decorin/dermatansulfate/chondroitinsulfate	[48, 295]
Bbk32	Fibronectin /heparansulfate/dermatansulfate	[63]
P66	Integrins	[87]
OspA	Plasminogen	[296]
OspC	Plasminogen	[297, 298]
Enolase	Plasminogen	[299]
Erps (OspE/F related proteins)	Factor H or FHL protein	[105]
CRASPs	Factor H	[105]
PAMPs	Mannose receptor on dendritic cells	[300]
Unknown	Neolacto-(Gal4GlcNAc3Gal4Glc1)-carrying glycoconjugates in human erythrocytes	[301]
VspB (*B.turicatae*)	GAG	[61]

Table 2 Summary of carbohydrate-binding proteins of *Anaplasma* recognizing tick or host receptors. The carbohydrate-binding proteins from *Anaplasma* are listed together with the recognized molecule from the vector or the host. Glycoproteins or glycans are listed as the recognized molecules depending on the available information

Anaplasma protein	Binding partner	Reference
MSP1a (MSP1 complex)	Vector binding partner: Unknown receptor in IDE8 tick cells	[189, 190]
Unknown molecule	Vector binding partner: Core α 1,3-fucose glycoprotein	[203]
Unknown adhesin-like molecule	Host binding partner: 1,3-Fuc and Sia in sialyl Lewis X, PSGL-1 in human neutrophils	[199, 200]
Unknown adhesin-like molecule	Host binding partner: 1,3-Fuc and Sia in sialyl Lewis X, PSGL-1 in murine neutrophils	[199]
Unknown adhesin-like molecule	Host binding partner: 1,3-Fuc and Sia in sialyl Lewis X, PSGL-1 in human myeloid HL-60 cells	[197, 201]
Unknown molecule of *A. phagocytophilum* NCH-1 strain	Host binding partner: 1,3-fucose in murine bone marrow-derived mast cells (BMMCs), murine peritoneal mast cells	[198]
Unknown molecule of *A. phagocytophilum* NCH-1 strain	Host binding partner: α 1,3-Fuc in human skin-derived mast cells	[198]
AmOmpA	Host binding partner: α2,3-sialylated and α1,3-fucosylated glycan of the sialyl Lewis x in myeloid cells	[182]
AmOmpA	Host binding partner: α2,3-sialylated and α1,3-fucosylated glycan of the 6- sulfo-sialyl Lewis x in endothelial cells	[180, 182]
AmOmpA	Host binding partner: α2,3-sialylated, α2,6-sialylated, α1,3-fucosylated glycan receptors in human and murine myeloid HL-60 cells, 6- sulpho-sialyl Lewis x in endothelial cells	[180–182]
Unknown	Host binding partner: α1,3-fucose	[203]

92

dissemination and chronic infection [18], and to overcome host immune system surveillance [19]. The concerted action of these structurally and functionally diverse *Borrelia* surface molecules helps the spirochete to successfully adapt and multiply in the host body.

The interacting molecules of *Borrelia* and the tick are often modified by glycosylation producing a diverse pool of structures. Moreover, glycosylation is a dynamic modification and can be readily altered upon environmental cues [20].

The presence of glycoconjugates on the surface of cultured *B. burgdorferi* has been demonstrated by the ability of *Borrelia* to bind a number of lectins [21]. In search of *B. burgdorferi* glycosylation patterns, increased attention has been paid to outer surface proteins that are produced at different stages of the *Borrelia* transmission cycle and represent points of interaction between the spirochetes and their hosts/vectors.

Borrelia outer surface proteins

Borrelia outer surface proteins A and B (*osp*A and *osp*B) are encoded on a bicistronic operon and extensively expressed on the surface of spirochetes in unfed ticks. OspA is one of the major and most comprehensively studied *Borrelia* proteins. While OspA mediates *Borrelia* attachment to the tick midgut when spirochetes are acquired by ticks during blood-feeding, OspB plays a key role in successful colonization of the tick midgut. OspA downregulation is important for *Borrelia* detachment, multiplication, and migration from the tick midgut to salivary glands [22–25]. When ticks are fed to engorgement, *Borrelia* clears OspA and OspB from the surface expressing instead another outer surface protein C (OspC) [22, 26].

OspC, encoded by *bbb19* mapped to the cp26 plasmid, is one of the most divergent genes in *Borrelia* genome, and is crucial for the early stages of mammalian host infection by the spirochete, but not required for acquisition of spirochetes by tick, tick colonization or migration from salivary glands to the gut [27–32].

Erps (OspE/F-related proteins) are a family of surface integrins with high affinity to factor H and encoded by *erp*-loci localised on each of the cp32 plasmids. Lyme disease spirochetes control Erp synthesis throughout the bacterial infectious tabacycle, producing the proteins during the infection of the host but downregulating their synthesis during tick infection stage. The best-characterized members are OspE and OspF proteins [33], their paralogues OspE/F-related proteins [34] and a group of OspE/F-like leader peptides (Elps) [35].

OspA, OspB and TROSPA

Earlier work had indicated that OspA and OspB are the major *Borrelia* glycosylated proteins [36], yet a later study showed that the suggested *N*-linked glycosylation does not occur [37]. Colonization of ticks by spirochetes requires the involvement of tick receptor(s). Although a tick receptor for OspB has not yet been identified, the tick receptor for OspA (TROSPA) is located in the tick gut and is heavily glycosylated. The blockade of TROSPA by TROSPA antisera or by downregulation of TROSPA *via* RNAi reduced *B. burgdorferi* adherence to the tick gut, hampering the spirochete transmission to the mammalian host. The number of potential posttranslational modification sites in TROSPA is unusually high (> 30), with a predominance of *O*-glycosylation sites [25].

OspC and Salp15

When transmitted from the tick vector to the host, *Borrelia* are delivered within the tick saliva. Tick saliva contains a plethora of bioactive molecules, which have been shown to be important for immunosuppression of the host responses [28]. One of the secreted salivary proteins is *Salp15* [29]. This protein specifically interacts with *B. burgdorferi* OspC which results in the protection of *Borrelia* from antibody-mediated killing and plays a critical role in establishing *B. burgdorferi* infection [27]. Whereas no data exists about the potential glycosylation of OspC, the glycosylation of Salp15 was demonstrated experimentally [30]. Salp15 from *I. ricinus* did not deliver the same protection to *B. garinii* and *B. afzelii* against antibody-mediated killing [31], presumably suggesting that the Salp15 binding for some species is an advantage for surviving in nature [31]. An explanation may lie in a different structural or spatial organization of the OspC or Salp15 molecule causing better access to the binding sites of each of the molecules in *B. burgdorferi*. Another hypothesis claims that *B. burgdorferi* OspC holds differently charged areas which interact in a way that favour formation of OspC multimers or even a lattice [38]. This structure, along with bound Salp15, might form a protective coating on the bacteria preventing an access of anti-OspC antibodies or *B. burgdorferi* antiserum [27]. In addition to the direct interplay between Salp15 and *B. burgdorferi*, Salp15 indirectly facilitates the host invasion by inhibiting dendritic cell activation by binding to the receptor/lectin DC-SIGN, localized on the surface of macrophages and dendritic cells [32].

Ixofin3D and Ixodes scapularis dystroglycan-like protein

Ixofin3D and *I. scapularis* dystroglycan-like protein (ISDLP) are glycoproteins expressed on the surface of midgut cells which were identified as candidate tick midgut binding partners of *B. burgdorferi* using a yeast surface display assay [39]. The expression of both Ixofin3D and ISDLP was elevated in *Borrelia*-infected tick midgut during feeding. Ixofin3D and ISDLP interact with spirochete cells as was confirmed *in vitro* by immunofluorescence assay and RNA interference. The RNAi-mediated reduction in expression of Ixofin3D and ISDLP resulted in decreased

Vechtova *et al. Parasites & Vectors*   (2018) 11:594

Page 6 of 27

spirochete burdens in the tick salivary glands and in the murine host as well [39, 40]. The full-length Ixofin3D contains four putative fibronectin type III domains. Ixofin3D is glycosylated as shown experimentally by periodic-acid Schiff's staining of a recombinant protein produced in *Drosophila* cells. Even though the importance of Ixofin3D for *Borrelia* infection was shown, the borrelial binding partner for Ixofin3D has not yet been identified [39].

The binding partner for ISDLP is also yet to be discovered. Like Ixofin3D, ISDLP silencing did not reduce the spirochete numbers in the gut but the transmigration process from gut to salivary glands was impaired. The mechanism remains unknown although the collected evidence implies that ISDLP may facilitate gut tissue remodelling or reduced barrier for spirochete transfer to salivary glands [40].

TSLPI

Tick salivary lectin pathway inhibitor (TSLPI) is a secreted salivary protein that protects *Borrelia* from complement-mediated killing. TSLPI facilitates spirochete transmission and acquisition through interference with the host mannose-binding lectin (MBL) and inhibition of the host lectin complement pathway [41]. *N*-linked glycosylation of recombinant *Drosophila*-expressed TSLPI appeared to be vital for its function as a lectin pathway inhibitor, suggesting that TSLPI *N*-glycans are involved in its binding to MBL carbohydrate recognition domains [42, 43].

Borrelia adhesins and extracellular matrix

Adhesion is the first and basic event in establishing an infection. The *Borrelia* cell surface is, at the time of host invasion, covered by adhesion proteins that can recognize and bind to various host cell types and/or extracellular matrix (ECM) components and thus promote *Borrelia* dissemination and settlement in various corners of the host body. Although *Borrelia* adhesins are not glycosylated, the presence of glycosylation has been confirmed in their tick receptors, suggesting a significant role of glycosylation in adhesin-receptor interaction.

Borrelia burgdorferi encodes a variety of adhesins and their characterization and role in the *Borrelia* infection cycle using different approaches was thoroughly described in a review by Coburn et al. [44]. With regard to their overlapping roles in *Borrelia* adhesion to the host tissue, it is important to note that only the concerted action of various adhesins guarantees an effective adhesion and transmigration of spirochetes to different hosts and their tissues [44].

A short overview of host ECM proteins
Glycosaminoglycans
Several ECM-associated molecules are specifically targeted by *Borrelia* adhesins. Exceptionally important seem to be the glycosaminoglycans (GAGs), large linear polysaccharides constructed of repeating disaccharide units (e.g. hyaluronan, chondroitin, dermatan, heparan, keratan) that decorate the ECM proteins. GAG chains are abundantly modified by sulphurylation, which imparts them a strong negative charge [45]. Numerous studies have shown that binding of GAGs by *B. burgdorferi* enables colonization of the host [46].

Fibronectin
A relevant ECM-associated molecule for *B. burgdorferi* attachment is fibronectin (Fn), a high-molecular weight, dimeric glycoprotein found in body fluids and in the ECM. *Borrelia burgdorferi* fails to bind to the ECM *in vitro* upon exposure to an anti-Fn antibody, implicating the Fn involvement in *Borrelia* attachment [47].

Decorins
Decorins are ubiquitous ECM proteoglycans, which are associated with collagen fibrils in the mammalian connective tissue [48]. Decorins are complex glycoproteins; apart from serine linked GAG chain, they are also modified by up to 3 N-glycans [49, 50]. Numerous studies associate decorins with *Borrelia* adhesin attachment and interestingly, the binding is promoted by intact decorin proteoglycan molecule rather than its protein core or GAG chain itself [48].

Laminin
Laminin is a large extracellular matrix multidomain glycoprotein. It is a critical molecule in the basement membrane assembly and, by extension, in tissue formation in the developing organism [51]. Besides its role in basement membrane architecture, it also mediates cellular interactions and provides a dense network for various cellular signalling and attachment events. The existence of different laminin isoforms gives space to developmental regulations mediated by differential responses to cells and newly forming tissues. Laminin, as well as other ECM forming molecules, possesses numerous glycosylation sites and its molecule is modified up to 32 % by N-linked glycans [52].

The carbohydrate portion of Laminin was proven to be a mediator of attachment in several bacterial species [53]. Laminin is also a potent target of several borrelial adhesins [54–56] although the direct involvement of the laminin carbohydrate moiety has not been reported yet.

Integrins
Integrins are glycosylated cell surface receptors mediating cell adhesions to the extracellular matrix and some important cell-cell interactions [57]. The presence of *N*-linked glycans in integrin molecule proves integral for the stability of the domain conformation and consequently affects integrin adhesive properties [58]. Integrins possess

Vechtova *et al. Parasites & Vectors*   (2018) 11:594

Page 7 of 27

a typical heterodimeric structure combining different α and β polypeptide chains and their combination determines the specificity of integrins [59]. Integrins are expressed on all mammalian cells except erythrocytes. The expression of different integrin subtypes produces unique cell surface signature of each cell type [60].

Borrelia adhesins
Vsps
Relapsing fever *Borrelia*, unlike Lyme disease-causing *Borrelia*, are vectored by soft ticks of the genus *Ornithodoros*. They are present in the blood of the mammalian host in high numbers which lead to high fevers followed by bouts of relapses. They recognize glycosaminoglycans (GAG), which mediates the attachment of *Borrelia* to mammalian cells. GAG recognition is partly dependent on the presence of some of the variable small proteins (Vsps). *Borrelia turicatae*, a relapsing fever borrelia that is vectored by *O. turicata*, recognizes GAGs *via* VspB which allows binding of *B. turicatae* to cultured mammalian cells as well as increased spread and replication in the mammalian host. *Borrelia hermsii* also attaches to cultured mammalian cells *via* GAGs; however, Vsps are not essential for this binding [61].

After the feeding of *O. hermsi* with *B. hermsii*-infected blood, the bacteria switched from expression of many bloodstream outer surface variable major proteins (Vmps) to a unique protein, variable tick protein (Vtp, Vsp33) [62].

BBK32, RevA and C1-inhibitor
Borrelia burgdorferi expresses at least two fibrinogen-binding proteins, BBK32 [63] and RevA [64]. BBK32 is a protein, whose attenuation does not block the spirochete transmission from the tick to the host [65], but lowers the bacterial loads in different tissues at different time points of infection [66]. *Borrelia burgdorferi* also attaches to endothelium in the vascular system through fibrinogen (Fn) and this interaction becomes stronger with increasing blood flow, allowing the spirochete to overcome fluid shear stress [67]. These stabilizing interactions are sustained by catch bond properties of BBK32 [68]. Following the binding to Fn, BBK32 binds to various kinds of GAGs, including heparin sulphates and dermatan sulphates of the host ECM [69–71]. It also seems to be involved in the modulation of the innate immunity. In particular, BBK32 binds the C1 complex of the classical innate immunity pathway, preventing its activation and thus obstructing classical pathway-mediated *Borrelia* lysis [72].

As *B. burgdorferi* BBK32 mutants are still able to bind fibronectin, an additional Fn-binding protein, RevA, was identified [58]. RevA expression on the *Borrelia* cell surface was upregulated in mammalian host compared to the tick vector. Furthermore, *Borrelia*-infected patients produced anti-RevA antibodies throughout various stages of Lyme disease suggesting its involvement in Lyme disease establishment and persistence in the host. RevA appears to have multiple binding sites which *Borrelia* uses to bind host cells *via* Fn [46, 73].

DbpA/DbpB
Decorin-binding proteins A and B (DbpA and DbpB) are adhesins found on the surface of *B. burgdorferi* [20, 45]. These proteins are critical for the virulence of *B. burgdorferi* [74, 75]. New data suggests that the decorin-binding proteins actually do not bind directly to the decorin protein core but interact with decorin *via* GAGs that are attached to the protein [76–78]. The binding studies of DbpA and DbpB from different *Borrelia* genospecies showed that there are clear differences in the decorin binding activity and that these differences may ultimately lead to the differences in tissue tropism and clinical manifestations associated with particular *Borrelia* genospecies [76, 79]. *In vivo* functional studies demonstrated the importance of DbpA/B adhesins for *Borrelia* invasion of the mammalian host especially in the early stages of infection [80].

Bgp
Borrelia burgdorferi glycosaminoglycan binding protein (Bgp) is a surface-exposed protein on intact spirochetes [70]. Recombinant Bgp bound the same GAG as the whole spirochete, agglutinated erythrocytes and inhibited binding of *B. burgdorferi* to the mammalian cells. A transposon mutant of the *Bgp* gene had less ability to adhere to host endothelial and epithelial cells *in vitro* and to colonize host target tissues leading to the reduced inflammatory manifestation of Lyme disease in the mouse model. The adherence was not fully disrupted due to the existence of other GAG-binding adhesins which facilitate host colonization and also highlights the importance of *Borrelia* GAG-binding ability for the completion of the infection cycle [81]. Although the Bgp attachment to GAG is not essential for disease establishment, the protein appears to be involved in the formation of an initial infectious niche in the host. Different spirochetes strains possess different GAG-binding preferences and their binding ability to multiple cells depends on the GAGs that they express [76].

BmpA
BmpA (*Borrelia* membrane protein A) and its three paralogues B, C, and D are all laminin-binding borrelial outer surface proteins [82]. Like other *Borrelia* surface proteins, BmpA is also antigenic. All bmp genes are located on the *Borrelia* chromosome, arranged in clusters that are differentially regulated [83]. The involvement in the development of arthritis in the mouse model was described for two Bmp proteins, BmpA and BmpB [84].

Borrelia adhesins and integrin-mediated interactions

Borrelia binds to host endothelial cells *via* the interaction of integrins $\alpha_{IIb}\beta_3$, $\alpha_V\beta_3$, and $\alpha_V\beta_1$ with *Borrelia* surface adhesins [59, 85]. It was also described that the causative agent of relapsing fever, *B. hermsii*, binds to human platelets promoted by the platelet glycoprotein integrin $\alpha_{IIb}\beta_3$ and is diminished by $\alpha_{IIb}\beta_3$ antagonists or by a genetic defect in this integrin [86].

P66

P66 is one of the candidate ligands for β_3-chain integrins (e.g. $\alpha_{IIb}\beta_3$, $\alpha_V\beta_3$) [87]. P66 also functions as a porin [88, 89], and structural predictions, as well as some experimental data, present the molecule as porin assuming the structure of β-barrel [90].

P66 mutants showed a dramatically reduced ability to attach to integrin $\alpha_V\beta_3$ [91]. Endothelial cells responded to wild-type *Borrelia* infection by upregulation of endothelial growth factor compared to a control infection with a P66 deletion mutant. The ability of P66 mutants to transmigrate through the cell monolayer was impaired, which suggests the role of P66 in *Borrelia* transendothelial migration, although its porin function does not play a role in the migration process [92].

Mammalian integrins typically contain an RGD (Arg-Gly-Asp tripeptide) consensus sequence in their binding domain, where aspartic acid is a key binding amino acid. P66 lacks this sequence; however, residues 205 and 207 of its 203–209 binding region are both aspartic acid [93]. P66 deletion mutants applied subcutaneously are readily cleared out of the site of infection, which refers to the possible involvement of the innate immune system and confirms the importance of this protein for host colonization together with other studies [94]. However, tick colonization is shown to be P66-independent [94].

BB0172

BB0172 is an outer membrane protein containing von Willebrand factor A domain which mediates intercellular and protein-protein interactions in ECM. It is, for example, involved in the attachment of platelets to the ECM in the site of damaged endothelial epithelium *via* platelet surface glycoprotein [95]. BB0172 showed a weak interaction with ECM-associated fibronectin. Importantly, a strong affinity was observed in the attachment of BB0172 to $\alpha_{III}\beta_1$ integrin. Moreover, the affinity was much stronger than the one observed in the interaction of borrelial P66 adhesins with β_3 chain integrins [95].

Borrelia adhesins interacting with mammalian complement

Mammalian innate immunity is alerted by a variety of surface-exposed molecules of invading pathogens. The first encounter of host antibodies with potentially harmful intruder activates the complement system which assists in tagging of the pathogen for destruction and also acts on pathogen clearance itself by the formation of membrane attack complex. Different pathways of the complement system progress in a cascade-like manner and its brisk response to pathogen invasion must be under the control of regulating mechanisms preventing complement from attacking host cells.

Invading a host organism, the pathogens have evolved different strategies to circumvent the immune response. Many of these strategies are in fact directed against components of the complement system. The most widespread strategy employs molecules recruiting or mimicking complement regulators, including the direct interaction of pathogens with complement proteins leading to the modulation or inhibition of their function or indirectly to the activation of complement proteins enzymatic degradation [96].

The complement regulators are represented by several serum proteins that are able to dampen the activity of complement and prevent host self-destruction. Two of them, complement factor H (FH) and its splice homologue Factor H-like (FHL) inhibit the alternative complement pathway response using host-|specific surface patterns like sialic acid or GAGs and thus promoting self-recognition processes [97, 98].

FH is a plasma glycoprotein containing 9 glycosylation sites [99] bearing complex, predominantly diantennary disialylated, fucosylated, and nonfucosylated glycans at eight of the nine glycosylation sites [100]. Similarly, FHL is also a plasma glycoprotein [101]. Both proteins possess a RGD motif which is assigned cell adhesive properties and thus can modulate cell adhesion. Additionally, FHL promotes anchorage-dependent cell attachment and spreading [102].

CRASPs and ERPs

The two complement regulators, FH and FHL are bound by *Borrelia* surface proteins hence preventing the activation at the central step of the complement cascade. Serum resistant *Borrelia* express adhesins on their surface, which are capable of interfering with different components of the host complement system leading to the modulation of host immune response and hampering the complement-mediated spirochete lysis [103, 104].

The two well-characterized types of complement interfering adhesins, complement regulator-acquiring surface proteins (CRASP) 1 and 2 [105], control the complement activity by binding complement regulating molecules such as FH and FHL-1 [104, 106]. Up to now, five different CRASPs (CRASP-1 to CRASP-5) have been described and each of them presents a different binding ability to FH, FHL-1, or plasminogen [98, 104, 106].

Vechtova *et al. Parasites & Vectors*   (2018) 11:594

Page 9 of 27

CRASP-1 (CspA, BBA68) has been studied the most extensively. It shows a strong affinity to the complement regulators which inactivate the complement response very efficiently [106, 107].

The expression of CRASP-1 is repressed in the tick vector and increases in the mammalian host, which suggests its role in spirochete transmission and evasion of the host immune response [108, 109]. CRASP-1 also confers serum resistance to *B. burgdorferi*. The role of CRASP-1 in complement inactivation is evident in the CRASP-1 knockout-mutants which inefficiently bound human FHL and attracted complement constituents more readily [110, 111].

Apart from *B. bavariensis*, all studied *Borrelia* species possess CRASP-1 orthologues conferring complement inactivation [112, 113]. The orthologues belong to the same protein family although the encoding genes do not share the same locus with the *B. burgdorferi* CspA [98].

CRASP-2 (CspZ) is another *Borrelia* adhesin binding both FH and FHL-1 independently of CRASP-1 and reinforcing *Borrelia* complement resistance [114, 115]. The CRASP-2 expression fluctuates in a somewhat similar manner to CRASP-1 during the *Borrelia* infectious cycle. Like CRASP-1, CRASP-2 is also upregulated during an established mammalian infection and is able to activate antibody-mediated immune response [116], which makes this adhesin important for the diagnosis of Lyme disease infection. The triggered immune response does not, however, provide the host with protective immunity and has no effect on spirochete dissemination [117].

Three members of the polymorphic Erp (OspE/F-related protein) protein family, ErpA (BBP38, CRASP-5), ErpC (CRASP-4) and ErpP (BBN38, CRASP-3), are plasminogen binding proteins that can simultaneously bind to FH and FH-related proteins [103, 107, 118–122].

The Erp proteins are most probably involved in different reservoir hosts infection due to differential binding abilities of particular Erp paralogues [123, 124]. Despite their complement regulator binding properties, none of the Erp proteins are necessary for the protection of *Borrelia* spirochetes against complement-mediated killing; CRASP-1/CRASP-2 deletion mutants expressing all Erp proteins were susceptible to serum mediated lysis [119, 120, 125].

Erps are not upregulated during *Borrelia* transmission but their expression gradually increases during Lyme disease progression, suggesting their role during mammalian infection [125]. Interestingly, *Borrelia* can regulate the expression of both Erps and CRASPs very dynamically as different isolates of *B. burgdorferi* (*s.l.*) reacted differently to complement-mediated killing [56, 126]. Moreover, some of the Erp members present multiple functions during *Borrelia* infection. For example, ErpX ability to bind complement regulators is complemented by its laminin binding properties [56]. The overlapping activities

of *Borrelia* surface molecules enhance the overall infectious potential of the spirochete.

Borrelia-specific host pattern-recognition receptors and lectins
Toll-like receptors
Recognition of pathogens is mediated by a set of pattern-recognition receptors (PRRs). The group of glycosylated proteins that comprise the Toll or Toll-like receptors family (TLRs) are transmembrane receptors that function as PRRs in mammals [127]. So far, eleven members that potentially participate in the recognition of invading pathogens have been identified in mammalian genomes [128] and glycosylation was shown to have a critical role in TLR presentation on the cell surface [129, 130].

There are several TLR members, whose role in spirochete recognition has been identified. The well-characterized TLR2 is presented on antigen-presenting cells, epithelial and endothelial cells [131]. It was able to recognize a variety of ligands and was important for macrophage activation and further triggering of the immune response in *Borrelia*-infected mammalian hosts when stimulated by OspA [132]. The signal transduction through TLR1/2 in response to *B. burgdorferi* invasion can elicit opposite immunoregulatory effects in the blood and CNS immune cells, affecting the different susceptibility of these compartments to infection [127].

TLR4 is expressed in macrophages and dendritic cells [130] and is upregulated upon *Borrelia* infection or stimulation by OspC [133, 134] and its main ligands are lipopolysaccharides (LPS) from gram-negative bacteria [135]. The role of TLR4 in *Borrelia* recognition remains unclear as *B. burgdorferi* does not express LPS on its surface.

TLR9 is responsible for recognition and further endosomal/lysosomal internalization of CpG motifs in bacterial DNA [136]. This process has been observed in sonicated *Borrelia*, which promoted the activation of murine cells *via* TLR9 [137].

Nucleotide-oligomerization domain-like receptors
Nucleotide-oligomerization domain-like receptors (NOD-like receptors or NLR) are a group of intracellular PRRs, capable of binding bacterial muropeptides, the molecules derived from bacterial peptidoglycans [138]. Together with TLRs, NOD-like receptors are crucial for recognition of *Borrelia* species. Contrary to other PRR families, NLRs bind bacterial ligands intracellularly, i.e. they are able to recognize the pathogen-associated molecular patterns (PAMPs) that enter the cell *via* phagocytosis or through the membrane pores induced during cellular stress [139].

There are several NLR protein members that can bind carbohydrate-associated PAMPs, although only a few of them were directly observed to be involved in Lyme

disease. NOD1 and NOD2 receptors are the most extensively investigated major PRRs [138, 140].

Borrelia-infected primary murine astrocytes upregulated NOD-proteins upon exposure to some TLR-ligands [138], while murine primary microglia infected by *Borrelia* only upregulated NOD2 and not the NOD1 [141]. NOD2 activation by *Borrelia* stimulated inflammatory cytokines release. Their activities are assigned to a host proinflammatory response, although their particular role in Lyme disease establishment remains unknown [142]. NOD2 stimulation by *Borrelia* induces inflammation during the early stages of Lyme disease but induces tolerance and suppresses *B. burgdorferi*-mediated Lyme arthritis and carditis in mice during later phases of infection [143]. *Borrelia* recognition in the host is conferred by the combined action of TLR and NOD2. The activation of both receptors at a time by *Borrelia* species is essential for an effective cytokine release. It has been concluded that TLR2 and NOD2 co-recognition of *Borrelia* surface receptors leads to both induction of a proper immune response and to inflammatory-induced pathology [144].

C-type lectin receptors

A family of calcium-dependent receptors that bind carbohydrate ligands include both soluble and cell-associated (transmembrane) lectins in vertebrates. C-type lectin receptors (CLRs) expressed by dendritic cells are crucial for tailoring immune response to pathogens. The transmembrane type is predominantly expressed by antigen-presenting cells functioning as PRRs recognizing PAMPs in bacteria [128]. Currently, 17 CLR subfamilies are described in vertebrates.

Mannose receptor represents a subgroup of CLRs binding mannose-containing bacterial transmembrane PAMPs. CLRs are involved in the recognition and phagocytosis of several microorganisms including *B. burgdorferi*. In particular, CLRs were upregulated in dendritic cells after *B. burgdorferi* activation and facilitated phagocytosis of *B. burgdorferi* by monocytes and macrophages [128]. However, the recognized borrelial protein is yet to be identified.

Surface glycolipids of *Borrelia burgdorferi*

Borrelia have an unusual composition of glycolipids in their outer membrane; they synthesize mono-α-galactosyl-diacylglycerol (MGalD) and cholesterol derived glycolipids cholesteryl-β-D-galacto-pyranoside, cholesteryl 6-O-acyl-β-D-galactopyranoside (ACG), or cholesteryl 6-O-palmitoyl-β-D-galactopyranoside (ACGal/BbGL-1) [145–147].

The *Borrelia* glycolipids induce inflammatory reactions; in particular, two glycolipids ACGal/BbGL-I and MGalD/BbGL-II, are probably immunogenic [145, 148]. The immunogenic epitope is recognized in the lipid part of the glycolipids [149]. An important constituent of the immunogenic epitope is the α-linked terminally bound galactose which is recognized by the T-cell receptor of invariant natural killer T cells (NKT) [150]. This then promotes their activation as well as the proliferation of Lyme disease-directed antibodies [151–153] which recognize glycolipids in the cell membrane of *Borrelia* but also *Ehrlichia* [154]. Importantly, the induced antibodies against the glycolipid fraction cross-react with gangliosides, which explains the phenomenon of neuroborreliosis [155].

The glycolipid recognition by invariant NKT cells seems to be an alternative system for innate immune system activation by bacteria lacking LPS, an otherwise typical antigenic determinant of most gram-negative bacteria [156].

Borrelia bind to GalCer (galactosylceramide) on Schwan cells [157], LacCer (lactosylceramide), ceramide trihexoside and gangliosides GD1a and GT1b. Moreover, *Borrelia* displays a specific affinity to disialoganglioside GD1a and trisialoganglioside GT1b carrying sialic acid. The ability to bind such a wide range of glycosphingolipids might provide an explanation for its ability to adhere to a wide spectrum of different cell types [158]. *Borrelia* did not bind gangliosides GM1, GD1b, GM2, GM3 and asialo-GM1 implying the requirement for terminally bound sialic acid in ganglioside recognized epitope and demonstrates the specific character of *Borrelia* and acidic gangliosides interaction. Interestingly, adhesion to GD1a and GT1b, as well as GalCer or LacCer was not compromised by free sialic acid, galactose or lactose, respectively [158, 159]. Conversely, GalCer-binding sites were saturable using free GalCer in CHO-K1 cells preventing spirochetes from attachment [148].

Vector-host glycosylated interactions

Similarly to *Borrelia*, the tick's successful evasion of the host response depends on its ability to conceal its activities from the host immune system. The pursuit of successful feeding drove ticks to equip their saliva with multiple pharmacologically active molecules which feature immunomodulatory activities. The myriad of diverse functions include cytolysis, vasodilatation, anticoagulation, anti-inflammation and immunosuppression. The comprehensive list of tick pharmacologically active salivary gland molecules is presented in a recent review [28].

P672 and CCL8

P672 is a chemokine binding protein (evasin). Evasins bind to multiple chemokines of different origin and their effects are thus pleiotropic. To date, several evasins originating in tick saliva have been identified [160, 161] and they inhibit responses of many chemokine sensitive molecules including neutrophiles or macrophages, which have been demonstrated in several tick species [28]. P672 was originally identified in *Rhipicephalus pulchellus* and its promiscuous binding abilities assign it 13 different chemokine partners showing different dissociation constants.

Mass spectrometric characterisation revealed the presence of several *N*-linked glycans and their deprival negatively influences the affinity of P672 to CCL8, although the underlying mechanism of this observation is yet to be uncovered [162].

Protease inhibitors

Many of the tick salivary proteins are glycosylated [163]. While the exact structure of the glycans attached to these proteins has not been studied, research has concentrated on the role of glycosylation with regard to the recognition of glycans by host immune systems. The importance of the glycan part for antibody recognition was shown for several proteins, such as AamS6 serpin [164], *R. microplus* serpins [165] or evasins 1 and 3 [166] confirming the need to use of glycosylated recombinant proteins in anti-tick vaccine preparations.

For proteins, where the role of glycosylation for the protein function was not confirmed, masking of the tick proteins antigenic epitopes and thus minimization of the immune response was speculated as the role of glycosylation [166].

Serpin 19

Serpin 19 is a serine protease inhibitor identified in the saliva of *Amblyomma americanum*. Serpin 19 displays a broad range of inhibitory activities: it interferes with the host homeostasis, coagulation and the development of inflammatory response. Importantly, the activity of many serine proteases is both positively and negatively regulated when bound to GAGs [167–169] and serpin 19 also contains several predicted GAG binding motives [170]. The functional validation further confirmed its GAG-binding properties and also extended the list of binding partners with heparin sulphate and heparin [170].

Variegin

The inhibition of blood coagulation cascade represents an important property of tick saliva that facilitates successful engorgement on the host. Variegin is a small thrombin-binding oligopeptide isolated from *A. variegatum* salivary glands. During tick feeding, variegin binds thrombin and disables its fibrinolytic activity and thus blocks the blood coagulation cascade. Despite its small size, variegin possesses a single *O*-linked glycan [171]. The synthetic *O*-glycosylated variegin analogues show significantly higher affinity to thrombin and consequently lower reaction kinetics of thrombin-mediated fibrinogenolysis compared to the non-glycosylated form, confirming the importance of its glycosylation. The functional analysis of the inhibition mechanism using macromolecular docking revealed the formation of some favourable hydrogen bonds between hydroxyl groups of the glycan and the allosterically important sites of thrombin [172].

Glycosylation in the *Anaplasma* infection cycle

Anaplasma is a genus of gram-negative rickettsial bacteria. They are obligate intracellular parasites infecting mammals including many domestic animals. The infection causes a reduction of the animal's body weight, abortions, reduces milk production and frequently leads to death [173–175]. In humans, *A. phagocytophilum* is the only confirmed pathogenic species causing human granulocytic anaplasmosis. Patients suffer from fever, headache, myalgias, chills, leukopenia, thrombocytopenia and liver damage manifested by elevated liver enzymes in serum [176]. The symptoms are usually mild but for some individuals, e.g. patients with a weakened immune system, it can be fatal. The infected vertebrate host serves as a reservoir where the bacterium can proliferate for many years and infect naïve ticks [177].

The main vectors of the genus *Anaplasma* are ticks, especially species of the genera *Ixodes*, *Dermacentor*, *Rhipicephalus* and *Amblyomma* [178, 179]. The initial phase of the infection during colonization of the host is the recognition of a suitable cell, attachment onto this cell, and entry into it. This process is facilitated by several specialized bacterial proteins (adhesins/invasins) that can recognize host surface molecules including glycans and glycoproteins and initiate signalling cascades to promote pathogen internalization. *Anaplasma* spp. express several surface proteins which are involved in binding to glycosylated host cells receptors and thus in the infection of the host and tick cells. These differ in glycan specificity and importance for the infection of various hosts and host cell types.

Anaplasma glycoprotein-binding surface proteins

As an intracellular pathogen, *Anaplasma* depends on a host cell to survive. *Anaplasma* infects two different types (groups) of organisms: the tick vector and the mammalian hosts, with various cell types being infected by the pathogen. Recognition of the cell type and of the infected organism is provided through binding of surface glycan epitopes or even several epitopes on a glycoprotein molecules.

Two groups of *Anaplasma* surface proteins were shown to recognize tick or host glycoproteins: outer membrane proteins (Omps) and major surface proteins (MSPs).

OmpA belongs to highly conserved genes among *A. phagocytophilum* isolates and is transcriptionally induced during feeding of *A. phagocytophilum*-infected ticks on mice and also during the invasion of mammalian but not tick cells [180, 181]. Pre-treatment of *A. phagocytophilum* or *A. marginale* bacteria with the respective OmpA antiserum reduces their ability to infect mammalian cells [181, 182]. Also, preincubation of mammalian cells with a recombinant ApOmpA effectively inhibits *A. phagocytophilum* infection of host cells.

Glycoproteins containing α1,3-fucose and either sLex or 6-sulfo sLex on host cells are recognized by the outer

Vechtova *et al. Parasites & Vectors*   (2018) 11:594

Page 12 of 27

membrane protein A (ApOmpA) of *A. phagocytophilum* [180, 181]. On the other hand, OmpA of *A. marginale* (AmOmpA), a species non-pathogenic for humans, binds only α1,3-fucose and sLex but not 6-sulfo-sLex glycans. *Anaplasma marginale* also produces AmOmpA in both the infected mammalian and tick cells. Pre-treatment of host cells with sialidase or trypsin reduces or nearly eliminates OmpA adhesion. Therefore, AmOmpA interacts with sialylated glycoproteins *via* an adhesin-receptor pair. Thus, both AmOmpA and ApOmpA recognize different receptor molecules even though these receptors share some structural similarity and thus provide a similar function to these two bacterial species [182].

Structures of *A. marginale* and *A. phagocytophilum* OmpA proteins are very similar and their binding domains are structurally conserved. The OmpA binding domain was identified within amino acids 59 to 74 and it is responsible for the recognition of α2,3-bound sialic acid and α1,3-fucose [180]. A recent study by Hebert et al. [182] describes the OmpA receptor-binding domain between the amino acids 19 to 74.

Another group of surface proteins interacting with host (glycosylated) molecules are the major surface proteins (MSPs) that are involved in the adhesion of host cells and the immunological reaction of the host [183–187]. MSP1 protein with its variants α, β1, and β2 and the MSP3 protein are present in *A. marginale*, while MSP2 and MSP4 in both *A. marginale* and *A. phagocytophilum* [188]. The MSP1 complex consists of two polypeptides MSP1a and MSP1b and both polypeptides participate in adhesion processes to both tick cells and bovine erythrocytes [183–186].

Similarly to OmpA, these proteins show glycan-binding activity. *Anaplasma marginale* MSP1 and MSP2 can hemagglutinate bovine erythrocytes [184] suggesting recognition of some erythrocyte surface saccharide molecules. Recombinant forms of the MSP1 isoforms are glycosylated; MSP1a recombinant glycoprotein contains glucose, galactose, mannose and xylose, while MSP1b contains glucose, galactose and mannose. The functional domain of MSP1a contains tandemly repeated peptides that are important for adhesion to tick cells and bovine erythrocytes. The MSP1a polypeptide backbone alone shows binding to tick cell extract proteins and the glycan in its N-terminus enhances this binding [189, 190]. The MSP2 protein binds to the mammalian PSGL-1 [191] and thus can be responsible for the above mentioned *Anaplasma* recognition of sialic acid on this protein. A hypervariable region is present in the middle of the MSP2 gene which allows the bacterium to express various paralogs of the protein on its surface, possibly enhancing immune system evasion [192, 193]. However, the glycan binding abilities of the various MSP2 paralogs were not studied.

In addition to the above-described receptor molecules, two other proteins, Asp14 and AipA, were found to be acting together with OmpA during the infection of host cells. However, neither of these two proteins were shown to bind glycans nor to be glycosylated [180]. Finally, during the past ten years, other novel *A. phagocytophilum* surface proteins Asp55, Asp62 and APH_1235, with possible function as adhesins and invasins have been identified [194–196]; however, their receptor molecules remain unknown.

Anaplasma-host interactions

A confirmation of *Anaplasma* recognition of host-surface glycans came by Goodman et al. [197] showing binding of *A. phagocytophilum* to the cell surface of the promyelocytic leukaemia cell line HL-60. Bacterial binding to the cell surface correlates with the expression of the sialyl Lewis x (sLex) or a closely related 6-sulpho sLex glycan-containing molecules glycan and α1,3-fucosylated molecules. On the other hand, α1,3-fucosylated glycans but not sialylated glycans, are essential for the infection of murine and human mast cells by *A. phagocytophilum* [180, 198]. These glycan epitopes are important for *Anaplasma in vivo* as has been shown by Carlyon et al. [199].

The protein part bearing the recognized glycans can be also important; thus, not any glycan molecule is recognized, only the one found on a specific protein. In humans and animal hosts, *A. phagocytophilum* exhibits, amongst others, a tropism for myeloid cells. As an adhesion molecule involved in the binding to the surface of human neutrophils, the P-selectin glycoprotein ligand-1, PSGL-1, has been identified [197, 199–202]. In the case of human PSGL-1, *A. phagocytophilum* cooperatively binds to a short amino acid sequence in its N-terminal region and an O-glycan containing a sialyl Lewis x (sLex) on PSGL-1 (NeuAcα2,3Galβ1,4[Fucα1,3]GlcNac) [202] or on another molecule. On the other hand, PSGL-1 is not the major ligand in mice [199, 200]. Thus, the terminal or core α1,3-fucosylated glycans seem to be a generally recognized receptor, while sialylated glycans and PSGL-1 enhance the infection of diverse types of mammalian host cells.

Anaplasma-vector interactions

In the pathogen-tick relationship, several tick glycosylated molecules can be induced in the presence of a pathogen in the tick tissues and help the pathogen to colonize the tick or enhance its infection. For example, α1,3-core-fucosylated glycans are required for tick colonization by *A. phagocytophilum* and silencing of the responsible fucosyltransferases results in the absence of *Anaplasma* in the infected ticks. To increase the number of its receptors in the tick, *A. phagocytophilum* induces the expression of α1,3-fucosyltransferases to enhance the colonization of *I. scapularis* ticks. Therefore, α 1,3-fucose is a unifying

Vechtova *et al. Parasites & Vectors* (2018) 11:594

Page 13 of 27

determinant that *A. phagocytophilum* targets to infect its natural murine and arthropod reservoirs and accidental human hosts as well. In addition, the presence or absence of these glycans does not affect the transmission of the pathogen from the tick vector to the vertebrate host. While the infection of the tick by *Anaplasma* depends on the presence of α1,3-core-fucosylated glycans, these epitopes do not seem to be important for the infection by another tick-borne pathogen, *B. burgdorferi* [203].

Furthermore, tandem repeat peptides of the MSP1a functional domain are important for the adhesion of bacteria to tick cells and the glycosylation of MSP1a probably plays a role during the adhesion of *A. marginale* to tick cells [189, 190].

Colonization of the tick by pathogens depends on the tick life-cycle; one of the crucial steps is the colonization of the midgut or survival in the midgut in the process of the blood meal digestion. For successful colonization, the tick midgut peritrophic matrix (PM) and bacterial biofilms formed in the midgut are critical. The PM forms a barrier between the midgut lumen and the epithelial cells lining the luminal side of the midgut and is formed by a thick matrix of mostly chitin with various proteins, such as chitin deacetylase, and glycoproteins [204]. One of the bacteria depending on the biofilm formation in the *I. scapularis* tick midgut is *A. phagocytophilum*. The presence of this bacterium affects the midgut microbial community and biofilm composition and it also decreases the expression of several genes for the glycoprotein peritrophin, one of the major PM components. This results also in decreased PM thickness. Furthermore, RNAi silencing of these genes significantly enhanced *Anaplasma* colonization of the tick [205]. *Anaplasma* further enhances its chances for a successful colonization of *I. scapularis* ticks by induction of an antifreeze protein (IAFGP) during the infection of ticks [205]. This secreted antifreeze glycoprotein inhibits bacterial biofilm formation through binding to the D-alanine residue of some bacteria peptidoglycan and was induced in response to *Anaplasma* infection [206, 207]. IAFGP expression resulted in thinning of the tick midgut PM and RNAi silencing of *iafgp* gene resulted in the absence of *Anaplasma* in the tick midgut [205].

Tick lectins

Ticks, like other arthropods, lack specific adaptive immunity. To defend themselves against invading microorganisms, ticks use the evolutionarily older nonspecific innate immune system, including both cellular and humoral immune responses. Cellular immune reactions involve haemocytes capable of phagocytosis, encapsulation or nodulation of foreign microorganisms and particles. The humoral immune response involves a range of non-specific pathogen-recognizing defence systems: PRRs, lectins, complement-like molecules, pro-phenoloxidase activation, haemolymph coagulation factors, antimicrobial peptides, reactive oxygen species, etc. Some of these molecules which function as mediators in the innate immune response are glycosylated and/or may recognize glycan-containing epitopes, e.g. recognition receptors for pathogens, complement-related molecules, or lectins (Table 3). In mammals, lectins play an important role in the recognition of specific glycosylated surface molecules of a variety of pathogens (PAMPs) and subsequent activation of the lectin pathway [208, 209]. MBL or ficolins known to recognize *N*-acetyl groups [210] serve as the recognition molecules, which are further integrated with the MBL-associated serine proteases to trigger the complement activation.

Fibrinogen-related proteins

Invertebrates contain a variety of fibrinogen-related proteins (FRePs), all of them sharing structural similarity with fibrinogen. A common feature of FRePs is their glycan-binding activity as they recognize the invading pathogen through its specific glycan epitopes. Their expression increases upon infection of the invertebrate by parasites or by pathogens [211, 212] with possibly a specific role in complement activation [213]. However, some of the tick FRePs family proteins (such as ixoderins described below) may have various other functions (Table 3).

Dorin M from the soft tick *Ornithodoros moubata*, the first lectin purified and characterized from any tick species, shows a strong similarity to ficolins but lacks the N-terminal collagen domain [214, 215]. Dorin M and its closest homologue OMFREP, also from *O. moubata*, share sequence similarity with the innate immune FRePs Tachylectin 5A and B from the horseshoe crab, *Tachypleus tridentatus* [215, 216]. It has a binding activity for sialic acid [214], its conjugates and *N*-acetyl-hexosamines. The protein has three *N*-glycosylation sites modified by high-mannose type glycans and core-fucosylated paucimannose glycans [217]. Other FRePs were later identified in the haemolymph of *D. marginatus*, *R. appendiculatus*, *R. pulchellus* and *R. sanguineus* based on the cross-reactivity with sera directed against Dorin M [218].

The hard tick *I. ricinus* contains several FReP encoding sequences in its genome (ixoderins A, B and C) and their analogues are present in *I. scapularis* as well. While proteins similar to ixoderins A and C are present also in other tick species, ixoderin B-like proteins are found only in the genus *Ixodes*. All these proteins contain predicted glycosylation sites and they contain the fibrinogen-like domain with carbohydrate-binding properties [213, 215]. In *I. ricinus*, the expression of ixoderin A is restricted to haemocytes, salivary glands, and midgut while ixoderin B is only expressed in salivary glands [215]. As expected based on published information on other invertebrate

Table 3 Overview of identified tick lectins. Lectins identified in different tick species are listed including the tissue where the lectin was identified. Lectin binding specificity, its function and molecular weight are also listed if known

Lectin	Species	Tick tissue	Specificity	MW (kDa)	Function	Reference
Galectins (OmGalec)	*O. moubata*	Haemocytes, midgut, SG, ovaries	Lactosamine-like disaccharides	37.4	Putative functions in tick development, immunity, and vector-pathogen interaction	[221]
Dorin M	*O. moubata*	Haemocytes	*N*-acetyl-D-hexosamines and Sialic acid specific	na	Pattern recognition molecules	[214]
OMFREP	*O. moubata*	Hemolymph, salivary glands	Probably similar to Dorin M	na	Probably similar to Dorin M	[215]
Ixoderin A	*I. ricinus*	Hemolymph, salivary glands, midgut	Peptidoglycan recognition protein?	na	Putative defence protein, identification of self-/non-self tissues	[215, 219]
Ixoderin B	*I. ricinus*	Salivary glands	Unknown	na	Unknown putative immunomodulatory function	[215, 219]
Hemelipoglycoprotein	*D. marginatus*	Haemocytes, salivary glands, gut	Galactose- and mannose-binding specificity	290, 2 subunits	Putative innate immunity	[220]
Unknown lectin	*I. ricinus*	Gut, hemolymph	Sialic acid, *N*-acetyl-glucosamine	85	Putative recognition molecule	[233]
Unknown lectin	*I. ricinus*	SGs	Sialic acid	70	Unknown	[233]
TSLPI	*I. scapularis*	Unknown	Mannan	na	Unknown	[42]
HlCLec	*H. longicornis*	Midgut, ovary	Unknown	60.2	Unknown	[223]
Serpin 19	*A. americanum*	Saliva	GAGs	43.0	Serine protease inhibitor	[170]

Abbreviations: *MW* molecular weight, *na* not available

FRePs, ixoderins are also involved in defence against pathogens. Namely, ixoderins A and B are involved in phagocytosis of some pathogens as shown for *Candida albicans* [219]. On the other hand, knockdown of these two ixoderins did not affect the phagocytosis of the tick-transmitted *B. afzelii* and knockdown of all three ixoderins does not affect its transmission [219]. The reason can be the missing protein glycosylation and thus the binding site for these lectins on the *Borrelia* surface [37]. Ixoderins and FRePs can be involved in other processes as well; ixoderin B may be involved in the matrix attachment processes and angiogenesis inhibition. Alternatively, it may antagonize the effect of host ficolin [215].

Finally, one of the tick storage proteins, hemelipoglycoprotein, from several hard tick species seems to share a structural similarity to FRePs with its primary sequence showing a high similarity to the fibrinogen domain [218, 220].

Other tick lectins

OmGalec from the soft tick *O. moubata* is the first member of galectin family identified in ticks with the specificity towards β1-3 and β1-4 bound galactose to GlcNAc, and Glc and α1-3 bound galactose to GalNAc [221]. Similar proteins are also present in *R. appendiculatus* and *I. scapularis* [188]. OmGalec contains two carbohydrate-binding domains which share low sequence similarity and thus possibly possesses a different saccharide-specificity. The protein is expressed in various life-stages and tissues, with the highest expression in haemocytes, midguts and ovaries [221]. It has been shown that galectins play a vital role in immune homeostasis by being pathogen recognition receptors [222].

C-type lectins are also present in the available tick genomes and transcriptomes [223, 224]. The only characterized C-type lectin from *Haemaphysalis longicornis* (HlCLec) contains three various carbohydrate-binding domains. Each of them has been shown to recognize the bacteria *E. coli* and *S. aureus* and participate in the tick defence against gram-negative bacteria, but they do not have a direct effect on bacterial growth. HlCLec also affects the blood-feeding process and affects larvae hatching and mortality. Expression of this lectin is increased during blood-feeding and is the highest in the midgut and ovary [223]. In mosquitoes, C-type lectins influence the midgut colonization by bacteria midgut microbiome [225] and facilitate infection with West Nile and dengue viruses [226, 227].

Calreticulin (CRT), a lectin chaperone responsible mainly for the control and proper folding of glycoproteins, is conserved in all tick species and is even used as the biomarker for human tick bites in *I. scapularis* [228]. In blood-feeding parasites, CRTs participate in evasion of the host defence mechanisms, namely the complement by binding the initiator of this pathway, the C1q protein, or factor Xa participating in the blood coagulation [229]. In

mammals, CRT on the surface of neutrophils also binds C1q as well as other immune-related lectins [230]. Similarly, the salivary secreted CRT from *A. americanum* binds host C1q. On the other hand, it does not bind the factor Xa and does not inhibit the activation of the classical complement cascade and host haemostasis. The *A. americanum* CRT shares a very high sequence similarity with other tick CRTs and thus similar functions of tick CRT can be expected [231].

Several other lectins are characterized in *I. ricinus*, but have not been identified to date: the 37, 60, 65, and 73 kDa lectins from midgut showing haemagglutination activity [163, 232]. The 37 kDa lectin has a binding specificity towards β1-3 glucan, while the 65 kDa protein binds bovine submaxillary mucin, containing a complicated mixture of various glycan structures and more specifically binds free sialic acid. Another lectin is present in haemolymph/haemocytes with a molecular weight of 85 kDa. It is a C-type lectin with specificity towards sialic acid and GlcNAc [233]. Several other lectins with haemagglutination activity have also been described in other ticks including *R. appendiculatus* [234, 235], *O. tartakovskyi, O. tholozani* and *A. polonicus* [233].

Tick glycans
Regarding the glycans and glycoproteins of blood-feeding arthropods, several studies describe these molecules using lectin staining and other indirect methods. Lectin studies show the presence of both *N*- and *O*-glycosylated proteins in tick tissues and some glycoproteins have been shown to be antigenic determinants for the immune response of the host [236–239]. In recent years, the direct determination of glycan structures and composition, mostly using mass spectrometry, has also been published, either from tick tissues and cells [203, 240] or purified proteins [220]. The three most interesting glycan structures related to host-parasite interaction and host immune system reaction are described below; representation of these structures in a glycan molecule is shown in Fig. 2. An overview of tick glycans with known structures is listed in Table 4.

Alpha-galactose epitope
Alpha-galactose epitopes (Galα1-3Gal; αGal) are abundant on glycolipids and glycoproteins of plants, arthropods and non-primate mammals [241]. αGal is a novel allergen identified first during clinical trials in 2004 in patients treated with cetuximab, a medical preparation for metastatic colorectal cancer treatment. Several cases of hypersensitivity reaction were registered soon after cetuximab administration into the blood due to the presence of αGal in its structure. The majority of sensitive individuals come from a population in south-eastern USA [242]. Furthermore, the geographical distribution of cases with cetuximab hypersensitivity corresponded

to the distribution of red meat allergy cases and tick prevalence. Additionally, patients with red meat allergy experienced a tick bite in the months preceding the allergy symptoms. The causative agent of the αGal sensitization in the south-eastern region of the USA is the lone star tick *A. americanum* [243]. Red meat allergy is also linked with *I. holocyclus* tick bite in the Australian population [244] . Conversely, a bite by the *I. scapularis* tick from the same genus in the USA does not seem to result in red meat allergy [243]. Lastly, Chinuki et al. [245] described the allergy development upon *H. longicornis* bite in Japan. Direct evidence on αGal epitopes presence in *I. ricinus* is provided by Hamsten et al. [246], specifically in the tick midgut. However, the presence of αGal just in the tick saliva is what is important for patient sensitization. In this regard, the presence of undigested complete host proteins and glycoproteins was described in the tick body and, importantly, in the tick saliva [240, 246, 247] and thus the presence of αGal originating in the blood of non-mammalian hosts from the previous blood-feeding can be expected in the saliva. The αGal epitope is only known to be present in the saliva of *A. sculptum*, a tick that until now has not been connected with red meat allergy cases [248].

Core α1,3-fucosylation
The allergenic core α1,3-fucose (α1,3-Fuc) attached on the proximal GlcNAc residue is widely present in plants and arthropods and is one of the well-known possible human allergens as it is usually absent in mammals. It can induce production of specific IgE antibodies associated with IgE-mediated allergic immune responses, which is mostly described for schistosomes or venoms of some species of the order Hymenoptera. However, such a response is not described after a tick bite [249–251]. It is rather surprising, as α1,3-fucosylated structures are present in the tick salivary glands as well as in saliva of both *I. ricinus* and *I. scapularis* [203, 252]. This can be explained by the structural features of the allergenic epitopes; for example, in the case of core α1,3-Fuc, terminal GlcNAc weakens the immune response [253]. Additionally, more than one epitope has to be present to trigger the allergic reaction and the presence of blocking IgG4 antibodies against this epitope can lower the immune reaction [249].

The α1,3-Fuc modification of the *N*-linked glycan core mediates an entrance of one of the tick-transmitted pathogens, *A. phagocytophilum*, into *I. scapularis* midgut cells, but it is not required for the transmission of the pathogen to a vertebrate host. Furthermore, *Anaplasma* increases the expression of α1,3-fucosyltransferases in the tick, further increasing its ability to infect the tick. On the other hand, the infection of the tick by *B. burgdorferi* was not affected by the presence or absence of core α1,3-Fuc [203].

Fig. 2 Scheme of a model complex-type glycan showing presented oligosaccharide structures. An example of an *N*-glycan bearing the three glycoepitopes immunogenic in the mammalian hosts are shown. The αGal epitope is formed by a terminal galactose bound to another galactose *via* an α1-3 bond. In the case of the core α1,3-fucose, both the specific α1,3 bond and the core (not terminal localization of fucose are important for the immunogenicity in mammals. Two types of sialic acid are present in Eukaryotes: the *N*-acetylneuraminic acid (Neu5Ac) and the *N*-glycolylneuraminic acid (Neu5Gc). As humans do not possess the enzymatic apparatus for the production of Neu5Gc into glycans, glycans terminated with this type of sialic acid are immunogenic in humans. The used symbol nomenclature is based on the Consortium for Functional Glycomics (http://www.functionalglycomics.org/)

Sialic acids

Sialic acids (Sia) are found typically in the terminal position of vertebrate complex *N*- or *O*-linked glycans. In insects, some studies have shown the ability of sialylation [254, 255] and the importance of sialylation for insect-development, even though the abundance of sialylated glycans is very low [256].

N-glycans terminated with Sia are present also in the organs of the tick *I. ricinus*, namely in the gut, salivary glands, ovary and Malpighian tubules [240, 257]. However, the sialylated proteins in the adult ticks originate most probably from the host blood [258]. Hypothetically, sialo-glycans present in the tick organs and in the secreted tick saliva can be engaged in molecular mimicry. We suppose that sialic acid is produced also by the tick itself in the ovary and eggs and later in larvae; the exact role of the tick sialylated proteins for the physiology and development of ticks is not yet known (unpublished results). Both eukaryotic types of sialic acids, *N*-acetyl-neuraminic acid and *N*-glycolyl-neuraminic acid (Fig. 2), were detected in the ticks [240].

N-linked glycans of flaviviruses

Tick-borne encephalitis virus (TBEV), a member of the genus *Flavivirus*, can cause serious infections in humans, which may result in encephalitis/meningoencephalitis. The viral single-stranded genomic RNA of positive polarity contains one open reading frame, which encodes a single polyprotein that is co-translationally and post-translationally cleaved by viral and cellular proteases into three structural and seven non-structural proteins (Table 4) [259].

Flaviviral non-structural proteins

Non-structural proteins of the flavivirus family (NS1, NS2A, NS2B, NS3, NS4A, NS4B and NS5) do not have their precise role elucidated, but they are generally considered as the effectors of viral replication, which occurs in close association with cellular membranes. Dramatic changes in the intracellular membrane structures including convoluted membranes, vesicle packets or paracrystalline arrays were observed as a result of dengue virus (DENV), TBEV or West Nile virus (WNV) replication [260–262]. Recently, NS1, NS4A and possibly also NS2A, were described to be involved in the formation of vesicle packets [263, 264]. Moreover, novel functions in terms of virus-host interactions were recently described for particular NS proteins; for example, TBEV NS5 protein acts as an inhibitor of interferon-activated Jak-STAT signalling [265].

Flaviviral structural proteins

Apart from seven non-structural proteins, the flaviviral genome encodes three structural proteins (C, M, E). The flaviviral nucleocapsid is composed of (+) ssRNA genome and the capsid protein (C), whereas the host-derived

Vechtova *et al. Parasites & Vectors*   (2018) 11:594

Page 17 of 27

Table 4 Overview of identified tick glycan structures composition. Monosaccharide compositions of the identified N-glycans are shown. Note that in some cases, the same composition can define various structures. For each glycan, the protein or the tick samples is listed, in which it was identified by mass spectrometry

Glycan composition				Protein/sample	Reference
Paucimannose glycans					
HexNAc	Hex	dHex	Sia		
2	3	0	0	Dorin M (position [41]NHS, [171]NGS, [129]NHS) from *O. moubata*	[217]
				I. ricinus fed female salivary glands	[240]
				I. ricinus fed female midgut	[240]
				I. scapularis salivary gland	[203]
2	4	0	0	Dorin M (position [41]NHS, [171]NGS, [129]NHS) from *O. moubata*	[217]
				I. ricinus fed female salivary glands	[240]
				I. ricinus fed female midgut	[240]
				I. scapularis salivary gland	[203]
High-mannose glycans					
HexNAc	Hex	dHex	Sia		
2	5	0	0	Dorin M (position [41]NHS, [129]NHS) from *O. moubata*	[217]
				I. ricinus fed female salivary glands	[240]
				I. ricinus fed female midgut	[240]
				I. scapularis salivary gland	[203]
2	6	0	0	Dorin M (position [41]NHS, [129]NHS) from *O. moubata*	[217]
				I. ricinus fed female salivary glands	[240]
				I. ricinus fed female midgut	[240]
				I. scapularis salivary gland	[203]
2	7	0	0	Dorin M (position [41]NHS, [129]NHS) from *O. moubata*	[217]
				I. ricinus fed female midgut	[240]
				I. scapularis salivary gland	[203]
2	8	0	0	Dorin M (position [41]NHS, [129]NHS) from *O. moubata*	[217]
				I. ricinus fed female midgut	[240]
				I. scapularis salivary gland	[203]
2	9	0	0	Dorin M (position [41]NHS, [129]NHS) from *O. moubata*	[217]
				I. ricinus fed female salivary glands	[240]
				I. ricinus fed female midgut	[240]
				D. marginatus Hemelipoglycoprotein	[220]
				I. scapularis salivary gland	[203]
2	10	0	0	*D. marginatus* Hemelipoglycoprotein	[220]
				I. scapularis salivary gland	[203]
Core-fucosylated glycans					
HexNAc	Hex	dHex	Sia		
2	3	1	0	Dorin M (position [171]NGS) from *O. moubata*	[217]
				I. ricinus fed female salivary glands	[240]
				I. ricinus fed female midgut	[240]
				I. scapularis salivary gland	[203]
2	4	1	0	Dorin M (position [171]NGS) from *O. moubata*	[217]
				I. ricinus fed female salivary glands	[240]
				I. ricinus fed female midgut	[240]

Table 4 Overview of identified tick glycan structures composition. Monosaccharide compositions of the identified N-glycans are shown. Note that in some cases, the same composition can define various structures. For each glycan, the protein or the tick samples is listed, in which it was identified by mass spectrometry *(Continued)*

Glycan composition				Protein/sample	Reference
				I. scapularis salivary gland	[203]
2	5	1	0	Dorin M (position [171]NGS) from *O. moubata*	[217]
				I. ricinus fed female salivary glands	[240]
				I. ricinus fed female midgut	[240]
				I. scapularis salivary gland	[203]
3	2	1	0	*I. ricinus* fed female salivary glands	[240]
3	3	1	0	*I. ricinus* fed female salivary glands	[240]
				I. ricinus fed female midgut	[240]
				I. scapularis salivary gland	[203]
4	3	1	0	*I. ricinus* fed female midgut	[240]
				I. scapularis salivary gland	[203]
4	4	1	0	*I. scapularis* salivary gland	[203]
4	5	1	0	*I. ricinus* fed female midgut	[240]
				I. scapularis salivary gland	[203]
4	6	1	0	*I. ricinus* fed female midgut	[240]
5	3	1	0	*I. ricinus* fed female salivary glands	[240]
				I. scapularis salivary gland	[203]
5	5	1	0	*I. ricinus* fed female midgut	[240]
6	6	1	0	*I. ricinus* fed female midgut	[240]
Complex glycans					
HexNAc	Hex	dHex	Sia		
3	4	0	0	*I. ricinus* fed female salivary glands	[240]
4	5	0	0	*I. ricinus* fed female salivary glands	[240]
				I. ricinus fed female midgut	[240]
4	6	0	0	*I. ricinus* fed female midgut	[240]
4	7	0	0	*D. marginatus* Hemelipoglycoprotein	[220]
4	8	0	0	*D. marginatus* Hemelipoglycoprotein	[220]
5	6	0	0	*I. ricinus* fed female midgut	[240]
6	2	0	0	*I. ricinus* fed female midgut	[240]
Sialylated glycans (containing either Neu5Ac or Neu5Gc)					
HexNAc	Hex	dHex	Sia		
4	5	0	1	*I. ricinus* fed female salivary glands	[240]
				I. ricinus fed female midgut	[240]
4	5	0	2	*I. ricinus* fed female midgut	[240]
5	6	0	1	*I. ricinus* fed female midgut	[240]
5	6	0	2	*I. ricinus* fed female midgut	[240]

Abbreviations: *HexNAc* N-acetyl-hexosamine (*N*-acetyl-glucosamine or *N*-acetyl-galactosamine), *Hex* hexose (mannose, glucose, galactose), *dHex* deoxyhexose (fucose), *Sia* sialic acid (*N*-acetyl-neuraminic acid, *N*-glycolyl-neuraminic acid)

envelope contains two glycoproteins, the membrane (prM/M) protein and the envelope (E) protein [266].

The E glycoprotein is localized in the viral envelope and is the main antigenic determinant of TBEV inducing a humoral immune response. It mediates fusion of TBEV with host cell membrane and thus facilitates the virus entry to the host cell. It forms heterodimers with the prM protein; the prM-E protein interaction is essential for proper folding of E protein [267]. The heterodimers then migrate to the ER membrane and eventually

Vechtova *et al. Parasites & Vectors*   (2018) 11:594

Page 19 of 27

bud off as nucleocapsid-containing immature virions [260, 268].

The M glycoprotein is an integral part of the viral envelope together with E protein. It forms heterodimers with the E protein and functions as a chaperon ensuring proper folding of E protein [267]. Non-infectious immature virions containing prM/E homodimers undergo maturation process in late trans-Golgi network by cleavage of pr part from the prM protein by host protease furin. The cleavage produces protein M and triggers re-organization of protein E to form homodimers [268, 269].

TBEV proteins glycosylation
The glycosylation of viral proteins increases their folding efficiency and promotes their intracellular transport by the interaction with host lectins [270]. In several viruses that cross the endoplasmic reticulum during their life-cycle, the protein glycosylation was proven important for virus growth, budding, secretion, and pathogenicity (reviewed in [271–273]). So far, only membrane glycoproteins prM/M and E are known to be *N*-glycosylated in TBEV (Table 5) [274–276]. α1,3-core fucosylated, high-mannose and hybrid N-glycans were shown to be present in the E protein of TBEV produced in chicken embryos by affinoblots [277]. E protein glycosylation was also confirmed recently also using cryo-electron microscopy, even though the exact glycan structure was not defined [278]. Another two sites (N130 and N207) in the NS1 protein are *N*-glycosylated in the case of dengue virus [274, 279]. One of these two *N*-glycosylation sites (N207) is present also in the TBEV NS1 protein; however, its glycosylation has not yet been shown (Table 5).

The E glycoprotein is a viral surface protein and thus contains major antigenic epitopes responsible for triggering the host immune system [280]. The *N*-glycosylation site at position N154 is present in the majority of TBEV strains and other flaviviruses. Moreover, a potential N361 glycosylation site is present in TBEV E protein as well.

Depending on the strain, zero to two glycans are attached [280, 281]. The investigation of the presence and position of E protein glycans showed that an increased number of E protein glycans elevate its expression. Conversely, the E protein glycosylation deletion mutants showed reduced E protein production, suggesting the importance of glycosylation for the viral life-cycle [276].

Importantly, the absence of E-protein glycosylation affects the E protein conformation and further the TBEV infectivity only in the mammalian host, but not in the tick vector. Different temperatures in the host (37 °C) and the vector (23 °C) do not affect the stability of the deglycosylated E protein [282]. In light of this evidence, the E protein glycosylation seems to represent one of the factors conferring different vector and host competence. Interestingly, the investigation of mosquito-borne flaviviruses, DENV and WNV, shows that glycans modifying E protein are important for virus propagation in both vector and host cells. However, the role of the particular *N*-linked glycosylation site varies depending on the invertebrate/vertebrate host [283–285]. For example, the importance of *N*-linked glycan at 154 aa of WNV E protein was proved in case of the vector (*Culex pipiens* and *Cx. tarsalis* mosquitoes) as well as the bird host (*Gallus gallus*) [286, 287].

The prM protein encodes for the precursor of membrane protein M and also contains one *N*-linked glycosylation consensus sequence in N32 position (Table 5) [267, 276]. During TBEV maturation, the structural proteins prM and E form heterodimer, where prM has a chaperone-like role in the folding and maturation of E protein [267], although the biological role of TBEV prM glycosylation, has not yet been elucidated. However, Goto et al. [279] suggest the participation of carbohydrate-mediated interaction for prM-E heterodimer formation; glycosylation-deficient mutant of prM reduces the secretion of E protein to 60% in comparison to the wild-type prM. Further evidence for the crucial role of prM glycan was described in the case of WNV.

Table 5 TBEV protein glycosylation overview. List of TBEV proteins and their functions. Identified or predicted N-linked glycosylation sites are listed as well. NetNGlyc 1.0 Server was used for N-linked glycosylation site prediction

	Protein	Function	*N*-linked glycosylation	Reference
Structural	C	Capsid protein; forming of nucleocapsid	None	
	prM/M	Envelope protein; E protein chaperone	N32	[265, 302]
	E	Envelope protein; binding and fusion	N154, N361	[263–265]
Non-structural	NS1	Replication	Predicted: N85, N207	
	NS2A	Assembly, replication	None	
	NS2B	NS3 serine-protease cofactor	None	
	NS3	Serine-protease, helicase, replication RNA triphosphatase	Predicted: N160, N499, N555	
	NS4A	Assembly, replication	None	
	NS4B	Assembly, induction of membrane rearrangements	Predicted: N188	
	NS5	Methyltransferase, RNA-dependent RNA polymerase	Predicted: N18, N175, N215	

Vechtova *et al. Parasites & Vectors*   (2018) 11:594

Page 20 of 27

The prM glycosylation-deficient mutants decreased the formation and release of virus-like particles as well as genome copies. However, the infectivity of prM glycosylation-deficient mutants was not affected in mosquito, avian or mammalian cell lines [284].

In summary, *N*-linked glycosylation of TBEV prM and E proteins represents a multifaceted factor which is involved in many steps of the viral life-cycle, especially in virion assembly/secretion, and host/vector competence. Despite various studies, there are many aspects which need to be elucidated, especially the role of viral protein *N*-linked glycans within tick vectors. Moreover, the presence of other *N*-linked glycans in predicted sites of NS1, NS3, NS4B, and NS5 remains to be determined as well as their potential function.

Conclusions

The recent decades have provided an outstanding amount of new data about glycoconjugates and a growing line of evidence highlights the importance of carbohydrate-based interactions in the complex pathogen-host environment [288]. Glycoconjugates have an enormous structural diversity in the glycan moieties and therefore fulfil a variety of biological roles [289]. Given the fact that glycoconjugates are the major components of the outer surface of animal cells [290], it is likely that all interactions of microbial pathogens with their hosts/vectors are affected to a certain degree by the pattern of glycans and glycan-binding molecules that each produces. Despite the fact that protein glycosylation in the field of tick-borne pathogens has become a subject of increased attention in the last decade [37, 218, 291], there is still a deep knowledge gap regarding the nature and the specific roles of the glycoconjugates in the infectious cycle of these pathogens. All the findings mentioned in this review have tackled the important, yet still inadequately explored, the field of the carbohydrate-based interactions at the pathogen-tick-host interface. The basis of these interactions needs to be further addressed to gain clearer insights into the intricate strategies that the parasites employ to successfully finish their life-cycles. Ultimately, the common goal of scientists working in any field dealing with infectious diseases is to find an effective countermeasure against the particular threat. Ticks transmit a great variety of bacterial, viral and protozoan pathogens and therefore the search for a potent vaccine against each of these parasites costs an enormous amount of effort and money. One of the most promising strategies to cope with all pathogens transmitted by ticks is the development of a general anti-tick vaccine [292]. The potentially important role of sugar moieties in such a tick vaccine has already been suggested, showing, for instance, the tick midgut protein Bm86 to be more immunogenic in glycosylated form than non-glycosylated [291]. However, the progress in this matter is still

insufficient and intense analysis of glycosylation needs to be addressed in future studies in order to be applied to the development of new therapeutics. Modern glycan sequencing technologies and strategies that allow site-specific mass-spectrometric identification of proteins with glycan modifications in a complex biological sample have shown that glycosylation could be much more extensive than previously thought [293].

Publisher's Note

Springer Nature remains neutral with regard to jurisdictional claims in published maps and institutional affiliations.

References

1. WHO. http://www.who.int/en/. 1948. Accessed 28 Mar 2018.
2. de la Fuente J, Antunes S, Bonnet S, Cabezas-Cruz A, Domingos AG, Estrada-Pena A, et al. Tick-pathogen interactions and vector competence:

Vechtova *et al. Parasites & Vectors*   (2018) 11:594

Page 21 of 27

identification of molecular drivers for tick-borne diseases. Front Cell Infect Microbiol. 2017;7:114.

3. Coumou J, Wagemakers A, Trentelman JJ, Nijhof AM, Hovius JW. Vaccination against Bm86 homologues in rabbits does not impair *Ixodes ricinus* feeding or oviposition. PLoS One. 2014;10:e0123495.

4. Semenza JC, Suk JE. Vector-borne diseases and climate change: a European perspective. FEMS Microbiol Lett. 2018;365:2.

5. Dinglasan RR, Jacobs-Lorena M. Insight into a conserved lifestyle: protein-carbohydrate adhesion strategies of vector-borne pathogens. Infect Immun. 2005;73:7797–807.

6. Severo MS, Choy A, Stephens KD, Sakhon OS, Chen G, Chung DW, et al. The E3 ubiquitin ligase XIAP restricts *Anaplasma phagocytophilum* colonization of *Ixodes scapularis* ticks. J Infect Dis. 2013;208:1830–40.

7. Varki ACR, Esko JD, et al. Essentials of Glycobiology. 3rd ed. Cold Spring Harbor: Cold Spring Harbor Laboratory Press; 2017.

8. Ritchie GE, Moffatt BE, Sim RB, Morgan BP, Dwek RA, Rudd PM. Glycosylation and the complement system. Chem Rev. 2002;102:305-20-19.

9. Bann JG, Bachinger HP. Glycosylation/hydroxylation-induced stabilization of the collagen triple helix. 4-trans-hydroxyproline in the Xaa position can stabilize the triple helix. J Biol Chem. 2000;275:24466–9.

10. Ault BH, Schmidt BZ, Fowler NL, Kashtan CE, Ahmed AE, Vogt BA, et al. Human factor H deficiency. Mutations in framework cysteine residues and block in H protein secretion and intracellular catabolism. J Biol Chem. 1997;272:25168–75.

11. Dijk M, Holkers J, Voskamp P, Giannetti BM, Waterreus WJ, van Veen HA, et al. How dextran sulfate affects C1-inhibitor activity: a model for polysaccharide potentiation. Structure. 2016;24:2182–9.

12. Stavenhagen K, Kayili HM, Holst S, Koeleman C, Engel R, Wouters D, et al. *N*- and *O*-glycosylation analysis of human C1-inhibitor reveals extensive mucin-type *O*-glycosylation. Mol Cell Proteomics. 2017;17:1225–38.

13. Minta JO. The role of sialic acid in the functional activity and the hepatic clearance of C1-INH. J Immunol. 1981;126:245–9.

14. Novotny MV, Alley WR. Recent trends in analytical and structural glycobiology. Curr Opin Chem Biol. 2013;17:832–40.

15. Oswald DM, Cobb BA. Emerging glycobiology tools: a Renaissance in accessibility. Cell Immunol. 2018; https://doi.org/10.1016/j.cellimm.2018.04.010.

16. Tytgat HL, van Teijlingen NH, Sullan RM, Douillard FP, Rasinkangas P, Messing M, et al. Probiotic gut microbiota isolate interacts with dendritic cells *via* glycosylated heterotrimeric pili. PLoS One. 2016;11:e0151824.

17. Barbour AG, Hayes SF. Biology of *Borrelia* species. Microbiol Rev. 1986; 50:381–400.

18. Coburn J, Fischer JR, Leong JM. Solving a sticky problem: new genetic approaches to host cell adhesion by the Lyme disease spirochete. Mol Microbiol. 2005;57:1182–95.

19. Berndtson K. Review of evidence for immune evasion and persistent infection in Lyme disease. Int J Gen Med. 2013;6:291–306.

20. Cohen M. Notable aspects of glycan-protein interactions. Biomolecules. 2015;5:2056–72.

21. Vancova M, Nebesarova J, Grubhoffer L. Lectin-binding characteristics of a Lyme borreliosis spirochete *Borrelia burgdorferi sensu stricto*. Folia Microbiol. 2005;50:229–38.

22. Stevenson B, Schwan TG, Rosa PA. Temperature-related differential expression of antigens in the Lyme disease spirochete, *Borrelia burgdorferi*. Infect Immun. 1995;63:4535–9.

23. Pal U, de Silva AM, Montgomery RR, Fish D, Anguita J, Anderson JF, et al. Attachment of *Borrelia burgdorferi* within *Ixodes scapularis* mediated by outer surface protein A. J Clin Invest. 2000;106:561–9.

24. Schwan TG, Piesman J. Vector interactions and molecular adaptations of Lyme disease and relapsing fever spirochetes associated with transmission by ticks. Emerg Infect Dis. 2002;8:115–21.

25. Fikrig E, Pal U, Chen M, Anderson JF, Flavell RA. OspB antibody prevents *Borrelia burgdorferi* colonization of *Ixodes scapularis*. Infect Immun. 2004;72:1755–9.

26. Schwan TG, Piesman J, Golde WT, Dolan MC, Rosa PA. Induction of an outer surface protein on *Borrelia burgdorferi* during tick feeding. Proc Natl Acad Sci USA. 1995;92:2909–13.

27. Ramamoorthi N, Narasimhan S, Pal U, Bao F, Yang XF, Fish D, et al. The Lyme disease agent exploits a tick protein to infect the mammalian host. Nature. 2005;436:573–7.

28. Simo L, Kazimirova M, Richardson J, Bonnet SI. The essential role of tick salivary glands and saliva in tick feeding and pathogen transmission. Front Cell Infect Microbiol. 2017;7:281.

29. Anguita J, Ramamoorthi N, Hovius JWR, Das S, Thomas V, Persinski R, et al. Salp15, an *Ixodes scapularis* salivary protein, inhibits CD4(+) T cell activation. Immunity. 2002;16:849–59.

30. Kolb P, Vorreiter J, Habicht J, Bentrop D, Wallich R, Nassal M. Soluble cysteine-rich tick saliva proteins Salp15 and Iric-1 from *E. coli*. FEBS Open Bio. 2015;5:42–55.

31. Hovius JW, Schuijt TJ, de Groot KA, Roelofs JJ, Oei GA, Marquart JA, et al. Preferential protection of *Borrelia burgdorferi sensu stricto* by a Salp15 homologue in *Ixodes ricinus* saliva. J Infect Dis. 2008;198:1189–97.

32. Hovius JW, de Jong MA, den Dunnen J, Litjens M, Fikrig E, van der Poll T, et al. Salp15 binding to DC-SIGN inhibits cytokine expression by impairing both nucleosome remodeling and mRNA stabilization. PLoS Pathog. 2008;4:e31.

33. Lam TT, Nguyen TP, Montgomery RR, Kantor FS, Fikrig E, Flavell RA. Outer surface proteins E and F of *Borrelia burgdorferi*, the agent of Lyme disease. Infect Immun. 1994;62:290–8.

34. Casjens S, van Vugt R, Tilly K, Rosa PA, Stevenson B. Homology throughout the multiple 32-kilobase circular plasmids present in Lyme disease spirochetes. J Bacteriol. 1997;179:217–27.

35. Akins DR, Caimano MJ, Yang X, Cerna F, Norgard MV, Radolf JD. Molecular and evolutionary analysis of *Borrelia burgdorferi* 297 circular plasmid-encoded lipoproteins with OspE- and OspF-like leader peptides. Infect Immun. 1999;67:1526–32.

36. Sambri V, Stefanelli C, Cevenini R. Detection of glycoproteins in *Borrelia burgdorferi*. Arch Microbiol. 1992;157:205–8.

37. Sterba J, Vancova M, Rudenko N, Golovchenko M, Tremblay TL, Kelly JF, et al. Flagellin and outer surface proteins from *Borrelia burgdorferi* are not glycosylated. J Bacteriol. 2008;190:2619–23.

38. Eicken C, Sharma V, Klabunde T, Lawrenz MB, Hardham JM, Norris SJ, et al. Crystal structure of Lyme disease variable surface antigen VlsE of *Borrelia burgdorferi*. J Biol Chem. 2002;277:21691–6.

39. Narasimhan S, Coumou J, Schuijt TJ, Boder E, Hovius JW, Fikrig E. A tick gut protein with fibronectin III domains aids *Borrelia burgdorferi* congregation to the gut during transmission. PLoS Pathog. 2014;10:e1004278.

40. Coumou J, Narasimhan S, Trentelman JJ, Wagemakers A, Koetsveld J, Ersoz JI, et al. *Ixodes scapularis* dystroglycan-like protein promotes *Borrelia burgdorferi* migration from the gut. J Mol Med (Berl). 2016;94:361–70.

41. Narasimhan S, Santiago F, Koski RA, Brei B, Anderson JF, Fish D, et al. Examination of the *Borrelia burgdorferi* transcriptome in *Ixodes scapularis* during feeding. J Bacteriol. 2002;184:3122–5.

42. Schuijt TJ, Coumou J, Narasimhan S, Dai J, Deponte K, Wouters D, et al. A tick mannose-binding lectin inhibitor interferes with the vertebrate complement cascade to enhance transmission of the Lyme disease agent. Cell Host Microbe. 2011;10:136–46.

43. Schuijt TJ, Narasimhan S, Daffre S, DePonte K, Hovius JW, Van't Veer C, et al. Identification and characterization of *Ixodes scapularis* antigens that elicit tick immunity using yeast surface display. PLoS One. 2011;6:e15926.

44. Coburn J, Leong J, Chaconas G. Illuminating the roles of the *Borrelia burgdorferi* adhesins. Trends Microbiol. 2013;21:372–9.

45. Leong JM, Robbins D, Rosenfeld L, Lahiri B, Parveen N. Structural requirements for glycosaminoglycan recognition by the Lyme disease spirochete, *Borrelia burgdorferi*. Infect Immun. 1998;66:6045–8.

46. Brissette CA, Gaultney RA. That's my story, and I'm sticking to it - an update on *B. burgdorferi* adhesins. Front Cell Infect Microbiol. 2014;4:41.

47. Szczepanski A, Furie MB, Benach JL, Lane BP, Fleit HB. Interaction between *Borrelia burgdorferi* and endothelium *in vitro*. J Clin Invest. 1990;85:1637–47.

48. Guo BP, Norris SJ, Rosenberg LC, Hook M. Adherence of *Borrelia burgdorferi* to the proteoglycan decorin. Infect Immun. 1995;63:3467–72.

49. Choi HU, Johnson TL, Pal S, Tang LH, Rosenberg L, Neame PJ. Characterization of the dermatan sulfate proteoglycans, DS-PGI and DS-PGII, from bovine articular cartilage and skin isolated by octyl-sepharose chromatography. J Biol Chem. 1989;264:2876–84.

50. Rosenberg LC, Choi HU, Tang LH, Johnson TL, Pal S, Webber C, et al. Isolation of dermatan sulfate proteoglycans from mature bovine articular cartilages. J Biol Chem. 1985;260:6304–13.

51. Sasaki T, Fassler R, Hohenester E. Laminin: the crux of basement membrane assembly. J Cell Biol. 2004;164:959–63.

52. Kumar AP, Nandini CD, Salimath PV. Structural characterization of N-linked oligosaccharides of laminin from rat kidney: changes during diabetes and modulation by dietary fiber and butyric acid. FEBS J. 2011;278:143–55.

53. Singh B, Fleury C, Jalalvand F, Riesbeck K. Human pathogens utilize host extracellular matrix proteins laminin and collagen for adhesion and invasion of the host. FEMS Microbiol Rev. 2012;36:1122–80.

Vechtova *et al. Parasites & Vectors*   (2018) 11:594

Page 22 of 27

54. Cabello FC, Hulinska D, Godfrey HP. Molecular Biology of Spirochetes. Amsterdam: IOS Press; 2006.

55. Brissette CA, Verma A, Bowman A, Cooley AE, Stevenson B. The *Borrelia burgdorferi* outer-surface protein ErpX binds mammalian laminin. Microbiology. 2009;155:863–72.

56. Brissette CA, Cooley AE, Burns LH, Riley SP, Verma A, Woodman ME, et al. Lyme borreliosis spirochete Erp proteins, their known host ligands, and potential roles in mammalian infection. Int J Med Microbiol. 2008;298(Suppl. 1):257–67.

57. Hynes RO. Integrins: a family of cell surface receptors. Cell. 1987;48:549–54.

58. Cai X, Thinn AMM, Wang Z, Shan H, Zhu J. The importance of *N*-glycosylation on β3 integrin ligand binding and conformational regulation. Sci Rep. 2017;7:4656.

59. Coburn J, Magoun L, Bodary SC, Leong JM. Integrins αvβ3 and α5β1 mediate attachment of Lyme disease spirochetes to human cells. Infect Immun. 1998;66:1946–52.

60. Hynes RO. Integrins: versatility, modulation, and signaling in cell adhesion. Cell. 1992;69:11–25.

61. Magoun L, Zuckert WR, Robbins D, Parveen N, Alugupalli KR, Schwan TG, et al. Variable small protein (Vsp)-dependent and Vsp-independent pathways for glycosaminoglycan recognition by relapsing fever spirochaetes. Mol Microbiol. 2000;36:886–97.

62. Porcella SF, Raffel SJ, Anderson DE Jr, Gilk SD, Bono JL, Schrumpf ME, et al. Variable tick protein in two genomic groups of the relapsing fever spirochete *Borrelia hermsii* in western North America. Infect Immun. 2005;73:6647–58.

63. Probert WS, Johnson BJ. Identification of a 47 kDa fibronectin-binding protein expressed by *Borrelia burgdorferi* isolate B31. Mol Microbiol. 1998;30:1003–15.

64. Brissette CA, Bykowski T, Cooley AE, Bowman A, Stevenson B. *Borrelia burgdorferi* RevA antigen binds host fibronectin. Infect Immun. 2009; 77:2802–12.

65. Li X, Liu X, Beck DS, Kantor FS, Fikrig E. *Borrelia burgdorferi* lacking BBK32, a fibronectin-binding protein, retains full pathogenicity. Infect Immun. 2006;74:3305–13.

66. Hyde JA, Weening EH, Chang M, Trzeciakowski JP, Hook M, Cirillo JD, et al. Bioluminescent imaging of *Borrelia burgdorferi in vivo* demonstrates that the fibronectin-binding protein BBK32 is required for optimal infectivity. Mol Microbiol. 2011;82:99–113.

67. Niddam AF, Ebady R, Bansal A, Koehler A, Hinz B, Moriarty TJ. Plasma fibronectin stabilizes *Borrelia burgdorferi*-endothelial interactions under vascular shear stress via a catch-bond mechanism. Proc Natl Acad Sci USA. 2017;114:E3490–E8.

68. Ebady R, Niddam AF, Boczula AE, Kim YR, Gupta N, Tang TT, et al. Biomechanics of *Borrelia burgdorferi* vascular interactions. Cell Rep. 2016;16:2593–604.

69. Lin YP, Chen Q, Ritchie JA, Dufour NP, Fischer JR, Coburn J, et al. Glycosaminoglycan binding by *Borrelia burgdorferi* adhesin BBK32 specifically and uniquely promotes joint colonization. Cell Microbiol. 2015;17:860–75.

70. Parveen N, Robbins D, Leong JM. Strain variation in glycosaminoglycan recognition influences cell-type-specific binding by Lyme disease spirochetes. Infect Immun. 1999;67:1743–9.

71. Moriarty TJ, Shi M, Lin YP, Ebady R, Zhou H, Odisho T, et al. Vascular binding of a pathogen under shear force through mechanistically distinct sequential interactions with host macromolecules. Mol Microbiol. 2012;86:1116–31.

72. Garcia BL, Zhi H, Wager B, Hook M, Skare JT. *Borrelia burgdorferi* BBK32 inhibits the classical pathway by blocking activation of the C1 complement complex. PLoS Pathog. 2016;12:e1005404.

73. Brissette CA, Rossmann E, Bowman A, Cooley AE, Riley SP, Hunfeld KP, et al. The borrelial fibronectin-binding protein RevA is an early antigen of human Lyme disease. Clin Vaccine Immunol. 2010;17:274–80.

74. Shi Y, Xu Q, McShan K, Liang FT. Both decorin-binding proteins A and B are critical for the overall virulence of *Borrelia burgdorferi*. Infect Immun. 2008;76:1239–46.

75. Salo J, Jaatinen A, Soderstrom M, Viljanen MK, Hytonen J. Decorin binding proteins of *Borrelia burgdorferi* promote arthritis development and joint specific post-treatment DNA persistence in mice. PLoS One. 2015;10:e0121512.

76. Benoit VM, Fischer JR, Lin YP, Parveen N, Leong JM. Allelic variation of the Lyme disease spirochete adhesin DbpA influences spirochetal binding to decorin, dermatan sulfate, and mammalian cells. Infect Immun. 2011;79:3501–9.

77. Morgan A, Sepuru KM, Feng W, Rajarathnam K, Wang X. Flexible linker modulates glycosaminoglycan affinity of decorin binding protein A. Biochemistry. 2015;54:5113–9.

78. Wang X. Solution structure of decorin-binding protein A from *Borrelia burgdorferi*. Biochemistry. 2012;51:8353–62.

79. Salo J, Loimaranta V, Lahdenne P, Viljanen MK, Hytonen J. Decorin binding by DbpA and B of *Borrelia garinii*, *Borrelia afzelii*, and *Borrelia burgdorferi sensu stricto*. J Infect Dis. 2011;204:65–73.

80. Imai DM, Samuels DS, Feng S, Hodzic E, Olsen K, Barthold SW. The early dissemination defect attributed to disruption of decorin-binding proteins is abolished in chronic murine Lyme borreliosis. Infect Immun. 2013;81:1663–73.

81. Schlachter S, Seshu J, Lin T, Norris S, Parveen N. The *Borrelia burgdorferi* glycosaminoglycan binding protein Bgp in the B31 strain is not essential for infectivity despite facilitating adherence and tissue colonization. Infect Immun. 2018;86:e00667–17.

82. Verma A, Brissette CA, Bowman A, Stevenson B. *Borrelia burgdorferi* BmpA is a laminin-binding protein. Infect Immun. 2009;77:4940–6.

83. Antonara S, Ristow L, Coburn J. Adhesion mechanisms of *Borrelia burgdorferi*. Adv Exp Med Biol. 2011;715:35–49.

84. Pal U, Wang P, Bao F, Yang X, Samanta S, Schoen R, et al. *Borrelia burgdorferi* basic membrane proteins A and B participate in the genesis of Lyme arthritis. J Exp Med. 2008;205:133–41.

85. Coburn J, Barthold SW, Leong JM. Diverse Lyme disease spirochetes bind integrin αIIbβ3 on human platelets. Infect Immun. 1994;62:5559–67.

86. Alugupalli KR, Michelson AD, Barnard MR, Robbins D, Coburn J, Baker EK, et al. Platelet activation by a relapsing fever spirochaete results in enhanced bacterium-platelet interaction *via* integrin αIIbβ3 activation. Mol Microbiol. 2001;39:330–40.

87. Coburn J, Chege W, Magoun L, Bodary SC, Leong JM. Characterization of a candidate *Borrelia burgdorferi* β3-chain integrin ligand identified using a phage display library. Mol Microbiol. 1999;34:926–40.

88. Skare JT, Mirzabekov TA, Shang ES, Blanco DR, Erdjument-Bromage H, Bunikis J, et al. The Oms66 (p66) protein is a *Borrelia burgdorferi* porin. Infect Immun. 1997;65:3654–61.

89. Barcena-Uribarri I, Thein M, Sacher A, Bunikis I, Bonde M, Bergstrom S, et al. P66 porins are present in both Lyme disease and relapsing fever spirochetes: a comparison of the biophysical properties of P66 porins from six *Borrelia* species. Biochim Biophys Acta. 1798;2010:1197–203.

90. Kenedy MR, Luthra A, Anand A, Dunn JP, Radolf JD, Akins DR. Structural modeling and physicochemical characterization provide evidence that P66 forms a β-barrel in the *Borrelia burgdorferi* outer membrane. J Bacteriol. 2014;196:859–72.

91. Coburn J, Cugini C. Targeted mutation of the outer membrane protein P66 disrupts attachment of the Lyme disease agent, *Borrelia burgdorferi*, to integrin αVβ3. Proc Natl Acad Sci USA. 2003;100:7301–6.

92. Ristow LC, Bonde M, Lin YP, Sato H, Curtis M, Wesley E, et al. Integrin binding by *Borrelia burgdorferi* P66 facilitates dissemination but is not required for infectivity. Cell Microbiol. 2015;17:1021–36.

93. Defoe G, Coburn J. Delineation of *Borrelia burgdorferi* p66 sequences required for integrin αIIbβ3 recognition. Infect Immun. 2001;69:3455–9.

94. Ristow LC, Miller HE, Padmore LJ, Chettri R, Salzman N, Caimano MJ, et al. The β3-integrin ligand of *Borrelia burgdorferi* is critical for infection of mice but not ticks. Mol Microbiol. 2012;85:1105–18.

95. Wood E, Tamborero S, Mingarro I, Esteve-Gassent MD. BB0172, a *Borrelia burgdorferi* outer membrane protein that binds integrin α3β1. J Bacteriol. 2013;195:3320–30.

96. Lambris JD, Ricklin D, Geisbrecht BV. Complement evasion by human pathogens. Nat Rev Microbiol. 2008;6:132–42.

97. Ricklin D, Hajishengallis G, Yang K, Lambris JD. Complement: a key system for immune surveillance and homeostasis. Nat Immunol. 2010;11:785–97.

98. Kraiczy P. Hide and seek: how Lyme disease spirochetes overcome complement attack. Front Immunol. 2016;7:385.

99. Rodriguez de Cordoba S, Esparza-Gordillo J, Goicoechea de Jorge E, Lopez-Trascasa M, Sanchez-Corral P. The human complement factor H: functional roles, genetic variations and disease associations. Mol Immunol. 2004;41:355–67.

100. Fenaille F, Le Mignon M, Groseil C, Ramon C, Riande S, Siret L, et al. Site-specific *N*-glycan characterization of human complement factor H. Glycobiology. 2007;17:932–44.

101. Kraiczy P, Wallich R. Borrelial complement-binding proteins. In: Embers ME, editor. The Pathogenic Spirochetes: Strategies for Evasion of Host Immunity and Persistence. Boston: Springer US; 2012. p. 63–88.

Vechtova *et al. Parasites & Vectors*   (2018) 11:594

Page 23 of 27

102. Hellwage J, Kuhn S, Zipfel PF. The human complement regulatory factor-H-like protein 1, which represents a truncated form of factor H, displays cell-attachment activity. Biochem J. 1997;326:321–7.

103. Metts MS, McDowell JV, Theisen M, Hansen PR, Marconi RT. Analysis of the OspE determinants involved in binding of factor H and OspE-targeting antibodies elicited during *Borrelia burgdorferi* infection in mice. Infect Immun. 2003;71:3587–96.

104. Wallich R, Pattathu J, Kitiratschky V, Brenner C, Zipfel PF, Brade V, et al. Identification and functional characterization of complement regulator-acquiring surface protein 1 of the Lyme disease spirochetes *Borrelia afzelii* and *Borrelia garinii*. Infect Immun. 2005;73:2351–9.

105. Kraiczy P, Skerka C, Kirschfink M, Brade V, Zipfel PF. Immune evasion of *Borrelia burgdorferi* by acquisition of human complement regulators FHL-1/reconectin and Factor H. Eur J Immunol. 2001;31:1674–84.

106. Kraiczy P, Hellwage J, Skerka C, Becker H, Kirschfink M, Simon MM, et al. Complement resistance of *Borrelia burgdorferi* correlates with the expression of BbCRASP-1, a novel linear plasmid-encoded surface protein that interacts with human factor H and FHL-1 and is unrelated to Erp proteins. J Biol Chem. 2004;279:2421–9.

107. Haupt K, Kraiczy P, Wallich R, Brade V, Skerka C, Zipfel PF. Binding of human factor H-related protein 1 to serum-resistant *Borrelia burgdorferi* is mediated by borrelial complement regulator-acquiring surface proteins. J Infect Dis. 2007;196:124–33.

108. von Lackum K, Miller JC, Bykowski T, Riley SP, Woodman ME, Brade V, et al. *Borrelia burgdorferi* regulates expression of complement regulator-acquiring surface protein 1 during the mammal-tick infection cycle. Infect Immun. 2005;73:7398–405.

109. Bykowski T, Woodman ME, Cooley AE, Brissette CA, Brade V, Wallich R, et al. Coordinated expression of *Borrelia burgdorferi* complement regulator-acquiring surface proteins during the Lyme disease spirochete's mammal-tick infection cycle. Infect Immun. 2007;75:4227–36.

110. Kenedy MR, Vuppala SR, Siegel C, Kraiczy P, Akins DR. CspA-mediated binding of human factor H inhibits complement deposition and confers serum resistance in *Borrelia burgdorferi*. Infect Immun. 2009;77:2773–82.

111. Hallstrom T, Siegel C, Morgelin M, Kraiczy P, Skerka C, Zipfel PF. CspA from *Borrelia burgdorferi* inhibits the terminal complement pathway. MBio. 2013;4: e00481-13.

112. Bhide MR, Travnicek M, Levkutova M, Curlik J, Revajova V, Levkut M. Sensitivity of *Borrelia* genospecies to serum complement from different animals and human: a host-pathogen relationship. FEMS Immunol Med Microbiol. 2005;43:165–72.

113. Herzberger P, Siegel C, Skerka C, Fingerle V, Schulte-Spechtel U, van Dam A, et al. Human pathogenic *Borrelia spielmanii* sp. nov. resists complement-mediated killing by direct binding of immune regulators factor H and factor H-like protein 1. Infect Immun. 2007;75:4817–25.

114. Hartmann K, Corvey C, Skerka C, Kirschfink M, Karas M, Brade V, et al. Functional characterization of BbCRASP-2, a distinct outer membrane protein of *Borrelia burgdorferi* that binds host complement regulators factor H and FHL-1. Mol Microbiol. 2006;61:1220–36.

115. Siegel C, Schreiber J, Haupt K, Skerka C, Brade V, Simon MM, et al. Deciphering the ligand-binding sites in the *Borrelia burgdorferi* complement regulator-acquiring surface protein 2 required for interactions with the human immune regulators factor H and factor H-like protein 1. J Biol Chem. 2008;283:34855–63.

116. Kraiczy P, Seling A, Brissette CA, Rossmann E, Hunfeld KP, Bykowski T, et al. *Borrelia burgdorferi* complement regulator-acquiring surface protein 2 (CspZ) as a serological marker of human Lyme disease. Clin Vaccine Immunol. 2008;15:484–91.

117. Coleman AS, Yang X, Kumar M, Zhang X, Promnares K, Shroder D, et al. *Borrelia burgdorferi* complement regulator-acquiring surface protein 2 does not contribute to complement resistance or host infectivity. PLoS One. 2008;3:3010e.

118. Alitalo A, Meri T, Lankinen H, Seppala L, Lahdenne P, Hefty PS, et al. Complement inhibitor factor H binding to Lyme disease spirochetes is mediated by inducible expression of multiple plasmid-encoded outer surface protein E paralogs. J Immunol. 2002;169:3847–53.

119. Hammerschmidt C, Hallstrom T, Skerka C, Wallich R, Stevenson B, Zipfel PF, et al. Contribution of the infection-associated complement regulator-acquiring surface protein 4 (ErpC) to complement resistance of *Borrelia burgdorferi*. Clin Dev Immunol. 2012;2012:349657.

120. Siegel C, Hallstrom T, Skerka C, Eberhardt H, Uzonyi B, Beckhaus T, et al. Complement factor H-related proteins CFHR2 and CFHR5 represent novel

121. Hovis KM, Tran E, Sundy CM, Buckles E, McDowell JV, Marconi RT. Selective binding of *Borrelia burgdorferi* OspE paralogs to factor H and serum proteins from diverse animals: possible expansion of the role of OspE in Lyme disease pathogenesis. Infect Immun. 2006;74:1967–72.

122. McDowell JV, Wolfgang J, Tran E, Metts MS, Hamilton D, Marconi RT. Comprehensive analysis of the factor H binding capabilities of *Borrelia* species associated with Lyme disease: delineation of two distinct classes of factor H binding proteins. Infect Immun. 2003;71:3597–602.

123. Stevenson B, Bono JL, Schwan TG, Rosa P. *Borrelia burgdorferi* erp proteins are immunogenic in mammals infected by tick bite, and their synthesis is inducible in cultured bacteria. Infect Immun. 1998;66:2648–54.

124. Fikrig E, Narasimhan S. *Borrelia burgdorferi*-traveling incognito? Microbes Infect. 2006;8:1390–9.

125. Brooks CS, Vuppala SR, Jett AM, Alitalo A, Meri S, Akins DR. Complement regulator-acquiring surface protein 1 imparts resistance to human serum in *Borrelia burgdorferi*. J Immunol. 2005;175:3299–308.

126. van Dam AP, Oei A, Jaspars R, Fijen C, Wilske B, Spanjaard L, et al. Complement-mediated serum sensitivity among spirochetes that cause Lyme disease. Infect Immun. 1997;65:1228–36.

127. Sun J, Duffy KE, Ranjith-Kumar CT, Xiong J, Lamb RJ, Santos J, et al. Structural and functional analyses of the human Toll-like receptor 3. Role of glycosylation. J Biol Chem. 2006;281:11144–51.

128. Berende A, Oosting M, Kullberg BJ, Netea MG, Joosten LA. Activation of innate host defense mechanisms by *Borrelia*. Eur Cytokine Netw. 2010;21:7–18.

129. Leifer CA, Medvedev AE. Molecular mechanisms of regulation of Toll-like receptor signaling. J Leukocyte Biol. 2016;100:927–41.

130. Medzhitov R, Preston-Hurlburt P, Janeway CA Jr. A human homologue of the *Drosophila* Toll protein signals activation of adaptive immunity. Nature. 1997;388:394–7.

131. Muzio M, Bosisio D, Polentarutti N, D'Amico G, Stoppacciaro A, Mancinelli R, et al. Differential expression and regulation of toll-like receptors (TLR) in human leukocytes: selective expression of TLR3 in dendritic cells. J Immunol. 2000;164:5998–6004.

132. Wooten RM, Ma Y, Yoder RA, Brown JP, Weis JH, Zachary JF, et al. Toll-like receptor 2 is required for innate, but not acquired, host defense to *Borrelia burgdorferi*. J Immunol. 2002;168:348–55.

133. Bernardino AL, Myers TA, Alvarez X, Hasegawa A, Philipp MT. Toll-like receptors: insights into their possible role in the pathogenesis of Lyme neuroborreliosis. Infect Immun. 2008;76:4385–95.

134. Salazar JC, Pope CD, Moore MW, Pope J, Kiely TG, Radolf JD. Lipoprotein-dependent and -independent immune responses to spirochetal infection. Clin Diagn Lab Immunol. 2005;12:949–58.

135. Hoshino K, Takeuchi O, Kawai T, Sanjo H, Ogawa T, Takeda Y, et al. Cutting edge: Toll-like receptor 4 (TLR4)-deficient mice are hyporesponsive to lipopolysaccharide: evidence for TLR4 as the Lps gene product. J Immunol. 1999;162:3749–52.

136. Hacker H, Mischak H, Miethke T, Liptay S, Schmid R, Sparwasser T, et al. CpG-DNA-specific activation of antigen-presenting cells requires stress kinase activity and is preceded by non-specific endocytosis and endosomal maturation. EMBO J. 1998;17:6230–40.

137. Hemmi H, Takeuchi O, Kawai T, Kaisho T, Sato S, Sanjo H, et al. A Toll-like receptor recognizes bacterial DNA. Nature. 2000;408:740–5.

138. Inohara N, Nunez G. NODs: intracellular proteins involved in inflammation and apoptosis. Nat Rev Immunol. 2003;3:371–82.

139. Franchi L, Warner N, Viani K, Nunez G. Function of Nod-like receptors in microbial recognition and host defense. Immunol Rev. 2009;227:106–28.

140. Kanneganti TD, Lamkanfi M, Nunez G. Intracellular NOD-like receptors in host defense and disease. Immunity. 2007;27:549–59.

141. Sterka D Jr, Marriott I. Characterization of nucleotide-binding oligomerization domain (NOD) protein expression in primary murine microglia. J Neuroimmunol. 2006;179:65–75.

142. Sterka D Jr, Marriott I. Functional expression of NOD2, a novel pattern recognition receptor for bacterial motifs, in primary murine astrocytes. Glia. 2006;53:322–30.

143. Petnicki-Ocwieja T, DeFrancesco AS, Chung E, Darcy CT, Bronson RT, Kobayashi KS, et al. Nod2 suppresses *Borrelia burgdorferi* mediated murine Lyme arthritis and carditis through the induction of tolerance. PLoS One. 2011;6:e17414.

144. Oosting M, Berende A, Sturm P, Ter Hofstede HJ, de Jong DJ, Kanneganti TD, et al. Recognition of *Borrelia burgdorferi* by NOD2 is central for the induction of an inflammatory reaction. J Infect Dis. 2010;201:1849–58.

145. Stubs G, Fingerle V, Wilske B, Gobel UB, Zahringer U, Schumann RR, et al. Acylated cholesteryl galactosides are specific antigens of *Borrelia* causing Lyme disease and frequently induce antibodies in late stages of disease. J Biol Chem. 2009;284:13326–34.

146. Ben-Menachem G, Kubler-Kielb J, Coxon B, Yergey A, Schneerson R. A newly discovered cholesteryl galactoside from *Borrelia burgdorferi*. Proc Natl Acad Sci USA. 2003;100:7913–8.

147. Radolf JD, Caimano MJ, Stevenson B, Hu LT. Of ticks, mice and men: understanding the dual-host lifestyle of Lyme disease spirochaetes. Nat Rev Microbiol. 2012;10:87–99.

148. Jones KL, Seward RJ, Ben-Menachem G, Glickstein LJ, Costello CE, Steere AC. Strong IgG antibody responses to *Borrelia burgdorferi* glycolipids in patients with Lyme arthritis, a late manifestation of the infection. Clin Immunol. 2009;132:93–102.

149. Comstock LE, Fikrig E, Shoberg RJ, Flavell RA, Thomas DD. A monoclonal antibody to OspA inhibits association of *Borrelia burgdorferi* with human endothelial cells. Infect Immun. 1993;61:423–31.

150. Wang J, Li Y, Kinjo Y, Mac TT, Gibson D, Painter GF, et al. Lipid binding orientation within CD1d affects recognition of *Borrelia burgorferi* antigens by NKT cells. Proc Natl Acad Sci USA. 2010;107:1535–40.

151. Garcia Monco JC, Wheeler CM, Benach JL, Furie RA, Lukehart SA, Stanek G, et al. Reactivity of neuroborreliosis patients (Lyme disease) to cardiolipin and gangliosides. J Neurol Sci. 1993;117:206–14.

152. Garcia-Monco JC, Seidman RJ, Benach JL. Experimental immunization with *Borrelia burgdorferi* induces development of antibodies to gangliosides. Infect Immun. 1995;63:4130–7.

153. Weller M, Stevens A, Sommer N, Dichgans J, Kappler B, Wietholter H. Ganglioside antibodies: a lack of diagnostic specificity and clinical utility? J Neurol. 1992;239:455–9.

154. Venkataswamy MM, Porcelli SA. Lipid and glycolipid antigens of CD1d-restricted natural killer T cells. Semin Immunol. 2010;22:68–78.

155. Hossain H, Wellensiek HJ, Geyer R, Lochnit G. Structural analysis of glycolipids from *Borrelia burgdorferi*. Biochimie. 2001;83:683–92.

156. Smith DG, Williams SJ. Immune sensing of microbial glycolipids and related conjugates by T cells and the pattern recognition receptors MCL and Mincle. Carbohydr Res. 2016;420:32–45.

157. Garcia Monco JC, Fernandez Villar B, Rogers RC, Szczepanski A, Wheeler CM, Benach JL. *Borrelia burgdorferi* and other related spirochetes bind to galactocerebroside. Neurology. 1992;42:1341–8.

158. Backenson PB, Coleman JL, Benach JL. *Borrelia burgdorferi* shows specificity of binding to glycosphingolipids. Infect Immun. 1995;63:2811–7.

159. Kaneda K, Masuzawa T, Yasugami K, Suzuki T, Suzuki Y, Yanagihara Y. Glycosphingolipid-binding protein of *Borrelia burgdorferi sensu lato*. Infect Immun. 1997;65:3180–5.

160. Hajnicka V, Kocakova P, Slavikova M, Slovak M, Gasperik J, Fuchsberger N, et al. Anti-interleukin-8 activity of tick salivary gland extracts. Parasite Immunol. 2001;23:483–9.

161. Frauenschuh A, Power CA, Deruaz M, Ferreira BR, Silva JS, Teixeira MM, et al. Molecular cloning and characterization of a highly selective chemokine-binding protein from the tick *Rhipicephalus sanguineus*. J Biol Chem. 2007;282:27250–8.

162. Eaton JRO, Alenazi Y, Singh K, Davies G, Geis-Asteggiante L, Kessler B, et al. The N-terminal domain of a tick evasin is critical for chemokine binding and neutralization and confers specific binding activity to other evasins. J Biol Chem. 2018; https://doi.org/10.1074/jbc.RA117.000487.

163. Uhlir J, Grubhoffer L, Borsky I, Dusbabek F. Antigens and glycoproteins of larvae, nymphs and adults of the tick *Ixodes ricinus*. Med Vet Entomol. 1994;8:141–50.

164. Mulenga A, Kim T, Ibelli AM. *Amblyomma americanum* tick saliva serine protease inhibitor 6 is a cross-class inhibitor of serine proteases and papain-like cysteine proteases that delays plasma clotting and inhibits platelet aggregation. Insect Mol Biol. 2013;22:306–19.

165. Tirloni L, Kim TK, Coutinho ML, Ali A, Seixas A, Termignoni C, et al. The putative role of *Rhipicephalus microplus* salivary serpins in the tick-host relationship. Insect Biochem Mol Biol. 2016;71:12–28.

166. Deruaz M, Frauenschuh A, Alessandri AL, Dias JM, Coelho FM, Russo RC, et al. Ticks produce highly selective chemokine binding proteins with antiinflammatory activity. J Exp Med. 2008;205:2019–31.

167. Pratt CW, Church FC. Heparin binding to protein C inhibitor. J Biol Chem. 1992;267:8789–94.

168. Rein CM, Desai UR, Church FC. Serpin-glycosaminoglycan interactions. Methods Enzymol. 2011;501:105–37.

169. Tollefsen DM. Heparin Cofactor II. In: Church FC, Cunningham DD, Ginsburg D, Hoffman M, Stone SR, Tollefsen DM, editors. Chemistry and Biology of Serpins (Advances in Experimental Medicine and Biology, Vol. 425). New York: Springer Science+Business Media; 1997.

170. Radulovic ZM, Mulenga A. Heparan sulfate/heparin glycosaminoglycan binding alters inhibitory profile and enhances anticoagulant function of conserved *Amblyomma americanum* tick saliva serpin 19. Insect Biochem Mol Biol. 2017;80:1–10.

171. Koh CY, Kazimirova M, Trimnell A, Takac P, Labuda M, Nuttall PA, et al. Variegin, a novel fast and tight binding thrombin inhibitor from the tropical bont tick. J Biol Chem. 2007;282:29101–13.

172. Shabareesh PRV, Kumar A, Salunke DM, Kaur KJ. Structural and functional studies of differentially *O*-glycosylated analogs of a thrombin inhibitory peptide - variegin. J Pept Sci. 2017;23:880–8.

173. Stuen S, Bergstrom K, Palmer E. Reduced weight gain due to subclinical *Anaplasma phagocytophilum* (formerly *Ehrlichia phagocytophila*) infection. Exp Appl Acarol. 2002;28:209–15.

174. Splitter EJ, Twiehaus MJ, Castro ER. Anaplasmosis in sheep in the United States. J Am Vet Med Assoc. 1955;127:244–5.

175. Melendez RD. Future perspectives on veterinary hemoparasite research in the tropics at the start of this century. Ann N Y Acad Sci. 2000;916:253–8.

176. Dumler JS, Bakken JS. Human ehrlichioses: newly recognized infections transmitted by ticks. Annu Rev Med. 1998;49:201–13.

177. Keesing F, Hersh MH, Tibbetts M, McHenry DJ, Duerr S, Brunner J, et al. Reservoir competence of vertebrate hosts for *Anaplasma phagocytophilum*. Emerg Infect Dis. 2012;18:2013–6.

178. Parola P, Raoult D. Ticks and tickborne bacterial diseases in humans: an emerging infectious threat. Clin Infect Dis. 2001;32:897–928.

179. Stafford KC, Station CAE. Tick management handbook: an integrated guide for homeowners, pest control operators, and public health officials for the prevention of tick-associated disease. New Haven: Connecticut Agricultural Experiment Station; 2007.

180. Seidman D, Hebert KS, Truchan HK, Miller DP, Tegels BK, Marconi RT, et al. Essential domains of *Anaplasma phagocytophilum* invasins utilized to infect mammalian host cells. PLoS Pathog. 2015;11:e1004669.

181. Ojogun N, Kahlon A, Ragland SA, Troese MJ, Mastronunzio JE, Walker NJ, et al. *Anaplasma phagocytophilum* outer membrane protein A interacts with sialylated glycoproteins to promote infection of mammalian host cells. Infect Immun. 2012;80:3748–60.

182. Hebert KS, Seidman D, Oki AT, Izac J, Emani S, Oliver LD Jr, et al. *Anaplasma marginale* outer membrane protein A is an adhesin that recognizes sialylated and fucosylated glycans and functionally depends on an essential binding domain. Infect Immun. 2017;85:e00968-16.

183. Barbet AF, Allred DR. The msp1β multigene family of *Anaplasma marginale*: nucleotide sequence analysis of an expressed copy. Infect Immun. 1991;59:971–6.

184. McGarey DJ, Allred DR. Characterization of hemagglutinating components on the *Anaplasma marginale* initial body surface and identification of possible adhesins. Infect Immun. 1994;62:4587–93.

185. de la Fuente J, Garcia-Garcia JC, Blouin EF, Kocan KM. Differential adhesion of major surface proteins 1a and 1b of the ehrlichial cattle pathogen *Anaplasma marginale* to bovine erythrocytes and tick cells. Int J Parasitol. 2001;31:145–53.

186. McGarey DJ, Barbet AF, Palmer GH, McGuire TC, Allred DR. Putative adhesins of *Anaplasma marginale*: major surface polypeptides 1a and 1b. Infect Immun. 1994;62:4594–601.

187. Contreras M, Alberdi P, Mateos-Hernandez L, Fernandez de Mera IG, Garcia-Perez AL, Vancova M, et al. *Anaplasma phagocytophilum* MSP4 and HSP70 proteins are involved in interactions with host cells during pathogen infection. Front Cell Infect Microbiol. 2017;7:307.

188. NCBI. 1988. https://www.ncbi.nlm.nih.gov/. Accessed 30 Nov 2017.

189. de la Fuente J, Garcia-Garcia JC, Blouin EF, Kocan KM. Characterization of the functional domain of major surface protein 1a involved in adhesion of the rickettsia *Anaplasma marginale* to host cells. Vet Microbiol. 2003;91:265–83.

190. Garcia-Garcia JC, de la Fuente J, Bell-Eunice G, Blouin EF, Kocan KM. Glycosylation of *Anaplasma marginale* major surface protein 1a and its putative role in adhesion to tick cells. Infect Immun. 2004;72:3022–30.

191. Park J, Choi KS, Dumler JS. Major surface protein 2 of *Anaplasma phagocytophilum* facilitates adherence to granulocytes. Infect Immun. 2003;71:4018–25.

192. Rejmanek D, Foley P, Barbet A, Foley J. Antigen variability in *Anaplasma phagocytophilum* during chronic infection of a reservoir host. Microbiology. 2012;158:2632–41.

193. Rejmanek D, Foley P, Barbet A, Foley J. Evolution of antigen variation in the tick-borne pathogen *Anaplasma phagocytophilum*. Mol Biol Evol. 2012;29:391–400.

194. Ge Y, Rikihisa Y. Identification of novel surface proteins of *Anaplasma phagocytophilum* by affinity purification and proteomics. J Bacteriol. 2007;189:7819–28.

195. Mastronunzio JE, Kurscheid S, Fikrig E. Postgenomic analyses reveal development of infectious *Anaplasma phagocytophilum* during transmission from ticks to mice. J Bacteriol. 2012;194:2238–47.

196. Troese MJ, Kahlon A, Ragland SA, Ottens AK, Ojogun N, Nelson KT, et al. Proteomic analysis of *Anaplasma phagocytophilum* during infection of human myeloid cells identifies a protein that is pronouncedly upregulated on the infectious dense-cored cell. Infect Immun. 2011;79:4696–707.

197. Goodman JL, Nelson CM, Klein MB, Hayes SF, Weston BW. Leukocyte infection by the granulocytic ehrlichiosis agent is linked to expression of a selectin ligand. J Clin Invest. 1999;103:407–12.

198. Ojogun N, Barnstein B, Huang B, Oskeritzian CA, Homeister JW, Miller D, et al. *Anaplasma phagocytophilum* infects mast cells *via* α1,3-fucosylated but not sialylated glycans and inhibits IgE-mediated cytokine production and histamine release. Infect Immun. 2011;79:2717–26.

199. Carlyon JA, Akkoyunlu M, Xia L, Yago T, Wang T, Cummings RD, et al. Murine neutrophils require α1,3-fucosylation but not PSGL-1 for productive infection with *Anaplasma phagocytophilum*. Blood. 2003;102:3387–95.

200. McEver RP, Cummings RD. Role of PSGL-1 binding to selectins in leukocyte recruitment. J Clin Invest. 1997;100(Suppl. 11):S97–103.

201. Yago T, Leppanen A, Carlyon JA, Akkoyunlu M, Karmakar S, Fikrig E, et al. Structurally distinct requirements for binding of P-selectin glycoprotein ligand-1 and sialyl Lewis x to *Anaplasma phagocytophilum* and P-selectin. J Biol Chem. 2003;278:37987–97.

202. Herron MJ, Nelson CM, Larson J, Snapp KR, Kansas GS, Goodman JL. Intracellular parasitism by the human granulocytic ehrlichiosis bacterium through the P-selectin ligand, PSGL-1. Science. 2000;288:1653–6.

203. Pedra JH, Narasimhan S, Rendic D, DePonte K, Bell-Sakyi L, Wilson IB, et al. Fucosylation enhances colonization of ticks by *Anaplasma phagocytophilum*. Cell Microbiol. 2010;12:1222–34.

204. Kariu T, Smith A, Yang X, Pal U. A chitin deacetylase-like protein is a predominant constituent of tick peritrophic membrane that influences the persistence of Lyme disease pathogens within the vector. PLoS One. 2013;8:e78376.

205. Abraham NM, Liu L, Jutras BL, Yadav AK, Narasimhan S, Gopalakrishnan V, et al. Pathogen-mediated manipulation of arthropod microbiota to promote infection. Proc Natl Acad Sci USA. 2017;114:E781–E90.

206. Heisig M, Abraham NM, Liu L, Neelakanta G, Mattessich S, Sultana H, et al. Antivirulence properties of an antifreeze protein. Cell Rep. 2014;9:417–24.

207. Neelakanta G, Sultana H, Fish D, Anderson JF, Fikrig E. *Anaplasma phagocytophilum* induces *Ixodes scapularis* ticks to express an antifreeze glycoprotein gene that enhances their survival in the cold. J Clin Invest. 2010;120:3179–90.

208. Ip WK, Takahashi K, Ezekowitz RA, Stuart LM. Mannose-binding lectin and innate immunity. Immunol Rev. 2009;230:9–21.

209. Matsushita M. Ficolins: complement-activating lectins involved in innate immunity. J Innate Immun. 2010;2:24–32.

210. Krarup A, Thiel S, Hansen A, Fujita T, Jensenius JC. L-ficolin is a pattern recognition molecule specific for acetyl groups. J Biol Chem. 2004;279:47513–9.

211. Kairies N, Beisel HG, Fuentes-Prior P, Tsuda R, Muta T, Iwanaga S, et al. The 2. 0-A crystal structure of tachylectin 5A provides evidence for the common origin of the innate immunity and the blood coagulation systems. Proc Natl Acad Sci USA. 2001;98:13519–24.

212. Hanington PC, Zhang SM. The primary role of fibrinogen-related proteins in invertebrates is defense, not coagulation. J Innate Immun. 2011;3:17–27.

213. Kopacek P, Hajdusek O, Buresova V. Tick as a model for the study of a primitive complement system. Adv Exp Med Biol. 2012;710:83–93.

214. Kovar V, Kopacek P, Grubhoffer L. Isolation and characterization of Dorin M, a lectin from plasma of the soft tick *Ornithodoros moubata*. Insect Biochem Mol Biol. 2000;30:195–205.

215. Rego ROM, Hajdusek O, Kovar V, Kopacek P, Grubhoffer L, Hypsa V. Molecular cloning and comparative analysis of fibrinogen-related proteins from the soft tick *Ornithodoros moubata* and the hard tick *Ixodes ricinus*. Insect Biochem Mol Biol. 2005;35:991–1004.

216. Rego ROM, Kovar V, Kopacek P, Weise C, Man P, Sauman I, et al. The tick plasma lectin, Dorin M, is a fibrinogen-related molecule. Insect Biochem Mol Biol. 2006;36:291–9.

217. Man P, Kovar V, Sterba J, Strohalm M, Kavan D, Kopacek P, et al. Deciphering Dorin M glycosylation by mass spectrometry. Eur J Mass Spectrom. 2008;14:345–54.

218. Sterba J, Dupejova J, Fiser M, Vancova M, Grubhoffer L. Fibrinogen-related proteins in ixodid ticks. Parasit Vectors. 2011;4:127.

219. Honig Mondekova H, Sima R, Urbanova V, Kovar V, Rego ROM, Grubhoffer L, et al. Characterization of *Ixodes ricinus* fibrinogen-related proteins (Ixoderins) discloses their function in the tick innate immunity. Front Cell Infect Microbiol. 2017;7:509.

220. Dupejova J, Sterba J, Vancova M, Grubhoffer L. Hemelipoglycoprotein from the ornate sheep tick, *Dermacentor marginatus*: structural and functional characterization. Parasit Vectors. 2011;4:4.

221. Huang X, Tsuji N, Miyoshi T, Nakamura-Tsuruta S, Hirabayashi J, Fujisaki K. Molecular characterization and oligosaccharide-binding properties of a galectin from the argasid tick *Ornithodoros moubata*. Glycobiology. 2007;17:313–23.

222. Vasta GR, Ahmed H, Nita-Lazar M, Banerjee A, Pasek M, Shridhar S, et al. Galectins as self/non-self recognition receptors in innate and adaptive immunity: an unresolved paradox. Front Immunol. 2012;3:199.

223. Maeda H, Miyata T, Kusakisako K, Galay RL, Talactac MR, Umemiya-Shirafuji R, et al. A novel C-type lectin with triple carbohydrate recognition domains has critical roles for the hard tick *Haemaphysalis longicornis* against Gram-negative bacteria. Dev Comp Immunol. 2016;57:38–47.

224. Smith AA, Pal U. Immunity-related genes in *Ixodes scapularis* - perspectives from genome information. Front Cell Infect Microbiol. 2014;4:116.

225. Pang X, Xiao X, Liu Y, Zhang R, Liu J, Liu Q, et al. Mosquito C-type lectins maintain gut microbiome homeostasis. Nat Microbiol. 2016;1:16023.

226. Cheng G, Cox J, Wang P, Krishnan MN, Dai J, Qian F, et al. A C-type lectin collaborates with a CD45 phosphatase homolog to facilitate West Nile virus infection of mosquitoes. Cell. 2010;142:714–25.

227. Neelakanta G, Sultana H. Viral receptors of the gut: vector-borne viruses of medical importance. Curr Opin Insect Sci. 2016;16:44–50.

228. Alarcon-Chaidez F, Ryan R, Wikel S, Dardick K, Lawler C, Foppa IM, et al. Confirmation of bite by detection of antibody to *Ixodes* calreticulin salivary protein. Clin Vaccine Immunol. 2006;13:1217–22.

229. Schroeder H, Skelly PJ, Zipfel PF, Losson B, Vanderplasschen A. Subversion of complement by hematophagous parasites. Dev Comp Immunol. 2009;33:5–13.

230. Eggleton P, Lieu TS, Zappi EG, Sastry K, Coburn J, Zaner KS, et al. Calreticulin is released from activated neutrophils and binds to C1q and mannan-binding protein. Clin Immunol Immunopathol. 1994;72:405–9.

231. Kim TK, Ibelli AM, Mulenga A. *Amblyomma americanum* tick calreticulin binds C1q but does not inhibit activation of the classical complement cascade. Ticks Tick Borne Dis. 2015;6:91–101.

232. Uhlir J, Grubhoffer L, Volf P. Novel agglutinin in the midgut of the tick *Ixodes ricinus*. Folia Parasitol (Praha). 1996;43:233–9.

233. Grubhoffer L, Kovar V, Rudenko N. Tick lectins: structural and functional properties. Parasitology. 2004;129:S113–S25.

234. Kamwendo SP, Ingram GA, Musisi FL, Molyneux DH. Haemagglutinin activity in tick (*Rhipicephalus appendiculatus*) haemolymph and extracts of gut and salivary gland. Ann Trop Med Parasitol. 1993;87:303–5.

235. Kamwendo SP, Ingram GA, Musisi FL, Trees AJ, Molyneux DH. Characteristics of tick, *Rhipicephalus appendiculatus*, glands distinguished by surface lectin binding. Ann Trop Med Parasitol. 1993;87:525–35.

236. Pal U, Li X, Wang T, Montgomery RR, Ramamoorthi N, Desilva AM, et al. TROSPA, an *Ixodes scapularis* receptor for *Borrelia burgdorferi*. Cell. 2004;119:457–68.

237. Grubhoffer L, Dusbabek F. Lectin binding analysis of *Argas polonicus* tissue glycoproteins. Vet Parasitol. 1991;38:235–47.

238. Vancova M, Zacharovova K, Grubhoffer L, Nebesarova J. Ultrastructure and lectin characterization of granular salivary cells from *Ixodes ricinus* females. J Parasitol. 2006;92:431–40.

239. Grubhoffer L, Hajdusek O, Vancova M, Sterba J, Rudenko N. Glycobiochemistry of ticks, vectors of infectious diseases: carbohydrate-binding proteins and glycans. FEBS J. 2009;276:141.

240. Vancova M, Sterba J, Dupejova J, Simonova Z, Nebesarova J, Novotny MV, et al. Uptake and incorporation of sialic acid by the tick *Ixodes ricinus*. J Insect Physiol. 2012;58:1277–87.

241. Thall A, Galili U. Distribution of Galα1-3Galβ1-4GlcNAc residues on secreted mammalian glycoproteins (thyroglobulin, fibrinogen, and immunoglobulin G) as measured by a sensitive solid-phase radioimmunoassay. Biochemistry. 1990;29:3959–65.

242. Chung CH, Mirakhur B, Chan E, Le QT, Berlin J, Morse M, et al. Cetuximab-induced anaphylaxis and IgE specific for galactose-α-1,3-galactose. N Engl J Med. 2008;358:1109–17.

Vechtova *et al. Parasites & Vectors*   (2018) 11:594

Page 26 of 27

243. Commins SP, James HR, Kelly LA, Pochan SL, Workman LJ, Perzanowski MS, et al. The relevance of tick bites to the production of IgE antibodies to the mammalian oligosaccharide galactose-α-1,3-galactose. J Allergy Clin Immunol. 2011;127:1286–93.e6.

244. Van Nunen SA, O'Connor KS, Clarke LR, Boyle RX, Fernando SL. An association between tick bite reactions and red meat allergy in humans. Med J Aust. 2009;190:510–1.

245. Chinuki Y, Ishiwata K, Yamaji K, Takahashi H, Morita E. *Haemaphysalis longicornis* tick bites are a possible cause of red meat allergy in Japan. Allergy. 2016;71:421–5.

246. Hamsten C, Starkhammar M, Tran TA, Johansson M, Bengtsson U, Ahlen G, et al. Identification of galactose-α-1,3-galactose in the gastrointestinal tract of the tick *Ixodes ricinus*; possible relationship with red meat allergy. Allergy. 2013;68:549–52.

247. Wang H, Nuttall PA. Excretion of host immunoglobulin in tick saliva and detection of IgG-binding proteins in tick haemolymph and salivary glands. Parasitology. 1994;109:525–30.

248. Valenzuela JG, Francischetti IMB, Pham VM, Garfield MK, Mather TN, Ribeiro JMC. Exploring the sialome of the tick *Ixodes scapularis*. J Exp Biol. 2002;205:2843–64.

249. Araujo RN, Franco PF, Rodrigues H, Santos LCB, McKay CS, Sanhueza CA, et al. *Amblyomma sculptum* tick saliva: α-Gal identification, antibody response and possible association with red meat allergy in Brazil. Int J Parasitol. 2016;46:213–20.

250. Altmann F. The role of protein glycosylation in allergy. Int Arch Allergy Immunol. 2007;142:99–115.

251. van Die I, Gomord V, Kooyman FN, van den Berg TK, Cummings RD, Vervelde L. Core α1->3-fucose is a common modification of *N*-glycans in parasitic helminths and constitutes an important epitope for IgE from *Haemonchus contortus* infected sheep. FEBS Lett. 1999;463:189–93.

252. Altmann F. Coping with cross-reactive carbohydrate determinants in allergy diagnosis. Allergo J Int. 2016;25:98–105.

253. Vancova M, Nebesarova J. Correlative fluorescence and scanning electron microscopy of labelled core fucosylated glycans using cryosections mounted on carbon-patterned glass slides. PLoS One. 2015;10:e0145034.

254. Bencurova M, Hemmer W, Focke-Tejkl M, Wilson IB, Altmann F. Specificity of IgG and IgE antibodies against plant and insect glycoprotein glycans determined with artificial glycoforms of human transferrin. Glycobiology. 2004;14:457–66.

255. North SJ, Koles K, Hembd C, Morris HR, Dell A, Panin VM, et al. Glycomic studies of *Drosophila melanogaster* embryos. Glycoconjugate J. 2006;23:345–54.

256. Koles K, Irvine KD, Panin VM. Functional characterization of *Drosophila* sialyltransferase. J Biol Chem. 2004;279:4346–57.

257. Repnikova E, Koles K, Nakamura M, Pitts J, Li H, Ambavane A, et al. Sialyltransferase regulates nervous system function in *Drosophila*. J Neurosci. 2010;30:6466–76.

258. Sterba J, Vancova M, Sterbova J, Bell-Sakyi L, Grubhoffer L. The majority of sialylated glycoproteins in adult *Ixodes ricinus* ticks originate in the host, not the tick. Carbohydr Res. 2014;389:93–9.

259. Gritsun TS, Lashkevich VA, Gould EA. Tick-borne encephalitis. Antiviral Res. 2003;57:129–46.

260. Welsch S, Miller S, Romero-Brey I, Merz A, Bleck CK, Walther P, et al. Composition and three-dimensional architecture of the dengue virus replication and assembly sites. Cell Host Microbe. 2009;5:365–75.

261. Gillespie LK, Hoenen A, Morgan G, Mackenzie JM. The endoplasmic reticulum provides the membrane platform for biogenesis of the flavivirus replication complex. J Virol. 2010;84:10438–47.

262. Offerdahl DK, Dorward DW, Hansen BT, Bloom ME. A three-dimensional comparison of tick-borne flavivirus infection in mammalian and tick cell lines. PLoS One. 2012;7:e47912.

263. Miorin L, Romero-Brey I, Maiuri P, Hoppe S, Krijnse-Locker J, Bartenschlager R, et al. Three-dimensional architecture of tick-borne encephalitis virus replication sites and trafficking of the replicated RNA. J Virol. 2013;87:6469–81.

264. Yu L, Takeda K, Gao Y. Characterization of virus-specific vesicles assembled by West Nile virus non-structural proteins. Virology. 2017;506:130–40.

265. Best SM, Morris KL, Shannon JG, Robertson SJ, Mitzel DN, Park GS, et al. Inhibition of interferon-stimulated JAK-STAT signaling by a tick-borne flavivirus and identification of NS5 as an interferon antagonist. J Virol. 2005;79:12828–39.

266. Lindenbach BD, Rice CM. Molecular biology of flaviviruses. Adv Virus Res. 2003;59:23–61.

267. Lorenz IC, Allison SL, Heinz FX, Helenius A. Folding and dimerization of tick-borne encephalitis virus envelope proteins prM and E in the endoplasmic reticulum. J Virol. 2002;76:5480–91.

268. Mackenzie JM, Westaway EG. Assembly and maturation of the flavivirus Kunjin virus appear to occur in the rough endoplasmic reticulum and along the secretory pathway, respectively. J Virol. 2001;75:10787–99.

269. Stadler K, Allison SL, Schalich J, Heinz FX. Proteolytic activation of tick-borne encephalitis virus by furin. J Virol. 1997;71:8475–81.

270. Mandl CW. Steps of the tick-borne encephalitis virus replication cycle that affect neuropathogenesis. Virus Res. 2005;111:161–74.

271. Heinz FX, Allison SL. Flavivirus structure and membrane fusion. Adv Virus Res. 2003;59:63–97.

272. Hammond C, Braakman I, Helenius A. Role of *N*-linked oligosaccharide recognition, glucose trimming, and calnexin in glycoprotein folding and quality control. Proc Natl Acad Sci USA. 1994;91:913–7.

273. Yoshii K, Yanagihara N, Ishizuka M, Sakai M, Kariwa H. *N*-linked glycan in tick-borne encephalitis virus envelope protein affects viral secretion in mammalian cells, but not in tick cells. J Gen Virol. 2013;94:2249–58.

274. Winkler G, Heinz FX, Kunz C. Studies on the glycosylation of flavivirus E proteins and the role of carbohydrate in antigenic structure. Virology. 1987;159:237–43.

275. Rey FA, Heinz FX, Mandl C, Kunz C, Harrison SC. The envelope glycoprotein from tick-borne encephalitis virus at 2 A resolution. Nature. 1995;375:291–8.

276. Lorenz IC, Kartenbeck J, Mezzacasa A, Allison SL, Heinz FX, Helenius A. Intracellular assembly and secretion of recombinant subviral particles from tick-borne encephalitis virus. J Virol. 2003;77:4370–82.

277. Grubhoffer L, Guirakhoo F, Heinz F, Kunz C. Interaction of tick-borne encephalitis virus protein E with labelled lectins. In: Lectins: Biology, Biochemistry and Clinical Biochemistry, vol. 7. St Louis: Sigma Chemical Company; 1990. p. 313–9.

278. Fuzik T, Formanova P, Ruzek D, Yoshii K, Niedrig M, Plevka P. Structure of tick-borne encephalitis virus and its neutralization by a monoclonal antibody. Nat Commun. 2018;9:436.

279. Goto A, Yoshii K, Obara M, Ueki T, Mizutani T, Kariwa H, et al. Role of the *N*-linked glycans of the prM and E envelope proteins in tick-borne encephalitis virus particle secretion. Vaccine. 2005;23:3043–52.

280. Putnak JR, Charles PC, Padmanabhan R, Irie K, Hoke CH, Burke DS. Functional and antigenic domains of the dengue-2 virus nonstructural glycoprotein NS-1. Virology. 1988;163:93–103.

281. Chambers TJ, Hahn CS, Galler R, Rice CM. Flavivirus genome organization, expression, and replication. Annu Rev Microbiol. 1990;44:649–88.

282. Heinz FX, Allison SL. Structures and mechanisms in flavivirus fusion. Adv Virus Res. 2000;55:231–69.

283. Hanna SL, Pierson TC, Sanchez MD, Ahmed AA, Murtadha MM, Doms RW. *N*-linked glycosylation of west nile virus envelope proteins influences particle assembly and infectivity. J Virol. 2005;79:13262–74.

284. Bryant JE, Calvert AE, Mesesan K, Crabtree MB, Volpe KE, Silengo S, et al. Glycosylation of the dengue 2 virus E protein at N67 is critical for virus growth *in vitro* but not for growth in intrathoracically inoculated *Aedes aegypti* mosquitoes. Virology. 2007;366:415–23.

285. Mondotte JA, Lozach PY, Amara A, Gamarnik AV. Essential role of dengue virus envelope protein *N*-glycosylation at asparagine-67 during viral propagation. J Virol. 2007;81:7136–48.

286. Moudy RM, Zhang B, Shi PY, Kramer LD. West Nile virus envelope protein glycosylation is required for efficient viral transmission by *Culex* vectors. Virology. 2009;387:222–8.

287. Murata R, Eshita Y, Maeda A, Maeda J, Akita S, Tanaka T, et al. Glycosylation of the West Nile virus envelope protein increases *in vivo* and *in vitro* viral multiplication in birds. Am J Trop Med Hyg. 2010;82:696–704.

288. Hyde JA. *Borrelia burgdorferi* keeps moving and carries on: a review of borrelial dissemination and invasion. Front Immunol. 2017;8:114.

289. Hooper LV, Gordon JI. Glycans as legislators of host-microbial interactions: spanning the spectrum from symbiosis to pathogenicity. Glycobiology. 2001;11:1R–10R.

290. Nizet V, Esko JD. Bacterial and viral infections. In: Varki A, Cummings RD, Esko JD, Freeze HH, Stanley P, Bertozzi CR, et al., editors. Essentials of Glycobiology. 2nd ed. Cold Spring Harbor: Cold Spring Harbour Laboratory Press; 2009.

291. de la Fuente J, Canales M, Kocan KM. The importance of protein glycosylation in development of novel tick vaccine strategies. Parasite Immunol. 2006;28:687–8.

292. Sprong H, Trentelman J, Seemann I, Grubhoffer L, Rego RO, Hajdusek O, et al. ANTIDotE: anti-tick vaccines to prevent tick-borne diseases in Europe. Parasit Vectors. 2014;7:77.
293. Boysen A, Palmisano G, Krogh TJ, Duggin IG, Larsen MR, Moller-Jensen J. A novel mass spectrometric strategy "BEMAP" reveals extensive *O*-linked protein glycosylation in enterotoxigenic *Escherichia coli*. Sci Rep. 2016;6:32016.
294. Parveen N, Leong JM. Identification of a candidate glycosaminoglycan-binding adhesin of the Lyme disease spirochete *Borrelia burgdorferi*. Mol Microbiol. 2000;35:1220–34.
295. Guo BP, Brown EL, Dorward DW, Rosenberg LC, Hook M. Decorin-binding adhesins from *Borrelia burgdorferi*. Mol Microbiol. 1998;30:711–23.
296. Fuchs H, Wallich R, Simon MM, Kramer MD. The outer surface protein A of the spirochete *Borrelia burgdorferi* is a plasmin(ogen) receptor. Proc Natl Acad Sci USA. 1994;91:12594–8.
297. Lagal V, Portnoi D, Faure G, Postic D, Baranton G. *Borrelia burgdorferi sensu stricto* invasiveness is correlated with OspC-plasminogen affinity. Microbes Infect. 2006;8:645–52.
298. Onder O, Humphrey PT, McOmber B, Korobova F, Francella N, Greenbaum DC, et al. OspC is potent plasminogen receptor on surface of *Borrelia burgdorferi*. J Biol Chem. 2012;2870:16860–8.
299. Floden AM, Watt JA, Brissette CA. *Borrelia burgdorferi* enolase is a surface-exposed plasminogen binding protein. PLoS One. 2011;6:e27502.
300. Cinco M, Cini B, Murgia R, Presani G, Prodan M, Perticarari S. Evidence of involvement of the mannose receptor in adhesion of *Borrelia burgdorferi* to monocyte/macrophages. Infect Immun. 2001;69:2743–7.
301. Guo BP, Teneberg S, Munch R, Terunuma D, Hatano K, Matsuoka K, et al. Relapsing fever *Borrelia* binds to neolacto glycans and mediates rosetting of human erythrocytes. Proc Natl Acad Sci USA. 2009;106:19280–5.
302. Kuismanen E, Hedman K, Saraste J, Pettersson RF. Uukuniemi virus maturation: accumulation of virus particles and viral antigens in the Golgi complex. Mol Cell Biol. 1982;2:1444–58.

Selinger, M., Tykalová, H., Štěrba, J., Věchtová, P., Vavrušková, Z., Lieskovská, J., Kohl, A., Schnettler, E., Grubhoffer, L., 2019: Tick-borne encephalitis virus downregulates rRNA synthesis and host protein production in human cells of neuronal origin. *PLoS Negl Trop Dis.* 13(9): e0007745. DOI: 10.1371/journal.pntd.0007745. (IF = 4.487)

Tick-borne encephalitis virus inhibits rRNA synthesis and host protein production in human cells of neural origin

Martin Selinger[1,2☯], Hana Tykalová[1,2☯], Ján Štěrba[1,2], Pavlína Věchtová[1,2], Zuzana Vavrušková[1], Jaroslava Lieskovská[2], Alain Kohl[3], Esther Schnettler[4,5]*, Libor Grubhoffer[1,2]*

1 Institute of Parasitology, Biology Centre of the Czech Academy of Sciences, Branišovská 31, České Budějovice, Czech Republic, **2** Faculty of Science, University of South Bohemia in České Budějovice, Branišovská, České Budějovice, Czech Republic, **3** MRC-University of Glasgow Centre for Virus Research, Glasgow, Scotland, United Kingdom, **4** Bernhard-Nocht-Institute for Tropical Medicine, Bernhard-Nocht-Str. 74, Hamburg, Germany, **5** German Centre for Infection Research (DZIF), partner site Hamburg-Luebeck-Borstel-Riems, Hamburg, Germany

☯ These authors contributed equally to this work.
* schnettler@bnitm.de (ES); liborex@paru.cas.cz (LG)

Abstract

Tick-borne encephalitis virus (TBEV), a member of the genus *Flavivirus* (*Flaviviridae*), is a causative agent of a severe neuroinfection. Recently, several flaviviruses have been shown to interact with host protein synthesis. In order to determine whether TBEV interacts with this host process in its natural target cells, we analysed *de novo* protein synthesis in a human cell line derived from cerebellar medulloblastoma (DAOY HTB-186). We observed a significant decrease in the rate of host protein synthesis, including the housekeeping genes HPRT1 and GAPDH and the known interferon-stimulated gene viperin. In addition, TBEV infection resulted in a specific decrease of RNA polymerase I (POLR1) transcripts, 18S and 28S rRNAs and their precursor, 45-47S pre-rRNA, but had no effect on the POLR3 transcribed 5S rRNA levels. To our knowledge, this is the first report of flavivirus-induced decrease of specifically POLR1 rRNA transcripts accompanied by host translational shut-off.

Author summary

Tick-borne encephalitis virus (TBEV) is a causative agent of a severe human neuroinfection that threatens Europe and Asia. Little is known about the interaction of this neurotropic virus with neural cells, even though this may be important to better understand why or how TBEV can cause high pathogenicity in humans, especially following neural cell infection. Here, we showed that TBEV induced host translational shut-off in cells of neural origin. In addition, TBEV interfered also with the expression of host ribosomal RNAs. Interestingly, the transcriptional shut-off was documented for rRNA species transcribed by RNA polymerase I (18S rRNA, 28S rRNA and their precursor 45-47S pre-rRNA), but not for RNA polymerase III rRNA transcripts (5S rRNA). Artificial inhibition

of host translation using cycloheximide resulted in the decrease of all rRNA species. Based on these data, TBEV seems to specifically target transcription of RNA polymerase I. These new findings further increase our understanding of TBEV interactions with a key target cell type.

Introduction

The *Flaviviridae* family contains arthropod-borne viruses including medically important pathogens with worldwide distribution and impact, such as dengue virus (DENV), yellow fever virus (YFV), West Nile virus (WNV), Japanese encephalitis virus (JEV), Zika virus (ZIKV), and tick-borne encephalitis virus (TBEV) [1].

TBEV causes a severe neuroinfection known as tick-borne encephalitis, which affects thousands of people across Eurasia annually [2, 3]. In recent years, an increase in TBEV infection rates in affected countries and in its geographical distribution has been observed, involving previously unaffected areas such as Switzerland and northern Germany [4–6]. Although the disease is not always fatal (mortality rate of 1–2%), a high percentage of patients (35–58%) suffer from permanent sequelae, such as cognitive or neuropsychiatric afflictions, balance disorders, headaches, dysphasia, hearing defects, and spinal paralysis after overcoming the main symptoms [2, 7]. Specific antiviral therapy for tick-borne encephalitis does not exist. Neurons are the primary target for TBEV infection in mice and humans, and according to *post mortem* studies of TBEV-infected patients, the cerebellum is one of the main foci affected [8–10]. Understanding the interaction between TBEV and human neural cells is essential as it could lead to possible new treatment targets and a better understanding of why TBEV infection can result in severe neurological symptoms. Like all flaviviruses, TBEV is an enveloped virus with a single-stranded RNA (ssRNA) genome of positive polarity (approx. 11 kb) with a 7-methylguanosine cap at the 5′end. The coding segment is flanked on both ends by untranslated regions (UTR). Viral proteins are encoded in a single open reading frame that is translated in one poly-protein which is then proteolytically processed into three structural (C, prM, E) and seven non-structural proteins (NS1, NS2A, NS2B, NS3, NS4A, NS4B, NS5) [11–13]. While the structural proteins are the main building units of the viral particle, the non-structural proteins are crucial in the TBEV life cycle. They are essential components of viral replication within the host endoplasmic reticulum or Golgi apparatus-derived membrane compartments and the virion assembly processes and are involved in immune response evasion/counteractions [14–16].

Virus replication is reliant on the host protein synthesis apparatus and manipulates it in favour of viral requirements. There are various strategies viruses use to accomplish this goal and generally aim at three levels: host translational shut-off, processing of host mRNA, and host transcriptional shut-off [17, 18]. Translation of eukaryotic and viral proteins is often controlled at the rate-limiting step of initiation and viruses such as Bunyamwera virus, influenza A virus or poliovirus were shown to target initiation factors [19–23]. More specifically for flaviviruses, a recent study [24] documented repression of the host translation initiation step during DENV infection and general translational repression was also recorded for WNV and ZIKV. While inducing host translational shut-off, viral proteins are still synthesised thanks to alternative translation initiation strategies, such as cap-independent translation [20, 25–27].

Transcription in eukaryotic organisms is carried out by three RNA polymerases: RNA polymerase I, II, and III. Each of the RNA polymerase complexes is responsible for the transcription of different genes. RNA polymerase I (POLR1) yields a single transcription unit 45-47S

118

pre-rRNA, which undergoes a complex maturation process that generates 5.8S, 18S, and 28S rRNA [28, 29]. RNA polymerase III (POLR3) produces 5S rRNA, tRNAs, and specific small RNAs [29]. RNA polymerase II (POLR2) transcribes protein-coding genes and certain small RNAs [30]. Out of all the transcripts synthesised in the eukaryotic cell, ribosomal RNA is the most abundant and a key component of ribosomes. Virus-induced interference with transcription and subsequent processing of host rRNA has been described for influenza A virus [31], herpes simplex virus type I [32], human papillomavirus type 8 [33], human cytomegalovirus [34], and human immunodeficiency virus (HIV) [35]. However, this was not described for flaviviruses.

Given the indications for flaviviruses affecting host translation [24], we aimed at exploring this topic further in TBEV infection of naturally permissive host cells of neural origin, that represent a key cell type responsible for tick-borne encephalitis manifestation. We found that TBEV triggered host translational shut-off that involved lowered expression of GAPDH and HPRT1 housekeeping genes as well as the interferon-induced protein viperin. TBEV further specifically impaired the production of POLR1-transcribed rRNAs. Therefore, we postulate that TBEV specifically targets POLR1-mediated transcription of rRNA and rate of host translation thus promoting virus replication.

Methods

Cell lines

The human medulloblastoma (DAOY HTB-186; ATCC), human lung adenocarcinoma (A549; a gift from R. Randall, University of St. Andrews, UK), and Vero (green monkey kidney; Biology Centre, CAS, CZ) cell lines were grown in low glucose DMEM medium supplemented with 10% foetal bovine serum (FBS), 1% antibiotics-antimycotics (amphotericin B 0.25 µg/ml, penicillin G 100 units/ml, streptomycin 100 µg/ml), and 1% L-alanyl-L-glutamine. DAOY HTB-186 cell line is derived from desmoplastic cerebellar medulloblastoma of a 4-year-old Caucasian male [36]. A549s are derived from a lung cancerous tissue (alveolar basal epithelial cells) of a 58-year-old Caucasian male [37]. Vero cells are derived from kidney epithelial cells from African green monkey (*Cercopithecus aethiops*). PS cells (porcine kidney stable) were grown in L15 medium with 3% new-born calf serum (NCS), 1% antibiotics-antimycotics, and 1% L-alanyl-L-glutamine [38]. The human osteosarcoma cell line MG-63 (Sigma-Aldrich) was grown in RPMI 1640 medium supplemented with 10% FBS, 1% antibiotics-antimycotics, 1% L-alanyl-L-glutamine, and 50 nM β-mercaptoethanol. These were explanted from a 14-year-old Caucasian male [39].

For metabolic labelling experiments, all cell lines were grown in RPMI 1640 medium supplemented with 10% FBS, 1% antibiotics-antimycotics, 1% L-alanyl-L-glutamine, and 50 nM β-mercaptoethanol. All cell lines were grown at 37°C and 5% CO_2; with the exception of PS cells (37°C without additional CO_2).

Transfection and plasmids

PolyJet *In Vitro* Transfection Reagent (SignaGen; #SL100688) was used for transfection. The procedure was carried out according to the manufacturer's protocol. For GFP and *Renilla* luciferase expression, the mammalian expression vectors phMGFP (Promega) and pRL-CMV (Promega) were used, respectively. The wt viperin mammalian expression vector was a kind gift from Lisa F.P. Ng (Singapore Immunology Network, Agency for Science, Technology and Research (A* STAR), Singapore), in which the viperin gene with C-terminal c-myc tag is transcribed under the control of the CMV promoter [40].

119

Viruses and infection

Two representatives of the West-European TBEV subtype with different degrees of virulence were used–medium (Neudoerfl) and severe (Hypr). Both strains differ in their coding sequences by only 12 nonconservative amino acid substitutions [41], and in the length and structure of the 3´UTR [42]. When mice were infected peripherally, the Hypr strain exhibited pronounced neuroinvasiveness and caused shorter survival than strain Neudoerfl [41]. The low passage TBEV strain, Neudoerfl (fourth passage in suckling mice brains; GenBank accession no. TEU27495), was provided by Prof. F.X. Heinz (Medical University of Vienna, Austria) [43]. The low passage TBEV strain, Hypr (fourth passage in suckling mice brains; GenBank accession no. TEU39292), is available at the Institute of Parasitology, Biology Centre of CAS, České Budějovice, Czech Republic [44]. Viruses were handled under biosafety level 3 conditions.

TBEV was added to the cells one day post seeding. Cells were then incubated for 2 hours, washed with PBS, and finally fresh pre-warmed medium was added. Brain suspension from uninfected suckling mice was used as a negative control.

Virus titration

Viral titres were determined by plaque assay as described [45], with minor modifications. Briefly, PS cell monolayers ($9x10^4$ cells per well) were grown in 24-well plates and incubated with 10x serial dilutions of infectious samples for 4 hours at 37˚C. The samples were then covered by 1:1 (v/v) overlay mixture (carboxymethyl cellulose and 2x L15 medium including 6% NCS, 2% antibiotics-antimycotics, and 2% L-glutamine). After five days, medium with overlay was removed, cells washed with physiological solution, subsequently fixed and stained (0.1% naphthalene black in 6% acetic acid solution) for 45 minutes. Virus-produced plaques were counted, and titres are stated as PFU/ml.

Antibodies and reagents

The following primary antibodies were used: anti-TBEV C polyclonal antibody (produced in-house), anti-TBEV NS3 polyclonal antibody (a kind gift from Dr. M. Bloom, NIAID, USA), anti-HPRT1 Polyclonal Antibody (Thermo Fisher Scientific; #PA5-22281), anti-GAPDH Antibody [EPR16891] (Abcam; #ab181602), Monoclonal Antibody to Mouse Viperin (Hycult Biotech; #HM1016), anti-NPM1 Monoclonal Antibody FC-61991 (Thermo Fisher Scientific; #MA1-1560), and anti-POLR1A Antibody (Abcam; ab222065). The following secondary/tertiary antibodies were used: HRP Goat Anti-Guinea Pig (Novex; #A18769), HRP Rabbit Anti-Chicken IgY (H+L) Secondary Antibody (Thermo Fisher Scientific; #A16130), HRP Horse Anti-Mouse IgG Antibody (VectorLabs; #PI-2000), HRP Goat Anti-Rabbit IgG Antibody (VectorLabs; #PI-1000), Biotinylated Anti-Streptavidin Antibody (VectorLabs; #BA-0500), AP-conjugated Streptavidin (VectorLabs; #SA-5100), Streptavidin-DyLight 549 (VectorLabs; Cat#SA-5549), Goat Anti-Rabbit IgG-DyLight 594 (Abcam; #ab96897), Goat Anti-Guinea Pig DyLight 594 (Abcam; #ab150188), and Goat Anti-Chicken IgY H&L-DyLight 488 (Abcam; #ab96947).

L-azidohomoalanine (Click Chemistry Tools; #1066–25) and 5-ethynyl-uridine (Click Chemistry Tools; #1261–25) were used for metabolic labelling of nascent proteins or RNA, respectively. Biotin-PEG4-Alkyne (Click Chemistry Tools; #TA105-25) and Biotin Picolyl Azide (Click Chemistry Tools; #1167–25) were used for subsequent detection of incorporated L-azidohomoalanine or 5-ethynyl-uridine, respectively. Cycloheximide was purchased from Sigma-Aldrich (#01810-1G).

120

Flow cytometry analysis

DAOY cells were seeded one day prior to infection in the 12-well plate at a density of 2.5×10^5 cells/well. At the indicated time intervals post-TBEV infection, cells were washed with PBS, trypsinized, and fixed by 4% paraformaldehyde in PBS (Roth). After permeabilization (0.1% Triton X-100), cells were stained using guinea pig anti-TBEV C antibodies (1:1500 dilution) and anti-guinea pig DyLight 594 (1:500 dilution) secondary antibodies. Flow cytometry was performed on a FACS Canto II cytometer and data analysed using FACS DIVA software v. 5.0 (BD Biosciences).

RNA isolation

Total cellular RNA was isolated using Trizol-based RNA Blue reagent (Top-Bio; #R013) according to the manufacturer's instructions. RNA pellets were dissolved in DEPC-treated water and directly used for either real-time PCR or analysis on an RNA denaturing gel.

rRNA quantification

The quantity and integrity of rRNA in total RNA samples were analysed on a 2100 Bioanalyzer using Agilent RNA 6000 Nano kit (Agilent Technologies; #5067–1511). The concentration of each sample was determined spectrophotometrically prior the Bioanalyzer measurement and samples were diluted according to the cell number ratio (resulting concentrations were between 10–20 ng/μl). 1 μl of the diluted RNA samples was loaded on the Bioanalyzer chip and the electrophoretic assay was performed according to the manufacturer's instructions. All samples were analysed in technical triplicates. 1.2% agarose MOPS-buffered denaturing gel (with 6.7% formaldehyde) was used for fractionation of isolated total RNA. RNA was visualised by addition of the GelRed dye (Biotium) into the gel. The signal was subsequently quantified using Fiji software.

Sample standardisation

We observed that the viability of TBEV Hypr-infected cells was negatively affected at 36 and 48 hours p.i. (Fig 1D). Therefore, in order to diminish the effect of this phenomenon on our data, we decided to standardise in our experiments to cell counts.

Normalisation to cell numbers was performed for real-time PCR, western blotting, northern blotting, and metabolic labelling analyses. For this, we established a viability-based method using alamarBlue reagent (Thermo Fisher Scientific; #DAL1025). Our data demonstrate that viability measurement is directly proportional to the cell number, and therefore this method is fully suitable for normalisation to the cell number (S1 Fig). The procedure was performed according to the manufacturer's instructions. Briefly, cells were washed with PBS and fresh pre-warmed growth medium with diluted alamarBlue reagent was added (1:10 dilution ratio; v/v). Cells were incubated for 2–2.5 hours and fluorescence of the reduced product was measured on a BioTek plate reader (λ_{ex} = 550 nm; λ_{em} = 590 nm). Growth medium with alamarBlue without cells was used as a blank. All samples were analysed in technical triplicates. Average fluorescence values for TBEV-treated sample were normalized to the respective mock control cells. The viability factor (f) was subsequently used as a normalisation factor for the calculation of RNA/protein input based on the pre-set mock control input.

$$f = \frac{viability_{sample}[a.u.]}{viability_{control}[a.u.]} \qquad\qquad V_{sample}[\mu l] = \frac{V_{control}[\mu l]}{f}$$

121
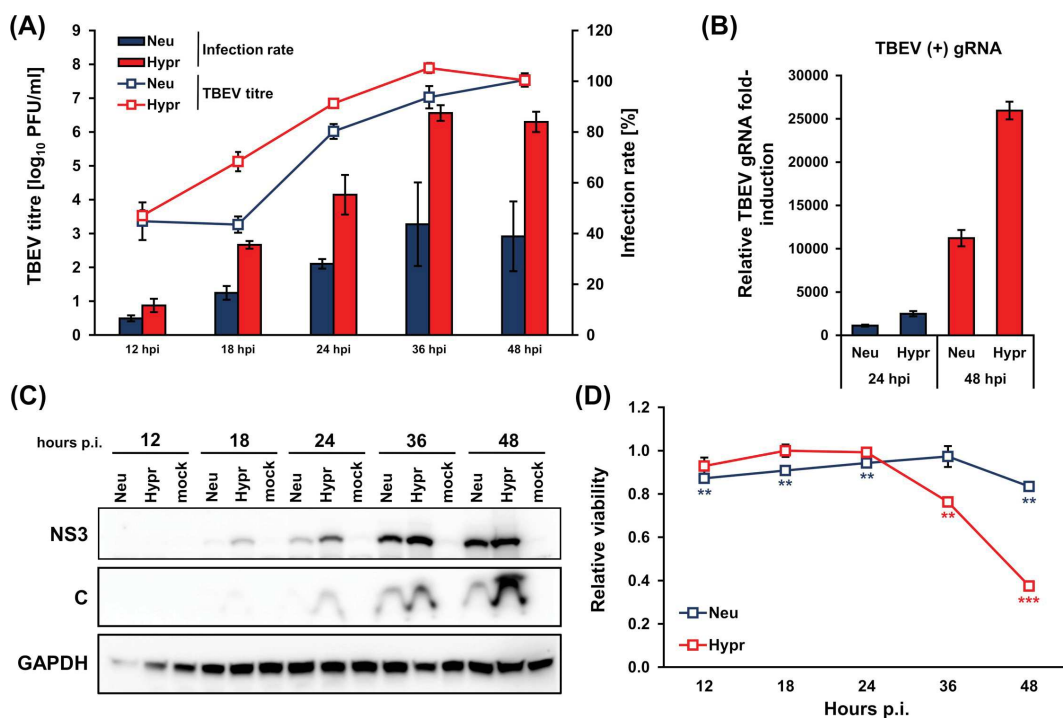
Fig 1. Characterization of TBEV Hypr and Neudoerfl infection kinetics in DAOY cells. DAOY cells were infected with TBEV Neudoerfl or Hypr strain (MOI 5). (A) Viral titres (indicated in trend lines) determined by plaque assay on PS cells and infection rate (indicated in bars) determined by flow-cytometric detection of TBEV C-stained cells were analysed at 12, 18, 24, 36, 48 hours p.i. Graphical summary of three independent experiments is shown with values expressed as mean with SEM. (B) Total RNA was isolated at 24 and 48 hours p.i. and relative qPCR quantification of TBEV gRNA using Δ-c_t method with normalisation to cell number was performed. Data are summary of three independent experiments and values in graphs are expressed as mean with SEM. (C) Levels of TBEV NS3 and C proteins in infected DAOY cells were determined by immunoblotting at 12, 18, 24, 36, 48 hours p.i. Data are summary of three independent experiments. (D) Viability of infected cells was determined using alamarBlue reagent, at the indicated time intervals p.i. Data are summary of three independent experiments and values are expressed as mean with SEM, normalised to mock infected cells; significant difference from control was calculated by unpaired Student's t-test (** $P<0.01$; *** $P<0.001$).

Real-time qPCR

For real-time qPCR analyses, the KAPA SYBR FAST Universal One-Step qRT-PCR Kit was used according to the manufacturer's protocol. Data obtained were processed via relative quantification using the delta c_t (Δ-c_t) method; the amount of RNA was adjusted to the cell number instead of the c_t values of the housekeeping reference gene. All samples were treated with dsDNase and subsequently 5× diluted in RNAse-free water before the real-time PCR analysis. All samples were analysed in technical triplicates. List of primers used can be found in S1 Table.

Western blotting

Cells were washed with PBS and RIPA buffer (25 mM Tris-HCl pH 7.6, 150 mM NaCl, 1% NP-40, 0.1% SDS, 1% sodium deoxycholate) with protease inhibitors (Thermo Fisher

122

Scientific; #78430) was added. Cell lysis was performed for 15 minutes on ice while gently shaking. Sonicated and cleared protein lysates in RIPA buffer were separated on 12% denaturing polyacrylamide gels and blotted onto PVDF membranes. The quantity of proteins was normalised to the cell number. Membranes were blocked (5% skimmed milk in PBS-T) and incubated with primary, secondary, and alternatively also tertiary antibodies; between each staining step, membranes were washed three times in PBS-T. Primary antibodies used were guinea pig anti-C (produced in-house; 1:1500), chicken anti-NS3 (M. Bloom laboratory; 1:5000), rabbit anti-GAPDH (Abcam; 1:1000), anti-HPRT1 (Thermo Fisher Scientific; 1:500), anti-viperin (Hycult Biotech; 1:500). Secondary/tertiary antibodies used were goat anti-rabbit HRP (VectorLabs; 1:1000), rabbit anti-chicken HRP (Thermo Fisher Scientific; 1:1000), and horse anti-mouse HRP (VectorLabs; 1:1000). Chemiluminescent signal was developed using either Novex CDP-Star kit for alkaline phosphatase (Thermo Fisher Scientific) or WesternBright Quantum kit for horseradish peroxidase (Advansta; #K-12042-D20). The signal was subsequently quantified using Fiji software [46]. For stripping of antibodies, membranes were incubated with stripping solution (62.5 mM Tris HCl pH 6.8, 2% SDS, 0.8% β-mercaptoethanol) for 45 minutes at 50°C. Subsequently, membranes were extensively washed six times with PBS. Following this, membranes were blocked, and immunostaining was again performed as described above.

Luciferase assay

For analyses of *Renilla* luciferase activity in CHX-treated cells, *Renilla* Luciferase Assay Kit from Promega (#E2810) was used according to the manufacturer's instructions. Briefly, 5×10^4 DAOY cells per well were seeded on a 96-well plate. Cells were transfected with 100 ng of pRL-CMV vector per well using PolyJet transfection reagent and incubated with cycloheximide (50–300 μg/ml) for 2, 4, 6, 14, and 24 hours. At 24 hours post-transfection, the viability of cells was measured using alamarBlue. Subsequently, cells were lysed and *Renilla* luciferase activity was determined.

Metabolic labelling of *de novo* synthesised proteins

Cells were seeded in 6-well plates at a density of 1×10^6 (Vero, A549) or 5×10^5 (DAOY, MG-63) cells per well. At indicated time intervals p.i., cells were washed with PBS and starved for 1 hour by addition of complete methionine-free RPMI medium (methionine-free RPMI medium containing 10% FBS, 1% L-alanyl-L-glutamine, 1% antibiotics/antimycotics, and 0.27 mM L-cystine). Subsequently, fresh complete methionine-free RPMI medium was added with 50 μM L-azidohomoalanine (AHA) and 1× AlamarBlue reagent. Metabolic labelling with AHA was performed for 2 hours. Afterwards, cell viability was measured as described earlier. Cells were then washed with PBS and lysed on ice for 15 minutes in 200 μl RIPA buffer with protease inhibitors (Halt Protease Inhibitor Single-Use Cocktail; Thermo Fisher Scientific). Lysates were separated on 12% polyacrylamide gels and transferred by electroblotting onto the PVDF membrane. The quantity of proteins loaded onto the gel was normalised to the cell numbers. Subsequently, the modified detection method Click-on-membrane was performed according to Kočová et al. (in preparation). Briefly, membranes were washed in 0.1 M potassium phosphate buffer pH 7.0 and the Click reaction was performed as follows: membranes were incubated in Click reaction buffer (0.1 M potassium phosphate buffer pH 7.0 with 0.25 mM sodium ascorbate, 0.5 mM THPTA, 0.1 mM $CuSO_4$, and 10 μM biotin-alkyne) for 1 hour in the dark at room temperature. Membranes were washed three times with PBS, blocked (5% skimmed milk in PBS-T) and incubated with primary (AP-streptavidin; VectorLabs; 1:500), secondary (biotinylated anti-streptavidin; VectorLabs; 1:1000) and tertiary antibodies (AP-

streptavidin; VectorLabs; 1:2000). Between each staining step, membranes were washed three times in PBS-T. Chemiluminescence signal was developed using Novex CDP-Star kit (Invitrogen; #WP20002). Signal was subsequently quantified using Fiji software [46].

Metabolic labelling of *de novo* synthesised RNA

DAOY cells were seeded in 6-well plates at a density of 5×10^5 cells per well. At the indicated time intervals p.i., 5-ethynyl uridine (5-EU) was added to the cells (final concentration of 5-EU was 1 mM) as well as alamarBlue reagent. Metabolic labelling with 5-EU was performed for 2 hours. Cell viability was measured as described earlier. Cells were then washed with PBS and lysed using RNA Blue reagent. Total RNA was isolated according to the manufacturer's instructions. Next, RNA was separated in MOPS-buffered denaturing gel, as described above. The quantity of RNA was normalised to the cell number. Capillary blotting of RNA to the PVDF membrane (GE Healthcare) using 20× SSC buffering system was performed afterwards. Subsequently, the modified detection method Click-on-membrane was performed according to the method described by Kočová et. al. (in preparation). Briefly, the UV-fixed membrane was washed in 0.1 M potassium phosphate buffer pH 7.0 and the Click reaction on membrane was performed as follows: membranes were incubated in Click reaction buffer (0.1 M potassium phosphate buffer pH 7.0 with 0.25 mM sodium ascorbate, 0.5 mM THPTA, 0.1 mM $CuSO_4$, and 10 μM picolyl biotin azide) for 1 hour in the dark at room temperature. Blocking and triple labelling using biotin-streptavidin system was performed as described above. The chemiluminescence signal was developed using Novex CDP-Star kit (Invitrogen; #WP20002), and signal was subsequently quantified using Fiji software [46].

Immunofluorescence

DAOY cells were seeded in chamber slides (0,3 cm^2/well; 5×10^3 cells/well) and at the indicated time intervals p.i. processed as previously described [47]. Rabbit anti-POLR1A (Abcam; 1:200) and chicken anti-NS3 (a kind gift from Dr. M. Bloom, NIAID, NIH; 1:5000) antibodies were used. As the secondary antibodies, anti-rabbit DyLight 594 (Abcam; 1:500) and anti-chicken DyLight 488 (Abcam; 1:500), were used. In the case of metabolic labelling of nascent RNA, the Click reaction was performed *in situ* before the blocking step. 10 μM Picolyl biotin azide was used for the detection of incorporated 5-EU. For subsequent fluorescent labelling, streptavidin conjugated with DyLight 549 was used (VectorLabs; 1:500). Slides were eventually mounted in Vectashield mounting medium (VectorLabs). The Olympus Fluoview FV10i confocal microscope was used for imaging and subsequent export of images was done in FV10-ASW software (v.1.7).

Statistical analyses

All statistical analyses were performed in MS Excel using one-sample two-tailed Student's t-test. Only in case of qPCR analysis of over-expressed viperin and GFP, an unpaired two-tailed Student's t-test was used. In this case, datasets were first tested for the equality of variances by F-test. If the experiment was performed in technical replicates, the statistics was performed using the means of the independent biological replicates.

Results

TBEV infection reduces host protein production

Recent studies have shown that DENV decreases the rate of *de novo* protein synthesis in host cells [24, 48]. In order to establish whether TBEV also affects translation, *de novo* protein

124

synthesis kinetics was measured in TBEV-infected cells using Click chemistry [49]. For this purpose, we utilized a suitable *in vitro* experimental system of the cerebellum-derived human medulloblastoma cell line DAOY HTB-186 to broaden previous findings [47]. Two closely related members of the European subtype of TBEV with different virulence were used for comparative purposes: a medium virulent prototype strain, Neudoerfl, and a highly virulent strain, Hypr [41]. Initially, we characterized the course of infection for both TBEV strains. DAOY cells were infected at an MOI of 5 with either strain and at 12, 18, 24, 36, 48 hours p.i., replication kinetics, infection rate, viral protein (C, NS3) production and viability of infected cells were determined. Both strains successfully replicated in DAOY cells, with the Hypr strain reaching at least one order of magnitude higher titres during the course of infection until 48 hours p.i., when both strains eventually produced equal titres (Fig 1A). The infection rate was also considerably higher for the Hypr strain, culminating at 36 hours p.i. (87.5% of infected cells), whereas the Neudoerfl strain infected only 43.6% of cells (Fig 1A). Relative quantification of genomic RNA at 24 and 48 hours p.i. revealed that Hypr replicated with higher efficiency than Neudoerfl (Fig 1B). TBEV C and TBEV NS3 protein detection corresponded to replication kinetics and for both strains proteins could be detected earliest at 18 hours p.i., increasing thereafter (Fig 1C). While TBEV Neudoerfl affected the viability of the infected cells only mildly (maximal decrease by 16.6% at 36 hours p.i.), TBEV Hypr lowered the viability of the infected cells by 23.8% and 62.5% in comparison to mock-infected control at 36 and 48 hours p.i., respectively (Fig 1D). Therefore, in order to compensate the potential bias originating from cell death, we standardised our experiments to viability which is directly proportional to the number of living cells (S1 Fig). In the following experiments we pursued interaction of TBEV with DAOY cells during the period of productive infection for both TBEV strains, ranging from 24 to 48 hours p.i.

After this detailed characterization of our *in vitro* model, *de novo* protein synthesis and quantification was performed. DAOY cells were infected with either TBEV Hypr or Neudoerfl and metabolic labelling was carried out for 2 hours at 24, 36, and 48 hours p.i. using the methionine analogue L-azidohomoalanine (AHA). At 24 hours p.i., translation levels were comparable in control and infected cells, but infection resulted in a significant decrease of AHA-labelled proteins at 36 and 48 hours p.i. in TBEV Hypr-infected cells and at 48 hours p.i. in TBEV Neudoerfl-infected cells (Fig 2A and 2B; S2A Fig). Interestingly, the viral NS3 protein levels increased over the course of the infection with both strains (Fig 2A, lower panel). Furthermore, TBEV-induced host translational shut-off was also documented for cell lines of non-neural origin (A549 cells, Vero cells, and MG-63 cells) at 48 hours p.i., for both TBEV strains (Fig 2C; S2B Fig). Interestingly, despite the observed host translational shut-off both TBEV strains were able to replicate (Fig 1B) successfully and reached high titres (Fig 1A) in DAOY cells throughout the infection.

Since these experiments revealed a significant decrease in host protein synthesis upon TBEV infection on a global level, we evaluated the specificity of this for particular host proteins. First, the effect of TBEV infection on common housekeeping genes GAPDH and HPRT1 was determined by analysing their mRNA and protein levels. Relative quantification of GAPDH and HPRT1 mRNAs revealed a strong inhibition of expression for both genes and TBEV strains at 48 hours p.i. (Fig 3A and 3B; upper panel). Similar results were observed for their protein levels, although the more virulent strain Hypr elicited a stronger reduction (Fig 3A and 3B; lower panel).

As the subversion of host translation process can be used as an immune evasion strategy by viruses [17], we investigated the effect of translational shut-off on the interferon-inducible gene viperin. Viperin has been described so far as an antiviral protein that interferes with TBEV on multiple levels [50]. A time course of viperin mRNA production in response to

125
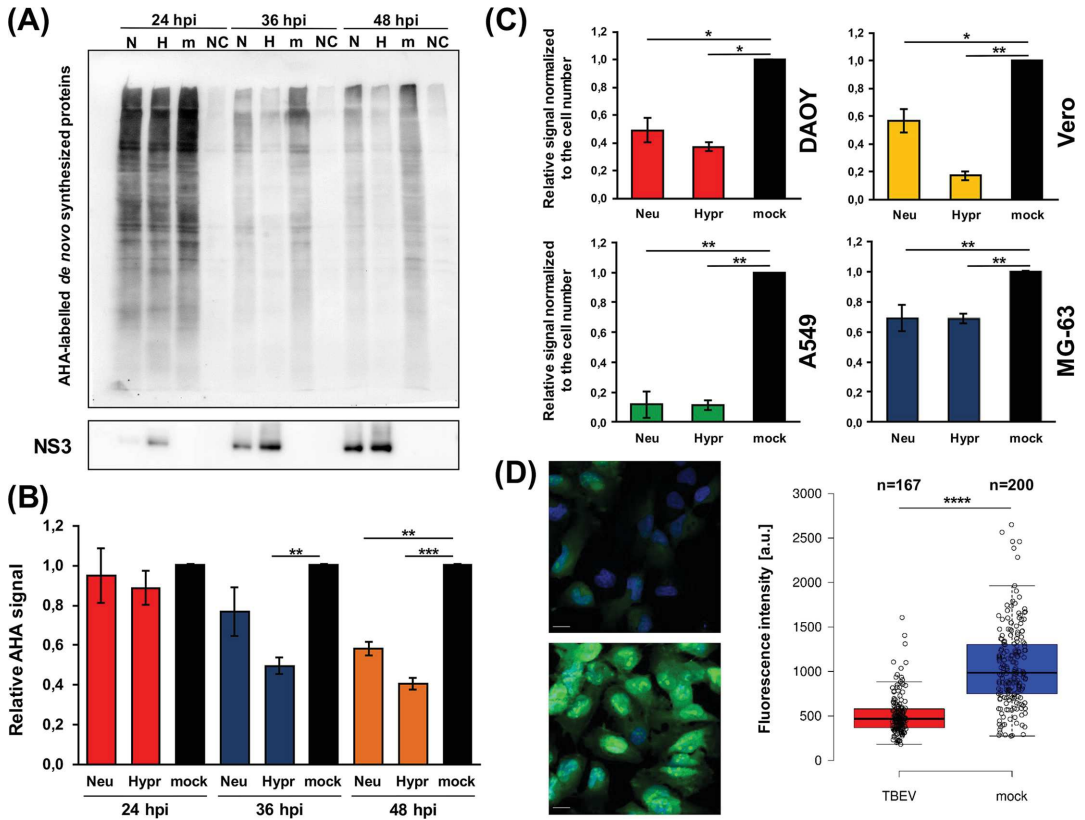
Fig 2. TBEV infection induces host translational shut-off. (A) DAOY cells were infected with TBEV Neudoerfl or Hypr strain (MOI 5) and *de novo* protein synthesis was assessed at 24, 36, and 48 hours p.i. by incorporation of methionine analogue L-azidohomoalanine (AHA). AHA-labelled proteins were visualised by immunodetection using HRP-conjugated antibodies; stripped membranes were subsequently used for the immunodetection of viral NS3 protein. Data are representative of three independent experiments; N–TBEV Neudoerfl strain (AHA-labelled), H–TBEV Hypr strain (AHA labelled), m–mock (AHA-labelled), NC–negative control (non-labelled). (B) Summary of *de novo* protein synthesis from (A) including all three performed experiments. Relative chemiluminescent signal was quantified using Fiji software and compared to mock-infected cells. Values were further normalised to the cell number and mock-infected cells were set to 1. Data are representative of three independent experiments and values are expressed as mean with SEM; significant difference from control was calculated by unpaired Student's t-test ($**$ P<0.01; $***$ P<0.001). (C) Summary of *de novo* protein synthesis rate in TBEV-infected DAOY, Vero, A549, and MG-63 cells. Cell lines were infected with either Neudoerfl or Hypr strain (MOI 5) and subsequently analysed for *de novo* protein synthesis at 48 hours p.i. Relative chemiluminescent signal was quantified using Fiji software and compared to mock-infected cells. Values were further normalised to the cell number and mock-infected cells were set to 1. Data are summary of three independent experiments and values are expressed as mean with SEM; significant difference from mock-infected cells was calculated by Student's t-test ($*$ P<0.05; $**$ P<0.01). (D) DAOY cells were infected with TBEV Hypr strain (MOI 5), and *de novo* protein synthesis was assessed at 36 hours p.i. by incorporation of methionine analogue L-azidohomoalanine (AHA). AHA-labelled proteins were visualised by Click reaction using AlexaFluor 488-conjugated alkyne. Representative images of TBEV-infected and control cells are shown on the left. Scale bar represents 100 µm. On the right, scatter plot is shown illustrating *de novo* protein synthesis rate measured by fluorescence intensity of the AlexaFluor 488 (fluorescence intensity per pixel; a.u.–arbitrary units). Data are representative of two independent experiments and values in graphs are expressed as mean, with whiskers extending to data points that are less than 1.5 x interquartile range away from 1st/3rd quartile (Tukey's boxplot); significant difference from mock-infected cells was calculated by Student's t-test ($****$ P<0.0001).

TBEV infection in DAOY cells was determined. Induction of viperin mRNA expression was detected at 24 hours p.i. and increasing throughout next 24 hours (Fig 3C; upper panel). Despite significantly increased viperin mRNA levels, none or very small amounts of viperin

126
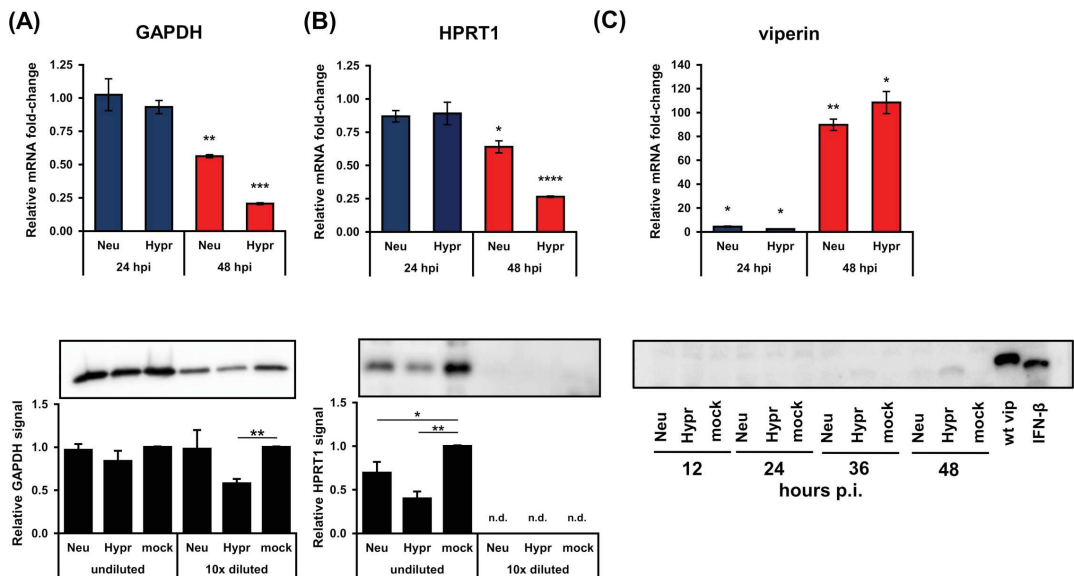
Fig 3. TBEV-induced translational arrest results in the decreased protein levels of GAPDH, HPRT1, and viperin. (A) Upper panel: DAOY cells were infected with either TBEV Neudoerfl or Hypr strain (MOI 5) and total RNA was isolated at indicated time intervals. Relative qPCR quantification of GAPDH mRNA using Δ-c_t method with normalisation to the cell number was performed. Lower panel: DAOY cells were infected with either Neudoerfl or Hypr TBEV strain (5 MOI) and lysed at 48 hours p.i. Western blot analysis of GAPDH protein levels was performed using protein-specific antibodies with undiluted and 10-times diluted samples. Relative chemiluminescent signal was quantified using Fiji software and compared to mock-infected cells. Values were further normalised to the cell number. Data are summary of three independent experiments and values in graphs are expressed as mean with SEM. Significant difference from mock-infected cells was calculated using one-sample Student's t-test (** $P<0.01$; *** $P<0,001$). (B) Upper panel: DAOY cells were infected with either TBEV Neudoerfl or Hypr strain (MOI 5) and total RNA was isolated at indicated time intervals. Relative qPCR quantification of HPRT1 mRNA using Δ-c_t method with normalisation to the cell number was performed. Lower panel: DAOY cells were infected with either Neudoerfl or Hypr TBEV strain (5 MOI) and lysed at 48 hours p.i. Western blot analysis of HPRT1 protein levels was performed using protein-specific antibodies with undiluted and 10-times diluted samples. Relative chemiluminescent signal was quantified using Fiji software and compared to mock-infected cells. Values were further normalised to the cell number. Data are summary of three independent experiments and values in graphs are expressed as mean with SEM. Significant difference from mock-infected cells was calculated using one-sample Student's t-test (* $P<0.05$; ** $P<0.01$; **** $P<0,0001$); n. d.–not detected. (C) Upper panel: DAOY cells were infected with either TBEV Neudoerfl or Hypr strain (MOI 5) and total RNA was isolated at the indicated time intervals. Relative qPCR quantification of viperin mRNA using Δ-c_t method with normalisation to the cell number was performed. Data are summary of three independent experiments and values are expressed as mean with standard error of mean (SEM). Lower panel: Immunodetection of viperin protein in TBEV-infected DAOY cells at indicated intervals p.i. (MOI 5). As a positive control, cells transfected with a c-myc-tagged viperin expression plasmid (wt vip) and cells treated with IFN-β (12 hours; 50 ng/ml) were used.

protein were detected in cell lysates from TBEV-infected DAOY cells by western blot analysis (Fig 3C; lower panel). As a positive control, DAOY cells treated with INF-β (12 hours; 50 ng/ml) as well as DAOY cells transfected with a human viperin expression vector [40] were used.

To assess whether the effect of TBEV on endogenous viperin production can be overcome by artificial over-expression, DAOY cells were first infected (TBEV Neudoerfl and Hypr; MOI 5) and subsequently transfected with a wt-viperin expression construct at 12 hours p.i. Viperin mRNA, as well as protein levels, were analysed at 12 hours post-transfection (S3A Fig). As a control, GFP expression construct was used. S3B Fig shows that viperin protein was produced; however, the protein levels were significantly reduced in TBEV-infected cells compared to control cells. Hypr strain infection also resulted in a statistically significant decrease in mRNA levels of viperin. As expected, GFP production in TBEV infected cells was negatively affected in case of both TBEV strains (S3C Fig). Again, Hypr strain infection also caused a significant

127
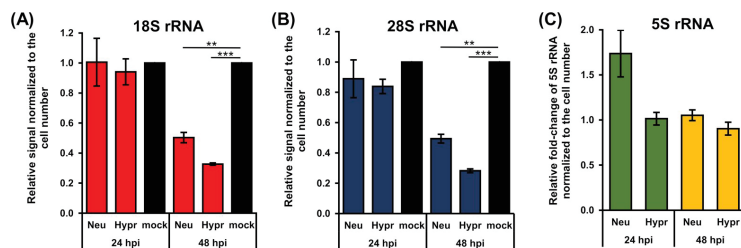
Fig 4. TBEV infection decrease levels of 18S and 28S rRNA but not 5S rRNA. (A, B) Total RNA was isolated from TBEV-infected DAOY cells (24 and 48 hours p.i.; MOI 5) and analysed using Bioanalyzer 2100. Graphs represent relative mean of areas for 18S (a) and 28S (b) peaks compared to mock-infected cells. Values were further normalised to the cell number. Data are representative of three independent experiments and values are expressed as mean with SEM. Significant difference from mock-infected cells was calculated using one-sample Student's t-test (** $P<0.01$; *** $P<0,001$). (C) Relative quantification of 5S rRNA in TBEV-infected DAOY cells at 24 and 48 hours p.i. (MOI 5) using the Δ-c_t method. Graph represents relative fold-induction of 5S rRNA levels in comparison to mock-infected cells with normalisation to cell number. Data are representative of three independent experiments and values are expressed as mean with SEM.

https://doi.org/10.1371/journal.pntd.0007745.g004

decrease in GFP mRNA. Consequently, TBEV induces a general translational shut-off, which can negatively affect even the production of overexpressed transcripts. Nevertheless, viral titres were increasing throughout the infection (Fig 1).

TBEV infection downregulates the levels of specific host rRNAs

Previous data revealed a significant decrease in RNA encoding genes including 5.8S rRNA and 7SL RNA following TBEV infection [47]. Here, we verified the link between the TBEV-induced translational shut-off and production of host rRNAs. We quantified the levels of 18S and 28S rRNAs in total cellular RNA from TBEV-infected DAOY cells at 24 and 48 hours p.i. We found that infection by both TBEV strains significantly decreased the 18S and 28S rRNA (S4 Fig). 18S rRNA levels decreased to $50 \pm 6\%$ or $33 \pm 1\%$ for TBEV Neudoerfl- or Hypr-infected cells compared to controls, respectively (Fig 4A). For 28S rRNA, its transcription levels fell to $49 \pm 5\%$ or $28 \pm 2\%$ for TBEV Neudoerfl- or Hypr-infected cells, respectively (Fig 4B). Both 18S and 28S rRNAs are transcripts of POLR1. Interestingly, the POLR3 transcript 5S rRNA levels remained unaffected by TBEV infection (Fig 4C). These data imply that the effect of TBEV infection on host cells also involves the transcription of specific ribosomal RNA genes.

TBEV interferes with *de novo* production of 45-47S pre-rRNA transcripts

In order to elucidate at which step TBEV interferes with rRNA production, we first analysed the integrity of mature rRNA molecules. No degradation products were observed following infection with either TBEV strains at 24 or 48 hours p.i. in DAOY cells (Fig 5A and 5B). Next, we investigated the rRNA expression and processing via quantification of *de novo* synthesised RNA in TBEV-infected DAOY cells. We labelled nascent RNA in TBEV-infected DAOY cells at 24, 36 and 48 hours p.i. with 5-ethynyl uridine (EU). Incorporated EU was visualised using Click chemistry and the biotin-streptavidin detection system. The presence of TBEV Hypr strain resulted in a decreased quantity of 45-47S pre-rRNA transcripts at 36 and 48 hours p.i., whereas infection with TBEV Neudoerfl strain reduced *de novo* synthesis of 45-47S pre-rRNA at 48 hours p.i. (Fig 5C).

128
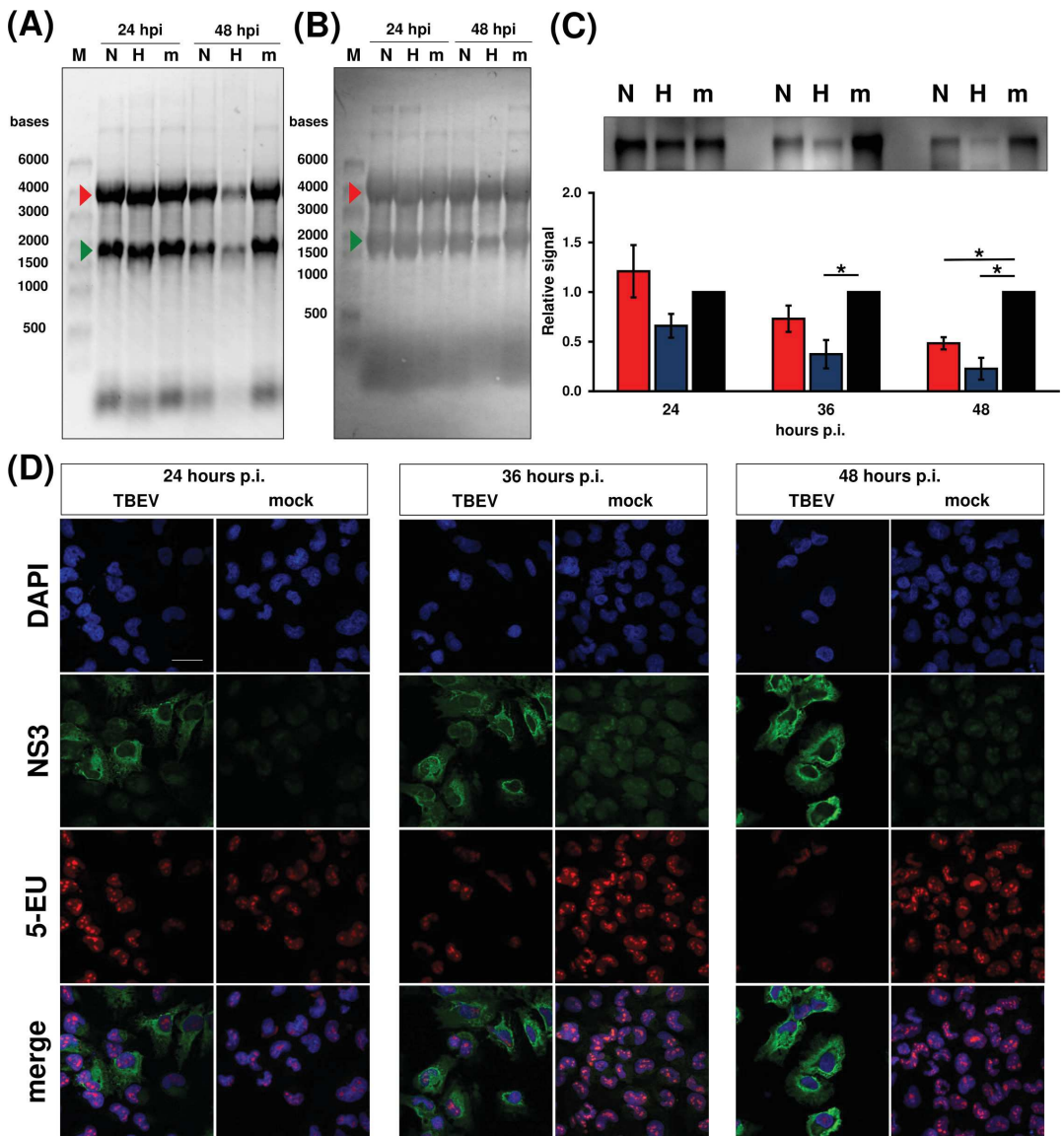
Fig 5. TBEV infection results in decrease of *de novo* synthesised 45-47S pre-rRNA. DAOY cells were either infected with Neudoerfl (N) or Hypr strain (H) at MOI 5 or mock-infected (m). Total RNA was isolated at indicated time post infection; 5-ethynyl uridine (1 mM) was added 2 hours before the collection interval. Data are representative of three independent experiments. (A) Integrity of 28S (red arrow) and 18S rRNA (green arrow), evaluated by using in-gel staining with GelRed. (B) Integrity of 28S (red arrow) and 18S rRNA (green arrow), evaluated by methylene blue staining after capillary transfer on PVDF membrane. (C) Upper panel: metabolic labelling of nascent 45-47S pre-rRNA was carried out using Click chemistry and biotin picolyl azide (10 μM) with subsequent chemiluminescent visualisation via biotin-streptavidin-alkaline phosphatase system. Lower panel: values are expressed as mean of three independent experiments with SEM. Significant difference from mock-

129

infected cells was calculated using one-sample Student's t-test (* $P<0.05$). (D) *In situ* metabolic labelling revealed TBEV-induced reduction of nascent RNA at 36 hours p.i. without change in RNA localization. DAOY cells were infected with TBEV Hypr strain (MOI 5) and at indicated time intervals incubated for 2 hours with 1 mM 5-ethynyl uridine (5-EU) in order to label nascent RNA. Detection of incorporated 5-EU was performed by Click reaction using 10 μM biotin picolyl azide followed by fluorescent labelling with streptavidin-DyLight549. Cells were co-stained with anti-NS3 antibodies; signal was further visualised using anti-chicken DyLight488 antibodies. Nuclei were stained with DAPI. Scale bar represents 200 μm.

Previously, a link between the inhibition of expression of 45-47S pre-rRNA and nucleolar stress was documented [31]. There are several hallmarks typical for nucleolar stress including disruption of nucleolus structure [51]. We, therefore, characterised the localization and production of nascent RNA at the cellular level and also investigated the structure of the nucleolus. DAOY cells infected with TBEV Hypr strain were analysed at 24, 36, and 48 hours p.i. using *in situ* Click reaction with 10 μM picolyl biotin azide and subsequent visualisation *via* streptavidin conjugated with DyLight-549. As shown in Fig 5D, the overall production of nascent RNA in TBEV-infected cells started to decrease from 36 hours p.i.; *de novo* synthesised RNA was exclusively detected in nuclei with foci of nascent RNA molecules localised in nucleoli. In addition, these nascent RNA foci were not structurally altered upon TBEV infection. The specificity of the labelling reaction was determined using EU-unlabelled cells in the Click reaction (S5A Fig). In order to further verify that TBEV did not induce nucleolar re-arrangement due to nucleolar stress, we analysed the nucleolar structure upon TBEV Hypr infection using nucleophosmin (NPM1; a nucleolar marker). As a positive control, cells were treated with 1 mM H_2O_2 for 45 minutes. No disruption of nucleoli in TBEV-infected cells was observed (S5B Fig). These data imply that TBEV inhibits 45-47S pre-rRNA production without triggering the nucleolar stress pathway.

TBEV infection affects POLR1 levels but not nucleolar localisation

Based on the observed TBEV interference with rRNA production on the transcriptional level, we sought to investigate if the levels and cellular localization of POLR1 changes in infected cells. As shown in Fig 6A and 6B, POLR1 was localised exclusively to the nuclei, and no translocation occurred in infected cells at any time interval tested. Nevertheless, POLR1 protein levels were impaired in TBEV Hypr-infected cells at 48 hours p.i. This may be a result of the previously mentioned translational shut-off since it coincided at 48 hours p.i. Besides, POLR1 mRNA levels were negatively affected by TBEV infection, too (Fig 6C). In particular, POLR1A (the largest subunit of the RNA polymerase I complex) mRNA levels dropped to 60 ± 5% or 25 ± 1% in TBEV Neudoerfl- or Hypr-infected DAOY cells at 48 hours p.i., respectively.

TBEV-induced translational shut-off and the decrease in production of nascent 45-47S pre-rRNA raised the question whether these processes are casually interconnected. We analysed the rate of rRNA production in DAOY cells after treatment with cycloheximide (CHX), an inhibitor of translation elongation. First, we determined the time- and dosage-dependent effect of CHX in DAOY cells using a *Renilla* (RL) luciferase-based reporter system. DAOY cells were first transfected with pRL-CMV and treated with CHX (50, 100, and 300 μg/ml). As shown in S6 Fig, all CHX concentrations tested decreased the production of luciferase. Moreover, the inhibition rate of luciferase production increased with longer exposure to CHX. Next, rRNA production in DAOY cells with decreased translational rate was assessed. Cells were treated with CHX (100 μg/ml) for 6 or 14 hours and *de novo* RNA synthesis in CHX-treated cells was subsequently determined. Fig 7A shows a statistically significant decrease in levels of nascent 45-47S pre-rRNA for both intervals. In particular, the levels decreased to 22 ± 9% or 56 ± 16% during CHX treatment for 14 or 6 hours, respectively. In addition, total levels of mature 18S and 28S rRNAs were quantified in CHX-treated cells. Significant

130
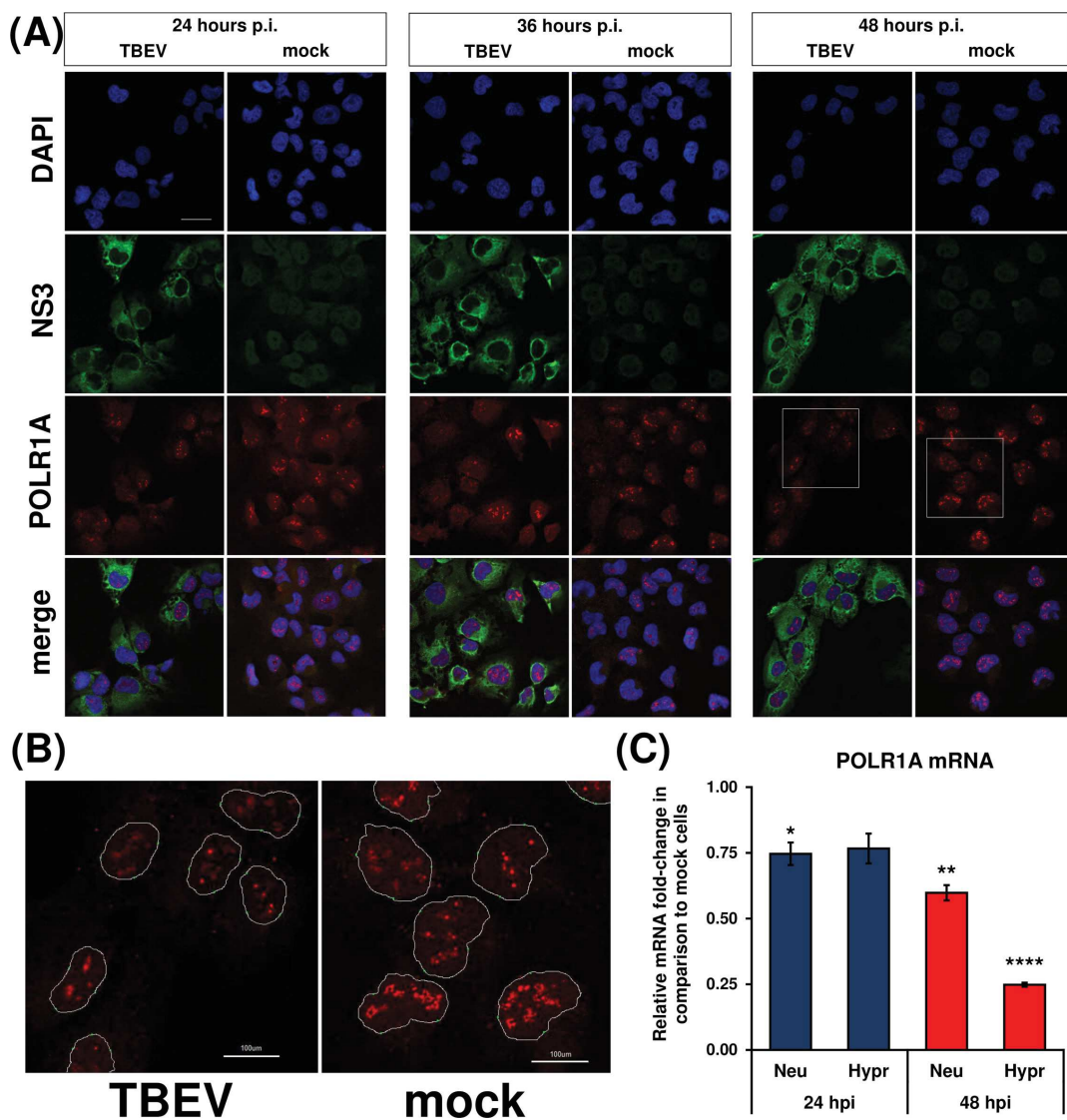
Fig 6. RNA polymerase I is not translocated upon TBEV infection. (A) DAOY cells were infected with TBEV Hypr strain (MOI 5) and at indicated time intervals fixed and POLR1A was detected using rabbit anti-POLR1A and anti-rabbit DyLight594 antibodies. Cells were further co-stained for viral NS3 protein using chicken anti-NS3 and anti-chicken DyLight488 antibodies. Nuclei were stained with DAPI. Scale bar represents 200 µm. (B) Zoomed images from panel (A) at 48 hours p.i. (areas marked by the white squares); POLR1 is localised in distinct foci in host nuclei without any observable virus-induced translocation. Scale bar represents 100 µm. (C) DAOY cells were infected with either TBEV Neudoerfl or Hypr strain (MOI 5) and total RNA was isolated at indicated time intervals. Relative qPCR quantification of POLR1A mRNA using Δ-c_t method with normalisation to the cell number was performed. Data are representative of three independent experiments and values are expressed as mean with SEM. Significant difference from mock-infected cells was calculated using one-sample Student's t-test (* P<0.05; ** P<0.01; **** P<0,0001).

131
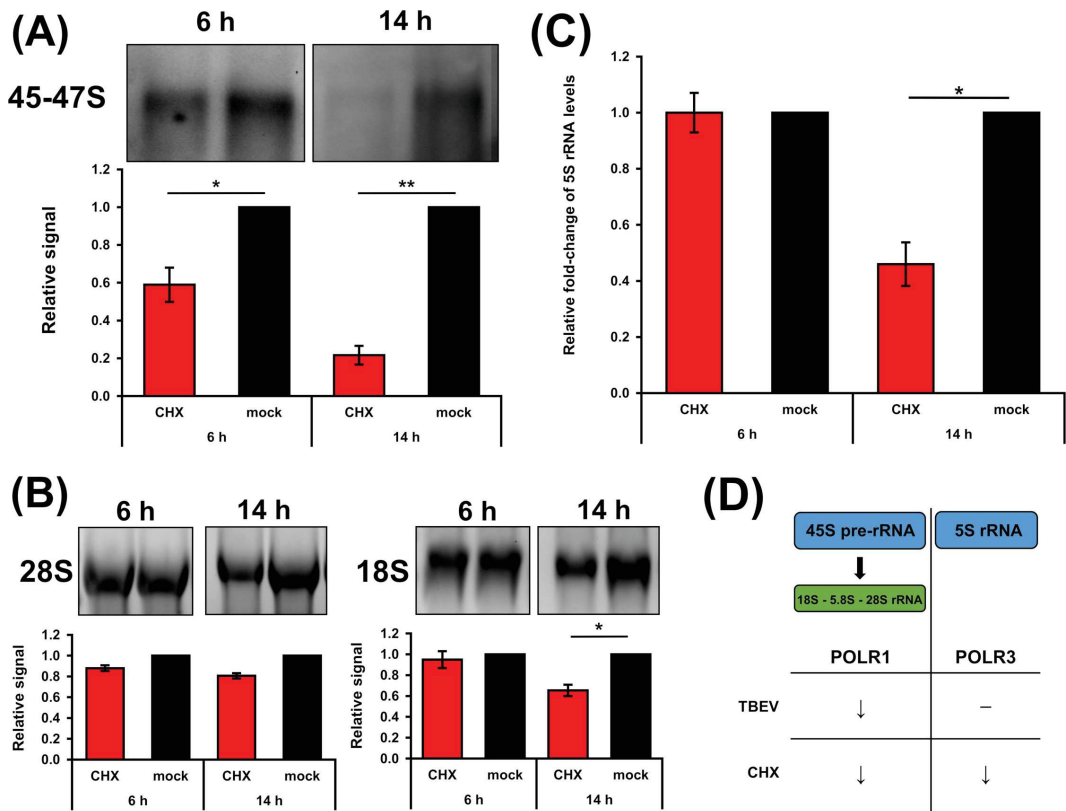
Fig 7. Cycloheximide (CHX) treatment decreases production of rRNA transcripts by POLR1 and POLR3. (A) DAOY cells were treated with CHX (100 μg/ml) for either 6 or 14 hours; for metabolic RNA labelling, 5-EU was added 2 hours before the sample collection. Cell viability was measured before the cell lysis. Isolated total RNA was transferred to a PVDF membrane and nascent RNA quantified using Click chemistry with 10 μM biotin picolyl azide before subsequent chemiluminescent detection. Data are representative of three independent experiments and values in graphs are expressed as mean with SEM, normalised to cell numbers and mock infected cells. Significant difference from the control was calculated using one-sample Student's t-test (* $P<0.05$; ** $P<0.01$). (B) Levels of 28S and 18S rRNA were analysed by in-gel RNA staining with GelRed before blotting. Data are representative of three independent experiments and values in graphs are expressed as mean with SEM, normalised to cell number and mock infected samples. Significant difference from the control was calculated using one-sample Student's t-test (* $P<0.05$). (C) Relative quantification of 5S rRNA in CHX-treated DAOY cells (6 and 14 hours post treatment; 100 μg/ml) using the Δ-c_t method. Graph represents relative fold-induction of 5S rRNA levels in comparison to mock-treated cells, with normalisation to cell number. Data are representative of three independent experiments and values are expressed as mean with SEM. Significant difference from the control was calculated using one-sample Student's t-test (* $P<0.05$). (D) Schematic summary of CHX versus TBEV effect on the expression of POLR1 and POLR3 transcripts. (↓) indicates observed decrease of the RNA levels and (—) indicates no change in RNA levels.

decreases in 18S rRNA levels were observed after a 14-hour incubation (65 ± 9%; Fig 7B). 28S rRNA levels were reduced to 81 ± 4% compared to control cells; however, this effect was not statistically significant (Fig 7B). Quantification of 5S rRNA, a POLR3 transcript, revealed a statistically significant decrease even for this rRNA species after 14 hours of CHX treatment (46 ± 11%; Fig 7C). These data demonstrated that during translation inhibition induced by CHX, the quantity of rRNA transcripts of both RNA polymerases (POLR1 and POLR3) were

132

decreased. In comparison to the general rRNA synthesis shut-down resulting from the action of CHX, TBEV infection induced only a decrease in POLR1 rRNA transcripts (Fig 7D). This suggests that TBEV infection specifically targeted POLR1, which may subsequently result in translational shut-off.

Discussion

TBEV infection is spreading through Europe, resulting in increased numbers of TBEV cases and emergence in previously unaffected areas. TBEV is known to be able to cause neurological symptoms in some infected patients, though little is known about its interplay with neural cells. The molecular basis of damage to the CNS following TBEV infection is still not fully understood. So far, it seems that it is a complex phenomenon combining multiple factors including host immune system [52]. Therefore, understanding the TBEV interaction with target cells and detailed description of processes of viral or host response can help to reveal new targets and ideas on how to treat this disease more successfully. To what extent the outcome of these infection-induced processes is reflected on longer term sequelae remains unrevealed.

Metabolic labelling experiments demonstrated that TBEV infection interferes with the global *de novo* protein synthesis in infected cells. Surprisingly, the effect of translational arrest was so robust that even the protein levels of two commonly used housekeeping genes, GAPDH and HPRT1, were significantly lowered (Fig 3A and 3B). Cell lines of both neural and non-neural origin underwent translational shut-off, demonstrating thus the general nature of this phenomenon upon TBEV infection. However, the rate of reduction varied substantially in individual cell lines suggesting cell-dependent effects. TBEV Hypr strain caused a greater translational shut-off in all cell lines compared to the Neudoerfl strain. This may be due to the increased virulence and neuroinvasiveness of the Hypr strain [53] or due to susceptibility and tropism of the virus strains to specific cell types. Recent studies have demonstrated that some flaviviruses can cause translation suppression via diverse mechanisms [24, 48]. These findings together with our results revise the idea of flaviviruses as "non-host cell protein synthesis influencers" [25, 54, 55]. Indeed, flaviviruses have been thought to avoid the host-cell protein synthesis shut-off as they replicate at a slower rate and global protein synthesis manipulation might have potentially deleterious effects on cell viability and virus yields [56, 57]. However, reduced synthesis of host proteins had no adverse effect on the production of viral NS3 and C proteins (Fig 1C), viral gRNA (Fig 1B) or production of viral progeny (Fig 1A). This suggests that protein synthesis shut-off does not stop TBEV from successful replication.

Viperin is a known interferon-stimulated gene (ISG) and has been described as a potent antiviral protein against members of the *Flaviviridae* family, especially TBEV [50, 58–61]. Thereby it is anticipated to see an increase in viperin mRNA levels upon TBEV infection in DAOY cells. However, the absence of endogenous viperin protein in TBEV-infected cells is surprising. Thus, translational shut-off may yield multiple advantages to TBEV. Apart from gearing the host protein synthesis apparatus to the purposes of the virus, it may also perform as an immune evasion strategy by preventing ISG production. A widely used stable overexpression approach in an ISG/viperin study [59] might therefore mask the real interactions among flaviviruses and host cells during the infection. In general, our data highlight the importance of careful experimental design when studying virus-host interactions and ISG function specifically.

To our knowledge virus-driven reduction in host rRNA levels has not been described before for any flavivirus. Only scarce information is available regarding the virus-induced reduction of rRNA expression, production, and maturation. For example, murine hepatitis virus directly reduces the levels of mature 28S rRNA [62]; *Autographa californica* multiple

133
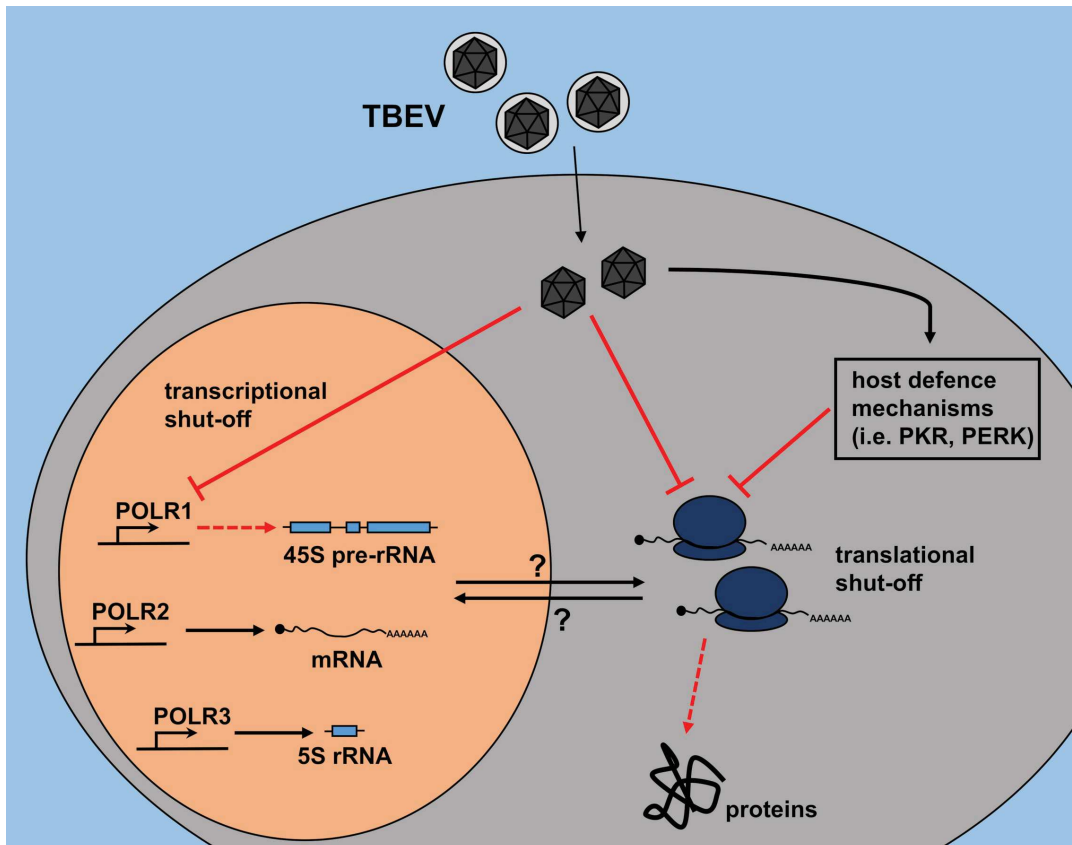
Fig 8. Schematic overview of potential pathways leading to TBEV-driven decrease in synthesis of host rRNA and proteins. TBEV may interfere directly with host translational processes, leading to decreased host protein levels. This decrease could negatively affect pre-rRNA synthesis and eventually rRNA levels. On the other hand, TBEV may also interfere directly with the synthesis of pre-rRNA first, which results in decreased levels of mature rRNAs. Insufficiency of rRNAs subsequently leads to the impairment of ribosome biogenesis and decrease of the translational rate in infected DAOY cells. TBEV infection could also trigger host defence mechanisms leading to the translational arrest. For example, protein kinase R (PKR) activated by dsRNA or PKR-like endoplasmic reticulum kinase (PERK) activated by ER stress could play a significant role in the observed translational shut-off as well.

https://doi.org/10.1371/journal.pntd.0007745.g008

nucleopolyhedrovirus was shown to decrease both, 18S and 28S rRNAs [63]. Additionally, over-expression of HIV Tat protein in *Drosophila melanogaster* led to the impairment of 45S pre-rRNA precursor processing [35]. Similarly, herpes simplex virus 1 decreased the rate of rRNA maturation despite unaltered levels of 45-47S pre-rRNA and unchanged POLR1 activity [32]. The reduction of rRNA levels can be associated with the induction of nucleolar stress, which is characterized by several hallmarks including nucleolar and ribosomal disruption eventually leading to the activation of the p53 signalling pathway. A possible link between fla-viviral pathogenesis and nucleolar stress was suggested previously. DENV and ZIKV, but not WNV were shown to induce nucleolar stress in infected cells by disruption of nucleoli, which

134

resulted in an increased rate of apoptosis via the p53 signalling cascade [64]. However, no disruption of nucleoli was observed in the case of TBEV-infected DAOY cells (S5B Fig), possibly not surprising as the TBEV infection specifically affects only the POLR1 activity.

We propose alternative ways by which TBEV could interfere with transcription and/or translation in DAOY cells: 1) TBEV negatively affects the translation of host proteins, including POLR1, transcription factors, and ribosomal proteins; their lower levels subsequently result in a decline in synthesis of all rRNA species; or 2) TBEV directly interferes with *de novo* synthesis of 45-47S pre-rRNA (but not 5S rRNA) via a POLR1 specific mechanism, which reduces the levels of 18S and 28S rRNAs and this leads to the decline of translational rate in host cells; 3) transcription and translation can be modified independently by both viral or cellular factors as a result of infection (summarised in Fig 8). Translational shut-off can otherwise be elicited by host cell defence mechanisms, such as activation of protein kinase R (PKR) or PKR-like endoplasmic reticulum kinase (PERK) [65–67]. To elucidate the exact mechanism of the inhibition of host protein and rRNA production and actual involvement of viral and host factors further experiments will be needed. These may for example assess whether viral proteins can directly inhibit transcription and/or translation. The present study does not elucidate this question and more work will be required to understand the processes; underlying the effects described here.

An overall translational inhibition induced by CHX treatment results in reduced *de novo* synthesis of 45-47S pre-rRNA precursor as well as the levels of 5S rRNA in DAOY cells. In contrast, TBEV infection only affected the 45-47S pre-rRNA precursor (and mature 18S and 28S rRNA levels) and did not affect 5S rRNA. This suggests TBEV-specific inhibition of POLR1 activity, which could result in reduced production of host proteins. Further analyses are needed to characterise the connection between rRNA production arrests and translational shut-off upon TBEV infection.

In summary, our results give new insights into the flavivirus-host interactions at the transcriptional/translational level. Moreover, a virus-induced rRNA decrease was described for flaviviral infection for the first time. The research here can contribute to understanding the mechanisms which determine at least to some extent the subsequent pathological processes. However, the relatively late onset of effects described in this study cannot completely rule out the possibility that our observations are due to cellular responses to TBEV infection rather than virus-mediated, or even combinations of both cellular and viral effects. More work is required to assess these possibilities in detail.

Supporting information

S1 Fig. Cell viability measurement using AlamarBlue in TBEV-infected DAOY cells. DAOY cells were infected with either TBEV Neudoerfl or Hypr strains (MOI 5) or untreated (mock); at indicated time intervals, cells were counted. A two-fold serial dilution was prepared with range from 50000 to 390 cells/well and cell viability was subsequently analysed by using alamarBlue reagent. Graphs represents fluorescent signal linked to the cell number at 24 hours p.i. (A) and 48 hours p.i. (B). Three independent experiments were performed and values are expressed as mean with SEM.
(TIF)

S2 Fig. TBEV induces host translational shut-off in infected cells. (A) Total protein pattern visualized using Coomassie blue (CBB) staining of the gel used for AHA detection presented in Fig 2A. (N) TBEV Neudoerfl, (H) TBEV Hypr, (m) mock control, (NC) non-labelled mock control. (B) DAOY, MG-63, A549, and Vero cells were infected with either Neudoerfl (N) of Hypr (H) strains of TBEV (MOI 5); as a negative control, mock-infected (m) cells were

included. Cells were starved for 1 hour in methionine-free medium and subsequently, nascent proteins were labelled using AHA (incubation for 2 hours; non-labelled negative controls, NC). Cell lysates analysed by SDS-PAGE followed by proteins transfer to PVDF membrane and Click reaction using biotin-alkyne. *De novo* synthesized proteins were further visualized by using biotin-streptavidin detection system along with conjugated alkaline phosphatase. Developed membranes were then stripped and NS3 viral protein detected. Total protein pattern was visualized using CBB staining of the gels after blotting. Representative images out of three independent experiments are shown.
(TIF)

S3 Fig. TBEV inhibits production of over-expressed viperin and GFP. (A) Schematic overview of experimental procedure: DAOY cells were first infected with either Neudoerfl or Hypr strain (MOI 5) and at 24 hours p.i. transfected either with wt-viperin or phMGFP expression constructs. (B) The relative quantification of overexpressed viperin and GFP mRNA in either TBEV Neudoerfl- (Neu) or TBEV Hypr-infected DAOY cells at 24 hours p.t. The Δ-c_t relative quantification method was used, with normalisation to the cell number. Mock-transfected cells (empty vector only) were used as a control. Data are representative of three independent experiments and values are expressed as mean with SEM. Significant difference from the control was calculated using unpaired two-sample Student's t-test (* $P<0.05$, ** $P<0.01$). (C) DAOY cells were first infected with either Neudoerfl or Hypr strain (MOI 5) and at 24 hours p.i. transfected with either viperin or GFP expression plasmids. Analysis of viperin and GFP protein levels was performed at 24 hours p.t. using viperin-specific immunodetection and GFP signal measurement. Relative amounts in comparison to uninfected cells with normalisation to cell numbers are shown for both proteins. Data are representative of three independent experiments and values are expressed as mean with SEM. Significant difference from the control was calculated using a one-sample Student's t-test (* $P<0.05$).
(TIF)

S4 Fig. Raw data of rRNA abundancy in TBEV-infected cells acquired from Bioanalyzer 2100. DAOY cells were infected with either TBEV Neudoerfl or Hypr strains (MOI 5) and total RNA was isolated with RNAblue at the indicated time intervals. Subsequent analysis was performed by using 30 ng of total RNA from mock-infected cells; RNA input of remaining samples was normalised to the cell number. Representative images from three independent experiments are shown.
(TIF)

S5 Fig. Specificity of Click reaction and visualization of nucleoli in DAOY cells. (A) DAOY cells were infected with TBEV Hypr strain (MOI 5) and at indicated time intervals incubated for 2 hours with EU-free cultivation medium. Fixed cells underwent the Click reaction using 10 μM biotin picolyl azide followed by fluorescent labelling with streptavidin-DyLight549. Cells were co-stained with anti-NS3 antibodies; signal was further visualized using anti-chicken DyLight488 antibodies. Scale bar represents 200 μm. (B) DAOY cells were either infected with TBEV Hypr strain (MOI 5) and fixed at 48 hours p.i. or treated with 1 mM hydrogen peroxide for 45 minutes before the fixation. Anti-NPM1 antibodies with the secondary DyLight594-conjugated antibodies were used for the visualization of nucleoli. Scale bar represents 80 μm.
(TIF)

S6 Fig. Cycloheximide (CHX) treatment results in decreased production of Renilla luciferase. DAOY cells were transfected with 100 ng of pRL-CMV reporter vector expressing RL and subsequently treated with CHX (50, 100 or 300 μg/ml) for time periods indicated. At 24 hours

136

p.t. cell viability as well as luciferase activity was analysed. Data are representative of two independent experiments and values are expressed as mean with SEM.
(TIF)

S1 Table. List of used primers.
(PDF)

Acknowledgments

We thank M. Bloom (National Institute of Allergy and Infectious Diseases, USA) for NS3 antibodies and valuable feedback and suggestions. We thank F. X. Heinz (Medical University of Vienna, Austria) for TBEV strain Neudoerfl. We also thank L. F.P. Ng (Singapore Immunology Network, Agency for Science, Technology and Research (A*STAR), Singapore) for providing the viperin expression construct. We thank R. Randall (University of St. Andrews, UK) for A549 cell line. We thank Dr Melanie McDonald and Dr Claire Donald for proofreading of the manuscript.

Author Contributions

Conceptualization: Martin Selinger, Hana Tykalová, Ján Štěrba, Alain Kohl, Esther Schnettler.

Funding acquisition: Ján Štěrba, Alain Kohl, Esther Schnettler, Libor Grubhoffer.

Investigation: Martin Selinger, Hana Tykalová, Pavlína Věchtová, Zuzana Vavrušková, Jaroslava Lieskovská.

Methodology: Martin Selinger, Ján Štěrba, Alain Kohl, Esther Schnettler.

Supervision: Alain Kohl, Esther Schnettler, Libor Grubhoffer.

Visualization: Martin Selinger.

Writing – original draft: Martin Selinger, Hana Tykalová.

Writing – review & editing: Martin Selinger, Hana Tykalová, Ján Štěrba, Alain Kohl, Esther Schnettler.

References

1. Simmonds P, Becher P, Bukh J, Gould EA, Meyers G, Monath T, et al. ICTV Virus Taxonomy Profile: Flaviviridae. J Gen Virol. 2017; 98(1):2–3. WOS:000396098700002. https://doi.org/10.1099/jgv.0.000672 PMID: 28218572

2. Dumpis U, Crook D, Oksi J. Tick-borne encephalitis. Clin Infect Dis. 1999; 28(4):882–90. https://doi.org/10.1086/515195 PMID: 10825054.

3. Kunz C, Heinz FX. Tick-borne encephalitis. Vaccine. 2003; 21:S1–S2. ISI:000181967400001.

4. Frimmel S, Krienke A, Riebold D, Loebermann M, Littmann M, Fiedler K, et al. Tick-borne encephalitis virus habitats in North East Germany: reemergence of TBEV in ticks after 15 years of inactivity. Biomed Res Int. 2014. WOS:000339315800001.

5. Boelke M, Bestehorn M, Marchwald B, Kubinski M, Liebig K, Glanz J, et al. First isolation and phylogenetic analyses of tick-borne encephalitis virus in Lower Saxony, Germany. Viruses-Basel. 2019; 11(5). ARTN 462 10.3390/v11050462. WOS:000472676600073.

6. Pagani SC, Malossa SF, Klaus C, Hoffmann D, Beretta O, Bomio-Pacciorini N, et al. First detection of TBE virus in ticks and sero-reactivity in goats in a non-endemic region in the southern part of Switzerland (Canton of Ticino). Ticks Tick-Borne Dis. 2019; 10(4):868–74. WOS:000468379800020. https://doi.org/10.1016/j.ttbdis.2019.04.006 PMID: 31047827

137

7. Haglund M, Gunther G. Tick-borne encephalitis—pathogenesis, clinical course and long-term follow-up. Vaccine. 2003; 21:S11–S8. ISI:000181967400003. https://doi.org/10.1016/s0264-410x(02)00811-3 PMID: 12628810

8. Gelpi E, Preusser M, Garzuly F, Holzmann H, Heinz FX, Budka H. Visualization of Central European tick-borne encephalitis infection in fatal human cases. J Neuropathol Exp Neurol. 2005; 64(6):506–12. Epub 2005/06/28. https://doi.org/10.1093/jnen/64.6.506 PMID: 15977642.

9. Kurhade C, Zegenhagen L, Weber E, Nair S, Michaelsen-Preusse K, Spanier J, et al. Type I Interferon response in olfactory bulb, the site of tick-borne flavivirus accumulation, is primarily regulated by IPS-1. J Neuroinflamm. 2016; 13. WOS:000368886900003.

10. Weber E, Finsterbusch K, Lindquist R, Nair S, Lienenklaus S, Gekara NO, et al. Type I interferon protects mice from fatal neurotropic infection with langat virus by systemic and local antiviral responses. J Virol. 2014; 88(21):12202–12. WOS:000343314900004. https://doi.org/10.1128/JVI.01215-14 PMID: 25122777

11. Gritsun TS, Lashkevich VA, Gould EA. Tick-borne encephalitis. Antiviral Res. 2003; 57(1–2):129–46. https://doi.org/10.1016/s0166-3542(02)00206-1 PMID: 12615309

12. Markoff L. 5'-and 3'-noncoding regions in flavivirus RNA. Adv Virus Res. 2003; 59:177–228. PMID: 14696330

13. Barrows NJ, Campos RK, Liao KC, Prasanth KR, Soto-Acosta R, Yeh SC, et al. Biochemistry and molecular biology of flaviviruses. Chem Rev. 2018; 118(8):4448–82. WOS:000431095200009. https://doi.org/10.1021/acs.chemrev.7b00719 PMID: 29652486

14. Murray CL, Jones CT, Rice CM. Architects of assembly: roles of *Flaviviridae* non-structural proteins in virion morphogenesis. Nat Rev Microbiol. 2008; 6(9):699–708. ISI:000258413100015. https://doi.org/10.1038/nrmicro1928 PMID: 18587411

15. Lindqvist R, Upadhyay A, Overby AK. Tick-borne flaviviruses and the type I interferon response. Viruses-Basel. 2018; 10(7). Tick-borne flaviviruses and the type I interferon response. WOS:000445153200002.

16. Apte-Sengupta S, Sirohi D, Kuhn RJ. Coupling of replication and assembly in flaviviruses. Curr Opin Virol. 2014; 9:134–42. WOS:000346958700022. https://doi.org/10.1016/j.coviro.2014.09.020 PMID: 25462445

17. Walsh D, Mathews MB, Mohr I. Tinkering with translation: protein synthesis in virus-infected cells. Csh Perspect Biol. 2013; 5(1). WOS:000315983600013.

18. Rivas HG, Schmaling SK, Gaglia MM. Shutof of host gene expression in influenza A virus and herpesviruses: similar mechanisms and common themes. Viruses-Basel. 2016; 8(4). WOS:000375157800015.

19. Blakqori G, van Knippenberg I, Elliott RM. Bunyamwera orthobunyavirus S-segment untranslated regions mediate poly(A) tail-independent translation. J Virol. 2009; 83(8):3637–46. WOS:000264327300021. https://doi.org/10.1128/JVI.02201-08 PMID: 19193790

20. Walsh D, Mohr I. Viral subversion of the host protein synthesis machinery. Nat Rev Microbiol. 2011; 9 (12):860–75. WOS:000297255800012. https://doi.org/10.1038/nrmicro2655 PMID: 22002165

21. Feigenblum D, Schneider RJ. Modification of eukaryotic initiation factor 4F during infection by influenza virus. J Virol. 1993; 67(6):3027–35. WOS:A1993LB79400008. PMID: 8098776

22. de Breyne S, Bonderoff JM, Chumakov KM, Lloyd RE, Hellen CUT. Cleavage of eukaryotic initiation factor eIF5B by enterovirus 3C proteases. Virology. 2008; 378(1):118–22. WOS:000258316100013. https://doi.org/10.1016/j.virol.2008.05.019 PMID: 18572216

23. Gradi A, Svitkin YV, Imataka H, Sonenberg N. Proteolysis of human eukaryotic translation initiation factor eIF4GII, but not eIF4GI, coincides with the shutoff of host protein synthesis after poliovirus infection. P Natl Acad Sci USA. 1998; 95(19):11089–94. WOS:000075957100017.

24. Roth H, Magg V, Uch F, Mutz P, Klein P, Haneke K, et al. Flavivirus infection uncouples translation suppression from cellular stress responses. Mbio. 2017; 8(1). WOS:000395835000058.

25. Edgil D, Polacek C, Harris E. Dengue virus utilizes a novel strategy for translation initiation when cap-dependent translation is inhibited. J Virol. 2006; 80(6):2976–86. WOS:000236131400039. https://doi.org/10.1128/JVI.80.6.2976-2986.2006 PMID: 16501107

26. Villas-Boas CSA, Conceicao TM, Ramirez J, Santoro ABM, Da Poian AT, Montero-Lomeli M. Dengue virus-induced regulation of the host cell translational machinery. Braz J Med Biol Res. 2009; 42 (11):1020–6. WOS:000271163100001. https://doi.org/10.1590/S0100-879X2009001100004 PMID: 19855901

27. Roberts L, Wieden HJ. Viruses, IRESs, and a universal translation initiation mechanism. Biotechnol Genet Eng Rev. 2018; 34(1):60–75. Epub 2018/05/29. 29804514. https://doi.org/10.1080/02648725.2018.1471567 PMID: 29804514

138

28. Henras AK, Plisson-Chastang C, O'Donohue MF, Chakraborty A, Gleizes PE. An overview of pre-ribosomal RNA processing in eukaryotes. Wiley Interdisciplinary Reviews: RNA. 2015; 6(2):225–42. Epub 2014/10/28. https://doi.org/10.1002/wrna.1269 PMID: 25346433; PubMed Central PMCID: PMC4361047.

29. Khatter H, Vorlander MK, Muller CW. RNA polymerase I and III: similar yet unique. Curr Opin Struc Biol. 2017; 47:88–94. WOS:000419413700013.

30. Chen FX, Smith ER, Shilatifard A. Born to run: control of transcription elongation by RNA polymerase II. Nat Rev Mol Cell Bio. 2018; 19(7):464–78. WOS:000435953700009.

31. Yan Y, Du Y, Wang G, Li K. Non-structural protein 1 of H3N2 influenza A virus induces nucleolar stress via interaction with nucleolin. Sci Rep. 2017; 7(1):17761. Epub 2017/12/21. https://doi.org/10.1038/s41598-017-18087-2 PMID: 29259342; PubMed Central PMCID: PMC5736645.

32. Belin S, Kindbeiter K, Hacot S, Albaret MA, Roca-Martinez JX, Therizols G, et al. Uncoupling ribosome biogenesis regulation from RNA polymerase I activity during herpes simplex virus type 1 infection. RNA. 2010; 16(1):131–40. Epub 2009/11/26. https://doi.org/10.1261/rna.1935610 PMID: 19934231; PubMed Central PMCID: PMC2802023.

33. Oswald E, Reinz E, Voit R, Aubin F, Alonso A, Auvinen E. Human papillomavirus type 8 E7 protein binds nuclear myosin 1c and downregulates the expression of pre-rRNA. Virus Genes. 2017; 53(6):807–13. Epub 2017/07/25. https://doi.org/10.1007/s11262-017-1491-6 PMID: 28733876.

34. Westdorp KN, Sand A, Moorman NJ, Terhune SS. Cytomegalovirus late protein pUL31 alters pre-rRNA expression and nuclear organization during infection. J Virol. 2017; 91(18). Epub 2017/07/01. https://doi.org/10.1128/JVI.00593-17 PMID: 28659485; PubMed Central PMCID: PMC5571270.

35. Ponti D, Troiano M, Bellenchi GC, Battaglia PA, Gigliani F. The HIV Tat protein affects processing of ribosomal RNA precursor. BMC cell biology. 2008; 9:32. Epub 2008/06/19. https://doi.org/10.1186/1471-2121-9-32 PMID: 18559082; PubMed Central PMCID: PMC2440370.

36. Jacobsen PF, Jenkyn DJ, Papadimitriou JM. Establishment of a human medulloblastoma cell line and its heterotransplantation into nude mice. J Neuropathol Exp Neurol. 1985; 44(5):472–85. Epub 1985/09/01. https://doi.org/10.1097/00005072-198509000-00003 PMID: 2993532.

37. Giard DJ, Aaronson SA, Todaro GJ, Arnstein P, Kersey JH, Dosik H, et al. In vitro cultivation of human tumors: establishment of cell lines derived from a series of solid tumors. J Natl Cancer Inst. 1973; 51(5):1417–23. Epub 1973/11/01. https://doi.org/10.1093/jnci/51.5.1417 PMID: 4357758.

38. Kozuch O, Mayer V. Pig kidney epithelial (PS) cells: a perfect tool for the study of flaviviruses and some other arboviruses. Acta Virol. 1975; 19(6):498. Epub 1975/11/01. 1999.

39. Billiau A, Edy VG, Heremans H, Van Damme J, Desmyter J, Georgiades JA, et al. Human interferon: mass production in a newly established cell line, MG-63. Antimicrob Agents Chemother. 1977; 12(1):11–5. Epub 1977/07/01. https://doi.org/10.1128/aac.12.1.11 PMID: 883813; PubMed Central PMCID: PMC352146.

40. Teng TS, Foo SS, Simamarta D, Lum FM, Teo TH, Lulla A, et al. Viperin restricts chikungunya virus replication and pathology. J Clin Invest. 2012; 122(12):4447–60. Epub 2012/11/20. https://doi.org/10.1172/JCI63120 PMID: 23160199; PubMed Central PMCID: PMC3533538.

41. Wallner G, Mandl CW, Ecker M, Holzmann H, Stiasny K, Kunz C, et al. Characterisation and complete genome sequences of high- and low-virulence variants of tick-borne encephalitis virus. J Gen Virol. 1996; 77:1035–42. WOS:A1996UJ08600027. https://doi.org/10.1099/0022-1317-77-5-1035 PMID: 8609469.

42. Asghar N, Lindblom P, Melik W, Lindqvist R, Haglund M, Forsberg P, et al. Tick-borne encephalitis virus sequenced directly from questing and blood-feeding ticks reveals quasispecies variance. Plos One. 2014; 9(7). WOS:000341354800074.

43. Heinz FX, Kunz C. Homogeneity of the structural glycoprotein from European isolates of tick-borne encephalitis virus: comparison with other flaviviruses. J Gen Virol. 1981; 57(Pt 2):263–74. Epub 1981/12/01. https://doi.org/10.1099/0022-1317-57-2-263 PMID: 6172553.

44. Pospisil L, Jandasek L. and Pesek J. Isolation of new strains of tick-borne encephalitis virus, Brno region, summer 1953. Lek List. 1954; 9:3–5. PMID: 13131921.

45. De Madrid AT, Porterfield JS. A simple micro-culture method for the study of group B arboviruses. Bull World Health Organ. 1969; 40(1):113–21. Epub 1969/01/01. PMID: 4183812; PubMed Central PMCID: PMC2554446.

46. Rueden CT, Schindelin J, Hiner MC, DeZonia BE, Walter AE, Arena ET, et al. ImageJ2: ImageJ for the next generation of scientific image data. BMC bioinformatics. 2017; 18(1):529. Epub 2017/12/01. https://doi.org/10.1186/s12859-017-1934-z PMID: 29187165; PubMed Central PMCID: PMC5708080.

47. Selinger M, Wilkie GS, Tong L, Gu Q, Schnettler E, Grubhoffer L, et al. Analysis of tick-borne encephalitis virus-induced host responses in human cells of neuronal origin and interferon-mediated protection. J

139

Gen Virol. 2017; 98(8):2043–60. Epub 2017/08/09. https://doi.org/10.1099/jgv.0.000853 PMID: 28786780; PubMed Central PMCID: PMC5817271.

48. Reid DW, Campos RK, Child JR, Zheng TL, Chan KWK, Bradrick SS, et al. Dengue virus selectively annexes endoplasmic reticulum-associated translation machinery as a strategy for co-opting host cell protein synthesis. J Virol. 2018; 92(7). WOS:000428409800013.

49. Best MD. Click chemistry and bioorthogonal reactions: unprecedented selectivity in the labeling of biological molecules. Biochemistry. 2009; 48(28):6571–84. Epub 2009/06/03. https://doi.org/10.1021/bi9007726 PMID: 19485420.

50. Lindqvist R, Overby AK. The role of viperin in antiflavivirus responses. DNA Cell Biol. 2018; 37(9):725–30. WOS:000443729600001. https://doi.org/10.1089/dna.2018.4328 PMID: 30059238

51. Yang K, Yang J, Yi J. Nucleolar Stress: hallmarks, sensing mechanism and diseases. Cell Stress. 2018; 2(6):125–40. Epub 10.5. 2018. https://doi.org/10.15698/cst2018.06.139 PMID: 31225478

52. Hayasaka D, Nagata N, Fujii Y, Hasegawa H, Sata T, Suzuki R, et al. Mortality following peripheral infection with Tick-borne encephalitis virus results from a combination of central nervous system pathology, systemic inflammatory and stress responses. Virology. 2009; 390(1):139–50. WOS:000268218200016. https://doi.org/10.1016/j.virol.2009.04.026 PMID: 19467556

53. Mandl CW, Ecker M, Holzmann H, Kunz C, Heinz FX. Infectious cDNA clones of tick-borne encephalitis virus European subtype prototypic strain Neudoerfl and high virulence strain Hypr. J Gen Virol. 1997; 78:1049–57. WOS:A1997WW48500010. https://doi.org/10.1099/0022-1317-78-5-1049 PMID: 9152422

54. Westaway EG. Proteins Specified by Group B Togaviruses in Mammalian-Cells during Productive Infections. Virology. 1973; 51(2):454–65. WOS:A1973P069000019. https://doi.org/10.1016/0042-6822(73)90444-3 PMID: 4632654

55. Heinz FX, Kunz C. Molecular epidemiology of tick-borne encephalitis virus: peptide mapping of large non-structural proteins of European isolates and comparison with other flaviviruses. J Gen Virol. 1982; 62(Oct):271–85. WOS:A1982PL98600008.

56. Emara MM, Brinton MA. Interaction of TIA-1/TIAR with West Nile and dengue virus products in infected cells interferes with stress granule formation and processing body assembly. P Natl Acad Sci USA. 2007; 104(21):9041–6. WOS:000246853700065.

57. Pena J, Harris E. Dengue virus modulates the unfolded protein response in a time-dependent manner. J Biol Chem. 2011; 286(16):14226–36. WOS:000289556200046. https://doi.org/10.1074/jbc.M111.222703 PMID: 21385877

58. Panayiotou C, Lindqvist R, Kurhade C, Vonderstein K, Pasto J, Edlund K, et al. Viperin restricts Zika virus and tick-borne encephalitis virus replication by targeting NS3 for proteasomal degradation. J Virol. 2018; 92(7). WOS:000428409800027.

59. Upadhyay AS, Vonderstein K, Pichlmair A, Stehling O, Bennett KL, Dobler G, et al. Viperin is an iron-sulfur protein that inhibits genome synthesis of tick-borne encephalitis virus via radical SAM domain activity. Cell Microbiol. 2014; 16(6):834–48. Epub 2013/11/20. https://doi.org/10.1111/cmi.12241 PMID: 24245804.

60. Van der Hoek KH, Eyre NS, Shue B, Khantisitthiporn O, Glab-Ampi K, Carr JM, et al. Viperin is an important host restriction factor in control of Zika virus infection. Sci Rep. 2017; 7. WOS:000404451300081.

61. Helbig KJ, Beard MR. The role of viperin in the innate antiviral response. J Mol Biol. 2014; 426(6):1210–9. WOS:000333487600005. https://doi.org/10.1016/j.jmb.2013.10.019 PMID: 24157441

62. Banerjee S, An S, Zhou A, Silverman RH, Makino S. RNase L-independent specific 28S rRNA cleavage in murine coronavirus-infected cells. J Virol. 2000; 74(19):8793–802. Epub 2000/09/12. https://doi.org/10.1128/jvi.74.19.8793-8802.2000 PMID: 10982321; PubMed Central PMCID: PMC102073.

63. Fujita R, Asano S, Sahara K, Bando H. Marked decrease of ribosomal RNA in BmN cells infected with AcMNPV. J Insect Biotechnol Sericol. 2005; 74(3):125–8. https://doi.org/10.11416/jibs.74.125

64. Slomnicki LP, Chung DH, Parker A, Hermann T, Boyd NL, Hetman M. Ribosomal stress and Tp53-mediated neuronal apoptosis in response to capsid protein of the Zika virus. Sci Rep. 2017; 7(1):16652. Epub 2017/12/02. https://doi.org/10.1038/s41598-017-16952-8 PMID: 29192272; PubMed Central PMCID: PMC5709411.

65. Herbert KM, Nag A. A tale of two RNAs during viral infection: how viruses antagonize mRNAs and small non-coding RNAs in the host cell. Viruses-Basel. 2016; 8(6). WOS:000378848600006.

66. Weber F, Kochs G, Haller O. Inverse interference: How viruses fight the interferon system. Viral Immunol. 2004; 17(4):498–515. WOS:000226043900005. https://doi.org/10.1089/vim.2004.17.498 PMID: 15671747

67. Valadao ALC, Aguiar RS, de Arruda LB. Interplay between inflammation and cellular stress triggered by flaviviridae viruses. Front Microbiol. 2016; 7. WOS:000381851000001.

140

5 Discussion

Flaviviruses represent a worldwide-distributed family of arboviruses with an enormous impact on the public health. Effective vaccines against some of the flaviviruses are at disposal, however, no specific treatment for flavivirus-induced disease exists so far. Thus, any kind of anti-flaviviral medicine is highly demanded. In order to develop such type of a cure, an identification of crucial flavivirus-host interactions on the molecular level may substantially help. Therefore, our laboratory tries to uncover the course of interactions between the neurotropic TBEV and the innate immune system in neural cells.

TBEV is a neurotropic tick-borne flavivirus causing the TBE disease in infected humans. The clinical outcome of TBE can vary from sub-clinical cases to severe encephalitis/meningoencephalitis accompanied by neurological sequelae. Geographical distribution of TBEV includes vast regions of Eurasia and is further expanding with approximately 12 000 cases of TBE reported annually [3, 39, 60].

In CNS, neurons in spinal cord, brainstem, cerebellum, and basal ganglia are believed to be the primary targets [52, 54]. However, other cell types of CNS, including astrocytes, were proved to be sensitive as well [51, 53]. In order to get a model relatively corresponding to the *in vivo* natural state, we employed human cell lines of neural origin for our *in vitro* studies. In particular, desmoplastic cerebellar medulloblastoma (DAOY HTB-186) [236], bone marrow metastasis of Evans stage 4 neuroblastoma (UKF-NB4) [237], and glioblastoma astrocytoma (U373 MG Uppsala) [238] human cell lines were used.

It has been previously shown that type I IFN pre-treatment of neuronal cells *in vitro* resulted in a decreased production of neurotropic WNV and SLEV [113]. We were the first to report a similar antiviral effect of type I IFN (IFN-β) pre-treatment in case of TBEV infection in DAOY cells [239, 240]. Without IFN pre-treatment, TBEV infection in DAOY cells results in high viral titres and strong cytopathic effect eventually leading to cell death. In order to get more detailed image of the mechanism behind the IFN-mediated protection, an unbiased transcriptomic analysis was

performed in DAOY cells (1) pre-treated with IFN-β, (2) infected with TBEV Neudoerfl strain, or (3) pre-treated with IFN-β with subsequent TBEV infection.

Analysis of differentially expressed (DE) genes upon TBEV infection revealed very interesting results. Surprisingly, no type I IFNs were expressed in response to TBEV infection. Instead, strong up-regulation of INF-λ1 was detected. IFN-λ1 was recently shown to play a significant role during WNV infection of CNS [126]. However, our results suggest no role of IFN-λ1 in defence against TBEV infection – despite its massive production, IFN-λ1 failed to elicit an effective antiviral response, since high levels of TBEV titres were produced and accompanied by significantly decreased viability of infected cells. The ineffectiveness of IFN-λ1 against TBEV was further demonstrated in pre-treatment experiments, when no antiviral effect was observed. On the other hand, pre-treatment with either IFN-β or IFN-λ1 resulted in an increased protection of A549 cells (human lung adenocarcinoma) against TBEV. This finding represents one of the main outcomes from this study – an evidence how important is the context of infection in terms of tissue response specificity to various IFNs. In accordance to our findings, the tissue and cell type specificity in terms of IFN signalling was described for both, IFN-β or IFN-λ [124, 200].

In addition to type III IFN, a wide panel of cytokines, chemokines and ISGs was up-regulated upon TBEV infection as well. Several studies have already described various cytokines and chemokines being up-regulated in response to TBEV infection in neural tissues [53, 241]. However, only a limited panel of custom-selected genes was analysed in case of both cited studies. Thus the complexity of the overall host response remained undetermined. Our transcriptomic data confirmed the up-regulation of five previously identified cytokines (CCL3/MIP1α, CCL4/MIP1β, CCL5/RANTES, CXCL10/IP-10, IL-6, and TNF-α) and identified five new (CXCL2/MIP2α, CXCL11/IP-9, IL-12α, IL-15 and IL-23α). The panel of up-regulated cytokines/chemokines as described here would mostly result in the activation/stimulation and chemotaxis of effector immune cells. This finding correlates with TBEV-associated immunopathogenesis in the brain [54, 55].

Among ISGs, whose expression was activated upon TBEV infection in DAOY cells IFIT1, IFIT2, RSAD2, OASL, IFIT3, OAS2, ISG15, and ISG20 proteins were the most induced ones (fold-change >2.5). Except ISGs with direct antiviral effect, expression of RIG-I and MDA5 was induced as well. Antiviral role of all mentioned ISGs is well described for many flaviviruses (chapter 2.2.2.4). However, for TBEV only RIG-I, MDA5, and RSAD2 were proved to have an important role in sensing TBEV and interfering with its replication [80, 197-199]. Although various ISGs were up-regulated, high TBEV titres were observed in DAOY cells, which suggests the presence of counteracting measures by TBEV against the host immune responses, at least in the infected cells.

On the other hand, the IFN-β pre-treatment of DAOY cells initiates a potent antiviral response which efficiently interferes with TBEV infection. It is not surprising that the panel of genes activated upon IFN-β treatment differs strongly from the panel of genes, whose expression is activated in response to TBEV infection naturally. Only 12.3 % and 29.2 % of the DE genes identified in mock- and TBEV-infected cells that had been pre-treated with IFN-β were also identified in TBEV-infected cells, respectively. Furthermore, the DE gene analysis revealed two highly striking phenomena: (1) two ISGs, IFI6 and IFI27, were shown to be, by far, the most up-regulated genes, (2) expression of a unique set of pro-inflammatory cytokines (CCL3/MIP1α, CSF3, CCL20/MIP3α, IL36RN, CXCL1/KC, CXCL2/MIP2α, CXCL3/MIP2β, CXCL5/ENA78, IL-1α, IL-1β, IL-6, IL-8 and IL-11) was decreased strongly. The latter observation of the anti-inflammatory effect of IFN-β is a well-documented phenomenon [242], suggesting that IFN-β may also reduce the immunopathogenic effect of TBEV infection in CNS. In connection to IFI6 and IFI27, both proteins belong to FAM14 family of ISGs [243] and were documented as mitochondrial proteins involved in apoptosis regulation [244-246]. Over-expression of IFI6 inhibited DENV-induced apoptosis of endothelial cells [245, 246], whereas IFI27 over-expression in human neurons resulted in decreased production of WNV, SLEV and MHV [113]. An elegant study by Richardson *et al.* revealed that IFI6 prophylactically protects uninfected cells against DENV, WNV, YFW, and ZIKV by preventing the formation of virus-induced ER membrane invaginations [247]. These data therefore suggest that IFI6 and IFI27 are promising candidate proteins that may be responsible for the inhibition of TBEV

infection in DAOY cells. However, further studies are needed in order to confirm this hypothesis.

Our transcriptomic data confirmed that TBEV infection triggers host innate immune system response *via* expression of specific ISGs and IFN-λ1 in DAOY cells. Nevertheless, despite the prompt host response, the infection resulted in high death rate. In further context with recent findings that have described a DENV-induced host translational shut-off [138, 208], we hypothesized that TBEV blocks the translation of host mRNAs in order to avoid the production of ISGs with possible restrictive effect on its replication. Truly, metabolic labelling experiments revealed a strong inhibition of host *de novo* protein synthesis in DAOY cells upon TBEV infection [248]. Cell lines of both neural and non-neural origin underwent translational shut-off, demonstrating thus the general nature of this phenomenon, however, the rate of reduction varied substantially in individual cell lines suggesting cell-dependent variability. In the case of DAOY cells, the observed translational shut-off involved also viperin, whose protein levels were surprisingly low, even despite an enormous enhancement of its mRNA production. Interestingly, the inhibitory effect of TBEV on the host translation was so robust that even the CMV promoter-driven over-expression of either viperin or GFP resulted in substantially decreased protein levels in the case of both proteins. The same situation was described in case of over-expressed OASLa variant (unpublished results). However, it is also possible that the translational arrest is induced upon the activation of UPR pathway, which was recently shown to be activated upon TBEV infection in osteosarcoma (U2OS) cells [211]. Unfortunately, we are currently not able to distinguish the exact rate of host and virus contribution to the observed translational shut-off.

Besides from the TBEV-induced host translational shut-off, we also described a decrease in mature 18S and 28S rRNA levels. Both, 18S and 28S, are derived from one pre-rRNA transcript, 45S pre-rRNA, which is transcribed by RNA polymerase I (POLR1). Metabolic labelling experiments showed that *de novo* synthesis of 45S pre-rRNA is significantly reduced upon TBEV infection. Intriguingly, levels of 5S rRNA, an RNA polymerase III (POLR3) transcript, were not affected negatively by TBEV infection, thus suggesting a targeted interference with RNA polymerase I only. To our knowledge, the virus-driven reduction in host

rRNA levels has not been described before for any flavivirus. Further analyses are in progress in order to describe the phenomena of transcriptional and translational shut-off in more detail.

The presence of both, transcriptional and translational arrest, raises a question whether these phenomena are triggered independently or not. It is highly probable that some kind of a connection exists, however, more work is required to fully describe the relationship between transcriptional and translational shut-off. We propose three alternative ways by which TBEV could interfere with transcription and/or translation in DAOY cells: 1) TBEV negatively affects the translation of host proteins, including POLR1, transcription factors, and ribosomal proteins; their lower levels subsequently result in a decline in synthesis of all rRNA species (UPR pathway could be involved as well); 2) TBEV directly interferes with the *de novo* synthesis of 45-47S pre-rRNA (but not 5S rRNA) *via* a POLR1 specific mechanism, which reduces the levels of 18S and 28S rRNAs and this leads to the decline of translational rate in host cells; 3) transcription and translation can be modified independently by both viral or cellular factors as a result of infection. We presented an indirect evidence in favour of the second hypothesis – treatment with cycloheximide (CHX; an inhibitor of translation elongation) resulted in decreased levels of both, POLR1 and POLR3, rRNA transcripts. This finding shows that general inhibition of translation does not discriminate and results in decrease of all rRNA species, whereas TBEV infection results only in decrease of POLR1-transcribed rRNAs.

The documented ability of TBEV to overcome the response of host innate immune system led us to a hypothesis that specific viral factor has to be responsible for such an interference. Truly, flaviviruses exploit many evasion strategies to avoid the host immune system (described in Chapter 2.3). Several possible candidates are being tested in our laboratory in co-operation with our colleagues from Prague, Brno, Glasgow, Hamburg, and Hamilton. So far, two studies were published and the results are discussed below.

During ZIKV outbreak in South America (2015-2016), we participated in the study describing the full genomic sequence of ZIKV Brazilian isolate PE243 and its interferon antagonistic properties [249]. The viral factor responsible for the inhibition of IFN-β expression was found to be ZIKV

sfRNA. In more detail, activity of IFN-β promoter was significantly reduced in the presence of ZIKV sfRNA when stimulated by poly I:C. The mode of ZIKV sfRNA action was determined as an interference with RIG-I and MDA5 signalling. In comparison to ZIKV, DENV sfRNA was proved to impair expression of IFN-β only *via* inhibition of RIG-I signalling pathway. This study further expanded the list of works identifying sfRNA as a potent modulator of host innate immune system in mammalian cells [73, 219, 220].

An enormous attention was recently given to sfRNA and its role during infection, with DENV and WNV sfRNA being studied the most extensively. On the other side, not much is known about TBEV sfRNA and its function in CNS. We confirmed the presence of sfRNA in TBEV-infected DAOY HTB-186 cells (unpublished results), however, its immunomodulatory effects still need to be further verified. Nevertheless, it is of high probability that the TBEV-derived sfRNA will contribute to the evasion of host immune system, since the importance of TBEV 3' UTR in the virulence has been already described [70]. Further experiments are in progress in order to get deeper insight into TBEV sfRNA function in neural cells.

Parallel studies in our laboratory focused also on the role of a newly identified uORF (upstream open reading frame) in several TBEV strains, which may possibly encode a minor polypeptide of 13 – 31 amino acids (depending on the strain). As described in Chapter 2.1.3, flaviviruses encode 10 major proteins. However, several studies have already documented the presence of minor proteins in flavivirus-infected cells. In the case of JEV and WNV, a prolonged version of NS1 protein, called NS1', was shown to be generated by -1 ribosomal frameshift event thanks to a pseudoknot structure in the NS2A gene [250-253]. Moreover, an additional N-NS4B/WARF4 minor protein was identified in WNV-infected cells [254, 255]. Based on the bioinformatic and experimental analyses, the presence of alternative ORFs is usually specific only for a narrow group of closely related strains, where even only a single nucleotide mutation was shown to critically impair the production of these minor proteins [250, 252, 253]. Surprisingly, these alternative proteins were shown to play an important role in neuroinvasiveness of the respective virus [250, 252]. Based on these data, we hypothesized that putative TuORF-coded peptide could play a role in the observed interference with

host response to TBEV infection. Therefore, we analysed the presence of TuORF-coded peptide in cells infected with TBEV Hypr strain (TuORF not present) and Neudoerfl strain (TuORF present). The putative peptide TuORF was not expressed on detectable levels in the Neudoerfl-infected human (DAOY HTB-186, UKF-NB4, U373) or tick (IRE/CTVM19) cell lines tested, thus its role during TBEV infection remains elusive [256]. However, it is possible that TuORF could have only regulatory function, since many mammalian uORFs act on the level of negative translation regulation without being expressed [257].

Another important factor, which plays a very significant role in virus-host interactions, is glycosylation. Both, glycosylated proteins and the glycan-binding proteins, of host or viral origin are crucial in many processes including viral entry, secretion, and tropism [258]. However, only a limited amount of information about glycobiology of flaviviruses is currently available. In the case of TBEV, the presence of *N*-linked glycans have been so far confirmed only in the structural proteins E and prM/M [259, 260] with described function in virus secretion and infectivity [261, 262]. Overall knowledge about the glycobiology interface of tick-host-pathogen relationships was summarized by our lab in Vechtova *et al.* [263].

6 Conclusions and future prospectives

In conclusion, this thesis provides novel insights into the response of neural cells to TBEV infection and the antiviral effects of type I and III IFNs. Moreover, new findings about TBEV-host interactions at the transcriptional/translational level were described together with the characterization of TuORF and ZIKV sfRNA expression profile and possible antagonistic effects in host cells. Published data can contribute to understanding the mechanisms which determine at least to some extent the pathological processes of neurotropic flaviviruses in CNS.

Currently, our main goal is to identify the mechanism and viral/host effectors responsible for the observed transcriptional and translational shut-off. So far, we ruled out the contribution of TuORF. The promising candidates are sfRNA and C protein. Various immunomodulatory effects were already described in case of sfRNA, thus we plan to analyse whether the presence of sfRNA derived from selected flaviviruses will result in transcriptional/translational shut-off. If our experiments will show a connection between the presence of sfRNA and host transcription/translation regulation, binding partners of sfRNA will be determined in order to describe the mechanistic nature of the sfRNA-induced changes in the host cells.

Except for the forming of viral capsid, no additional roles of the C protein are known. Several studies have described its unusual nuclear localization, however, its role in the nucleus remains elusive. Our preliminary results show that C protein localizes in the nucleolus, an organelle composed mainly of rDNA clusters where rRNA is produced and processed, and where ribosome biogenesis takes place. This finding points towards a connection between the observed transcriptional/translational shut-off and possible involvement of C protein in this phenomenon. In order to uncover the role of C protein in nucleolus, we plan to identify the binding partners of C protein (both RNA and proteins). In addition to this, we plan to characterize the role of C protein during flaviviral life cycle in host cells using TBEV mutants lacking specific regions of C gene analogical over-expression experiments as in the case of sfRNA.

The *in vitro* system we used in our studies relies on the human cancer cell lines derived from different brain parts. Even though this model was thoroughly characterized and thus represents a reliable system for the experiments, the cancer nature of cells may bias the observations in comparison to the *in vivo* state. Therefore, we started to utilize primary human neurons and astrocytes instead. These cells were proved to behave differently upon TBEV infection. Therefore, we plan to employ two TBEV strains of different virulence and both, neurons and astrocytes, in order to describe the principles of different outcome of infection in dependence on the cell type and severity of the virus strain. The analysis will be based on the transcriptomic changes in the pools of poly-(A) RNAs and small RNAs, thus giving a complex information about the overall response in terms of gene expression and its regulation.

7 References

1.   **Flaviviridae**   [https://talk.ictvonline.org/ictv-
        reports/ictv_online_report/positive-sense-rna-viruses/w/flaviviridae]

2.   Diamond MS, Pierson TC: **Molecular Insight into Dengue Virus
        Pathogenesis and Its Implications for Disease Control**. *Cell*
        2015, **162**(3):488-492.

3.   Gould EA, Solomon T: **Pathogenic flaviviruses**. *Lancet (London,
        England)* 2008, **371**(9611):500-509.

4.   **DENV - Fact Sheet** [https://www.who.int/news-room/fact-
        sheets/detail/dengue-and-severe-dengue]

5.   Bhatt S, Gething PW, Brady OJ, Messina JP, Farlow AW, Moyes CL,
        Drake JM, Brownstein JS, Hoen AG, Sankoh O *et al*: **The global
        distribution and burden of dengue**. *Nature* 2013, **496**(7446):504-
        507.

6.   Villar L, Dayan GH, Arredondo-Garcia JL, Rivera DM, Cunha R,
        Deseda C, Reynales H, Costa MS, Morales-Ramirez JO,
        Carrasquilla G *et al*: **Efficacy of a tetravalent dengue vaccine in
        children in Latin America**. *The New England journal of medicine*
        2015, **372**(2):113-123.

7.   Godoi IP, Lemos LL, de Araujo VE, Bonoto BC, Godman B, Guerra
        Junior AA: **CYD-TDV dengue vaccine: systematic review and
        meta-analysis of efficacy, immunogenicity and safety**. *Journal of
        comparative effectiveness research* 2017, **6**(2):165-180.

8.   Douam F, Ploss A: **Yellow Fever Virus: Knowledge Gaps
        Impeding the Fight Against an Old Foe**. *Trends in microbiology*
        2018, **26**(11):913-928.

9.   Monath TP, Vasconcelos PF: **Yellow fever**. *Journal of clinical
        virology : the official publication of the Pan American Society for
        Clinical Virology* 2015, **64**:160-173.

10.   **YFV - Fact Sheet** [https://www.who.int/news-room/fact-
        sheets/detail/yellow-fever]

11.   Yun SI, Lee YM: **Japanese encephalitis: the virus and vaccines**.
        Human vaccines & immunotherapeutics 2014, **10**(2):263-279.

12.   Mansfield KL, Hernandez-Triana LM, Banyard AC, Fooks AR,
        Johnson N: **Japanese encephalitis virus infection, diagnosis and**

control in domestic animals. *Veterinary microbiology* 2017, **201**:85-92.

13. **JEV - Fact Sheet** [https://www.who.int/news-room/fact-sheets/detail/japanese-encephalitis]

14. Petersen LR, Brault AC, Nasci RS: **West Nile virus: review of the literature**. *Jama* 2013, **310**(3):308-315.

15. Rossi SL, Ross TM, Evans JD: **West Nile virus**. *Clinics in laboratory medicine* 2010, **30**(1):47-65.

16. Dick GW, Kitchen SF, Haddow AJ: **Zika virus. I. Isolations and serological specificity**. *Transactions of the Royal Society of Tropical Medicine and Hygiene* 1952, **46**(5):509-520.

17. Macnamara FN: **Zika virus: a report on three cases of human infection during an epidemic of jaundice in Nigeria**. *Transactions of the Royal Society of Tropical Medicine and Hygiene* 1954, **48**(2):139-145.

18. Faye O, Freire CC, Iamarino A, Faye O, de Oliveira JV, Diallo M, Zanotto PM, Sall AA: **Molecular evolution of Zika virus during its emergence in the 20(th) century**. *PLoS neglected tropical diseases* 2014, **8**(1):e2636.

19. Musso D, Gubler DJ: **Zika Virus**. *Clinical microbiology reviews* 2016, **29**(3):487-524.

20. Lee I, Bos S, Li G, Wang S, Gadea G, Despres P, Zhao RY: **Probing Molecular Insights into Zika Virus(-)Host Interactions**. *Viruses* 2018, **10**(5).

21. **ZIKV - Fact Sheet** [https://www.who.int/news-room/fact-sheets/detail/zika-virus]

22. Mead PS, Hills SL, Brooks JT: **Zika virus as a sexually transmitted pathogen**. *Current opinion in infectious diseases* 2018, **31**(1):39-44.

23. Musso D, Nhan T, Robin E, Roche C, Bierlaire D, Zisou K, Shan Yan A, Cao-Lormeau VM, Broult J: **Potential for Zika virus transmission through blood transfusion demonstrated during an outbreak in French Polynesia, November 2013 to February 2014**. *Euro surveillance : bulletin Europeen sur les maladies transmissibles = European communicable disease bulletin* 2014, **19**(14).

24. Driggers RW, Ho CY, Korhonen EM, Kuivanen S, Jaaskelainen AJ, Smura T, Rosenberg A, Hill DA, DeBiasi RL, Vezina G *et al*: **Zika Virus Infection with Prolonged Maternal Viremia and Fetal Brain Abnormalities**. *The New England journal of medicine* 2016, **374**(22):2142-2151.

25. Lindqvist R, Upadhyay A, Overby AK: **Tick-Borne Flaviviruses and the Type I Interferon Response**. *Viruses* 2018, **10**(7).

26. Mc LD, Donohue WL: **Powassan virus: isolation of virus from a fatal case of encephalitis**. *Canadian Medical Association journal* 1959, **80**(9):708-711.

27. Hermance ME, Thangamani S: **Powassan Virus: An Emerging Arbovirus of Public Health Concern in North America**. *Vector borne and zoonotic diseases (Larchmont, NY)* 2017, **17**(7):453-462.

28. Work TH, Trapido H: **Summary of preliminary report of investigations of the Virus Research Centre on an epidemic disease affecting forest villagers and wild monkeys of Shimoga District, Mysore**. *Indian journal of medical sciences* 1957, **11**(5):341-342.

29. Holbrook MR: **Kyasanur forest disease**. *Antiviral research* 2012, **96**(3):353-362.

30. Zilber L: **Spring-summer tick-borne encephalitis**. *Arkhiv Biol Nauk* 1939, **56**:255-261.

31. Jahfari S, de Vries A, Rijks JM, Van Gucht S, Vennema H, Sprong H, Rockx B: **Tick-Borne Encephalitis Virus in Ticks and Roe Deer, the Netherlands**. *Emerging infectious diseases* 2017, **23**(6):1028-1030.

32. de Graaf JA, Reimerink JH, Voorn GP, Bij de Vaate EA, de Vries A, Rockx B, Schuitemaker A, Hira V: **First human case of tick-borne encephalitis virus infection acquired in the Netherlands, July 2016**. *Euro surveillance : bulletin Europeen sur les maladies transmissibles = European communicable disease bulletin* 2016, **21**(33).

33. Ecker M, Allison SL, Meixner T, Heinz FX: **Sequence analysis and genetic classification of tick-borne encephalitis viruses from Europe and Asia**. *The Journal of general virology* 1999, **80 (Pt 1)**:179-185.

34. Grard G, Moureau G, Charrel RN, Lemasson JJ, Gonzalez JP, Gallian P, Gritsun TS, Holmes EC, Gould EA, de Lamballerie X:

Genetic characterization of tick-borne flaviviruses: new insights into evolution, pathogenetic determinants and taxonomy. *Virology* 2007, **361**(1):80-92.

35.   Hubalek Z, Rudolf I: **Tick-borne viruses in Europe**. *Parasitology research* 2012, **111**(1):9-36.

36.   Golovljova I, Vene S, Sjolander KB, Vasilenko V, Plyusnin A, Lundkvist A: **Characterization of tick-borne encephalitis virus from Estonia**. *Journal of medical virology* 2004, **74**(4):580-588.

37.   Jaaskelainen AE, Tikkakoski T, Uzcategui NY, Alekseev AN, Vaheri A, Vapalahti O: **Siberian subtype tickborne encephalitis virus, Finland**. *Emerging infectious diseases* 2006, **12**(10):1568-1571.

38.   Jaaskelainen AE, Sironen T, Murueva GB, Subbotina N, Alekseev AN, Castren J, Alitalo I, Vaheri A, Vapalahti O: **Tick-borne encephalitis virus in ticks in Finland, Russian Karelia and Buryatia**. *The Journal of general virology* 2010, **91**(Pt 11):2706-2712.

39.   Gritsun TS, Lashkevich VA, Gould EA: **Tick-borne encephalitis**. *Antiviral research* 2003, **57**(1-2):129-146.

40.   Michelitsch A, Wernike K, Klaus C, Dobler G, Beer M: **Exploring the Reservoir Hosts of Tick-Borne Encephalitis Virus**. *Viruses* 2019, **11**(7).

41.   Rehacek J: **Transovarial transmission of tick-borne encephalitis virus by ticks**. *Acta virologica* 1962, **6**:220-226.

42.   Labuda M, Jones LD, Williams T, Danielova V, Nuttall PA: **Efficient transmission of tick-borne encephalitis virus between cofeeding ticks**. *Journal of medical entomology* 1993, **30**(1):295-299.

43.   Labuda M, Kozuch O, Zuffova E, Eleckova E, Hails RS, Nuttall PA: **Tick-borne encephalitis virus transmission between ticks cofeeding on specific immune natural rodent hosts**. *Virology* 1997, **235**(1):138-143.

44.   Gresikova-Kohutova M: **[Persistence of the virus of tick-borne encephalitis in milk & milk products]**. *Ceskoslovenska epidemiologie, mikrobiologie, imunologie* 1959, **8**(1):26-32.

45.   Hudopisk N, Korva M, Janet E, Simetinger M, Grgic-Vitek M, Gubensek J, Natek V, Kraigher A, Strle F, Avsic-Zupanc T: **Tick-borne encephalitis associated with consumption of raw goat**

milk, Slovenia, 2012. *Emerging infectious diseases* 2013, **19**(5):806-808.

46.   Markovinovic L, Kosanovic Licina ML, Tesic V, Vojvodic D, Vladusic Lucic I, Kniewald T, Vukas T, Kutlesa M, Krajinovic LC: **An outbreak of tick-borne encephalitis associated with raw goat milk and cheese consumption, Croatia, 2015**. *Infection* 2016, **44**(5):661-665.

47.   Labuda M, Austyn JM, Zuffova E, Kozuch O, Fuchsberger N, Lysy J, Nuttall PA: **Importance of localized skin infection in tick-borne encephalitis virus transmission**. *Virology* 1996, **219**(2):357-366.

48.   Thangamani S, Hermance ME, Santos RI, Slovak M, Heinze D, Widen SG, Kazimirova M: **Transcriptional Immunoprofiling at the Tick-Virus-Host Interface during Early Stages of Tick-Borne Encephalitis Virus Transmission**. *Frontiers in cellular and infection microbiology* 2017, **7**:494.

49.   Mustafa YM, Meuren LM, Coelho SVA, de Arruda LB: **Pathways Exploited by Flaviviruses to Counteract the Blood-Brain Barrier and Invade the Central Nervous System**. *Frontiers in microbiology* 2019, **10**:525.

50.   Miner JJ, Diamond MS: **Mechanisms of restriction of viral neuroinvasion at the blood-brain barrier**. *Current opinion in immunology* 2016, **38**:18-23.

51.   Palus M, Vancova M, Sirmarova J, Elsterova J, Perner J, Ruzek D: **Tick-borne encephalitis virus infects human brain microvascular endothelial cells without compromising blood-brain barrier integrity**. *Virology* 2017, **507**:110-122.

52.   Gelpi E, Preusser M, Garzuly F, Holzmann H, Heinz FX, Budka H: **Visualization of Central European tick-borne encephalitis infection in fatal human cases**. *Journal of neuropathology and experimental neurology* 2005, **64**(6):506-512.

53.   Palus M, Bily T, Elsterova J, Langhansova H, Salat J, Vancova M, Ruzek D: **Infection and injury of human astrocytes by tick-borne encephalitis virus**. *The Journal of general virology* 2014, **95**(Pt 11):2411-2426.

54.   Gelpi E, Preusser M, Laggner U, Garzuly F, Holzmann H, Heinz FX, Budka H: **Inflammatory response in human tick-borne encephalitis: analysis of postmortem brain tissue**. *Journal of neurovirology* 2006, **12**(4):322-327.

55. Ruzek D, Salat J, Palus M, Gritsun TS, Gould EA, Dykova I, Skallova A, Jelinek J, Kopecky J, Grubhoffer L: **CD8+ T-cells mediate immunopathology in tick-borne encephalitis**. *Virology* 2009, **384**(1):1-6.

56. **TBEV - Fact Sheet** [https://www.who.int/immunization/diseases/tick_encephalitis/en/]

57. Suss J: **Tick-borne encephalitis 2010: epidemiology, risk areas, and virus strains in Europe and Asia-an overview**. *Ticks and tick-borne diseases* 2011, **2**(1):2-15.

58. **TBE Cases by year: Number of TBE cases, regardless of the applied case definition, by year reported in 16 EU/EFTA countries, 2000–2010 (n= 29 381)** [https://www.ecdc.europa.eu/en/publications-data/tbe-cases-year-number-tbe-cases-regardless-applied-case-definition-year-reported]

59. Haglund M, Gunther G: **Tick-borne encephalitis--pathogenesis, clinical course and long-term follow-up**. *Vaccine* 2003, **21 Suppl 1**:S11-18.

60. Lindquist L, Vapalahti O: **Tick-borne encephalitis**. *Lancet (London, England)* 2008, **371**(9627):1861-1871.

61. Kaiser R: **The clinical and epidemiological profile of tick-borne encephalitis in southern Germany 1994-98: a prospective study of 656 patients**. *Brain : a journal of neurology* 1999, **122 (Pt 11)**:2067-2078.

62. Barrows NJ, Campos RK, Liao KC, Prasanth KR, Soto-Acosta R, Yeh SC, Schott-Lerner G, Pompon J, Sessions OM, Bradrick SS *et al*: **Biochemistry and Molecular Biology of Flaviviruses**. *Chemical reviews* 2018, **118**(8):4448-4482.

63. Pulkkinen LIA, Butcher SJ, Anastasina M: **Tick-Borne Encephalitis Virus: A Structural View**. *Viruses* 2018, **10**(7).

64. Wengler G, Wengler G, Gross HJ: **Studies on virus-specific nucleic acids synthesized in vertebrate and mosquito cells infected with flaviviruses**. *Virology* 1978, **89**(2):423-437.

65. Wallner G, Mandl CW, Kunz C, Heinz FX: **The flavivirus 3'-noncoding region: extensive size heterogeneity independent of evolutionary relationships among strains of tick-borne encephalitis virus**. *Virology* 1995, **213**(1):169-178.

66.   Mandl CW: **Steps of the tick-borne encephalitis virus replication cycle that affect neuropathogenesis**. *Virus research* 2005, **111**(2):161-174.

67.   Filomatori CV, Lodeiro MF, Alvarez DE, Samsa MM, Pietrasanta L, Gamarnik AV: **A 5' RNA element promotes dengue virus RNA synthesis on a circular genome**. *Genes & development* 2006, **20**(16):2238-2249.

68.   Rouha H, Hoenninger VM, Thurner C, Mandl CW: **Mutational analysis of three predicted 5'-proximal stem-loop structures in the genome of tick-borne encephalitis virus indicates different roles in RNA replication and translation**. *Virology* 2011, **417**(1):79-86.

69.   Hodge K, Tunghirun C, Kamkaew M, Limjindaporn T, Yenchitsomanus PT, Chimnaronk S: **Identification of a Conserved RNA-dependent RNA Polymerase (RdRp)-RNA Interface Required for Flaviviral Replication**. *The Journal of biological chemistry* 2016, **291**(33):17437-17449.

70.   Sakai M, Yoshii K, Sunden Y, Yokozawa K, Hirano M, Kariwa H: **Variable region of the 3' UTR is a critical virulence factor in the Far-Eastern subtype of tick-borne encephalitis virus in a mouse model**. *The Journal of general virology* 2014, **95**(Pt 4):823-835.

71.   Neufeldt CJ, Cortese M, Acosta EG, Bartenschlager R: **Rewiring cellular networks by members of the Flaviviridae family**. *Nature reviews Microbiology* 2018, **16**(3):125-142.

72.   Pijlman GP, Funk A, Kondratieva N, Leung J, Torres S, van der Aa L, Liu WJ, Palmenberg AC, Shi PY, Hall RA *et al*: **A highly structured, nuclease-resistant, noncoding RNA produced by flaviviruses is required for pathogenicity**. *Cell host & microbe* 2008, **4**(6):579-591.

73.   Chang RY, Hsu TW, Chen YL, Liu SF, Tsai YJ, Lin YT, Chen YS, Fan YH: **Japanese encephalitis virus non-coding RNA inhibits activation of interferon by blocking nuclear translocation of interferon regulatory factor 3**. *Veterinary microbiology* 2013, **166**(1-2):11-21.

74.   Schnettler E, Sterken MG, Leung JY, Metz SW, Geertsema C, Goldbach RW, Vlak JM, Kohl A, Khromykh AA, Pijlman GP: **Noncoding flavivirus RNA displays RNA interference suppressor activity in insect and Mammalian cells**. *Journal of virology* 2012, **86**(24):13486-13500.

75. Schnettler E, Tykalova H, Watson M, Sharma M, Sterken MG, Obbard DJ, Lewis SH, McFarlane M, Bell-Sakyi L, Barry G *et al*: **Induction and suppression of tick cell antiviral RNAi responses by tick-borne flaviviruses**. *Nucleic acids research* 2014, **42**(14):9436-9446.

76. Welsch S, Miller S, Romero-Brey I, Merz A, Bleck CK, Walther P, Fuller SD, Antony C, Krijnse-Locker J, Bartenschlager R: **Composition and three-dimensional architecture of the dengue virus replication and assembly sites**. *Cell host & microbe* 2009, **5**(4):365-375.

77. Gillespie LK, Hoenen A, Morgan G, Mackenzie JM: **The endoplasmic reticulum provides the membrane platform for biogenesis of the flavivirus replication complex**. *Journal of virology* 2010, **84**(20):10438-10447.

78. Miorin L, Romero-Brey I, Maiuri P, Hoppe S, Krijnse-Locker J, Bartenschlager R, Marcello A: **Three-dimensional architecture of tick-borne encephalitis virus replication sites and trafficking of the replicated RNA**. *Journal of virology* 2013, **87**(11):6469-6481.

79. Bily T, Palus M, Eyer L, Elsterova J, Vancova M, Ruzek D: **Electron Tomography Analysis of Tick-Borne Encephalitis Virus Infection in Human Neurons**. *Scientific reports* 2015, **5**:10745.

80. Overby AK, Popov VL, Niedrig M, Weber F: **Tick-borne encephalitis virus delays interferon induction and hides its double-stranded RNA in intracellular membrane vesicles**. *Journal of virology* 2010, **84**(17):8470-8483.

81. Miorin L, Albornoz A, Baba MM, D'Agaro P, Marcello A: **Formation of membrane-defined compartments by tick-borne encephalitis virus contributes to the early delay in interferon signaling**. *Virus research* 2012, **163**(2):660-666.

82. Mackenzie JM, Westaway EG: **Assembly and maturation of the flavivirus Kunjin virus appear to occur in the rough endoplasmic reticulum and along the secretory pathway, respectively**. *Journal of virology* 2001, **75**(22):10787-10799.

83. Kashem SW, Haniffa M, Kaplan DH: **Antigen-Presenting Cells in the Skin**. *Annual review of immunology* 2017, **35**:469-499.

84. Diamond MS, Shrestha B, Marri A, Mahan D, Engle M: **B cells and antibody play critical roles in the immediate defense of disseminated infection by West Nile encephalitis virus**. *Journal of virology* 2003, **77**(4):2578-2586.

85. Kaufman BM, Summers PL, Dubois DR, Cohen WH, Gentry MK, Timchak RL, Burke DS, Eckels KH: **Monoclonal antibodies for dengue virus prM glycoprotein protect mice against lethal dengue infection**. *The American journal of tropical medicine and hygiene* 1989, **41**(5):576-580.

86. Kimura-Kuroda J, Yasui K: **Protection of mice against Japanese encephalitis virus by passive administration with monoclonal antibodies**. *Journal of immunology (Baltimore, Md : 1950)* 1988, **141**(10):3606-3610.

87. Jacobs SC, Stephenson JR, Wilkinson GW: **High-level expression of the tick-borne encephalitis virus NS1 protein by using an adenovirus-based vector: protection elicited in a murine model**. *Journal of virology* 1992, **66**(4):2086-2095.

88. Falgout B, Bray M, Schlesinger JJ, Lai CJ: **Immunization of mice with recombinant vaccinia virus expressing authentic dengue virus nonstructural protein NS1 protects against lethal dengue virus encephalitis**. *Journal of virology* 1990, **64**(9):4356-4363.

89. Hawkes RA: **ENHANCEMENT OF THE INFECTIVITY OF ARBOVIRUSES BY SPECIFIC ANTISERA PRODUCED IN DOMESTIC FOWLS**. *The Australian journal of experimental biology and medical science* 1964, **42**:465-482.

90. Halstead SB: **In vivo enhancement of dengue virus infection in rhesus monkeys by passively transferred antibody**. *The Journal of infectious diseases* 1979, **140**(4):527-533.

91. Blum JS, Wearsch PA, Cresswell P: **Pathways of antigen processing**. *Annual review of immunology* 2013, **31**:443-473.

92. Shrestha B, Diamond MS: **Role of CD8+ T cells in control of West Nile virus infection**. *Journal of virology* 2004, **78**(15):8312-8321.

93. Yauch LE, Zellweger RM, Kotturi MF, Qutubuddin A, Sidney J, Peters B, Prestwood TR, Sette A, Shresta S: **A protective role for dengue virus-specific CD8+ T cells**. *Journal of immunology (Baltimore, Md : 1950)* 2009, **182**(8):4865-4873.

94. Larena M, Regner M, Lee E, Lobigs M: **Pivotal role of antibody and subsidiary contribution of CD8+ T cells to recovery from infection in a murine model of Japanese encephalitis**. *Journal of virology* 2011, **85**(11):5446-5455.

95.   Sitati EM, Diamond MS: **CD4+ T-cell responses are required for clearance of West Nile virus from the central nervous system**. *Journal of virology* 2006, **80**(24):12060-12069.

96.   Rivino L, Kumaran EA, Jovanovic V, Nadua K, Teo EW, Pang SW, Teo GH, Gan VC, Lye DC, Leo YS *et al*: **Differential targeting of viral components by CD4+ versus CD8+ T lymphocytes in dengue virus infection**. *Journal of virology* 2013, **87**(5):2693-2706.

97.   Gomez I, Marx F, Saurwein-Teissl M, Gould EA, Grubeck-Loebenstein B: **Characterization of tick-borne encephalitis virus-specific human T lymphocyte responses by stimulation with structural TBEV proteins expressed in a recombinant baculovirus**. *Viral immunology* 2003, **16**(3):407-414.

98.   Hayasaka D, Nagata N, Fujii Y, Hasegawa H, Sata T, Suzuki R, Gould EA, Takashima I, Koike S: **Mortality following peripheral infection with tick-borne encephalitis virus results from a combination of central nervous system pathology, systemic inflammatory and stress responses**. *Virology* 2009, **390**(1):139-150.

99.   Caligiuri MA: **Human natural killer cells**. *Blood* 2008, **112**(3):461-469.

100.   Azeredo EL, De Oliveira-Pinto LM, Zagne SM, Cerqueira DI, Nogueira RM, Kubelka CF: **NK cells, displaying early activation, cytotoxicity and adhesion molecules, are associated with mild dengue disease**. *Clinical and experimental immunology* 2006, **143**(2):345-356.

101.   Blom K, Braun M, Pakalniene J, Lunemann S, Enqvist M, Dailidyte L, Schaffer M, Lindquist L, Mickiene A, Michaelsson J *et al*: **NK Cell Responses to Human Tick-Borne Encephalitis Virus Infection**. *Journal of immunology (Baltimore, Md : 1950)* 2016, **197**(7):2762-2771.

102.   Quaresma JA, Barros VL, Pagliari C, Fernandes ER, Andrade HF, Jr., Vasconcelos PF, Duarte MI: **Hepatocyte lesions and cellular immune response in yellow fever infection**. *Transactions of the Royal Society of Tropical Medicine and Hygiene* 2007, **101**(2):161-168.

103.   Vargin VV, Semenov BF: **Changes of natural killer cell activity in different mouse lines by acute and asymptomatic flavivirus infections**. *Acta virologica* 1986, **30**(4):303-308.

104. Shrestha B, Samuel MA, Diamond MS: **CD8+ T cells require perforin to clear West Nile virus from infected neurons**. *Journal of virology* 2006, **80**(1):119-129.

105. Conde JN, Silva EM, Barbosa AS, Mohana-Borges R: **The Complement System in Flavivirus Infections**. *Frontiers in microbiology* 2017, **8**:213.

106. Mehlhop E, Whitby K, Oliphant T, Marri A, Engle M, Diamond MS: **Complement activation is required for induction of a protective antibody response against West Nile virus infection**. *Journal of virology* 2005, **79**(12):7466-7477.

107. Fuchs A, Lin TY, Beasley DW, Stover CM, Schwaeble WJ, Pierson TC, Diamond MS: **Direct complement restriction of flavivirus infection requires glycan recognition by mannose-binding lectin**. *Cell host & microbe* 2010, **8**(2):186-195.

108. Mehlhop E, Ansarah-Sobrinho C, Johnson S, Engle M, Fremont DH, Pierson TC, Diamond MS: **Complement protein C1q inhibits antibody-dependent enhancement of flavivirus infection in an IgG subclass-specific manner**. *Cell host & microbe* 2007, **2**(6):417-426.

109. Jensen S, Thomsen AR: **Sensing of RNA viruses: a review of innate immune receptors involved in recognizing RNA virus invasion**. *Journal of virology* 2012, **86**(6):2900-2910.

110. Melchjorsen J: **Learning from the messengers: innate sensing of viruses and cytokine regulation of immunity - clues for treatments and vaccines**. *Viruses* 2013, **5**(2):470-527.

111. Diamond MS, Roberts TG, Edgil D, Lu B, Ernst J, Harris E: **Modulation of Dengue virus infection in human cells by alpha, beta, and gamma interferons**. *Journal of virology* 2000, **74**(11):4957-4966.

112. Anderson JF, Rahal JJ: **Efficacy of interferon alpha-2b and ribavirin against West Nile virus in vitro**. *Emerging infectious diseases* 2002, **8**(1):107-108.

113. Cho H, Proll SC, Szretter KJ, Katze MG, Gale M, Jr., Diamond MS: **Differential innate immune response programs in neuronal subtypes determine susceptibility to infection in the brain by positive-stranded RNA viruses**. *Nature medicine* 2013, **19**(4):458-464.

114.   Lindqvist R, Mundt F, Gilthorpe JD, Wolfel S, Gekara NO, Kroger A, Overby AK: **Fast type I interferon response protects astrocytes from flavivirus infection and virus-induced cytopathic effects**. *Journal of neuroinflammation* 2016, **13**(1):277.

115.   Weber E, Finsterbusch K, Lindquist R, Nair S, Lienenklaus S, Gekara NO, Janik D, Weiss S, Kalinke U, Overby AK *et al*: **Type I interferon protects mice from fatal neurotropic infection with Langat virus by systemic and local antiviral responses**. *Journal of virology* 2014, **88**(21):12202-12212.

116.   McNab F, Mayer-Barber K, Sher A, Wack A, O'Garra A: **Type I interferons in infectious disease**. *Nature reviews Immunology* 2015, **15**(2):87-103.

117.   Schroder K, Hertzog PJ, Ravasi T, Hume DA: **Interferon-gamma: an overview of signals, mechanisms and functions**. *Journal of leukocyte biology* 2004, **75**(2):163-189.

118.   Shrestha B, Wang T, Samuel MA, Whitby K, Craft J, Fikrig E, Diamond MS: **Gamma interferon plays a crucial early antiviral role in protection against West Nile virus infection**. *Journal of virology* 2006, **80**(11):5338-5348.

119.   Schneider WM, Chevillotte MD, Rice CM: **Interferon-stimulated genes: a complex web of host defenses**. *Annual review of immunology* 2014, **32**:513-545.

120.   Kotenko SV, Gallagher G, Baurin VV, Lewis-Antes A, Shen M, Shah NK, Langer JA, Sheikh F, Dickensheets H, Donnelly RP: **IFN-lambdas mediate antiviral protection through a distinct class II cytokine receptor complex**. *Nature immunology* 2003, **4**(1):69-77.

121.   Sheppard P, Kindsvogel W, Xu W, Henderson K, Schlutsmeyer S, Whitmore TE, Kuestner R, Garrigues U, Birks C, Roraback J *et al*: **IL-28, IL-29 and their class II cytokine receptor IL-28R**. *Nature immunology* 2003, **4**(1):63-68.

122.   Marcello T, Grakoui A, Barba-Spaeth G, Machlin ES, Kotenko SV, MacDonald MR, Rice CM: **Interferons alpha and lambda inhibit hepatitis C virus replication with distinct signal transduction and gene regulation kinetics**. *Gastroenterology* 2006, **131**(6):1887-1898.

123.   Bolen CR, Ding S, Robek MD, Kleinstein SH: **Dynamic expression profiling of type I and type III interferon-stimulated hepatocytes reveals a stable hierarchy of gene expression**. *Hepatology (Baltimore, Md)* 2014, **59**(4):1262-1272.

124. Sommereyns C, Paul S, Staeheli P, Michiels T: **IFN-lambda (IFN-lambda) is expressed in a tissue-dependent fashion and primarily acts on epithelial cells in vivo**. *PLoS pathogens* 2008, **4**(3):e1000017.

125. Palma-Ocampo HK, Flores-Alonso JC, Vallejo-Ruiz V, Reyes-Leyva J, Flores-Mendoza L, Herrera-Camacho I, Rosas-Murrieta NH, Santos-Lopez G: **Interferon lambda inhibits dengue virus replication in epithelial cells**. *Virology journal* 2015, **12**:150.

126. Lazear HM, Daniels BP, Pinto AK, Huang AC, Vick SC, Doyle SE, Gale M, Jr., Klein RS, Diamond MS: **Interferon-lambda restricts West Nile virus neuroinvasion by tightening the blood-brain barrier**. *Science translational medicine* 2015, **7**(284):284ra259.

127. Bayer A, Lennemann NJ, Ouyang Y, Bramley JC, Morosky S, Marques ET, Jr., Cherry S, Sadovsky Y, Coyne CB: **Type III Interferons Produced by Human Placental Trophoblasts Confer Protection against Zika Virus Infection**. *Cell host & microbe* 2016, **19**(5):705-712.

128. Meurs E, Chong K, Galabru J, Thomas NS, Kerr IM, Williams BR, Hovanessian AG: **Molecular cloning and characterization of the human double-stranded RNA-activated protein kinase induced by interferon**. *Cell* 1990, **62**(2):379-390.

129. Nanduri S, Carpick BW, Yang Y, Williams BR, Qin J: **Structure of the double-stranded RNA-binding domain of the protein kinase PKR reveals the molecular basis of its dsRNA-mediated activation**. *The EMBO journal* 1998, **17**(18):5458-5465.

130. Romano PR, Garcia-Barrio MT, Zhang X, Wang Q, Taylor DR, Zhang F, Herring C, Mathews MB, Qin J, Hinnebusch AG: **Autophosphorylation in the activation loop is required for full kinase activity in vivo of human and yeast eukaryotic initiation factor 2alpha kinases PKR and GCN2**. *Molecular and cellular biology* 1998, **18**(4):2282-2297.

131. Pakos-Zebrucka K, Koryga I, Mnich K, Ljujic M, Samali A, Gorman AM: **The integrated stress response**. *EMBO reports* 2016, **17**(10):1374-1395.

132. Ank N, West H, Bartholdy C, Eriksson K, Thomsen AR, Paludan SR: **Lambda interferon (IFN-lambda), a type III IFN, is induced by viruses and IFNs and displays potent antiviral activity against select virus infections in vivo**. *Journal of virology* 2006, **80**(9):4501-4509.

133.   Schulz O, Pichlmair A, Rehwinkel J, Rogers NC, Scheuner D, Kato H, Takeuchi O, Akira S, Kaufman RJ, Reis e Sousa C: **Protein kinase R contributes to immunity against specific viruses by regulating interferon mRNA integrity**. *Cell host & microbe* 2010, **7**(5):354-361.

134.   Pham AM, Santa Maria FG, Lahiri T, Friedman E, Marie IJ, Levy DE: **PKR Transduces MDA5-Dependent Signals for Type I IFN Induction**. *PLoS pathogens* 2016, **12**(3):e1005489.

135.   Noguchi T, Satoh S, Noshi T, Hatada E, Fukuda R, Kawai A, Ikeda S, Hijikata M, Shimotohno K: **Effects of mutation in hepatitis C virus nonstructural protein 5A on interferon resistance mediated by inhibition of PKR kinase activity in mammalian cells**. *Microbiology and immunology* 2001, **45**(12):829-840.

136.   Samuel MA, Whitby K, Keller BC, Marri A, Barchet W, Williams BR, Silverman RH, Gale M, Jr., Diamond MS: **PKR and RNase L contribute to protection against lethal West Nile Virus infection by controlling early viral spread in the periphery and replication in neurons**. *Journal of virology* 2006, **80**(14):7009-7019.

137.   Balachandran S, Roberts PC, Brown LE, Truong H, Pattnaik AK, Archer DR, Barber GN: **Essential role for the dsRNA-dependent protein kinase PKR in innate immunity to viral infection**. *Immunity* 2000, **13**(1):129-141.

138.   Roth H, Magg V, Uch F, Mutz P, Klein P, Haneke K, Lohmann V, Bartenschlager R, Fackler OT, Locker N *et al*: **Flavivirus Infection Uncouples Translation Suppression from Cellular Stress Responses**. *mBio* 2017, **8**(1).

139.   Rajsbaum R, Garcia-Sastre A, Versteeg GA: **TRIMmunity: the roles of the TRIM E3-ubiquitin ligase family in innate antiviral immunity**. *Journal of molecular biology* 2014, **426**(6):1265-1284.

140.   Hatakeyama S: **TRIM Family Proteins: Roles in Autophagy, Immunity, and Carcinogenesis**. *Trends in biochemical sciences* 2017, **42**(4):297-311.

141.   Wang K, Zou C, Wang X, Huang C, Feng T, Pan W, Wu Q, Wang P, Dai J: **Interferon-stimulated TRIM69 interrupts dengue virus replication by ubiquitinating viral nonstructural protein 3**. *PLoS pathogens* 2018, **14**(8):e1007287.

142.   Taylor RT, Lubick KJ, Robertson SJ, Broughton JP, Bloom ME, Bresnahan WA, Best SM: **TRIM79alpha, an interferon-stimulated gene product, restricts tick-borne encephalitis virus replication**

by degrading the viral RNA polymerase. *Cell host & microbe* 2011, **10**(3):185-196.

143. Yang D, Li NL, Wei D, Liu B, Guo F, Elbahesh H, Zhang Y, Zhou Z, Chen GY, Li K: **The E3 ligase TRIM56 is a host restriction factor of Zika virus and depends on its RNA-binding activity but not miRNA regulation, for antiviral function**. *PLoS neglected tropical diseases* 2019, **13**(6):e0007537.

144. Manocha GD, Mishra R, Sharma N, Kumawat KL, Basu A, Singh SK: **Regulatory role of TRIM21 in the type-I interferon pathway in Japanese encephalitis virus-infected human microglial cells**. *Journal of neuroinflammation* 2014, **11**:24.

145. Diamond MS, Farzan M: **The broad-spectrum antiviral functions of IFIT and IFITM proteins**. *Nature reviews Immunology* 2013, **13**(1):46-57.

146. Fensterl V, Sen GC: **Interferon-induced Ifit proteins: their role in viral pathogenesis**. *Journal of virology* 2015, **89**(5):2462-2468.

147. Abbas YM, Pichlmair A, Gorna MW, Superti-Furga G, Nagar B: **Structural basis for viral 5'-PPP-RNA recognition by human IFIT proteins**. *Nature* 2013, **494**(7435):60-64.

148. Katibah GE, Lee HJ, Huizar JP, Vogan JM, Alber T, Collins K: **tRNA binding, structure, and localization of the human interferon-induced protein IFIT5**. *Molecular cell* 2013, **49**(4):743-750.

149. Yang Z, Liang H, Zhou Q, Li Y, Chen H, Ye W, Chen D, Fleming J, Shu H, Liu Y: **Crystal structure of ISG54 reveals a novel RNA binding structure and potential functional mechanisms**. *Cell research* 2012, **22**(9):1328-1338.

150. Hui DJ, Bhasker CR, Merrick WC, Sen GC: **Viral stress-inducible protein p56 inhibits translation by blocking the interaction of eIF3 with the ternary complex eIF2.GTP.Met-tRNAi**. *The Journal of biological chemistry* 2003, **278**(41):39477-39482.

151. Terenzi F, Pal S, Sen GC: **Induction and mode of action of the viral stress-inducible murine proteins, P56 and P54**. *Virology* 2005, **340**(1):116-124.

152. Saikia P, Fensterl V, Sen GC: **The inhibitory action of P56 on select functions of E1 mediates interferon's effect on human papillomavirus DNA replication**. *Journal of virology* 2010, **84**(24):13036-13039.

153.   Pichlmair A, Lassnig C, Eberle CA, Gorna MW, Baumann CL, Burkard TR, Burckstummer T, Stefanovic A, Krieger S, Bennett KL *et al*: **IFIT1 is an antiviral protein that recognizes 5'-triphosphate RNA**. *Nature immunology* 2011, **12**(7):624-630.

154.   Kumar P, Sweeney TR, Skabkin MA, Skabkina OV, Hellen CU, Pestova TV: **Inhibition of translation by IFIT family members is determined by their ability to interact selectively with the 5'-terminal regions of cap0-, cap1- and 5'ppp- mRNAs**. *Nucleic acids research* 2014, **42**(5):3228-3245.

155.   Habjan M, Hubel P, Lacerda L, Benda C, Holze C, Eberl CH, Mann A, Kindler E, Gil-Cruz C, Ziebuhr J *et al*: **Sequestration by IFIT1 impairs translation of 2'O-unmethylated capped RNA**. *PLoS pathogens* 2013, **9**(10):e1003663.

156.   Abbas YM, Laudenbach BT, Martinez-Montero S, Cencic R, Habjan M, Pichlmair A, Damha MJ, Pelletier J, Nagar B: **Structure of human IFIT1 with capped RNA reveals adaptable mRNA binding and mechanisms for sensing N1 and N2 ribose 2'-O methylations**. *Proceedings of the National Academy of Sciences of the United States of America* 2017, **114**(11):E2106-e2115.

157.   Kimura T, Katoh H, Kayama H, Saiga H, Okuyama M, Okamoto T, Umemoto E, Matsuura Y, Yamamoto M, Takeda K: **Ifit1 inhibits Japanese encephalitis virus replication through binding to 5' capped 2'-O unmethylated RNA**. *Journal of virology* 2013, **87**(18):9997-10003.

158.   Szretter KJ, Daniels BP, Cho H, Gainey MD, Yokoyama WM, Gale M, Jr., Virgin HW, Klein RS, Sen GC, Diamond MS: **2'-O methylation of the viral mRNA cap by West Nile virus evades ifit1-dependent and -independent mechanisms of host restriction in vivo**. *PLoS pathogens* 2012, **8**(5):e1002698.

159.   Cho H, Shrestha B, Sen GC, Diamond MS: **A role for Ifit2 in restricting West Nile virus infection in the brain**. *Journal of virology* 2013, **87**(15):8363-8371.

160.   Perreira JM, Chin CR, Feeley EM, Brass AL: **IFITMs restrict the replication of multiple pathogenic viruses**. *Journal of molecular biology* 2013, **425**(24):4937-4955.

161.   Bailey CC, Zhong G, Huang IC, Farzan M: **IFITM-Family Proteins: The Cell's First Line of Antiviral Defense**. *Annual review of virology* 2014, **1**:261-283.

162. Brass AL, Huang IC, Benita Y, John SP, Krishnan MN, Feeley EM, Ryan BJ, Weyer JL, van der Weyden L, Fikrig E *et al*: **The IFITM proteins mediate cellular resistance to influenza A H1N1 virus, West Nile virus, and dengue virus**. *Cell* 2009, **139**(7):1243-1254.

163. Jiang D, Weidner JM, Qing M, Pan XB, Guo H, Xu C, Zhang X, Birk A, Chang J, Shi PY *et al*: **Identification of five interferon-induced cellular proteins that inhibit west nile virus and dengue virus infections**. *Journal of virology* 2010, **84**(16):8332-8341.

164. Savidis G, Perreira JM, Portmann JM, Meraner P, Guo Z, Green S, Brass AL: **The IFITMs Inhibit Zika Virus Replication**. *Cell reports* 2016, **15**(11):2323-2330.

165. Zhu X, He Z, Yuan J, Wen W, Huang X, Hu Y, Lin C, Pan J, Li R, Deng H *et al*: **IFITM3-containing exosome as a novel mediator for anti-viral response in dengue virus infection**. *Cellular microbiology* 2015, **17**(1):105-118.

166. Haas AL, Ahrens P, Bright PM, Ankel H: **Interferon induces a 15-kilodalton protein exhibiting marked homology to ubiquitin**. *The Journal of biological chemistry* 1987, **262**(23):11315-11323.

167. Blomstrom DC, Fahey D, Kutny R, Korant BD, Knight E, Jr.: **Molecular characterization of the interferon-induced 15-kDa protein. Molecular cloning and nucleotide and amino acid sequence**. *The Journal of biological chemistry* 1986, **261**(19):8811-8816.

168. Loeb KR, Haas AL: **The interferon-inducible 15-kDa ubiquitin homolog conjugates to intracellular proteins**. *The Journal of biological chemistry* 1992, **267**(11):7806-7813.

169. Perng YC, Lenschow DJ: **ISG15 in antiviral immunity and beyond**. *Nature reviews Microbiology* 2018, **16**(7):423-439.

170. Giannakopoulos NV, Luo JK, Papov V, Zou W, Lenschow DJ, Jacobs BS, Borden EC, Li J, Virgin HW, Zhang DE: **Proteomic identification of proteins conjugated to ISG15 in mouse and human cells**. *Biochemical and biophysical research communications* 2005, **336**(2):496-506.

171. Zhao C, Denison C, Huibregtse JM, Gygi S, Krug RM: **Human ISG15 conjugation targets both IFN-induced and constitutively expressed proteins functioning in diverse cellular pathways**. *Proceedings of the National Academy of Sciences of the United States of America* 2005, **102**(29):10200-10205.

172.   Zhao C, Hsiang TY, Kuo RL, Krug RM: **ISG15 conjugation system targets the viral NS1 protein in influenza A virus-infected cells**. *Proceedings of the National Academy of Sciences of the United States of America* 2010, **107**(5):2253-2258.

173.   Zhang X, Bogunovic D, Payelle-Brogard B, Francois-Newton V, Speer SD, Yuan C, Volpi S, Li Z, Sanal O, Mansouri D *et al*: **Human intracellular ISG15 prevents interferon-alpha/beta over-amplification and auto-inflammation**. *Nature* 2015, **517**(7532):89-93.

174.   Sanyal S, Ashour J, Maruyama T, Altenburg AF, Cragnolini JJ, Bilate A, Avalos AM, Kundrat L, Garcia-Sastre A, Ploegh HL: **Type I interferon imposes a TSG101/ISG15 checkpoint at the Golgi for glycoprotein trafficking during influenza virus infection**. *Cell host & microbe* 2013, **14**(5):510-521.

175.   Hsiao NW, Chen JW, Yang TC, Orloff GM, Wu YY, Lai CH, Lan YC, Lin CW: **ISG15 over-expression inhibits replication of the Japanese encephalitis virus in human medulloblastoma cells**. *Antiviral research* 2010, **85**(3):504-511.

176.   Dai J, Pan W, Wang P: **ISG15 facilitates cellular antiviral response to dengue and west nile virus infection in vitro**. *Virology journal* 2011, **8**:468.

177.   Broering R, Zhang X, Kottilil S, Trippler M, Jiang M, Lu M, Gerken G, Schlaak JF: **The interferon stimulated gene 15 functions as a proviral factor for the hepatitis C virus and as a regulator of the IFN response**. *Gut* 2010, **59**(8):1111-1119.

178.   Malathi K, Dong B, Gale M, Jr., Silverman RH: **Small self-RNA generated by RNase L amplifies antiviral innate immunity**. *Nature* 2007, **448**(7155):816-819.

179.   Donovan J, Rath S, Kolet-Mandrikov D, Korennykh A: **Rapid RNase L-driven arrest of protein synthesis in the dsRNA response without degradation of translation machinery**. *RNA (New York, NY)* 2017, **23**(11):1660-1671.

180.   Rath S, Prangley E, Donovan J, Demarest K, Wingreen NS, Meir Y, Korennykh A: **Concerted 2-5A-Mediated mRNA Decay and Transcription Reprogram Protein Synthesis in the dsRNA Response**. *Molecular cell* 2019, **75**(6):1218-1228.e1216.

181.   Hornung V, Hartmann R, Ablasser A, Hopfner KP: **OAS proteins and cGAS: unifying concepts in sensing and responding to**

cytosolic nucleic acids. *Nature reviews Immunology* 2014, **14**(8):521-528.

182.   Zhu J, Ghosh A, Sarkar SN: **OASL-a new player in controlling antiviral innate immunity**. *Current opinion in virology* 2015, **12**:15-19.

183.   Deo S, Patel TR, Dzananovic E, Booy EP, Zeid K, McEleney K, Harding SE, McKenna SA: **Activation of 2' 5'-oligoadenylate synthetase by stem loops at the 5'-end of the West Nile virus genome**. *PloS one* 2014, **9**(3):e92545.

184.   Lim JK, Lisco A, McDermott DH, Huynh L, Ward JM, Johnson B, Johnson H, Pape J, Foster GA, Krysztof D *et al*: **Genetic variation in OAS1 is a risk factor for initial infection with West Nile virus in man**. *PLoS pathogens* 2009, **5**(2):e1000321.

185.   Lin RJ, Yu HP, Chang BL, Tang WC, Liao CL, Lin YL: **Distinct antiviral roles for human 2',5'-oligoadenylate synthetase family members against dengue virus infection**. *Journal of immunology (Baltimore, Md : 1950)* 2009, **183**(12):8035-8043.

186.   Hartmann R, Olsen HS, Widder S, Jorgensen R, Justesen J: **p59OASL, a 2'-5' oligoadenylate synthetase like protein: a novel human gene related to the 2'-5' oligoadenylate synthetase family**. *Nucleic acids research* 1998, **26**(18):4121-4128.

187.   Rebouillat D, Marie I, Hovanessian AG: **Molecular cloning and characterization of two related and interferon-induced 56-kDa and 30-kDa proteins highly similar to 2'-5' oligoadenylate synthetase**. *European journal of biochemistry* 1998, **257**(2):319-330.

188.   Marques J, Anwar J, Eskildsen-Larsen S, Rebouillat D, Paludan SR, Sen G, Williams BR, Hartmann R: **The p59 oligoadenylate synthetase-like protein possesses antiviral activity that requires the C-terminal ubiquitin-like domain**. *The Journal of general virology* 2008, **89**(Pt 11):2767-2772.

189.   Ishibashi M, Wakita T, Esumi M: **2',5'-Oligoadenylate synthetase-like gene highly induced by hepatitis C virus infection in human liver is inhibitory to viral replication in vitro**. *Biochemical and biophysical research communications* 2010, **392**(3):397-402.

190.   Guo X, Li X, Xu Y, Sun T, Yang G, Wu Z, Li E: **Identification of OASL d, a splice variant of human OASL, with antiviral activity**. *The international journal of biochemistry & cell biology* 2012, **44**(7):1133-1138.

191.   Zhu H, Cong JP, Shenk T: **Use of differential display analysis to assess the effect of human cytomegalovirus infection on the accumulation of cellular RNAs: induction of interferon-responsive RNAs**. *Proceedings of the National Academy of Sciences of the United States of America* 1997, **94**(25):13985-13990.

192.   Helbig KJ, Beard MR: **The role of viperin in the innate antiviral response**. *Journal of molecular biology* 2014, **426**(6):1210-1219.

193.   Lindqvist R, Overby AK: **The Role of Viperin in Antiflavivirus Responses**. *DNA and cell biology* 2018, **37**(9):725-730.

194.   Helbig KJ, Eyre NS, Yip E, Narayana S, Li K, Fiches G, McCartney EM, Jangra RK, Lemon SM, Beard MR: **The antiviral protein viperin inhibits hepatitis C virus replication via interaction with nonstructural protein 5A**. *Hepatology (Baltimore, Md)* 2011, **54**(5):1506-1517.

195.   Wang S, Wu X, Pan T, Song W, Wang Y, Zhang F, Yuan Z: **Viperin inhibits hepatitis C virus replication by interfering with binding of NS5A to host protein hVAP-33**. *The Journal of general virology* 2012, **93**(Pt 1):83-92.

196.   Wang X, Hinson ER, Cresswell P: **The interferon-inducible protein viperin inhibits influenza virus release by perturbing lipid rafts**. *Cell host & microbe* 2007, **2**(2):96-105.

197.   Upadhyay AS, Vonderstein K, Pichlmair A, Stehling O, Bennett KL, Dobler G, Guo JT, Superti-Furga G, Lill R, Overby AK *et al*: **Viperin is an iron-sulfur protein that inhibits genome synthesis of tick-borne encephalitis virus via radical SAM domain activity**. *Cellular microbiology* 2014, **16**(6):834-848.

198.   Vonderstein K, Nilsson E, Hubel P, Nygard Skalman L, Upadhyay A, Pasto J, Pichlmair A, Lundmark R, Overby AK: **Viperin Targets Flavivirus Virulence by Inducing Assembly of Noninfectious Capsid Particles**. *Journal of virology* 2018, **92**(1).

199.   Panayiotou C, Lindqvist R, Kurhade C, Vonderstein K, Pasto J, Edlund K, Upadhyay AS, Overby AK: **Viperin Restricts Zika Virus and Tick-Borne Encephalitis Virus Replication by Targeting NS3 for Proteasomal Degradation**. *Journal of virology* 2018, **92**(7).

200.   Lindqvist R, Kurhade C, Gilthorpe JD, Overby AK: **Cell-type- and region-specific restriction of neurotropic flavivirus infection by viperin**. *Journal of neuroinflammation* 2018, **15**(1):80.

201. Chan YL, Chang TH, Liao CL, Lin YL: **The cellular antiviral protein viperin is attenuated by proteasome-mediated protein degradation in Japanese encephalitis virus-infected cells**. *Journal of virology* 2008, **82**(21):10455-10464.

202. Chin KC, Cresswell P: **Viperin (cig5), an IFN-inducible antiviral protein directly induced by human cytomegalovirus**. *Proceedings of the National Academy of Sciences of the United States of America* 2001, **98**(26):15125-15130.

203. Boudinot P, Riffault S, Salhi S, Carrat C, Sedlik C, Mahmoudi N, Charley B, Benmansour A: **Vesicular stomatitis virus and pseudorabies virus induce a vig1/cig5 homologue in mouse dendritic cells via different pathways**. *The Journal of general virology* 2000, **81**(Pt 11):2675-2682.

204. Dixit E, Boulant S, Zhang Y, Lee AS, Odendall C, Shum B, Hacohen N, Chen ZJ, Whelan SP, Fransen M *et al*: **Peroxisomes are signaling platforms for antiviral innate immunity**. *Cell* 2010, **141**(4):668-681.

205. Seo JY, Yaneva R, Hinson ER, Cresswell P: **Human cytomegalovirus directly induces the antiviral protein viperin to enhance infectivity**. *Science (New York, NY)* 2011, **332**(6033):1093-1097.

206. Ron D, Walter P: **Signal integration in the endoplasmic reticulum unfolded protein response**. *Nature reviews Molecular cell biology* 2007, **8**(7):519-529.

207. Hetz C: **The unfolded protein response: controlling cell fate decisions under ER stress and beyond**. *Nature reviews Molecular cell biology* 2012, **13**(2):89-102.

208. Reid DW, Campos RK, Child JR, Zheng T, Chan KWK, Bradrick SS, Vasudevan SG, Garcia-Blanco MA, Nicchitta CV: **Dengue Virus Selectively Annexes Endoplasmic Reticulum-Associated Translation Machinery as a Strategy for Co-opting Host Cell Protein Synthesis**. *Journal of virology* 2018, **92**(7).

209. Sharma M, Bhattacharyya S, Sharma KB, Chauhan S, Asthana S, Abdin MZ, Vrati S, Kalia M: **Japanese encephalitis virus activates autophagy through XBP1 and ATF6 ER stress sensors in neuronal cells**. *The Journal of general virology* 2017, **98**(5):1027-1039.

210. Yu C, Achazi K, Niedrig M: **Tick-borne encephalitis virus triggers inositol-requiring enzyme 1 (IRE1) and transcription factor 6**

(ATF6) pathways of unfolded protein response. *Virus research* 2013, **178**(2):471-477.

211. Carletti T, Zakaria MK, Faoro V, Reale L, Kazungu Y, Licastro D, Marcello A: **Viral priming of cell intrinsic innate antiviral signaling by the unfolded protein response**. *Nature communications* 2019, **10**(1):3889.

212. Courtney SC, Scherbik SV, Stockman BM, Brinton MA: **West nile virus infections suppress early viral RNA synthesis and avoid inducing the cell stress granule response**. *Journal of virology* 2012, **86**(7):3647-3657.

213. Hou S, Kumar A, Xu Z, Airo AM, Stryapunina I, Wong CP, Branton W, Tchesnokov E, Gotte M, Power C *et al*: **Zika Virus Hijacks Stress Granule Proteins and Modulates the Host Stress Response**. *Journal of virology* 2017, **91**(16).

214. Tan Z, Zhang W, Sun J, Fu Z, Ke X, Zheng C, Zhang Y, Li P, Liu Y, Hu Q *et al*: **ZIKV infection activates the IRE1-XBP1 and ATF6 pathways of unfolded protein response in neural cells**. *Journal of neuroinflammation* 2018, **15**(1):275.

215. Mackenzie JM, Khromykh AA, Parton RG: **Cholesterol manipulation by West Nile virus perturbs the cellular immune response**. *Cell host & microbe* 2007, **2**(4):229-239.

216. Ramanathan A, Robb GB, Chan SH: **mRNA capping: biological functions and applications**. *Nucleic acids research* 2016, **44**(16):7511-7526.

217. Daffis S, Szretter KJ, Schriewer J, Li J, Youn S, Errett J, Lin TY, Schneller S, Zust R, Dong H *et al*: **2'-O methylation of the viral mRNA cap evades host restriction by IFIT family members**. *Nature* 2010, **468**(7322):452-456.

218. Chang DC, Hoang LT, Mohamed Naim AN, Dong H, Schreiber MJ, Hibberd ML, Tan MJA, Shi PY: **Evasion of early innate immune response by 2'-O-methylation of dengue genomic RNA**. *Virology* 2016, **499**:259-266.

219. Bidet K, Dadlani D, Garcia-Blanco MA: **G3BP1, G3BP2 and CAPRIN1 are required for translation of interferon stimulated mRNAs and are targeted by a dengue virus non-coding RNA**. *PLoS pathogens* 2014, **10**(7):e1004242.

220. Manokaran G, Finol E, Wang C, Gunaratne J, Bahl J, Ong EZ, Tan HC, Sessions OM, Ward AM, Gubler DJ *et al*: **Dengue subgenomic**

RNA binds TRIM25 to inhibit interferon expression for epidemiological fitness. *Science (New York, NY)* 2015, **350**(6257):217-221.

221. Goertz GP, Fros JJ, Miesen P, Vogels CBF, van der Bent ML, Geertsema C, Koenraadt CJM, van Rij RP, van Oers MM, Pijlman GP: **Noncoding Subgenomic Flavivirus RNA Is Processed by the Mosquito RNA Interference Machinery and Determines West Nile Virus Transmission by Culex pipiens Mosquitoes**. *Journal of virology* 2016, **90**(22):10145-10159.

222. Arjona A, Ledizet M, Anthony K, Bonafe N, Modis Y, Town T, Fikrig E: **West Nile virus envelope protein inhibits dsRNA-induced innate immune responses**. *Journal of immunology (Baltimore, Md : 1950)* 2007, **179**(12):8403-8409.

223. Bhuvanakantham R, Ng ML: **West Nile virus and dengue virus capsid protein negates the antiviral activity of human Sec3 protein through the proteasome pathway**. *Cellular microbiology* 2013, **15**(10):1688-1706.

224. Bhuvanakantham R, Li J, Tan TT, Ng ML: **Human Sec3 protein is a novel transcriptional and translational repressor of flavivirus**. *Cellular microbiology* 2010, **12**(4):453-472.

225. Samuel GH, Wiley MR, Badawi A, Adelman ZN, Myles KM: **Yellow fever virus capsid protein is a potent suppressor of RNA silencing that binds double-stranded RNA**. *Proceedings of the National Academy of Sciences of the United States of America* 2016, **113**(48):13863-13868.

226. Xia H, Luo H, Shan C, Muruato AE, Nunes BTD, Medeiros DBA, Zou J, Xie X, Giraldo MI, Vasconcelos PFC *et al*: **An evolutionary NS1 mutation enhances Zika virus evasion of host interferon induction**. *Nature communications* 2018, **9**(1):414.

227. Beatty PR, Puerta-Guardo H, Killingbeck SS, Glasner DR, Hopkins K, Harris E: **Dengue virus NS1 triggers endothelial permeability and vascular leak that is prevented by NS1 vaccination**. *Science translational medicine* 2015, **7**(304):304ra141.

228. Liu WJ, Chen HB, Wang XJ, Huang H, Khromykh AA: **Analysis of adaptive mutations in Kunjin virus replicon RNA reveals a novel role for the flavivirus nonstructural protein NS2A in inhibition of beta interferon promoter-driven transcription**. *Journal of virology* 2004, **78**(22):12225-12235.

229.   Anglero-Rodriguez YI, Pantoja P, Sariol CA: **Dengue virus subverts the interferon induction pathway via NS2B/3 protease-IkappaB kinase epsilon interaction**. *Clinical and vaccine immunology : CVI* 2014, **21**(1):29-38.

230.   Munoz-Jordan JL, Laurent-Rolle M, Ashour J, Martinez-Sobrido L, Ashok M, Lipkin WI, Garcia-Sastre A: **Inhibition of alpha/beta interferon signaling by the NS4B protein of flaviviruses**. *Journal of virology* 2005, **79**(13):8004-8013.

231.   Dalrymple NA, Cimica V, Mackow ER: **Dengue Virus NS Proteins Inhibit RIG-I/MAVS Signaling by Blocking TBK1/IRF3 Phosphorylation: Dengue Virus Serotype 1 NS4A Is a Unique Interferon-Regulating Virulence Determinant**. *mBio* 2015, **6**(3):e00553-00515.

232.   Best SM, Morris KL, Shannon JG, Robertson SJ, Mitzel DN, Park GS, Boer E, Wolfinbarger JB, Bloom ME: **Inhibition of interferon-stimulated JAK-STAT signaling by a tick-borne flavivirus and identification of NS5 as an interferon antagonist**. *Journal of virology* 2005, **79**(20):12828-12839.

233.   Ashour J, Laurent-Rolle M, Shi PY, Garcia-Sastre A: **NS5 of dengue virus mediates STAT2 binding and degradation**. *Journal of virology* 2009, **83**(11):5408-5418.

234.   Laurent-Rolle M, Boer EF, Lubick KJ, Wolfinbarger JB, Carmody AB, Rockx B, Liu W, Ashour J, Shupert WL, Holbrook MR *et al*: **The NS5 protein of the virulent West Nile virus NY99 strain is a potent antagonist of type I interferon-mediated JAK-STAT signaling**. *Journal of virology* 2010, **84**(7):3503-3515.

235.   Cook BW, Cutts TA, Court DA, Theriault S: **The generation of a reverse genetics system for Kyasanur Forest Disease Virus and the ability to antagonize the induction of the antiviral state in vitro**. *Virus research* 2012, **163**(2):431-438.

236.   Jacobsen PF, Jenkyn DJ, Papadimitriou JM: **Establishment of a human medulloblastoma cell line and its heterotransplantation into nude mice**. *Journal of neuropathology and experimental neurology* 1985, **44**(5):472-485.

237.   Cinatl J, Gussetis, E.S., Cinatl, J., JR., Ebener, U., Mainke, M., Schwabe, D., Doerr, H.W., Kornhuber, B. and Gerein, V.: **Differentiation arrest in neuroblastoma cell culture.** *J Cancer Res Clin Oncol (Suppl)* 1990, **116**(9).

238.   Ponten J, Macintyre EH: **Long term culture of normal and neoplastic human glia**. *Acta pathologica et microbiologica Scandinavica* 1968, **74**(4):465-486.

239.   Selinger M, Wilkie GS, Tong L, Gu Q, Schnettler E, Grubhoffer L, Kohl A: **Analysis of tick-borne encephalitis virus-induced host responses in human cells of neuronal origin and interferon-mediated protection**. *The Journal of general virology* 2017, **98**(8):2043-2060.

240.   Selinger M, Wilkie GS, Tong L, Gu Q, Schnettler E, Grubhoffer L, Kohl A: **Corrigendum: Analysis of tick-borne encephalitis virus-induced host responses in human cells of neuronal origin and interferon-mediated protection**. *The Journal of general virology* 2018, **99**(8):1147-1149.

241.   Palus M, Vojtiskova J, Salat J, Kopecky J, Grubhoffer L, Lipoldova M, Demant P, Ruzek D: **Mice with different susceptibility to tick-borne encephalitis virus infection show selective neutralizing antibody response and inflammatory reaction in the central nervous system**. *Journal of neuroinflammation* 2013, **10**:77.

242.   Benveniste EN, Qin H: **Type I interferons as anti-inflammatory mediators**. *Science's STKE : signal transduction knowledge environment* 2007, **2007**(416):pe70.

243.   Parker N, Porter AC: **Identification of a novel gene family that includes the interferon-inducible human genes 6-16 and ISG12**. *BMC genomics* 2004, **5**(1):8.

244.   Rosebeck S, Leaman DW: **Mitochondrial localization and pro-apoptotic effects of the interferon-inducible protein ISG12a**. *Apoptosis : an international journal on programmed cell death* 2008, **13**(4):562-572.

245.   Huang J, Li Y, Qi Y, Zhang Y, Zhang L, Wang Z, Zhang X, Gui L: **Coordinated regulation of autophagy and apoptosis determines endothelial cell fate during Dengue virus type 2 infection**. *Molecular and cellular biochemistry* 2014, **397**(1-2):157-165.

246.   Qi Y, Li Y, Zhang Y, Zhang L, Wang Z, Zhang X, Gui L, Huang J: **IFI6 Inhibits Apoptosis via Mitochondrial-Dependent Pathway in Dengue Virus 2 Infected Vascular Endothelial Cells**. *PloS one* 2015, **10**(8):e0132743.

247.   Richardson RB, Ohlson MB, Eitson JL, Kumar A, McDougal MB, Boys IN, Mar KB, De La Cruz-Rivera PC, Douglas C, Konopka G *et al*: **A CRISPR screen identifies IFI6 as an ER-resident interferon**

effector that blocks flavivirus replication. *Nature microbiology* 2018, **3**(11):1214-1223.

248.   Selinger M, Tykalova H, Sterba J, Vechtova P, Vavruskova Z, Lieskovska J, Kohl A, Schnettler E, Grubhoffer L: **Tick-borne encephalitis virus inhibits rRNA synthesis and host protein production in human cells of neural origin**. *PLoS neglected tropical diseases* 2019, **13**(9):e0007745.

249.   Donald CL, Brennan B, Cumberworth SL, Rezelj VV, Clark JJ, Cordeiro MT, Freitas de Oliveira Franca R, Pena LJ, Wilkie GS, Da Silva Filipe A *et al*: **Full Genome Sequence and sfRNA Interferon Antagonist Activity of Zika Virus from Recife, Brazil**. *PLoS neglected tropical diseases* 2016, **10**(10):e0005048.

250.   Melian EB, Hinzman E, Nagasaki T, Firth AE, Wills NM, Nouwens AS, Blitvich BJ, Leung J, Funk A, Atkins JF *et al*: **NS1' of flaviviruses in the Japanese encephalitis virus serogroup is a product of ribosomal frameshifting and plays a role in viral neuroinvasiveness**. *Journal of virology* 2010, **84**(3):1641-1647.

251.   Firth AE, Atkins JF: **A conserved predicted pseudoknot in the NS2A-encoding sequence of West Nile and Japanese encephalitis flaviviruses suggests NS1' may derive from ribosomal frameshifting**. *Virology journal* 2009, **6**:14.

252.   Ye Q, Li XF, Zhao H, Li SH, Deng YQ, Cao RY, Song KY, Wang HJ, Hua RH, Yu YX *et al*: **A single nucleotide mutation in NS2A of Japanese encephalitis-live vaccine virus (SA14-14-2) ablates NS1' formation and contributes to attenuation**. *The Journal of general virology* 2012, **93**(Pt 9):1959-1964.

253.   Sun J, Yu Y, Deubel V: **Japanese encephalitis virus NS1' protein depends on pseudoknot secondary structure and is cleaved by caspase during virus infection and cell apoptosis**. *Microbes and infection* 2012, **14**(11):930-940.

254.   Faggioni G, Ciammaruconi A, De Santis R, Pomponi A, Scicluna MT, Barbaro K, Masuelli L, Autorino G, Bei R, Lista F: **Evidence of a humoral response to a novel protein WARF4 embedded in the West Nile virus NS4B gene encoded by an alternative open reading frame**. *International journal of molecular medicine* 2009, **23**(4):509-512.

255.   Faggioni G, Pomponi A, De Santis R, Masuelli L, Ciammaruconi A, Monaco F, Di Gennaro A, Marzocchella L, Sambri V, Lelli R *et al*: **West Nile alternative open reading frame (N-NS4B/WARF4) is produced in infected West Nile Virus (WNV) cells and induces**

humoral response in WNV infected individuals. *Virology journal* 2012, **9**:283.

256.   Cerny J, Selinger M, Palus M, Vavruskova Z, Tykalova H, Bell-Sakyi L, Sterba J, Grubhoffer L, Ruzek D: **Expression of a second open reading frame present in the genome of tick-borne encephalitis virus strain Neudoerfl is not detectable in infected cells**. *Virus genes* 2016, **52**(3):309-316.

257.   Calvo SE, Pagliarini DJ, Mootha VK: **Upstream open reading frames cause widespread reduction of protein expression and are polymorphic among humans**. *Proceedings of the National Academy of Sciences of the United States of America* 2009, **106**(18):7507-7512.

258.   Raman R, Tharakaraman K, Sasisekharan V, Sasisekharan R: **Glycan-protein interactions in viral pathogenesis**. *Current opinion in structural biology* 2016, **40**:153-162.

259.   Winkler G, Heinz FX, Kunz C: **Studies on the glycosylation of flavivirus E proteins and the role of carbohydrate in antigenic structure**. *Virology* 1987, **159**(2):237-243.

260.   Rey FA, Heinz FX, Mandl C, Kunz C, Harrison SC: **The envelope glycoprotein from tick-borne encephalitis virus at 2 A resolution**. *Nature* 1995, **375**(6529):291-298.

261.   Lorenz IC, Kartenbeck J, Mezzacasa A, Allison SL, Heinz FX, Helenius A: **Intracellular assembly and secretion of recombinant subviral particles from tick-borne encephalitis virus**. *Journal of virology* 2003, **77**(7):4370-4382.

262.   Yoshii K, Yanagihara N, Ishizuka M, Sakai M, Kariwa H: **N-linked glycan in tick-borne encephalitis virus envelope protein affects viral secretion in mammalian cells, but not in tick cells**. *The Journal of general virology* 2013, **94**(Pt 10):2249-2258.

263.   Vechtova P, Sterbova J, Sterba J, Vancova M, Rego ROM, Selinger M, Strnad M, Golovchenko M, Rudenko N, Grubhoffer L: **A bite so sweet: the glycobiology interface of tick-host-pathogen interactions**. *Parasites & vectors* 2018, **11**(1):594.

8 List of abbreviations

A549	human alveolar adenocarcinoma cell line
ADE	antibody-dependent enhancement
ADP	adenosine diphosphate
AIM2	absent in melanoma 2
ALR	augmenter of liver regeneration
APC	antigen-presenting cell
ARIH1	Ariadne RBR E3 ubiquitin protein ligase 1
ATF6	activating transcription factor 6
ATP	adenosine triphosphate
BBB	blood-brain barrier
CCL	chemokine C-C motif ligand
CD	cluster of differentiation
CLR	C-type lectin receptors
CMV	cytomegalovirus
CNS	central nervous system
CSF3	colony-stimulating factor 3
CTLs	cytotoxic T lymphocytes
CXCL	chemokine C-X-C motif ligand
DAI	DNA-dependent activator of IFN-regulatory factors
DAOY	human desmoplastic cerebellar medulloblastoma cell line
DC	dendritic cell
DC-SIGN	Dendritic Cell-Specific Intercellular adhesion molecule-3-Grabbing Non-integrin
DE genes	differentially expressed genes
DENV	dengue virus
DNA	deoxyribonucleic acid
dsRNA	double-stranded ribonucleic acid
EF1α	elongation factor 1 alpha

eIF2α	eukaryotic initiation factor 2 alpha
ENA78	Epithelial neutrophil- activating protein 78
ER	endoplasmic reticulum
ERAD	endoplasmic reticulum associated degradation
GAF	gamma interferon-activated factor
GAS	gamma interferon activation site
GCN2	general control nonderepressible 2
HBMEC	primary human microvascular endothelial cells
HCMV	human cytomegalovirus
HCV	hepatitis C virus
HEK293T	human embryonal kidney cell line containing the SV40 T-antigen
HERC5	HECT And RLD Domain Containing E3 Ubiquitin Protein Ligase 5
HRI	heme-regulated inhibitor
HTH	helix-turn-helix
hVAP-33	human VAMP-Associated Protein A
IAV	influenza A virus
IFI	Interferon Alpha Inducible Protein
IFIT	Interferon-induced protein with tetratricopeptide repeats
IFITM	Interferon-induced transmembrane protein
IFN	interferon
IFNAR1	Interferon-alpha/beta receptor alpha chain
IFNAR2	Interferon-alpha/beta receptor beta chain
IFNGR1	Interferon gamma receptor 1
IFNGR2	Interferon gamma receptor 2
IFNLR1	Interferon Lambda Receptor 1
IKKε	IκB kinase epsilon
IL10Rβ	Interleukin 10 Receptor Beta
IL-11	interleukin 11
IL-12α	interleukin 12 alpha

178

IL-15	interleukin 15
IL-1α	interleukin 1 alpha
IL-1β	interleukin 1 beta
IL-23α	interleukin 23 alpha
IL28Rα	Interleukin 28 Receptor Alpha
IL36RN	interleukin 36 receptor antagonist
IL-6	interleukin 6
IP-10	Interferon gamma-induced protein 10
IP-9	Interferon gamma-induced protein 9
IRE/CTVM19	*Ixodes ricinus*-derived embryonic cell line
IRE1	inositol-requiring protein 1
IRF	Interferon regulatory factor
ISG	interferon-stimulated gene
ISGF3	Interferon-stimulated gene factor 3
JAK1	Janus kinase 1
JEV	japanese encephalitis virus
kDa	kilodaltons
KFD	kyasanur forest disease
KFDV	kyasanur forest disease virus
LGP2	laboratory of genetics and physiology 2
LGTV	langat virus
LIV	louping ill virus
MAPK	mitogen-activated protein kinase
MAVS	Mitochondrial antiviral-signaling protein
MDA5	melanoma differentiation-associated protein 5
MHC	main histocompatibility complex
MHV	mouse hepatitis virus
MIP	macrophage inflammatory protein
mRNA	messenger RNA
Mx	Myxovirus resistance protein
MyD88	Myeloid differentiation primary response 88

NF-κB	nuclear factor kappa-light-chain-enhancer of activated B cells
NHL	NHL repeat (ncl-1, HT2A and lin-41)
NK	natural killer
NLR	NOD-like receptor
NLRP3	NOD-, LRR- and pyrin domain-containing protein 3
NOD2	nucleotide-binding oligomerization domain-containing protein 2
nt	nucleotide
OAS	2'-5'-oligoadenylate synthethase
OASL	2'-5'-oligoadenylate synthethase like
OHFV	Omsk haemorrhagic fever virus
ORF	open reading frame
PAMP	pathogen-associated molecular patterns
PERK	PKR-like ER kinase
PHD domain	Plant Homeodomain
PKR	protein kinase R
POLR1	RNA polymerase I
POLR3	RNA polymerase III
poly I:C	Polyinosinic:polycytidylic acid
POWV	powassan virus
PRR	Pattern recognition receptor
RANTES	Regulated on Activation, Normal T Cell Expressed and Secreted
rDNA	ribosomal deoxyribonucleic acid
RIG-I	Retinoic acid-inducible gene I
RING domain	Really Interesting New Gene domain
RIPK1	Receptor Interacting Serine/Threonine Kinase 1
RLR	RIG-I-like receptors
RNA	ribonucleic acid
rRNA	ribosomal ribonucleic acid
RSAD2	radical SAM domain-containing 2

SAM	S-adenosyl methionine
Sec3p	SECretory 3p
sfRNA	subgenomic ribonucleic acid
SLEV	Saint Louis encephalitis viruy
SOCS	Suppressor of cytokine signaling
SPRY domain	SPla and the RYanodine Receptor domain
ssRNA	single-stranded ribonucelic acid
STAT	Signal transducer and activator of transcription
STING	Stimulator of interferon *genes*
TANK	TRAF family member-associated NF-kappa-B activator
TBE	tick-borne encephalitis
TBEV	tick-borne encephalitis virus
TBEV-EU	western european TBEV subtype
TBEV-FE	far-eastern TBEV subtype
TBEV-Sib	siberian TBEV subtype
TBK1	TANK Binding Kinase 1
TLR	toll-like receptor
TNF-α	tumor necrosis factor alpha
TPR	Translocated Promoter Region
TRAF	TNF receptor-associated factor
TRIF	TIR-domain-containing adaptor-inducing interferon-β
TRIM	tripartite motif
tRNA	transfer ribonucleic acid
TSG101	Tumor susceptibility gene 101
TuORF	TBEV upstream open reading frame
TYK	Non-receptor tyrosine-protein kinase
U2OS	human osteosarcoma cell lim
U373	human glioma astrocytoma cell line
UBE1L	Ubiquitin-Activating Enzyme E1-Like
UBCH8	E2 Ubiquitin-Conjugating Enzyme L6

UKF-NB4	human neuroblastoma cells
uORF	upstream open reading frame
UPR	unfolded protein response
USP18	Ubiquitin Specific Peptidase 18
UTR	untranslated regions
VPs	vesicle packets
VSV	vesicular stomatitis virus
WARF4	West Nile alternative open reading frame N-NS4B
WHO	World Health Organization
WNV	west nile virus
XRN1	5'-3' exoribonuclease 1
YFV	yellow fever virus
ZIKV	Zika virus

9 *Curriculum vitae*

Mgr. Martin Selinger

E-mail: selinger@paru.cas.cz, selinm01@prf.jcu.cz
Date and place of birth: 24.9. 1988, České Budějovice, Czech Republic

Education:

2013 – present **University of South Bohemia, Faculty of Science**
- Ph.D. student of Cell and Molecular Biology and Genetics study program
- Ph.D. thesis: Molecular factors of cell antiviral immunity

2011 – 2013 **University of South Bohemia, Faculty of Science**
- Master degree in Experimental Biology study (graduated with honours)
- diploma thesis: Expression of target mRNAs during *Pospiviroid* pathogenesis in leaf factory system

2008 – 2011 **University of South Bohemia, Faculty of Science**
- Bachelor degree in Biology study program (graduated with honours)
- Bachelor thesis: Activation of selected plant promoters in leaf factory system dependent on the presence of silencing suppressors and viroid infection

Academic career:

2017 - now   Research assistant at the Institute of Chemistry and Biochemistry, Faculty of Science, University of South Bohemia (PI: dr. Jan Sterba)

2013 - now   Ph.D. student in the Laboratory of Molecular Ecology of Vectors and Pathogens at the Institute of Parasitology, Biology Centre, CAS (PI: prof. Libor Grubhoffer)

2007 - 2013   Bachelor and master student in the Laboratory of Molecular Genetics at the Institute of Plant Molecular Biology, Biology Centre, CAS (PI: dr. Jaroslav Matoušek)

Research internships:

2016   Internship in the Laboratory of Arboviruses at the MRC-University of Glasgow Centre for Virus Research (PI: prof. Alain Kohl)

Awards:

2013   Rector's award for excellent scientific results in master thesis at the Faculty of Science, University of South Bohemia
Dean's award for excellent scientific results in master thesis at the Faculty of Science, University of South Bohemia

Research funding (principal investigator):

2014   Characterization of viperin antiviral effect during TBEV infection (Grant Agency of University of South Bohemia)

Teaching:

2013 - now   Laboratory assistant in Biochemistry Laboratory 1 and Biochemistry Laboratory 2 courses (Faculty of Science, University of South Bohemia)

Attended courses:

2016	Osvědčení o odborné způsobilosti k navrhování pokusů a projektů pokusů podle § 15d odst. 3 zákona č. 246/1992 Sb., na ochranu zvířat proti týrání, ve znění pozdějších předpisů
2014	A PREDEMICS training course - Workshop on zoonotic features of viral infections: from the animal reservoir to pandemic emergence (Rome, Italy, April 2014)
2014	19th International Bioinformatics Workshop on Virus Evolution and Molecular Epidemiology (Rome, Italy, September 2014)
2013	TOEFL ITP: 637 points – C1 CEFR level

Publications with impact factor:

Selinger, M., Tykalová, H., Štěrba, J., Věchtová, P., Vavrušková, Z., Lieskovská, J., Kohl, A., Schnettler, E., Grubhoffer, L., 2019: Tick-borne encephalitis virus downregulates rRNA synthesis and host protein production in human cells of neuronal origin. *PLoS Negl Trop Dis.* 13(9): e0007745. doi: 10.1371/journal.pntd.0007745.

Dzyuba, V., Sampels, S., Ninhaus-Silveira, A., Kahanec, M., Veríssimo-Silveira, R., Rodina, M., Cosson, J., Boryshpolets, S., **Selinger, M.**, Sterba, J. and Dzyuba, B. (2019) Sperm motility and lipid composition in internally fertilizing ocellate river stingray *Potamotrygon motoro*. Theriogenology 130:26-35. doi: 10.1016/j.theriogenology.2019.02.029

Vechtova, P., Sterbova, J., Sterba, J., Vancova, M., Rego, R.O.M., **Selinger, M.**, Strnad, M., Golovchenko, M., Rudenko, N. and Grubhoffer, L. (2018) A bite so sweet: thy glycobiology interface of tick-host-pathogen interactions. *Parasit. Vectors* 11(1):594. doi: 10.1186/s13071-018-3062-7

Selinger, M., Wilkie, G.S., Tong, L., Gu, Q., Schnettler, E., Grubhoffer, L. and Kohl, A. (2017) Analysis of tick-borne encephalitis virus-induced host responses in human cells of neuronal origin and interferon-mediated protection. *J. Gen. Virol.* 98(8):2043-2060. doi:10.1099/jgv.0.000853

Donald, C.L., Brennan, B., Cumberworth, S.L., Rezelj, V.V., Clark J.J., Cordeiro, M.T., Freitas de Oliveira França, R., Pena, L.J., Wilkie, G.S., Da Silva Filipe, A., Davis, C., Hughes, J., Varjak, M., **Selinger, M.**, Zuvanov, L., Owsianka, A.M., Patel, A.H., McLauchlan, J., Lindenbach, B.D., Fall, G., Sall, A.A., Biek, R., Rehwinkel, J., Schnettler, E., Kohl, A. (2016) Full Genome Sequence and sfRNA Interferon Antagonist Activity of Zika Virus from Recife, Brazil. *PloS Negl. Trop. Dis.* 10(10):e0005048. doi: 10.1371/journal.pntd.0005048.

Černý, J., **Selinger, M.**, Palus, M., Vavrušková, Z., Černá Bolfíková, B., Tykalová, H., Grubhoffer, L., Růžek, D. (2016) Expression of a second open reading frame present in the genome of tick-borne encephalitis virus strain Neudoerfl is not detectable in infected cells. *Virus Genes* 52(3):309-16. doi: 10.1007/s11262-015-1273-y.

Number of publications in WoS: 6

Citations without self-citations (8.11. 2019): 62

H-index: 2

Molecular factors of cell antiviral immunity
Ph.D. Thesis Series, 2019, No. 20